ISSN 1007-9327 (print)
ISSN 2219-2840 (online)

World Journal of *Gastroenterology*

World J Gastroenterol 2018 December 28; 24(48): 5415-5536

Published by Baishideng Publishing Group Inc

World Journal of Gastroenterology

Contents

Weekly Volume 24 Number 48 December 28, 2018

World Journal of Gastroenterology

Contents

Weekly Volume 24 Number 48 December 28, 2018

Contents

World Journal of Gastroenterology
Volume 24 Number 48 December 28, 2018

ABOUT COVER

Editorial board member of *World Journal of Gastroenterology*, Harald Peter Hoensch, MD, Emeritus Professor, Marien Hospital Medical Department, Private Practice in Internal Medicine and Gastroenterology, Darmstadt D-64285, Germany

AIMS AND SCOPE

World Journal of Gastroenterology (*World J Gastroenterol*, *WJG*, print ISSN 1007-9327, online ISSN 2219-2840, DOI: 10.3748) is a peer-reviewed open access journal. *WJG* was established on October 1, 1995. It is published weekly on the 7th, 14th, 21st, and 28th each month. The *WJG* Editorial Board consists of 642 experts in gastroenterology and hepatology from 59 countries.

The primary task of *WJG* is to rapidly publish high-quality original articles, reviews, and commentaries in the fields of gastroenterology, hepatology, gastrointestinal endoscopy, gastrointestinal surgery, hepatobiliary surgery, gastrointestinal oncology, gastrointestinal radiation oncology, gastrointestinal imaging, gastrointestinal interventional therapy, gastrointestinal infectious diseases, gastrointestinal pharmacology, gastrointestinal pathophysiology, gastrointestinal pathology, evidence-based medicine in gastroenterology, pancreatology, gastrointestinal laboratory medicine, gastrointestinal molecular biology, gastrointestinal immunology, gastrointestinal microbiology, gastrointestinal genetics, gastrointestinal translational medicine, gastrointestinal diagnostics, and gastrointestinal therapeutics. *WJG* is dedicated to become an influential and prestigious journal in gastroenterology and hepatology, to promote the development of above disciplines, and to improve the diagnostic and therapeutic skill and expertise of clinicians.

INDEXING/ABSTRACTING

World Journal of Gastroenterology (*WJG*) is now indexed in Current Contents®/Clinical Medicine, Science Citation Index Expanded (also known as SciSearch®), Journal Citation Reports®, Index Medicus, MEDLINE, PubMed, PubMed Central and Directory of Open Access Journals. The 2018 edition of Journal Citation Reports® cites the 2017 impact factor for *WJG* as 3.300 (5-year impact factor: 3.387), ranking *WJG* as 35th among 80 journals in gastroenterology and hepatology (quartile in category Q2).

NAME OF JOURNAL
World Journal of Gastroenterology

ISSN
ISSN 1007-9327 (print)
ISSN 2219-2840 (online)

LAUNCH DATE
October 1, 1995

FREQUENCY
Weekly

EDITORIAL OFFICE
Ze-Mao Gong, Director
World Journal of Gastroenterology
Baishideng Publishing Group Inc
7901 Stoneridge Drive, Suite 501,
Pleasanton, CA 94588, USA
Telephone: +1-925-2238242
Fax: +1-925-2238243
E-mail: editorialoffice@wjgnet.com
Help Desk: https://www.f6publishing.com/helpdesk
https://www.wjgnet.com

PUBLISHER
Baishideng Publishing Group Inc
7901 Stoneridge Drive, Suite 501,
Pleasanton, CA 94588, USA
Telephone: +1-925-2238242
Fax: +1-925-2238243
E-mail: bpgoffice@wjgnet.com
Help Desk: https://www.f6publishing.com/helpdesk
https://www.wjgnet.com

PUBLICATION DATE
December 28, 2018

INSTRUCTIONS TO AUTHORS
Full instructions are available online at https://www.wjgnet.com/bpg/gerinfo/204

ONLINE SUBMISSION
https://www.f6publishing.com

World Journal of Gastroenterology

Submit a Manuscript: https://www.f6publishing.com

World J Gastroenterol 2018 December 28; 24(48): 5415-5417

DOI: 10.3748/wjg.v24.i48.5415

ISSN 1007-9327 (print) ISSN 2219-2840 (online)

EDITORIAL

Role of cenicriviroc in the management of nonalcoholic fatty liver disease

Georgios Neokosmidis, Konstantinos Tziomalos

Georgios Neokosmidis, Konstantinos Tziomalos, First Propedeutic Department of Internal Medicine, Medical School, Aristotle University of Thessaloniki, AHEPA Hospital, Thessaloniki 54636, Greece

ORCID number: Georgios Neokosmidis (0000-0003-1858-9098); Konstantinos Tziomalos (0000-0002-3172-1594).

Author contributions: Neokosmidis G drafted the editorial; Tziomalos K critically revised the draft.

Conflict-of-interest statement: All authors declare no conflict of interest related to this publication.

Manuscript source: Invited manuscript

Corresponding author: Konstantinos Tziomalos, MD, PhD, Assistant Professor, First Propedeutic Department of Internal Medicine, Medical School, Aristotle University of Thessaloniki, AHEPA Hospital, 1 Stilponos Kyriakidi Street, Thessaloniki 54636, Greece. ktziomalos@yahoo.com
Telephone: +30-2310-994621
Fax: +30-2310-994773

Received: September 28, 2018
Peer-review started: September 28, 2018
First decision: October 23, 2018
Revised: October 27, 2018
Accepted: November 8, 2018
Article in press: November 8, 2018
Published online: December 28, 2018

Abstract

Nonalcoholic fatty liver disease (NAFLD) is the commonest chronic liver disease in high-income countries and is associated with increased morbidity and mortality. Macrophages appear to play an important role in the development and progression of hepatic fibrosis in patients with NAFLD. Accordingly, modulation of macrophage trafficking might represent an attractive therapeutic strategy in this population. Cenicriviroc is an oral inhibitor of the chemokine ligand 2/C-C chemokine receptor 2 pathway, which plays an important role in the hepatic recruitment of the macrophages. Preclinical studies and a phase 2b study in humans suggest that this agent might hold promise in the management of NAFLD.

Key words: Cenicriviroc; Macrophages; Nonalcoholic fatty liver disease; Fibrosis; Nonalcoholic steatohepatitis

Core tip: Macrophages appear to play an important role in the development and progression of hepatic fibrosis in patients with nonalcoholic fatty liver disease (NAFLD). Accordingly, modulation of macrophage trafficking might represent an attractive therapeutic strategy in this population. Cenicriviroc is an oral inhibitor of the chemokine ligand 2/C-C chemokine receptor 2 pathway, which plays an important role in the hepatic recruitment of the macrophages. Preclinical studies and a phase 2b study in humans suggest that this agent might hold promise in the management of NAFLD.

Neokosmidis G, Tziomalos K. Role of cenicriviroc in the management of nonalcoholic fatty liver disease. *World J Gastroenterol* 2018; 24(48): 5415-5417
URL: https://www.wjgnet.com/1007-9327/full/v24/i48/5415.htm
DOI: https://dx.doi.org/10.3748/wjg.v24.i48.5415

INTRODUCTION

The prevalence of nonalcoholic fatty liver disease (NAFLD)

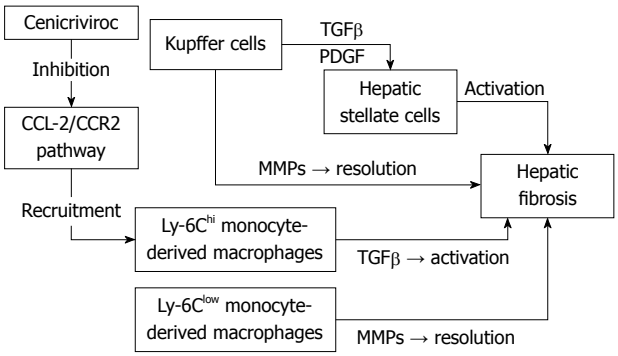

Figure 1 Molecular pathway through which cenicriviroc acts. TGFβ: Transforming growth factor β; PDGF: Platelet-derived growth factor; MMPs: Matrix metalloproteinases; CCL-2/CCR2: Chemokine (C-C motif) ligand 2/ C-C chemokine receptor 2.

is increasing worldwide and NAFLD has become the most predominant liver disease in Western countries due to the pandemic of obesity, metabolic syndrome and type 2 diabetes[1]. The histopathological spectrum of NAFLD ranges from isolated steatosis to nonalcoholic steatohepatitis (NASH) and cirrhosis, and NAFLD is associated with increased risk for hepatocellular carcinoma (HCC)[2].

The mainstay of treatment of NAFLD is weight loss through diet and exercise[2]. However, many patients cannot achieve or sustain weight loss[2]. Accordingly, pharmacotherapy is required in a considerable proportion of patients with NAFLD, particularly those with advanced fibrosis, who are at higher risk for liver-related complications[2,3].

Hepatic macrophages play an important role in the pathogenesis of acute and chronic liver injury[4,5]. Hepatic macrophages are a heterogenous population, consisting of Kupffer cells (KCs) and monocyte-derived macrophages (MoMF), which are recruited from the circulation to the liver[4,5]. KCs activate hepatic stellate cells (HSCs) through the production of pro-fibrotic cytokines transforming growth factor β (TGFβ) and platelet-derived growth factor (PDGF)[4,5]. On the other hand, KCs also secrete matrix metalloproteinases (MMPs), resulting in resolution of fibrosis[4,5]. Therefore, hepatic macrophages appear to exert both pro- and anti-fibrotic functions[4,5]. In cases of hepatic injury, Ly-6C^{hi} monocytes differentiate into proinflammatory macrophages, which interact with HSCs to promote fibrosis through the production of TGFβ[4,5]. The chemokine (C-C motif) ligand (CCL) 2/C-C chemokine receptor 2 (CCR2) pathway plays an important role in the hepatic recruitment of the Ly-6C^{hi} monocytes[4,5]. On the other hand, a recent study showed that phagocytosis of cellular debris facilitates a phenotypic switch from Ly-6C^{hi} macrophages to Ly-6C^{low} macrophages[4,5]. The Ly-6C^{low} monocyte is the main source of MMPs and promotes fibrosis resolution[4,5] (Figure 1).

CENICRIVIROC IN NAFLD

Given the important role of hepatic macrophages in the pathogenesis of liver fibrosis, targeting these cells might represent a promising approach in the management of NAFLD. Krenkel *et al*[6] recently reported an increased number of CCR2$^+$ macrophages in patients with NASH and either advanced fibrosis (stage 3) or cirrhosis (stage 4). It was also shown that cenicriviroc (CVC), an oral CCR2/CCR5 antagonist, prevents macrophage trafficking and hepatic infiltration by CCR2$^+$ MoMFs and might therefore be useful in the prevention and/or resolution of hepatic fibrosis in patients with NAFLD[6].

Several animal studies evaluated the antifibrotic potential of CVC. Kruger *et al*[7] administered CVC 10 mg/(kg•d) or 30 mg/(kg•d) for 4 wk and 20 mg/(kg•d) or 30 mg/(kg•d) for 14 wk in mice fed with a choline-deficient, L-amino acid- defined, high-fat diet (CDAHFD). A second group of mice was fed with standard chow and did not receive CVC. At 4 and 14 wk, livers were harvested for histology and flow cytometric analyses of intrahepatic cells. Serum alanine transaminase (ALT) and aspartate transaminase (AST) levels were normal in the standard chow group but were elevated in CDAHFD-fed, untreated control mice. In contrast, the CDAHFD-fed mice that were treated with CVBC 10 mg/(kg•d) and 30 mg/(kg•d) for 4 wk experienced a reduction in ALT levels. Moreover, after 4 wk of high-dose CVC treatment, a significant decrease in the number of intrahepatic Ly6-C^{high} macrophages was observed relative to the vehicle control. The intrahepatic CCR2$^+$ macrophages also decreased with 4 wk of CVC treatment whereas CCR5$^+$ macrophages were not affected. Therefore, CVC appears to have greater affinity for CCR2 than for CCR5 in mice. Kruger *et al*[7] also noticed a significant decrease in hepatic fibrosis in mice that received high-dose CVC treatment for 14 wk compared with vehicle controls. In another study, CVC reduced monocyte/macrophage recruitment at doses > 20 mg/(kg•d) in a mouse model of thiaglycalate-induced peritonitis[8]. At these doses, CVC also prevented hepatic fibrosis in a rat model of thioacetamide-induced liver fibrosis and in a mouse model of diet-induced NASH. A reduction in NAFLD activity score (NAS) and in plasma ALT levels was also observed with CVC treatment[8]. In another animal model of carbon tetrachloride-induced acute liver injury, mice received CVC or a vehicle control solution orally before the administration of carbon tetrachloride and after 12 h and 24 h[9]. CVC treatment reduced the number of F4/80 positive macrophages in the liver, particularly in the periportal and necrotic areas. Reductions in ALT levels and in the necrotic area at 36 h were also observed[9].

Recently, the results of the CENTAUR study were published[10]. This was a phase 2b, double-blind, placebo-controlled, multinational study that randomized 289 patients with NASH, NAS ⩾ 4 with ⩾ 1 in each component and stage 1-3 liver fibrosis to receive CVC 150 mg per os once daily or placebo. After 1 year of treatment, the primary endpoint (⩾ 2-point improvement in NAS with ⩾ 1-point reduction in either lobular inflammation or hepatocellular ballooning and no worsening of fibrosis) in the intent-to-treat population was achieved in a similar proportion of subjects on CVC and placebo

(16% *vs* 19%, respectively; $P = 0.52$). Resolution of steatohepatitis and no worsening of fibrosis, a key secondary outcome, was also observed in similar rates in the 2 groups (8% *vs* 6%, respectively; $P = 0.49$). However, improvement in fibrosis by $\geqslant$ 1 stage and no worsening of steatohepatitis, another key secondary outcome, was observed in more patients on CVC than placebo (20% *vs* 10%, respectively; $P = 0.02$). Patients with higher NAS, prominent hepatocellular ballooning, higher fibrosis stage, mild or no portal inflammation and with higher body mass index showed greater improvements with CVC treatment. The levels of biomarkers of systemic inflammation (high-sensitivity C-reactive protein, interleukin-6 and 1β, and fibrinogen) and of monocyte activation (sCD14) decreased in patients treated with CVC. On the other hand, CCL-2 and -4 increased in CVC-treated patients, confirming CCR2 and CCR5 blockade by CVC. Importantly, safety and tolerability of CVC were comparable to placebo[10]. AURORA, a phase Ⅲ study, will evaluate the effects of CVC on hepatic fibrosis in 2000 patients with NASH and is expected to be completed in 2019[11].

CONCLUSION

Cenicriviroc appears to represent a promising tool in the management of patients with NAFLD. However, larger studies are needed to clearly define the safety and efficacy of this novel agent in this highly prevalent disease.

REFERENCES

1 **Younossi ZM**, Koenig AB, Abdelatif D, Fazel Y, Henry L, Wymer M. Global epidemiology of nonalcoholic fatty liver disease-Meta-analytic assessment of prevalence, incidence, and outcomes. *Hepatology* 2016; **64**: 73-84 [PMID: 26707365 DOI: 10.1002/hep.28431]

2 **Chalasani N**, Younossi Z, Lavine JE, Diehl AM, Brunt EM, Cusi K, Charlton M, Sanyal AJ. The diagnosis and management of nonalcoholic fatty liver disease: practice Guideline by the American Association for the Study of Liver Diseases, American College of Gastroenterology, and the American Gastroenterological Association. *Hepatology* 2012; **55**: 2005-2023 [PMID: 22488764 DOI: 10.1002/hep.25762]

3 **Ekstedt M**, Hagström H, Nasr P, Fredrikson M, Stål P, Kechagias S, Hultcrantz R. Fibrosis stage is the strongest predictor for disease-specific mortality in NAFLD after up to 33 years of follow-up. *Hepatology* 2015; **61**: 1547-1554 [PMID: 25125077 DOI: 10.1002/hep.27368]

4 **Ju C**, Tacke F. Hepatic macrophages in homeostasis and liver diseases: from pathogenesis to novel therapeutic strategies. *Cell Mol Immunol* 2016; **13**: 316-327 [PMID: 26908374 DOI: 10.1038/cmi.2015.104]

5 **Raeman R**, Anania FA. Therapy for steatohepatitis: Do macrophages hold the clue? *Hepatology* 2018; **67**: 1204-1206 [PMID: 29091293 DOI: 10.1002/hep.29630]

6 **Krenkel O**, Puengel T, Govaere O, Abdallah AT, Mossanen JC, Kohlhepp M, Liepelt A, Lefebvre E, Luedde T, Hellerbrand C, Weiskirchen R, Longerich T, Costa IG, Anstee QM, Trautwein C, Tacke F. Therapeutic inhibition of inflammatory monocyte recruitment reduces steatohepatitis and liver fibrosis. *Hepatology* 2018; **67**: 1270-1283 [PMID: 28940700 DOI: 10.1002/hep.29544]

7 **Kruger AJ**, Fuchs BC, Masia R, Holmes JA, Salloum S, Sojoodi M, Ferreira DS, Rutledge SM, Caravan P, Alatrakchi N, Vig P, Lefebvre E, Chung RT. Prolonged cenicriviroc therapy reduces hepatic fibrosis despite steatohepatitis in a diet-induced mouse model of nonalcoholic steatohepatitis. *Hepatol Commun* 2018; **2**: 529-545 [PMID: 29761169 DOI: 10.1002/hep4.1160]

8 **Lefebvre E**, Moyle G, Reshef R, Richman LP, Thompson M, Hong F, Chou HL, Hashiguchi T, Plato C, Poulin D, Richards T, Yoneyama H, Jenkins H, Wolfgang G, Friedman SL. Antifibrotic Effects of the Dual CCR2/CCR5 Antagonist Cenicriviroc in Animal Models of Liver and Kidney Fibrosis. *PLoS One* 2016; **11**: e0158156 [PMID: 27347680 DOI: 10.1371/journal.pone.0158156]

9 **Puengel T**, Krenkel O, Kohlhepp M, Lefebvre E, Luedde T, Trautwein C, Tacke F. Differential impact of the dual CCR2/CCR5 inhibitor cenicriviroc on migration of monocyte and lymphocyte subsets in acute liver injury. *PLoS One* 2017; **12**: e0184694 [PMID: 28910354 DOI: 10.1371/journal.pone.0184694]

10 **Friedman SL**, Ratziu V, Harrison SA, Abdelmalek MF, Aithal GP, Caballeria J, Francque S, Farrell G, Kowdley KV, Craxi A, Simon K, Fischer L, Melchor-Khan L, Vest J, Wiens BL, Vig P, Seyedkazemi S, Goodman Z, Wong VW, Loomba R, Tacke F, Sanyal A, Lefebvre E. A randomized, placebo-controlled trial of cenicriviroc for treatment of nonalcoholic steatohepatitis with fibrosis. *Hepatology* 2018; **67**: 1754-1767 [PMID: 28833331 DOI: 10.1002/hep.29477]

11 Phase 3 Study for the Efficacy and Safety of CVC for the Treatment of Liver Fibrosis in Adults With NASH. In: Clinical Trials.gov [Internet]. Available from: URL: https://clinicaltrials.gov/ct2/show/NCT03028740?term=cenicrivirocrank=10 Clinical Trials.gov Identifier: NCT03028740

P- Reviewer: Kim DJ, Sherif Z, Zhu HF **S- Editor**: Wang XJ
L- Editor: A **E- Editor**: Yin SY

World Journal of Gastroenterology

Submit a Manuscript: https://www.f6publishing.com

World J Gastroenterol 2018 December 28; 24(48): 5418-5432

DOI: 10.3748/wjg.v24.i48.5418

ISSN 1007-9327 (print) ISSN 2219-2840 (online)

REVIEW

Colorectal cancer vaccines: Tumor-associated antigens *vs* neoantigens

Sandra Wagner, Christina S Mullins, Michael Linnebacher

Sandra Wagner, Christina S Mullins, Michael Linnebacher, Section of Molecular Oncology and Immunotherapy, General Surgery, University Medical Center, Rostock D-18057, Germany

ORCID number: Sandra Wagner (0000-0002-8112-4392); Christina S Mullins (0000-0003-2296-2027); Michael Linnebacher (0000-0001-8054-1402).

Author contributions: Wagner S and Linnebacher M wrote the manuscript and critically reviewed the final version of the manuscript. Mullins CS was involved in the design of the figures; critically reviewed the revised manuscript and language edited the manuscript as a native speaker.

Supported by Ministerium für Wirtschaft, Arbeit und Gesundheit Mecklenburg-Vorpommern, No. TBI-V-1-241-VBW-084.

Conflict-of-interest statement: Ms. Wagner has nothing to disclose. Dr. Mullins is supported by the Robert Bosch Stiftung with a Fast Track scholarship. Dr. Linnebacher reports grants from Ministerium für Wirtschaft, Arbeit und Gesundheit Mecklenburg-Vorpommern, during the conduct of the study.

Manuscript source: Invited manuscript

Corresponding author: Michael Linnebacher, PhD, Academic Fellow, Department of General Surgery, Section of Molecular Oncology and Immunotherapy, University Medical Center, Schillingallee 35, Rostock D-18057, Germany. michael.linnebacher@med.uni-rostock.de
Telephone: +49-381-4946043
Fax: +49-381-4946002

Received: October 13, 2018
Peer-review started: October 14, 2018
First decision: November 8, 2018
Revised: December 11, 2018
Accepted: December 20, 2018
Article in press: December 21, 2018
Published online: December 28, 2018

Abstract

Therapeutic options for the treatment of colorectal cancer (CRC) are diverse but still not always satisfying. Recent success of immune checkpoint inhibition treatment for the subgroup of CRC patients suffering from hypermutated tumors suggests a permanent role of immune therapy in the clinical management of CRC. Substantial improvement in treatment outcome could be achieved by development of efficient patient-individual CRC vaccination strategies. This mini-review summarizes the current knowledge on the two general classes of targets: tumor-associated antigens (TAAs) and tumor-specific antigens. TAAs like carcinoembryonic antigen and melanoma associated antigen are present in and shared by a subgroup of patients and a variety of clinical studies examined the efficacy of different TAA-derived peptide vaccines. Combinations of several TAAs as the next step and the development of personalized TAA-based peptide vaccines are discussed. Improvements of peptide-based vaccines achievable by adjuvants and immune-stimulatory chemotherapeutics are highlighted. Finally, we sum up clinical studies using tumor-specific antigens - in CRC almost exclusively neoantigens - which revealed promising results; particularly no severe adverse events were reported so far. Critical progress for clinical outcomes can be expected by individualizing neoantigen-based peptide vaccines and combining them with immune-stimulatory chemotherapeutics and immune checkpoint inhibitors. In light of these data and latest developments, truly personalized neoantigen-based peptide vaccines can be expected to fulfill modern precision medicine's requirements and will manifest as treatment pillar for routine clinical management of CRC.

Key words: Cancer vaccines; Colorectal neoplasm; Immunotherapy; Neoplasm antigen; Tumor-associated antigens; Tumor-specific antigens; Neoantigen(s)

Core tip: Peptide vaccines are a promising tool for colorectal cancer (CRC) treatment. Direct comparison of tumor-associated antigens (TAAs) and neoantigens reveals clear superiority of the latter for several reasons. TAAs, albeit easier to identify and even shared by many patients, did not prove effective in clinical trials. Additionally, and due to their unspecificity, they frequently trigger severe adverse events. This risk is neglectable for tumor-specific neoantigens - thus compensating for the costly and laborious identification of such antigens expressed in individual patient tumors. Intelligent modern CRC vaccines will likely combine several or even many individual neoantigen-derived peptides with immuno-chemotherapy, adjuvants or further immuno-modulators.

Wagner S, Mullins CS, Linnebacher M. Colorectal cancer vaccines: Tumor-associated antigens *vs* neoantigens. *World J Gastroenterol* 2018; 24(48): 5418-5432
URL: https://www.wjgnet.com/1007-9327/full/v24/i48/5418.htm
DOI: https://dx.doi.org/10.3748/wjg.v24.i48.5418

INTRODUCTION

Therapy of colorectal carcinoma (CRC) has been improved over the years with advanced surgical and chemotherapeutic procedures but challenges in sight of efficiency and adverse effects must still be accomplished. Especially late stage CRC patients still have a relatively poor prognosis. Only recently, immunotherapy has reached general clinical acceptance with the break-through results of immune checkpoint inhibition for selected cancer types or subgroups - also for CRC.

One approach further improving this type of CRC therapy is the vaccination with peptides alone, peptide-expressing viruses, peptide-loaded antigen presenting cells or application of peptide-specific T cells. Historically, the development of such cancer vaccines started with peptides derived from tumor-associated antigens (TAAs).

TAAs

TAAs are proteins that are significantly over-expressed in cancer compared to normal cells and are therefore also abundantly presented on the cancer cell's surface. Peptides of these TAAs bound to human leukocyte antigen (HLA) can be recognized by T cells initiating an anti-cancer immune response (Figure 1). Therefore, these TAAs have been used as target structures for the development of cancer vaccines (see Table 1 for an overview of CRC focused clinical studies).

Carcinoembryonic antigen

One of the first TAAs ever identified was the carcino-embryonic antigen (CEA) which is also overexpressed in CRC[1]. In initial *in vitro* experiments, it could be proven that CEA-derived peptide-loaded dendritic cells (DCs) are able to induce CEA-specific cytotoxic T lymphocyte (CTL) activity[2]. However, a CEA-derived peptide with low avidity led to an inefficient immune response lacking activated CTLs[3]. The explanation for such inefficient T cell activation lies in the fact that TAAs like CEA are not really cancer specific but are also expressed by normal epithelial cells. Therefore, the organism must, for the most part, be tolerant to such TAAs in order to prevent autoimmunity.

Consequently, different approaches for modifying CEA vaccines were developed to overcome or weaken this immune tolerance. Using an altered peptide ligand of CEA with higher HLA binding affinity could efficiently activate specific CTLs *in vitro*[4]. Another way to enhance specific T cell activation was the development of DNA vaccines encoding the CEA-derived peptide(s) together with sequences for stimulating cytokines, adjuvants or supportive T helper cell epitopes. In murine models, this kind of vaccine showed higher T cell activation in comparison to peptide-only vaccines[5,6]. However, in clinical trials, the efficacy of CEA peptide vaccines was overall not satisfying, clinical response rate did not exceed 17 %[7-10].

Melanoma associated antigen

The melanoma associated antigen (MAGE), first discovered in melanomas, belongs to the group of cancer/testis antigens. This subgroup of TAAs is expressed only in testis and cancer cells. MAGE has subsequently been found to be expressed in the majority of adenocarcinomas. The rate of CRCs identified as being MAGE-positive strongly varied between different studies and MAGE variants: 14 % for MAGE-A[11], 51 % for MAGE-A1-6[12] and 28 % for MAGE-A3[13].

A clinical benefit by a MAGE-directed vaccination therapy could be shown in a case study by Takahashi *et al*[14]. They reported that a synthesized helper/killer-hybrid epitope long peptide of MAGE-A4 is able to induce an orchestrated $CD4^+$ and $CD8^+$ immune response leading to a slightly decreased tumor growth and resulting in stable disease. In a vaccination study investigating different TAAs, an increase in specific CTLs could be detected but clinical response was not observed[15].

Other TAAs

Progress in CRC vaccine development was made also with a variety of other TAAs. A peptide vaccination consisting of two different 9-mers derived from MUC-1 combined with CpG oligonucleotides and granulocyte macrophage colony-stimulating factor (GM-CSF) as adjuvants reduced tumor burden in a MUC1.Tg mouse model. In the prophylactic setting, even a complete

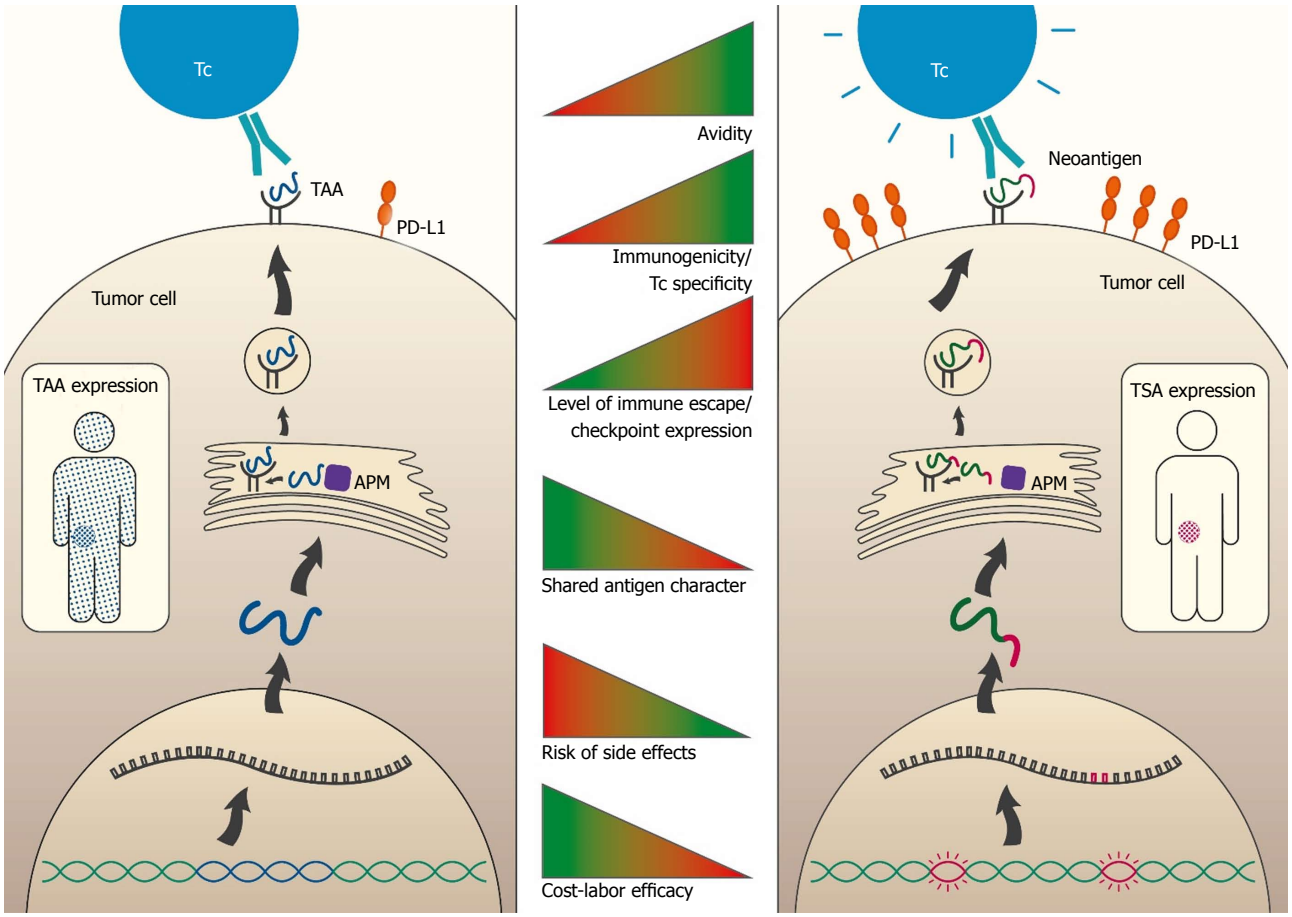

Figure 1 Comparison of tumor-associated antigens and tumor-specific antigens properties. The figure depicts properties and processing steps of antigens which are either tumor associated (TAA; blue; left side) or tumor specific (TSA; pink; right side). The course until antigen processing includes the following steps: transcription of genomic locus (TAA, blue) or mutation containing locus (TSA; pink), translation and RNA processing, protein degradation and MHC molecule loading and finally presentation of the antigen (TAA or TSA) on the cell surface embedded in MHC molecules. TAA-proteins are expressed to a high level in the tumor and to a low level in other organs and tissues (blue sprinkled patient). The neo-antigenic part of the TSA-protein is solely expressed in the tumor (pink sprinkled tumor). Recognition of the tumor cell by T cells (Tc, *e.g.*, CTL) takes place *via* the T cell receptor (TCR; green). The avidity is increased for TSAs (indicated by the "speedlines" on the right side of the Tc). The tumor may counteract the immune recognition by expression of immune checkpoint molecules such as PD-L1 (orange). This occurs to a much higher extent in TSA baring than in merely TAA baring tumors. The middle panel indicates the degree of T cell avidity (first bar), extent of immunogenicity/T cell specificity (second bar), level of immune escape / checkpoint expression (third bar), shared antigen character (fourth bar), risk of side effects (fifth bar) and cost-labor efficacy (sixth bar) ranging from low (red) to high (green). APM: Antigen-presenting machinery; TAA: Tumor-associated antigens; TCR: T cell receptor; TSA: Tumor-specific antigen.

protection against a syngeneic colon cancer cell line was achieved and attributed to the MUC 1-specific activation of the immune system[16]. However, these promising results could not be proven in clinical trials. Although an increase in anti MUC1 IgGs could be detected, neither cellular nor clinical response was observed[17-19].

CRC patients treated with survivin-derived peptide-pulsed DCs showed an increased number of specific CTLs[20,21]. In a minority of patients, also a drop in level of tumor markers and even in total tumor volume was witnessed[21].

Furthermore, success was achieved in CRC-focused studies on vaccination with peptides obtained from Wilms tumor 1 protein[22], transmembrane 4 superfamily member 5 protein[23], mitotic centromere associated kinesin[24] and epidermal growth factor receptor[25].

Of note and in contrast to other tumor entities, NY-ESO-1 is not overexpressed in CRC[11,26,27] and has therefore not been exploited as a target for immunotherapy.

COMBINATION OF TAAs

Single peptide vaccines often showed a significant immune response which was, however, not accompanied by a significant reduction of tumor burden. Thus, subsequent vaccination studies included more than one TAA-derived peptide to ameliorate clinical response.

After the identification of the ring finger protein 43 (RNF43) as a CTL-inducing peptide[28], it was often investigated in combination with other peptides. At first Okuno *et al*[29] combined chemotherapy with a RNF43 and a 34-kDa translocase of the outer mitochondrial membrane (TOMM34) peptide in a phase I clinical trial which resulted in 83 % stable disease and a mean survival time of 24 mo, but no reduction in tumor burden was observed. The efficiency of inducing specific CTLs by RNF43 and TOMM34 was also proven by additional

Table 1 Clinical vaccination trials focused on colorectal cancer patients

Target type	Target molecule	Vaccination strategy	Therapy	No. of CRC Patients	Clinical response	Ref.
TAA	CEA	Altered peptide loaded on DC		10/12	2 CR, 2 SD, 1 MR, 7 PD	[8]
TAA	CEA	CEA peptides pulsed DC		10	2 SD, 8 PD	[9]
TAA	CEA	CEA peptides pulsed DC		10	7 had CTL increase	[10]
TAA	MAGE	MAGE-A-pulsed DC		21	21 PD	[15]
TAA	MAGE	synthesized helper/killer-hybrid epitope long peptide (H/K-HELP) of MAGE-A4		1	SD	[14]
TAA	MUC1	MUC1-mannan fusion protein	Chemo-therapy	18	2 SD, 16 PD	[17]
TAA	MUC1	100-amino acid synthetic MUC1 peptide with Poly-ICLC		39	20 responders (IgG), 19 non-responders	[18]
TAA	MUC1	irradiated allogeneic colorectal carcinoma cell lines with GM-CSF-producing bystander cell line (K562)		9	4 CR, 5 PD	[19]
TAA	Survivin	survivin-2B peptide		15	1 MR, 3 SD, 11 PD	[21]
TAA	WT1	HLA-A or HLA-DR restricted peptides on DCs	Chemo-therapy	3	3 SD	[22]
TAA	RNF43, TOMM34	peptides,with Montanide ISA 51	Chemo-therapy	21	16 SD	[29]
TAA	RNF43, TOMM34	HLA-A*2402-restricted peptides	Chemo-therapy	22	13 CTL induction	[31]
TAA	RNF43, TOMM34	Peptides with Montanide ISA 51		24	6 SD, 18 PD	[30]
TAA + VEGFR	RNF43, TOMM34, FOXM1, MELK, HJURP, VEGFR-1, VEGFR-2	HLA-A2402-restricted peptides with Montanide ISA 51	Chemo-therapy	30	3 PR, 15 SD, 12 PD	[32]
TAA + VEGFR	RNF43, TOMM34, KOC1, VEGFR-1, VEGFR-2	HLA-A*2402-restricted peptides with Montanide ISA 51		19	1 CR, 6 SD, 12 PD	[33]
PPV TAA	cypB, Ick, SART 1-3, ART4	2-4 HLA-A24-restricted Peptides matching to patient's pre-vaccination immune response with Montanide ISA 51		10	1 PR, 1 SD, 8 PD	[34]
PPV TAA	SART3, Lck, WHS, HNR, MRP3, PAP, EZH2, CEA, PSCA, UBE, Her2/neu, PSA, CypB	2-4 HLA-A24- or HLA-A2 restricted Peptides matching to patient's pre-vaccination immune response with Montanide ISA 51	Chemo-therapy	7	1 SD, 6 PD	[35]
PPV TAA	SART2-3, Lck, MRP3, EIF4EBP, WHSC2, CypB, CEA, UBE, Her2/neu,	2-4 HLA-A24- or HLA-A2 restricted Peptides matching to patient's pre-vaccination immune response with Montanide ISA 51	Chemo-therapy	14	3 MR, 3 SD, 8 PD	[36]
Neoantigen	AIM2(-1), HT001(-1), TAF1B(-1)	Frameshift peptides with Montanide ISA 51		22	16 immune response (CTL/IgG induction)	[52]
Neoantigen	KRAS	13-mer ras peptide with Detox adjuvant		10	1 SD, 2 cytotoxic activity	[62]
Neoantigen	KRAS	13-mer ras peptide with Detox adjuvant		7	4 remained with no evidence of disease	[64]
Neoantigen	KRAS	13-mer ras peptide with Il-2 or GM-CSF or both		38	4 SD, 34 PD	[66]

CRC: Colorectal cancer; CR: Complete response; CTL: Cytotoxic T lymphocyte; DC: Dendritic cell; GM-CSF: Granulocyte macrophage colony-stimulating factor; HLA: Human leukocyte antigen; MR: Minor response; PD: Progressive disease; PR: Partial response; SD: Stable disease; CEA: Carcinoembryonic antigen; TAA: Tumor-associated antigen.

studies[30,31].

To further improve clinical response, Okuno *et al*[32] tested a seven peptide vaccine containing peptides from RNF43, TOMM34, forkhead box M1, maternal embryonic leucine zipper-kinase, holliday junction recognizing-protein and vascular endothelial growth factor receptor 1 and 2 (VEGFR-1 and VEGFR-2). In 9 out of 30 vaccinated patients, a CTL response to all 7 peptides could be detected including two of the three partial responders of the study. Moreover, there was a correlation between the number of vaccine peptide-specific CTL responses and overall survival[32]. Similar results were observed in a vaccination study with peptides from RNF43, TOMM34, VEGFR-1 and VEGFR-2 as well as insulin-like growth factor-Ⅱ mRNA binding protein 3[33].

PERSONALIZED PEPTIDE VACCINES

To further enhance the efficiency of cancer vaccines, the next wave of trials focused on personalized pep-

tide vaccines. This personalization was achieved by measuring existing peptide-specific CTL precursors in the patients' blood, as well as screening for peptide-specific IgGs, followed by vaccination with CTL-reactive peptides.

In a phase Ⅰ clinical trial, Sato *et al*[34] treated 10 CRC patients with 2-4 matching peptides derived from cytochrom B, intestinal cell kinase, squamous cell carcinoma antigen recognized by T cells (SART)1-3 and ADP-ribosyltransferase 4. Peptide specific CTLs increased in 50 % of patients, peptide specific IgGs in 60 %. In half of the patients an elevated functional CTL activity was observed in cytotoxicity assays. In spite of this enhanced immune response, only two patients could clinically benefit from vaccination and had a partial response (reduction of metastasis' volume) and a stable disease, respectively.

In a subsequent study, the effect of a personalized peptide vaccine in combination with a 5-fluorouracil derivative was investigated[35]. After six vaccinations, six out of seven patients responded to at least one peptide with increased CTL and IgG levels. But only one patient showed stable disease. He responded to peptides derived from SART3, Tyrosine-protein kinase Lck and Wolf-Hirschhorn syndrome protein.

The combination of personalized peptide vaccination and chemotherapy resulting in clinical benefit was also proven in a further study. Hattori et al. vaccinated 14 metastatic CRC patients with up to four personal HLA-matched peptides. This was combined with a 5-fluoruracil based standard chemotherapy[36]. Although neither partial nor complete responses were obtained, three patients showed minor response, defined as a reduction in tumor size. Furthermore, three additional patients had stable disease. The strongest immune responses were induced by peptides derived from SART2/3, multidrug resistance-associated protein 3, Her2/neu, cytochrome B, ubiquitin-conjugating enzyme E2 and CEA.

Besides, it could be proven that the number of peptides with increased CTL responses after vaccination was also significantly predictive of favorable overall survival[37] similar to the correlation found in studies with combinations of TAA vaccines[32].

NEOANTIGENS - TRULY TUMOR-SPECIFIC ANTIGENS

The stepwise acquisition and accumulation of mutations has been generally recognized as major mechanism for cancer initiation and progression. It not only leads to enhanced or reduced expression of genes but also to the expression of sequence-modified proteins - the so-called neoantigens (see Figure 1). Hence, the probability of creating neoantigens is rising simply with the number of mutations present in a given cancer cell[38]. But the mutational burden and therefore the potential of expressing neoantigens varies clearly between different cancer entities. The highest somatic mutation frequency of around 10 mutations per megabase is found in cancers of the skin, lung and colorectum resulting in the expression of approximately 150 nonsynonymous mutations within expressed genes[39].

A hyper-mutational burden is caused by a deficiency in the mismatch repair system. This leads to replication errors especially in regions with repetitive nucleotides which are found in coding microsatellites. A mismatch repair deficient tumor shows microsatellite instability (MSI) with a huge variety of mutations. A similar or even still higher mutational burden can be caused by a mutation in the catalytic subunit of DNA polymerase epsilon (POLE) leading to hypermutation independent of MSI.

Because high neoantigen load of CRC has repeatedly been correlated with improved patient survival[40,41], neoantigens have only recently been accepted as ideal targets for successful immunotherapy. In addition, as neoantigens are truly tumor-specific antigens (TSA) only presented by cancer cells but not by normal cells, the immune system can easily distinguish between malignant and healthy tissue - minimizing the risk of vaccination-induced severe adverse events (SAEs).

TGFBRII and other frameshift mutations

Studies focused on single nucleotide insertions or deletions in coding microsatellites and identified several proteins frequently affected by frameshift mutations in MSI^{high} CRCs. Early a short form of the transforming growth factor beta receptor 2 (TGFβRⅡ) was identified as such a frameshifted and therefore truncated protein with a role in tumor progression.

It could be proven that a 23-mer peptide derived from frameshift mutated TGFβRⅡ is able to induce T cell proliferation predominantly in $CD4^+$ T (helper) cells[42]. This promising result was confirmed by results from a frameshift mutated TGFβRⅡ-derived 9-mer peptide[43]. But in contrast to the former study, the induced T cells were predominantly $CD8^+$ and, more important, these activated T cells were able to lyse TGFβRⅡ-mutated CRC cells in a HLA-restricted fashion.

TGFβRⅡ-mutation-reactive T cells were also able to decrease tumor load in a mouse model and even significantly prolong survival[44] underlining the potential of frameshifted TGFβRⅡ as immunotherapeutic target.

In further studies, it was proven that peptides derived from frameshifted caspase 5, mut-S homologue 3 and O-linked N-acetylglucosamine transferase gene are able to induce CTLs with cytotoxic activity against CRC cells[45-47]. In another approach, an antibody response directed against frameshifted homeobox protein CDX2 was detected in serum of a CRC patient[48].

There are several further candidate genes frequently presenting with frameshift mutations in coding microsatellites: PTHL3, HT001, AC1, ACVR2, SLC23A1, BAX, TCF-4 and MSH3[49]. In addition peptides derived from frameshift-mutated MARCKS-1, MARCKS-2, TAF1B - 1, PCNXL2-2, TCF7L2-2, Baxα+1[50] as well as CREBBP, AIM2, EP300 and TTK[51] have been suggested to be taken into consideration for developing cancer vaccines for MSI^{high} CRCs as auspicious experimental and bio-

informatic data proved their importance.

In a first clinical trial, 22 CRC patients received vaccines containing peptides of frameshifted AIM2, HT001 and TAF1B[52]. No vaccine-related SAEs were observed and the induced immune response was significant: all patients responded to at least one of the peptides.

KRAS: an example of point mutated genes

In the process of cancer development mutations resulting in neoantigens can emerge in every coding region of the DNA. Neoantigens caused by KRAS are one example for point mutations in CRC. KRAS plays a major role in intracellular signaling cascades and is found mutated in more than 40 % of CRCs[53,54]. Most frequent mutations are located at codon 12 (G12D or G12V mutation) or 13 (G13D mutation) of the *KRAS* gene and result in single amino acid substitutions in the expressed protein[55,56]. Early approaches could prove that peptides derived from mutated KRAS can stimulate CTLs *in vitro*[57,58] as well as in pancreatic[59,60] and colorectal cancer[61]. A subsequent study also investigated the cytotoxic activity of mutated KRAS peptide-induced CTLs[62]. Only 2 of 10 CRC patients showed induction of peptide specific $CD8^+$ but in addition, these cytotoxic T cells were able to lyse HLA-A2-positive target cells incubated with the 10-mer mutant peptide. Similar results were obtained in a xenograft study, where peptide-specific T cells were able to delay the growth of KRAS mutant pancreatic tumors[63].

In vaccination trials with peptides derived from mutated KRAS, clinical benefits for patients could be achieved. Although only two of seven CRC patients responded positive to a mutated KRAS peptide vaccination, four remained with no evidence of disease[64]. In a case report, one CRC patient was treated with activated T cells recognizing G12D KRAS[65]. After a single infusion, all seven lung metastases regressed for 9 mo until 1 metastatic lesion progressed.

To further enhance the immunological response in CRC patients, Rahma et al. combined the peptide vaccination of mutated KRAS with IL-2 or GM-CSF[66]. The strongest immune response could be detected in the group with GM-CSF as adjuvant; all CRC patients had an increase in interferon producing, specifically-activated T cells. Despite the high immune response rate, no patient showed clinical response and disease progressed in all cases. An increase in regulatory T cells, detectable in all CRC patients of this group, is a likely explanation for this negative result.

Other neoantigens

Besides point and frameshift mutations there are further possibilities in creating neoantigens. Mutations at somatic splice sites as well as deregulated splicing factors can lead to alternative splice variants. A large-scale systematic investigation revealed that alternative splice variants in CRC are mainly caused by exon skipping, alternative promoter or terminator and intron retention[67]. A comparison between CRC and normal cells demonstrated that there are alternative splice variants exclusively expressed by cancer cells[68,69]. That these altered peptides can be presented by HLA was already proven in a study focusing on melanoma[70]. Therefore, further investigation in this field of alternative splice variants could lead to an extended range of target structures for cancer vaccines.

Ditzel *et al*[71] found a completely different mechanism of neoantigen generation. They proved that the apoptotic markers cytokeratin 8 and 18 are only proteolytically truncated in CRC tissue but not in normal colon epithelia. The cancer-associated forms of cytokeratin 8 and 18 are early apoptosis markers and recognized by a human antibody specific for a heterotypic conformational epitope. However, this and similar epitopes can hardly serve as target structures for T cell-specific immunotherapies.

CHALLENGES FOR DEVELOPING A CRC VACCINE

Genetic configuration and target selection

One important property for the development of a CRC vaccine is the genetic subtype of the patient. Around 15 % of CRCs are MSI^{high} and provide therefore a variety of mutations leading to neoantigens which are, as described above, often derived from frameshift mutations. Another form of hypermutated CRC is caused by POLE mutations - but only 3 % of CRC patients fit into this category. MSI^{high} or POLE mutations are responsible for a high mutational burden which is regularly correlated with increased lymphocyte infiltration into the tumors mirroring higher pre-vaccination antitumoral activity of the patients' immune system. Especially the intratumoral presence of $CD8^+$ $CD45RO^+$ T cells correlates with improved survival[72]. A CRC vaccine could further enhance or re-activate this anticancer activity and result in tumor reduction.

But also CRCs without MSI or POLE mutations show multiple genetic alterations. These immunogenic mutations, TAAs or neoantigens, need to be identified for vaccine development. Modern next-generation sequencing approaches open up the possibility of easy and fast sequencing but challenges in form of tumor heterogeneity are still to be accomplished. The whole mutational profile of a tumor is difficult to be depicted and for individualized vaccine development, it has to be considered that tumor sequencing can reveal only mutations of a subset of cells and at the time point of operation. The mutational profile of residual metastatic cells might differ[73,74].

One promising approach is to focus on driver mutations that are responsible for maintenance of the transformed status and/or the progression of the individual tumor. Aiming at driver mutations is of advantage in comparison to passenger mutations, as the tumor cell's survival is dependent on these dysregulated gene products and therefore, immune escape by switching off or reverting such mutations is less likely to occur.

The concept of personalized peptide vaccination follows another approach. CRC patients are screened for the presence of CTLs and IgGs against known TAAs and neoantigens in addition to the determination of their HLA profile. Having the knowledge of the patients' HLA layout as well as the natural immunogenicity of the tumor, the vaccine can be adapted by choosing matching peptides for vaccination. This lowers the risk of SAEs by only enhancing the existing antitumoral immune response.

VACCINE DESIGN

When a promising target is found, the design of the vaccine starts. As mentioned before, suiting (better ideal) peptides as well as adjuvants and administration schedules need to be selected. Due to space restrictions, we focus here on peptide-based vaccination strategies and omit recombinant protein- and tumor lysate-based ones.

Single peptides, peptide-loaded antigen-presenting cells or ex vivo expanded T cells?

Peptides used for vaccination can vary in length. When they directly bind into the peptide-binding groove of the HLA molecules, 8-10-mers (HLA-A/-B/-C) or 13-18-mers (HLA-DP/-DQ/-DR) are typically used. But the binding affinities of peptides to different HLA isoforms deviate. In addition, as the patient is restricted to its individual set of HLA alleles, the efficiency of a peptide vaccine is dependent on the selection of peptides and their best matching HLA. Furthermore, most of the current studies have only investigated peptides restricted to the most common HLA alleles HLA-A2 or HLA-A24, thereby limiting the number of patients benefitting from this therapy.

To circumvent HLA restriction, longer peptides (15-30-mer), so called synthetic long peptides, can be used as these peptides are internalized, processed and presented by antigen presenting cells. The risk of digestion by proteases is also decreased as long peptides form a tertiary structure and have therefore a longer half-life[75,76].

Alternatively, using (autologous) cellular vaccine strategies, completely evades the problem of HLA-restriction and peptide degradation. They can be composed of antigen presenting cells (DCs, B cells or artificial antigen presenting cells[77]) which present the selected peptide(s) to both $CD4^+$ helper as well as $CD8^+$ effector T cells or the direct approach of applying T cells carrying tumor-antigen-specific T cell receptor(s). For the latter approach, patient specific T cells need to be isolated, expanded and stimulated *in vitro*. After this complex *ex vivo* procedure, a defined amount of functional T cells can be given back to the patient. By including also T helper cells or peptides activating T helper cells, a humoral immune response can be induced, too[14].

Adjuvants

To further enhance the strength of a vaccine, formulations typically include also adjuvants. Incomplete Freund's adjuvant, alum, gold or nanoparticles as well as heat shock proteins and GM-CSF are such adjuvants which improve antigen stability, delivery, processing and presentation to T cells[78,79]. This is achieved by forming a depot at the injection site resulting in slow and prolonged peptide release and/or by induction of proliferation and migration of antigen presenting cells. GM-CSF, as well as TNF receptor ligands and TLR agonists like CpG oligonucleotides, additionally aim at enhancing costimulatory signals for T cell activation. Furthermore, cytokines like interferons or interleukins lead to enhanced immune response in different clinical trials[80,81].

ADVERSE EVENTS

Cancer vaccines are characterized by a high safety and low toxicity profile. Different studies evaluated SAEs grade Ⅲ/Ⅳ after cancer vaccine therapy in around 5500 cancer patients and observed a frequency of < 3%[82,83]. But especially by using vaccination approaches with TAAs, the possibility of damaging healthy tissue should not be neglected. As mentioned above, TAAs are not restricted to the tumor tissue but only expressed at higher levels compared to (some) normal cells.

In a study with engineered anti-CEA T cells, the CEA levels decreased and even tumor regression was seen in one patient; but all treated patients experienced severe transient inflammatory colitis[84]. The treatment with autologous anti-MAGE-A3/A9/A12 engineered T cells led in another clinical trial to severe neurological toxicity in 3 out of 9 cancer patients[85]. Recognition of different MAGE-A proteins in normal human brain by engineered T cells caused even treatment related mortality in 2 patients. Similarly, the use of engineered T cells showing off-target effects by recognizing un-targeted proteins is associated with an increased risk of SAEs. Linette et al. used an affinity-enhanced T cell receptor against MAGE-A3 and the first two treated patients developed a cardiogenic shock and died within a few days[86]. Recognition of the striated muscle-specific protein titin by these T cells led to severe cardiogenic damage.

As neoantigens are not presented by healthy cells, the risk of SAEs is decreased by using neoantigen-targeting vaccines. To date, vaccine studies focusing on neoantigens in CRC patients observed no SAEs; only mild side effects that resolved spontaneously have been described (*e.g.,* injections site reactions, fever)[52,62,64,66].

CANCER VACCINES: THE SOLUTION TO IMMUNE EVASION?

The tumor microenvironment is characterized by immunosuppressive signals leading to immune evasion of the tumor. An accumulation of regulatory T cells is responsible for the downregulation of other infiltrating and tumor attacking T cells in an antigen-dependent manner or by secretion of IL-10 or TGF-β[87]. Furthermore, these signal molecules are able to suppress the maturation of

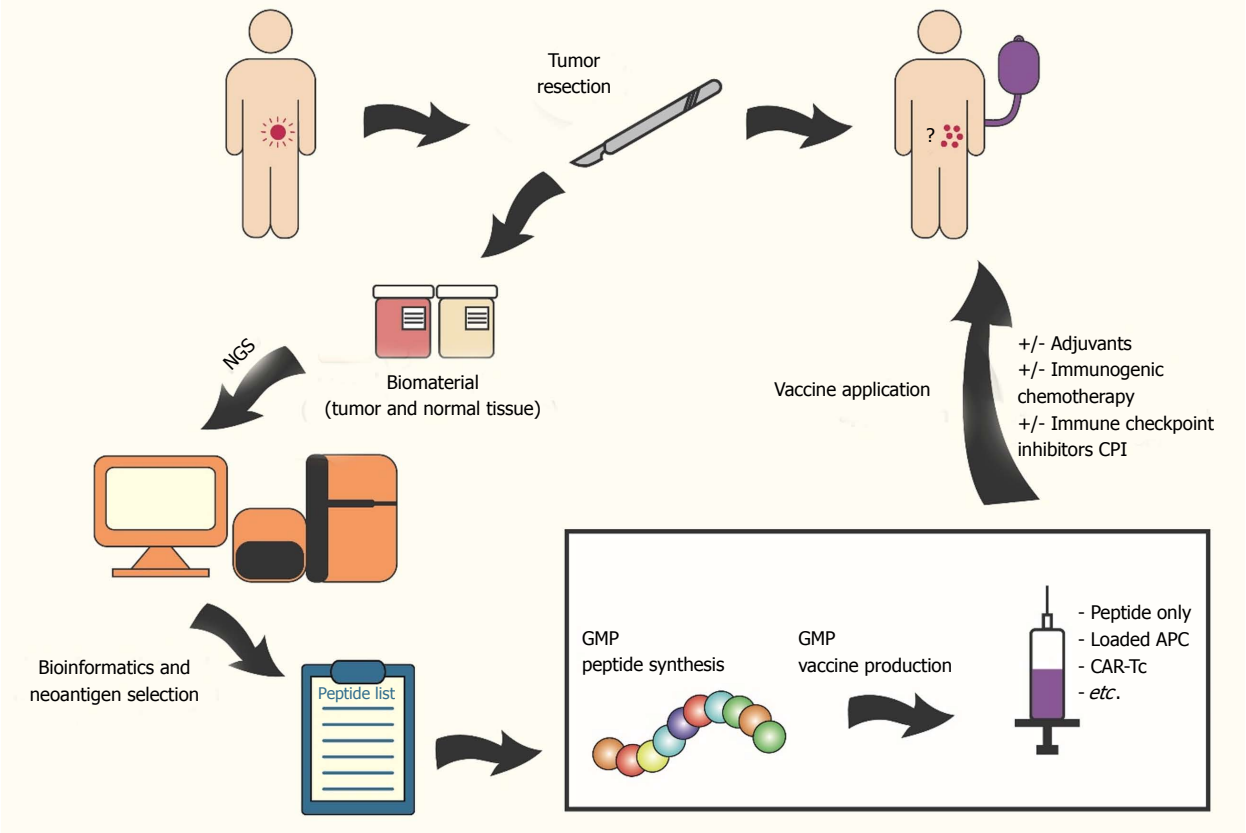

Figure 2 Workflow: preparation of individualized vaccine (using neoantigen targets). The figure shows the possible work flow for individualized cancer vaccination. The colorectal cancer patient (tumor in pink) undergoes tumor resection surgery and biomaterial (tumor (red container) and matching normal (beige container) tissue) is collected. Next generation sequencing and comparative bioinformatics analysis of these biomaterials reveal (tumor-specific) neoantigens and selected peptides are synthesized under GMP conditions. The vaccine consists of synthesized peptides, peptide-loaded antigen-presenting cells, *ex vivo* expanded T cells or chimeric antigen receptor T cells and can be combined with adjuvants, immunogenic chemotherapeutics and/or immune checkpoint inhibitors to further enhance vaccine efficacy. The patient will receive first vaccine shots ideally even before chemotherapeutic intervention. Residual tumor cells (in the colon or circulating as well as micrometastases in other organs) should be eliminated hereby. Exact vaccination scheme will depend on vaccine type, medical facility, *etc*.

DCs resulting in reduced antigen presentation[88]. Tumor-associated macrophages as well as myeloid suppressor cells are also present in the tumor microenvironment and act as immune suppressors[87,89].

But in addition to creating an inhospitable environment for tumor attacking immune cells, tumor cells can also hide from immune cells by modifying their surface to escape recognition. More than 50 % of MSI^{high} CRC patients' tumor harbor mutations that lower the functionality of HLA presentation of antigens[90]: mutations regarding regulation of HLA expression (*e.g.*, NLRC5 mutation[90]), peptide transport (*e.g.*, TAP1/2 and tapasin[90-92]) as well as HLA itself (*e.g.*, heavy chain[90] and B2M mutation[91-93]). To overcome this dissembling mechanism, the use of specific chemotherapeutics can be helpful, leading to an effective antitumor immune response by apoptosis (discussed below).

Furthermore, cancer cells take advantage of the control mechanism of nonsense mediated RNA-decay (NMRD). This system is responsible for degrading mRNA with premature stop codons and it has been suggested that this must inhibit the presentation of neoantigens[94]. However, it could be shown that only a part of the so far identified neoantigens are sensitive to NMRD[51].

Last but not least, cancer cells can not only influence cells of the microenvironment to express immune checkpoint molecules but they frequently express such molecules themselves to downregulate T cell activity. Immune checkpoint inhibitors are a precious device in overcoming this tumor-induced immune suppression.

IMMUNE CHECK POINT INHIBITORS

The field of studies exploring immune checkpoint inhibitors is growing. Targeted immune checkpoints like CTLA-4, PD-1, PD-L1 and LAG-3 are highly expressed in MSI^{high} tumors, thereby creating an immune suppressive microenvironment[95]. Besides, T cells infiltrating in MSI^{high} tumors frequently express PD-L1 making a PD-1 blocking antibody (*e.g.*, Pembrolizumab) a helpful instrument[96]: In clinical trials, almost 80 % of MSI high CRC patients benefitted from PD-1 blockade whereas microsatellite stable (MSS) CRC patients rarely did[96,97]. This can be explained by the difference in mutational burden of MSI^{high} and MSS patients, as a correlation of mutational burden/number of neoantigens and clinical response could be proven already[98,99]. Moreover, this clinical observation suggests that a substantial part of

Table 2 Current clinical vaccination studies including colorectal cancer patients

Target type	Target molecule	Vaccination strategy	Therapy	Number of patients	Trial identifier
TAA	CEA	alphavirus replicon (VRP) encoding CEA		12	NCT01890213
TAA	CEA	ETBX-011 ad-CEA, ALT-803 (IL-15)		3	NCT03127098
TAA	CEA	anti-CEA CAR-T cells		18	NCT03682744
TAA	CEA	anti-CEA CAR-T cells		5	NCT02850536
TAA	CEA	anti-CEA CAR-T cells, SIR-Sphere		8	NCT02416466
TAA	Her2	2 Her2 peptides in Montanide ISA 720		36	NCT01376505
TAA	Her2/neu	B-Cell and monocytes with HER2/neu antigen		9	NCT03425773
TAA	Brachyury, CEA, MUC1	ETBX-051; adenoviral brachyury vaccine, ETBX-061; adenoviral MUC1 vaccine, ETBX-011; adenoviral CEA vaccine		32	NCT03384316
TAA	7 cancer testis antigens	6 synthetic peptides in Montanide	Standard-of care maintenance	15	NCT03391232
Immune stimulation, TAA	MUC1	activated CIK and CD3-MUC1 bispecific antibody	cryotherapy	90	NCT03524274
TAA	HPV	DPX-E7		44	NCT02865135
TAA	hTERT	INO-1400 or INO-1401 alone or in combination with INO-9012		93	NCT02960594
TAA	MUC1	anti-MUC1 CAR-pNK cells		10	NCT02839954
TAA	MUC1	MUC1 peptide-poly-ICLC		110	NCT02134925
TAA	EpCAM	CAR T Cells targeting EpCAM		60	NCT03013712
Immune checkpoint, TAA	PD-1, p53	Pembrolizumab, modified vaccinia virus Ankara vaccine expressing p53		19	NCT02432963
Neoantigen		frameshift-derived neoantigen-loaded DC		25	NCT01885702
Neoantigen		personalized neoepitope yeast-based vaccine, YE-NEO-001		16	NCT03552718
Neoantigen		mRNA-based vaccine targeting neoantigens		64	NCT03480152
Neoantigen		ADXS-NEO (Advaxis NEO expressing personalized tumor antigens)		48	NCT03265080
Neoantigen	ras	anti-KRAS G12 V mTCR	Cyclophosphamide, Fludarabine, Aldesleukin	110	NCT03190941
Immune checkpoint	PD-L1	Avelumab, autologous dendritic cells		33	NCT03152565
Immune checkpoint	PD-1	Pembrolizumab, GVAX (allogeneic colon cancer GM-CSF secreting cells)	Cyclophosphamide	17	NCT02981524
Immune checkpoint	PD-L1	Atezolizumab, Imprime PGG (PAMP recognized by innate immune effector cells)	Regorafenib/ Isatuximab/ Bevacizumab	120	NCT03555149
Immune checkpoint	A2aR, A2bR	AB928 (A2aR and A2bR antagonist)	FOLFOX	98	NCT03720678
Immune checkpoint, TAA	PD-1, CEA, MUC-1	Nivolumab, MVA-BN-CV301 (modified vaccinia Ankara-Bavarian Nordic encoding CEA, MUC1, B7-1, ICAM-1 and LFA-3)	FOLFOX	78	NCT03547999
Immune checkpoint, TAA	PD-L1	Atezolizumab, RO7198457 (mRNA-based individualized, TAAs vaccine)		567	NCT03289962
Immune checkpoint, TAA	PD-L1, CEA	Avelumab + Ad-CEA	FOLFOX, Bevacizumab, Capecitabine	81	NCT03050814
Immune checkpoint, TAA, Immune stimulation	CEA, Her2/neu, Brachyury, MUC1, RAS, NK cells ICI	Aldoxorubicin, ETBX-011, ETBX-021, ETBX-051, ETBX-061, GI-4000, GI-6207, GI-6301, haNK, avelumab, HCI, ALT-803	Capecitabine, Cetuximab, Cyclophosphamide, Fluorouracil, Leucovorin, Nab-paclitaxel, Oxaliplatin, Regorafenib, SBRT, Trastuzumab	332	NCT03563157
Immune checkpoint, Mutated proteins	PD-1	Personalized peptides, Pembrolizumab		60	NCT02600949
Immune stimulation		GVAX (allogeneic colon cancer GM-CSF secreting cells)	Cyclophosphamide, SGI-110 (DNA Methyltransferase Inhibitor)	18	NCT01966289
Immune stimulation		GVAX (allogeneic colon cancer GM-CSF secreting cells)		15	NCT01952730

Immune stimulation		OncoVAX (non-dividing tumor cells)	Surgery	550	NCT02448173
Immune stimulation		Autologous or allogeneic immune stimulatory tumor cells		50	NCT00722228
Immune stimulation		autologous dendritic cells loaded with autologous tumour homogenate + IL-2		19	NCT02919644
Immune stimulation		autologous dendritic cells loaded with tumor antigens		58	NCT01348256
Immune stimulation		autologous dendritic cells loaded with tumor lysate antigens		30	NCT03214939
Oncolytic virus		GL-ONC1 oncolytic vaccinia virus, which disrupts nonessential genes and expression of the foreign gene expression		36	NCT02714374
Oncolytic virus, Immune checkpoint	PD-L1	Talimogene Laherparepvec, Atezolizumab		36	NCT03256344

CEA: Carcinoembryonic antigen; GM-CSF: Granulocyte macrophage colony-stimulating factor; TAA: Tumor-associated antigen.

these antitumoral immune responses must be HLA-unrestricted, since more than the expected 50% of MSI^{high} patients with functional HLA-presentation responded well. The interplay of adaptive (antitumoral) immune cells with cells of the innate arm of the immune system might partly explain this somewhat surprising finding. Consequently, this would also imply that modern neoantigen-specific vaccines (Figure 2) have a good chance to be beneficial for patients with hypermutated tumors despite the fact that HLA-presentation is corrupted due to immune escape phenomena.

Studies comparing infiltrating lymphocytes in MSS and MSI^{high} CRC patients revealed, that the amount of infiltrating cells is clearly higher in MSI^{high} tumors, but the correlation between infiltrating lymphocytes and overall survival is only in MSS patients significant[100,101]. Therefore, a combined immunotherapy with blocking immune checkpoints on the one hand and stimulating the immune system with a peptide vaccine on the other hand could help MSS as well as MSI^{high} CRC patients. A first animal study demonstrated increased cytolysis rate, tumor suppression and survival with a DNA vaccine consisting of PD-1 fused with survivin and MUC-1 peptides[102]. Clinical trials investigating the effect of immune checkpoint inhibitors with other forms of immunotherapy in CRC patients are still ongoing (Table 2).

CANCER VACCINES AND IMMUNOGENIC CELL DEATH

The dogma that chemotherapy is immunosuppressive has been disproved. Contrarily, it could be shown that selected chemotherapeutics are able to induce a special kind of cell death which improves tumor immune recognition. This so called immunogenic cell death is characterized by damage-associated molecular patterns on the surface of the tumor cell (calreticulin and heat shock proteins) which are "eat me" signals for immune cells and act as co-stimulators[103]. Inducers of immunogenic cell death are anthracyclines like doxorubicin[104], DNA alkylating cyclophosphamide[105] as well as the common platinum derivative for CRC treatment, oxaliplatin[106]. The studies combining TAAs with different chemotherapeutic agents also observed no immune suppressive effects but induction of specific immune responses[29,35,36]. Therefore, the combination of immunogenic cell death inducing chemotherapeutics and cancer-specific vaccination is an auspicious approach for future treatment of CRC patients (Figure 2).

Immunogenic cell death can also be induced by oncolytic viruses which preferentially infect cancer cells. *In vitro* studies revealed that viral treatment can lead to killing of CRC cells, especially tumor initiating cells or cancer stem cells[107,108]. First clinical studies with a combination of oncolytic viruses and immune checkpoint inhibitors in melanoma patients showed response rates up to 62 %[109-111]. These promising combinations are currently investigated in clinical trials also including CRC patients (Table 2).

CONCLUSION

Cancer vaccines are a promising instrument for treatment of cancers. The development started with peptides derived from TAAs. These targets can be detected easily and are shared by many patients. Therefore, a variety of studies investigated the effect of TAA-derived peptide vaccines with mediocre results. Low immunogenicity, HLA restriction as well as increased risk of SAEs limit the efficiency and clinical usefulness of this vaccine type.

These problems can likely be solved with novel vaccination approaches focusing on TSAs, mainly neoantigens. They clearly differ from proteins of healthy cells and thus neither self-tolerance nor SAEs are likely to limit clinical application of TSA-based vaccines (see Figure 1). First *in vitro* and *in vivo* studies revealed promising results. It can be envisioned that these advantages will on the longer run compensate for the time and money intense identification of patient-individual neoantigens and peptide composition. Pure peptide vaccines, peptide-loaded antigen presenting cells or adoptively transferred T cells will be exploited.

To further enhance the effect of neoantigen vaccines, adjuvants will be included. These improve peptide stability and also act as immune stimulators. Besides, the combination of these new generation individual cancer vaccines with immune checkpoint inhibitors and/or immunogenic cell death-inducing chemotherapeutic agents is an utterly promising concept that will be extensively investigated in the near future. Such multifactorial approaches even have the potential to solve the difficulties in targeting MSS CRC. However, concepts to select the best-suited combinations of vaccines, adjuvants and chemotherapeutic on a patient-individual basis still have to be developed and - possibly even more ambitious - adapted to the clinical routine.

ACKNOWLEDGMENTS

The authors would like to thank Jenny Burmeister for her excellent help with the figure designs.

REFERENCES

1 **Gold P**, Freedman SO. Demonstration of tumor-specific antigens in human colonic carcinomata by immunological tolerance and absorption techniques. *J Exp Med* 1965; **121**: 439-462 [PMID: 14270243]

2 **Nair SK**, Hull S, Coleman D, Gilboa E, Lyerly HK, Morse MA. Induction of carcinoembryonic antigen (CEA)-specific cytotoxic T-lymphocyte responses in vitro using autologous dendritic cells loaded with CEA peptide or CEA RNA in patients with metastatic malignancies expressing CEA. *Int J Cancer* 1999; **82**: 121-124 [PMID: 10360830]

3 **Alves PM**, Viatte S, Fagerberg T, Michielin O, Bricard G, Bouzourene H, Vuilleumier H, Kruger T, Givel JC, Lévy F, Speiser DE, Cerottini JC, Romero P. Immunogenicity of the carcinoembryonic antigen derived peptide 694 in HLA-A2 healthy donors and colorectal carcinoma patients. *Cancer Immunol Immunother* 2007; **56**: 1795-1805 [PMID: 17447064 DOI: 10.1007/s00262-007-0323-2]

4 **Zaremba S**, Barzaga E, Zhu M, Soares N, Tsang KY, Schlom J. Identification of an enhancer agonist cytotoxic T lymphocyte peptide from human carcinoembryonic antigen. *Cancer Res* 1997; **57**: 4570-4577 [PMID: 9377571]

5 **Park JS**, Kim HS, Park HM, Kim CH, Kim TG. Efficient induction of anti-tumor immunity by a TAT-CEA fusion protein vaccine with poly(I:C) in a murine colorectal tumor model. *Vaccine* 2011; **29**: 8642-8648 [PMID: 21945963 DOI: 10.1016/j.vaccine.2011.09.052]

6 **Salucci V**, Mennuni C, Calvaruso F, Cerino R, Neuner P, Ciliberto G, La Monica N, Scarselli E. CD8+ T-cell tolerance can be broken by an adenoviral vaccine while CD4+ T-cell tolerance is broken by additional co-administration of a Toll-like receptor ligand. *Scand J Immunol* 2006; **63**: 35-41 [PMID: 16398699 DOI: 10.1111/j.1365-3083.2006.01706.x]

7 **Fong L**, Hou Y, Rivas A, Benike C, Yuen A, Fisher GA, Davis MM, Engleman EG. Altered peptide ligand vaccination with Flt3 ligand expanded dendritic cells for tumor immunotherapy. *Proc Natl Acad Sci USA* 2001; **98**: 8809-8814 [PMID: 11427731 DOI: 10.1073/pnas.141226398]

8 **Lesterhuis WJ**, de Vries IJ, Schuurhuis DH, Boullart AC, Jacobs JF, de Boer AJ, Scharenborg NM, Brouwer HM, van de Rakt MW, Figdor CG, Ruers TJ, Adema GJ, Punt CJ. Vaccination of colorectal cancer patients with CEA-loaded dendritic cells: antigen-specific T cell responses in DTH skin tests. *Ann Oncol* 2006; **17**: 974-980 [PMID: 16600979 DOI: 10.1093/annonc/mdl072]

9 **Liu KJ**, Wang CC, Chen LT, Cheng AL, Lin DT, Wu YC, Yu WL, Hung YM, Yang HY, Juang SH, Whang-Peng J. Generation of carcinoembryonic antigen (CEA)-specific T-cell responses in HLA-A*0201 and HLA-A*2402 late-stage colorectal cancer patients after vaccination with dendritic cells loaded with CEA peptides. *Clin Cancer Res* 2004; **10**: 2645-2651 [PMID: 15102666 DOI: 10.1158/1078-0432.CCR-03-0430]

10 **Okuno K**, Sugiura F, Itoh K, Yoshida K, Tsunoda T, Nakamura Y. Recent advances in active specific cancer vaccine treatment for colorectal cancer. *Curr Pharm Biotechnol* 2012; **13**: 1439-1445 [PMID: 22339221 DOI: 10.2174/138920112800784998]

11 **Kerkar SP**, Wang ZF, Lasota J, Park T, Patel K, Groh E, Rosenberg SA, Miettinen MM. MAGE-A is More Highly Expressed Than NY-ESO-1 in a Systematic Immunohistochemical Analysis of 3668 Cases. *J Immunother* 2016; **39**: 181-187 [PMID: 27070449 DOI: 10.1097/CJI.0000000000000119]

12 **Choi J**, Chang H. The expression of MAGE and SSX, and correlation of COX2, VEGF, and survivin in colorectal cancer. *Anticancer Res* 2012; **32**: 559-564 [PMID: 22287745]

13 **Shantha Kumara HM**, Grieco MJ, Caballero OL, Su T, Ahmed A, Ritter E, Gnjatic S, Cekic V, Old LJ, Simpson AJ, Cordon-Cardo C, Whelan RL. MAGE-A3 is highly expressed in a subset of colorectal cancer patients. *Cancer Immun* 2012; **12**: 16 [PMID: 23390371]

14 **Takahashi N**, Ohkuri T, Homma S, Ohtake J, Wakita D, Togashi Y, Kitamura H, Todo S, Nishimura T. First clinical trial of cancer vaccine therapy with artificially synthesized helper/killer-hybrid epitope long peptide of MAGE-A4 cancer antigen. *Cancer Sci* 2012; **103**: 150-153 [PMID: 22221328 DOI: 10.1111/j.1349-7006.2011.02106.x]

15 **Kavanagh B**, Ko A, Venook A, Margolin K, Zeh H, Lotze M, Schillinger B, Liu W, Lu Y, Mitsky P, Schilling M, Bercovici N, Loudovaris M, Guillermo R, Lee SM, Bender J, Mills B, Fong L. Vaccination of metastatic colorectal cancer patients with matured dendritic cells loaded with multiple major histocompatibility complex class I peptides. *J Immunother* 2007; **30**: 762-772 [PMID: 17893568 DOI: 10.1097/CJI.0b013e318133451c]

16 **Mukherjee P**, Pathangey LB, Bradley JB, Tinder TL, Basu GD, Akporiaye ET, Gendler SJ. MUC1-specific immune therapy generates a strong anti-tumor response in a MUC1-tolerant colon cancer model. *Vaccine* 2007; **25**: 1607-1618 [PMID: 17166639 DOI: 10.1016/j.vaccine.2006.11.007]

17 **Karanikas V**, Thynne G, Mitchell P, Ong CS, Gunawardana D, Blum R, Pearson J, Lodding J, Pietersz G, Broadbent R, Tait B, McKenzie IF. Mannan mucin-1 peptide immunization: influence of cyclophosphamide and the route of injection. *J Immunother* 2001; **24**: 172-183 [PMID: 11265775]

18 **Kimura T**, McKolanis JR, Dzubinski LA, Islam K, Potter DM, Salazar AM, Schoen RE, Finn OJ. MUC1 vaccine for individuals with advanced adenoma of the colon: a cancer immunoprevention feasibility study. *Cancer Prev Res* (Phila) 2013; **6**: 18-26 [PMID: 23248097 DOI: 10.1158/1940-6207.CAPR-12-0275]

19 **Zheng L**, Edil BH, Soares KC, El-Shami K, Uram JN, Judkins C, Zhang Z, Onners B, Laheru D, Pardoll D, Jaffee EM, Schulick RD. A safety and feasibility study of an allogeneic colon cancer cell vaccine administered with a granulocyte-macrophage colony stimulating factor-producing bystander cell line in patients with metastatic colorectal cancer. *Ann Surg Oncol* 2014; **21**: 3931-3937 [PMID: 24943235 DOI: 10.1245/s10434-014-3844-x]

20 **Idenoue S**, Hirohashi Y, Torigoe T, Sato Y, Tamura Y, Hariu H, Yamamoto M, Kurotaki T, Tsuruma T, Asanuma H, Kanaseki T, Ikeda H, Kashiwagi K, Okazaki M, Sasaki K, Sato T, Ohmura T, Hata F, Yamaguchi K, Hirata K, Sato N. A potent immunogenic general cancer vaccine that targets survivin, an inhibitor of apoptosis proteins. *Clin Cancer Res* 2005; **11**: 1474-1482 [PMID: 15746049 DOI: 10.1158/1078-0432.CCR-03-0817]

21 **Tsuruma T**, Hata F, Torigoe T, Furuhata T, Idenoue S, Kurotaki T, Yamamoto M, Yagihashi A, Ohmura T, Yamaguchi K, Katsuramaki T, Yasoshima T, Sasaki K, Mizushima Y, Minamida H, Kimura H, Akiyama M, Hirohashi Y, Asanuma H, Tamura Y, Shimozawa K, Sato N, Hirata K. Phase I clinical study of anti-apoptosis protein, survivin-derived peptide vaccine therapy for patients with advanced or recurrent colorectal cancer. *J Transl Med* 2004; **2**: 19 [PMID: 15193151 DOI: 10.1186/1479-5876-2-19]

22 **Shimodaira S**, Sano K, Hirabayashi K, Koya T, Higuchi Y, Mizuno Y, Yamaoka N, Yuzawa M, Kobayashi T, Ito K, Koizumi T. Dendritic Cell-Based Adjuvant Vaccination Targeting Wilms' Tumor 1 in

Patients with Advanced Colorectal Cancer. *Vaccines (Basel)* 2015; **3**: 1004-1018 [PMID: 26690485 DOI: 10.3390/vaccines3041004]
23 **Kwon S**, Kim YE, Park JA, Kim DS, Kwon HJ, Lee Y. Therapeutic effect of a TM4SF5-specific peptide vaccine against colon cancer in a mouse model. *BMB Rep* 2014; **47**: 215-220 [PMID: 24286311 DOI: 10.5483/BMBRep.2014.47.4.157]
24 **Kawamoto M**, Tanaka F, Mimori K, Inoue H, Kamohara Y, Mori M. Identification of HLA-A*0201/-A*2402-restricted CTL epitope-peptides derived from a novel cancer/testis antigen, MCAK, and induction of a specific antitumor immune response. *Oncol Rep* 2011; **25**: 469-476 [PMID: 21165574 DOI: 10.3892/or.2010.1101]
25 **Foy KC**, Wygle RM, Miller MJ, Overholser JP, Bekaii-Saab T, Kaumaya PT. Peptide vaccines and peptidomimetics of EGFR (HER-1) ligand binding domain inhibit cancer cell growth in vitro and in vivo. *J Immunol* 2013; **191**: 217-227 [PMID: 23698748 DOI: 10.4049/jimmunol.1300231]
26 **Jungbluth AA**, Chen YT, Stockert E, Busam KJ, Kolb D, Iversen K, Coplan K, Williamson B, Altorki N, Old LJ. Immunohistochemical analysis of NY-ESO-1 antigen expression in normal and malignant human tissues. *Int J Cancer* 2001; **92**: 856-860 [PMID: 11351307 DOI: 10.1002/ijc.1282]
27 **Stockert E**, Jäger E, Chen YT, Scanlan MJ, Gout I, Karbach J, Arand M, Knuth A, Old LJ. A survey of the humoral immune response of cancer patients to a panel of human tumor antigens. *J Exp Med* 1998; **187**: 1349-1354 [PMID: 9547346]
28 **Uchida N**, Tsunoda T, Wada S, Furukawa Y, Nakamura Y, Tahara H. Ring finger protein 43 as a new target for cancer immunotherapy. *Clin Cancer Res* 2004; **10**: 8577-8586 [PMID: 15623641 DOI: 10.1158/1078-0432.CCR-04-0104]
29 **Okuno K**, Sugiura F, Hida JI, Tokoro T, Ishimaru E, Sukegawa Y, Ueda K. Phase I clinical trial of a novel peptide vaccine in combination with UFT/LV for metastatic colorectal cancer. *Exp Ther Med* 2011; **2**: 73-79 [PMID: 22977472 DOI: 10.3892/etm.2010.182]
30 **Kawamura J**, Sugiura F, Sukegawa Y, Yoshioka Y, Hida JI, Hazama S, Okuno K. Multicenter, phase Ⅱ clinical trial of peptide vaccination with oral chemotherapy following curative resection for stage III colorectal cancer. *Oncol Lett* 2018; **15**: 4241-4247 [PMID: 29541190 DOI: 10.3892/ol.2018.7905]
31 **Taniguchi H**, Iwasa S, Yamazaki K, Yoshino T, Kiryu C, Naka Y, Liew EL, Sakata Y. Phase 1 study of OCV-C02, a peptide vaccine consisting of two peptide epitopes for refractory metastatic colorectal cancer. *Cancer Sci* 2017; **108**: 1013-1021 [PMID: 28266765 DOI: 10.1111/cas.13227]
32 **Okuno K**, Sugiura F, Inoue K, Sukegawa Y. Clinical trial of a 7-peptide cocktail vaccine with oral chemotherapy for patients with metastatic colorectal cancer. *Anticancer Res* 2014; **34**: 3045-3052 [PMID: 24922671]
33 **Hazama S**, Nakamura Y, Takenouchi H, Suzuki N, Tsunedomi R, Inoue Y, Tokuhisa Y, Iizuka N, Yoshino S, Takeda K, Shinozaki H, Kamiya A, Furukawa H, Oka M. A phase I study of combination vaccine treatment of five therapeutic epitope-peptides for metastatic colorectal cancer; safety, immunological response, and clinical outcome. *J Transl Med* 2014; **12**: 63 [PMID: 24612787 DOI: 10.1186/1479-5876-12-63]
34 **Sato Y**, Maeda Y, Shomura H, Sasatomi T, Takahashi M, Une Y, Kondo M, Shinohara T, Hida N, Katagiri K, Sato K, Sato M, Yamada A, Yamana H, Harada M, Itoh K, Todo S. A phase I trial of cytotoxic T-lymphocyte precursor-oriented peptide vaccines for colorectal carcinoma patients. *Br J Cancer* 2004; **90**: 1334-1342 [PMID: 15054451 DOI: 10.1038/sj.bjc.6601711]
35 **Sato Y**, Fujiwara T, Mine T, Shomura H, Homma S, Maeda Y, Tokunaga N, Ikeda Y, Ishihara Y, Yamada A, Tanaka N, Itoh K, Harada M, Todo S. Immunological evaluation of personalized peptide vaccination in combination with a 5-fluorouracil derivative (TS-1) for advanced gastric or colorectal carcinoma patients. *Cancer Sci* 2007; **98**: 1113-1119 [PMID: 17459063 DOI: 10.1111/j.1349-7006.2007.00498.x]
36 **Hattori T**, Mine T, Komatsu N, Yamada A, Itoh K, Shiozaki H, Okuno K. Immunological evaluation of personalized peptide vaccination in combination with UFT and UZEL for metastatic colorectal carcinoma patients. *Cancer Immunol Immunother* 2009; **58**: 1843-1852 [PMID: 19396597 DOI: 10.1007/s00262-009-0695-6]
37 **Kibe S**, Yutani S, Motoyama S, Nomura T, Tanaka N, Kawahara A, Yamaguchi T, Matsueda S, Komatsu N, Miura M, Hinai Y, Hattori S, Yamada A, Kage M, Itoh K, Akagi Y, Sasada T. Phase Ⅱ study of personalized peptide vaccination for previously treated advanced colorectal cancer. *Cancer Immunol Res* 2014; **2**: 1154-1162 [PMID: 25351849 DOI: 10.1158/2326-6066.CIR-14-0035]
38 **Rooney MS**, Shukla SA, Wu CJ, Getz G, Hacohen N. Molecular and genetic properties of tumors associated with local immune cytolytic activity. *Cell* 2015; **160**: 48-61 [PMID: 25594174 DOI: 10.1016/j.cell.2014.12.033]
39 **Schumacher TN**, Schreiber RD. Neoantigens in cancer immunotherapy. *Science* 2015; **348**: 69-74 [PMID: 25838375 DOI: 10.1126/science.aaa4971]
40 **Brown SD**, Warren RL, Gibb EA, Martin SD, Spinelli JJ, Nelson BH, Holt RA. Neo-antigens predicted by tumor genome meta-analysis correlate with increased patient survival. *Genome Res* 2014; **24**: 743-750 [PMID: 24782321 DOI: 10.1101/gr.165985.113]
41 **Giannakis M**, Mu XJ, Shukla SA, Qian ZR, Cohen O, Nishihara R, Bahl S, Cao Y, Amin-Mansour A, Yamauchi M, Sukawa Y, Stewart C, Rosenberg M, Mima K, Inamura K, Nosho K, Nowak JA, Lawrence MS, Giovannucci EL, Chan AT, Ng K, Meyerhardt JA, Van Allen EM, Getz G, Gabriel SB, Lander ES, Wu CJ, Fuchs CS, Ogino S, Garraway LA. Genomic Correlates of Immune-Cell Infiltrates in Colorectal Carcinoma. *Cell Rep* 2016; **15**: 857-865 [PMID: 27149842 DOI: 10.1016/j.celrep.2016.03.075]
42 **Saeterdal I**, Bjørheim J, Lislerud K, Gjertsen MK, Bukholm IK, Olsen OC, Nesland JM, Eriksen JA, Møller M, Lindblom A, Gaudernack G. Frameshift-mutation-derived peptides as tumor-specific antigens in inherited and spontaneous colorectal cancer. *Proc Natl Acad Sci USA* 2001; **98**: 13255-13260 [PMID: 11687624 DOI: 10.1073/pnas.231326898]
43 **Linnebacher M**, Gebert J, Rudy W, Woerner S, Yuan YP, Bork P, von Knebel Doeberitz M. Frameshift peptide-derived T-cell epitopes: a source of novel tumor-specific antigens. *Int J Cancer* 2001; **93**: 6-11 [PMID: 11391614 DOI: 10.1002/ijc.1298]
44 **Inderberg EM**, Wälchli S, Myhre MR, Trachsel S, Almåsbak H, Kvalheim G, Gaudernack G. T cell therapy targeting a public neoantigen in microsatellite instable colon cancer reduces *in vivo* tumor growth. *Oncoimmunology* 2017; **6**: e1302631 [PMID: 28507809 DOI: 10.1080/2162402X.2017.1302631]
45 **Garbe Y**, Maletzki C, Linnebacher M. An MSI tumor specific frameshift mutation in a coding microsatellite of MSH3 encodes for HLA-A0201-restricted CD8+ cytotoxic T cell epitopes. *PLoS One* 2011; **6**: e26517 [PMID: 22110587 DOI: 10.1371/journal.pone.0026517]
46 **Ripberger E**, Linnebacher M, Schwitalle Y, Gebert J, von Knebel Doeberitz M. Identification of an HLA-A0201-restricted CTL epitope generated by a tumor-specific frameshift mutation in a coding microsatellite of the OGT gene. *J Clin Immunol* 2003; **23**: 415-423 [PMID: 14601650]
47 **Schwitalle Y**, Linnebacher M, Ripberger E, Gebert J, von Knebel Doeberitz M. Immunogenic peptides generated by frameshift mutations in DNA mismatch repair-deficient cancer cells. *Cancer Immun* 2004; **4**: 14 [PMID: 15563124]
48 **Ishikawa T**, Fujita T, Suzuki Y, Okabe S, Yuasa Y, Iwai T, Kawakami Y. Tumor-specific immunological recognition of frameshift-mutated peptides in colon cancer with microsatellite instability. *Cancer Res* 2003; **63**: 5564-5572 [PMID: 14500396]
49 **Woerner SM**, Benner A, Sutter C, Schiller M, Yuan YP, Keller G, Bork P, Doeberitz Mv, Gebert JF. Pathogenesis of DNA repair-deficient cancers: a statistical meta-analysis of putative Real Common Target genes. *Oncogene* 2003; **22**: 2226-2235 [PMID: 12700659 DOI: 10.1038/sj.onc.1206421]
50 **Speetjens FM**, Lauwen MM, Franken KL, Janssen-van Rhijn CM, van Duikeren S, Bres SA, van de Velde CJ, Melief CJ, Kuppen PJ, van der Burg SH, Morreau H, Offringa R. Prediction of the immunogenic potential of frameshift-mutated antigens in microsatellite instable cancer. *Int J Cancer* 2008; **123**: 838-845 [PMID: 18506693 DOI:

10.1002/ijc.23570]
51 **Williams DS**, Bird MJ, Jorissen RN, Yu YL, Walker F, Zhang HH, Nice EC, Burgess AW. Nonsense mediated decay resistant mutations are a source of expressed mutant proteins in colon cancer cell lines with microsatellite instability. *PLoS One* 2010; **5**: e16012 [PMID: 21209843 DOI: 10.1371/journal.pone.0016012]
52 **Kloor M**, Reuschenbach M, Karbach J, Rafiyan M, Al-Batran S-E, Pauligk C, Jaeger E, Knebel Doeberitz M von. Vaccination of MSI-H colorectal cancer patients with frameshift peptide antigens: A phase I/IIa clinical trial. *J Clin Oncol* 2015; **33**: 3020
53 **Karapetis CS**, Khambata-Ford S, Jonker DJ, O'Callaghan CJ, Tu D, Tebbutt NC, Simes RJ, Chalchal H, Shapiro JD, Robitaille S, Price TJ, Shepherd L, Au HJ, Langer C, Moore MJ, Zalcberg JR. K-ras mutations and benefit from cetuximab in advanced colorectal cancer. *N Engl J Med* 2008; **359**: 1757-1765 [PMID: 18946061 DOI: 10.1056/NEJMoa0804385]
54 **Vaughn CP**, Zobell SD, Furtado LV, Baker CL, Samowitz WS. Frequency of KRAS, BRAF, and NRAS mutations in colorectal cancer. *Genes Chromosomes Cancer* 2011; **50**: 307-312 [PMID: 21305640 DOI: 10.1002/gcc.20854]
55 **Andreyev HJ**, Norman AR, Cunningham D, Oates JR, Clarke PA. Kirsten ras mutations in patients with colorectal cancer: the multicenter "RASCAL" study. *J Natl Cancer Inst* 1998; **90**: 675-684 [PMID: 9586664]
56 **Bos JL**, Fearon ER, Hamilton SR, Verlaan-de Vries M, van Boom JH, van der Eb AJ, Vogelstein B. Prevalence of ras gene mutations in human colorectal cancers. *Nature* 1987; **327**: 293-297 [PMID: 3587348 DOI: 10.1038/327293a0]
57 **Gedde-Dahl T 3rd**, Fossum B, Eriksen JA, Thorsby E, Gaudernack G. T cell clones specific for p21 ras-derived peptides: characterization of their fine specificity and HLA restriction. *Eur J Immunol* 1993; **23**: 754-760 [PMID: 8449222 DOI: 10.1002/eji.1830230328]
58 **Peace DJ**, Chen W, Nelson H, Cheever MA. T cell recognition of transforming proteins encoded by mutated ras proto-oncogenes. *J Immunol* 1991; **146**: 2059-2065 [PMID: 2005390]
59 **Gjertsen MK**, Bakka A, Breivik J, Saeterdal I, Gedde-Dahl T 3rd, Stokke KT, Sølheim BG, Egge TS, Søreide O, Thorsby E, Gaudernack G. Ex vivo ras peptide vaccination in patients with advanced pancreatic cancer: results of a phase I/Ⅱ study. *Int J Cancer* 1996; **65**: 450-453 [PMID: 8621226 DOI: 10.1002/(SICI)1097-0215(19960208)65:4<450::AID-IJC10>3.0.CO;2-E]
60 **Gjertsen MK**, Bakka A, Breivik J, Saeterdal I, Solheim BG, Søreide O, Thorsby E, Gaudernack G. Vaccination with mutant ras peptides and induction of T-cell responsiveness in pancreatic carcinoma patients carrying the corresponding RAS mutation. *Lancet* 1995; **346**: 1399-1400 [PMID: 7475823 DOI: 10.1016/S0140-6736(95)92408-6]
61 **Shono Y**, Tanimura H, Iwahashi M, Tsunoda T, Tani M, Tanaka H, Matsuda K, Yamaue H. Specific T-cell immunity against Ki-ras peptides in patients with pancreatic and colorectal cancers. *Br J Cancer* 2003; **88**: 530-536 [PMID: 12592366 DOI: 10.1038/sj.bjc.6600697]
62 **Khleif SN**, Abrams SI, Hamilton JM, Bergmann-Leitner E, Chen A, Bastian A, Bernstein S, Chung Y, Allegra CJ, Schlom J. A phase I vaccine trial with peptides reflecting ras oncogene mutations of solid tumors. *J Immunother* 1999; **22**: 155-165 [PMID: 10093040]
63 **Wang QJ**, Yu Z, Griffith K, Hanada K, Restifo NP, Yang JC. Identification of T-cell Receptors Targeting KRAS-Mutated Human Tumors. *Cancer Immunol Res* 2016; **4**: 204-214 [PMID: 26701267 DOI: 10.1158/2326-6066.CIR-15-0188]
64 **Toubaji A**, Achtar M, Provenzano M, Herrin VE, Behrens R, Hamilton M, Bernstein S, Venzon D, Gause B, Marincola F, Khleif SN. Pilot study of mutant ras peptide-based vaccine as an adjuvant treatment in pancreatic and colorectal cancers. *Cancer Immunol Immunother* 2008; **57**: 1413-1420 [PMID: 18297281 DOI: 10.1007/s00262-008-0477-6]
65 **Tran E**, Robbins PF, Lu YC, Prickett TD, Gartner JJ, Jia L, Pasetto A, Zheng Z, Ray S, Groh EM, Kriley IR, Rosenberg SA. T-Cell Transfer Therapy Targeting Mutant KRAS in Cancer. *N Engl J Med* 2016; **375**: 2255-2262 [PMID: 27959684 DOI: 10.1056/NEJMoa1609279]
66 **Rahma OE**, Hamilton JM, Wojtowicz M, Dakheel O, Bernstein S, Liewehr DJ, Steinberg SM, Khleif SN. The immunological and clinical effects of mutated ras peptide vaccine in combination with IL-2, GM-CSF, or both in patients with solid tumors. *J Transl Med* 2014; **12**: 55 [PMID: 24565030 DOI: 10.1186/1479-5876-12-55]
67 **Li Y**, Sahni N, Pancsa R, McGrail DJ, Xu J, Hua X, Coulombe-Huntington J, Ryan M, Tychhon B, Sudhakar D, Hu L, Tyers M, Jiang X, Lin SY, Babu MM, Yi S. Revealing the Determinants of Widespread Alternative Splicing Perturbation in Cancer. *Cell Rep* 2017; **21**: 798-812 [PMID: 29045845 DOI: 10.1016/j.celrep.2017.09.071]
68 **Gardina PJ**, Clark TA, Shimada B, Staples MK, Yang Q, Veitch J, Schweitzer A, Awad T, Sugnet C, Dee S, Davies C, Williams A, Turpaz Y. Alternative splicing and differential gene expression in colon cancer detected by a whole genome exon array. *BMC Genomics* 2006; **7**: 325 [PMID: 17192196 DOI: 10.1186/1471-2164-7-325]
69 **Thorsen K**, Sørensen KD, Brems-Eskildsen AS, Modin C, Gaustadnes M, Hein AM, Kruhøffer M, Laurberg S, Borre M, Wang K, Brunak S, Krainer AR, Tørring N, Dyrskjøt L, Andersen CL, Orntoft TF. Alternative splicing in colon, bladder, and prostate cancer identified by exon array analysis. *Mol Cell Proteomics* 2008; **7**: 1214-1224 [PMID: 18353764 DOI: 10.1074/mcp.M700590-MCP200]
70 Retained Introns Can Produce Tumor-Specific Neoepitopes in Melanoma. *Cancer Discov* 2018; **8**: 1206 [PMID: 30143520 DOI: 10.1158/2159-8290.CD-RW2018-144]
71 **Ditzel HJ**, Strik MC, Larsen MK, Willis AC, Waseem A, Kejling K, Jensenius JC. Cancer-associated cleavage of cytokeratin 8/18 heterotypic complexes exposes a neoepitope in human adenocarcinomas. *J Biol Chem* 2002; **277**: 21712-21722 [PMID: 11923318 DOI: 10.1074/jbc.M202140200]
72 **Koelzer VH**, Lugli A, Dawson H, Hädrich M, Berger MD, Borner M, Mallaev M, Galván JA, Amsler J, Schnüriger B, Zlobec I, Inderbitzin D. CD8/CD45RO T-cell infiltration in endoscopic biopsies of colorectal cancer predicts nodal metastasis and survival. *J Transl Med* 2014; **12**: 81 [PMID: 24679169 DOI: 10.1186/1479-5876-12-81]
73 **Mogensen MB**, Rossing M, Østrup O, Larsen PN, Heiberg Engel PJ, Jørgensen LN, Hogdall EV, Eriksen J, Ibsen P, Jess P, Grauslund M, Nielsen HJ, Nielsen FC, Vainer B, Osterlind K. Genomic alterations accompanying tumour evolution in colorectal cancer: tracking the differences between primary tumours and synchronous liver metastases by whole-exome sequencing. *BMC Cancer* 2018; **18**: 752 [PMID: 30029640 DOI: 10.1186/s12885-018-4639-4]
74 **Sylvester BE**, Vakiani E. Tumor evolution and intratumor heterogeneity in colorectal carcinoma: insights from comparative genomic profiling of primary tumors and matched metastases. *J Gastrointest Oncol* 2015; **6**: 668-675 [PMID: 26697200 DOI: 10.3978/j.issn.2078-6891.2015.083]
75 **Bijker MS**, van den Eeden SJ, Franken KL, Melief CJ, van der Burg SH, Offringa R. Superior induction of anti-tumor CTL immunity by extended peptide vaccines involves prolonged, DC-focused antigen presentation. *Eur J Immunol* 2008; **38**: 1033-1042 [PMID: 18350546 DOI: 10.1002/eji.200737995]
76 **Srinivasan M**, Domanico SZ, Kaumaya PT, Pierce SK. Peptides of 23 residues or greater are required to stimulate a high affinity class Ⅱ-restricted T cell response. *Eur J Immunol* 1993; **23**: 1011-1016 [PMID: 8386663 DOI: 10.1002/eji.1830230504]
77 **Eggermont LJ**, Paulis LE, Tel J, Figdor CG. Towards efficient cancer immunotherapy: advances in developing artificial antigen-presenting cells. *Trends Biotechnol* 2014; **32**: 456-465 [PMID: 24998519 DOI: 10.1016/j.tibtech.2014.06.007]
78 **Awate S**, Babiuk LA, Mutwiri G. Mechanisms of action of adjuvants. *Front Immunol* 2013; **4**: 114 [PMID: 23720661 DOI: 10.3389/fimmu.2013.00114]
79 **Parmiani G**, Castelli C, Pilla L, Santinami M, Colombo MP, Rivoltini L. Opposite immune functions of GM-CSF administered as vaccine adjuvant in cancer patients. *Ann Oncol* 2007; **18**: 226-232 [PMID: 17116643 DOI: 10.1093/annonc/mdl158]
80 **Decker WK**, Safdar A. Cytokine adjuvants for vaccine therapy of neoplastic and infectious disease. *Cytokine Growth Factor Rev* 2011; **22**: 177-187 [PMID: 21862380 DOI: 10.1016/j.cytogfr.2011.07.001]
81 **Dummer R**, Hauschild A, Henseler T, Burg G. Combined interferon-alpha and interleukin-2 as adjuvant treatment for melanoma.

Lancet 1998; **352**: 908-909 [PMID: 9743016 DOI: 10.1016/S0140-6736(05)60052-9]
82 **Rahma OE**, Gammoh E, Simon RM, Khleif SN. Is the "3+3" dose-escalation phase I clinical trial design suitable for therapeutic cancer vaccine development? A recommendation for alternative design. *Clin Cancer Res* 2014; **20**: 4758-4767 [PMID: 25037736 DOI: 10.1158/1078-0432.CCR-13-2671]
83 **Yoshida K**, Noguchi M, Mine T, Komatsu N, Yutani S, Ueno T, Yanagimoto H, Kawano K, Itoh K, Yamada A. Characteristics of severe adverse events after peptide vaccination for advanced cancer patients: Analysis of 500 cases. *Oncol Rep* 2011; **25**: 57-62 [PMID: 21109957 DOI: 10.3892/or_00001041]
84 **Parkhurst MR**, Yang JC, Langan RC, Dudley ME, Nathan DA, Feldman SA, Davis JL, Morgan RA, Merino MJ, Sherry RM, Hughes MS, Kammula US, Phan GQ, Lim RM, Wank SA, Restifo NP, Robbins PF, Laurencot CM, Rosenberg SA. T cells targeting carcinoembryonic antigen can mediate regression of metastatic colorectal cancer but induce severe transient colitis. *Mol Ther* 2011; **19**: 620-626 [PMID: 21157437 DOI: 10.1038/mt.2010.272]
85 **Morgan RA**, Chinnasamy N, Abate-Daga D, Gros A, Robbins PF, Zheng Z, Dudley ME, Feldman SA, Yang JC, Sherry RM, Phan GQ, Hughes MS, Kammula US, Miller AD, Hessman CJ, Stewart AA, Restifo NP, Quezado MM, Alimchandani M, Rosenberg AZ, Nath A, Wang T, Bielekova B, Wuest SC, Akula N, McMahon FJ, Wilde S, Mosetter B, Schendel DJ, Laurencot CM, Rosenberg SA. Cancer regression and neurological toxicity following anti-MAGE-A3 TCR gene therapy. *J Immunother* 2013; **36**: 133-151 [PMID: 23377668 DOI: 10.1097/CJI.0b013e3182829903]
86 **Linette GP**, Stadtmauer EA, Maus MV, Rapoport AP, Levine BL, Emery L, Litzky L, Bagg A, Carreno BM, Cimino PJ, Binder-Scholl GK, Smethurst DP, Gerry AB, Pumphrey NJ, Bennett AD, Brewer JE, Dukes J, Harper J, Tayton-Martin HK, Jakobsen BK, Hassan NJ, Kalos M, June CH. Cardiovascular toxicity and titin cross-reactivity of affinity-enhanced T cells in myeloma and melanoma. *Blood* 2013; **122**: 863-871 [PMID: 23770775 DOI: 10.1182/blood-2013-03-490565]
87 **Whiteside TL**. The tumor microenvironment and its role in promoting tumor growth. *Oncogene* 2008; **27**: 5904-5912 [PMID: 18836471 DOI: 10.1038/onc.2008.271]
88 **Zou W**. Immunosuppressive networks in the tumour environment and their therapeutic relevance. *Nat Rev Cancer* 2005; **5**: 263-274 [PMID: 15776005 DOI: 10.1038/nrc1586]
89 **Murdoch C**, Muthana M, Coffelt SB, Lewis CE. The role of myeloid cells in the promotion of tumour angiogenesis. *Nat Rev Cancer* 2008; **8**: 618-631 [PMID: 18633355 DOI: 10.1038/nrc2444]
90 **Ozcan M**, Janikovits J, von Knebel Doeberitz M, Kloor M. Complex pattern of immune evasion in MSI colorectal cancer. *Oncoimmunology* 2018; **7**: e1445453 [PMID: 29900056 DOI: 10.1080/2162402X.2018.1445453]
91 **Atkins D**, Breuckmann A, Schmahl GE, Binner P, Ferrone S, Krummenauer F, Störkel S, Seliger B. MHC class I antigen processing pathway defects, ras mutations and disease stage in colorectal carcinoma. *Int J Cancer* 2004; **109**: 265-273 [PMID: 14750179 DOI: 10.1002/ijc.11681]
92 **Cabrera CM**, Jiménez P, Cabrera T, Esparza C, Ruiz-Cabello F, Garrido F. Total loss of MHC class I in colorectal tumors can be explained by two molecular pathways: beta2-microglobulin inactivation in MSI-positive tumors and LMP7/TAP2 downregulation in MSI-negative tumors. *Tissue Antigens* 2003; **61**: 211-219 [PMID: 12694570]
93 **Bicknell DC**, Kaklamanis L, Hampson R, Bodmer WF, Karran P. Selection for beta 2-microglobulin mutation in mismatch repair-defective colorectal carcinomas. *Curr Biol* 1996; **6**: 1695-1697 [PMID: 8994836]
94 **Bokhari A**, Jonchere V, Lagrange A, Bertrand R, Svrcek M, Marisa L, Buhard O, Greene M, Demidova A, Jia J, Adriaenssens E, Chassat T, Biard DS, Flejou JF, Lejeune F, Duval A, Collura A. Targeting nonsense-mediated mRNA decay in colorectal cancers with microsatellite instability. *Oncogenesis* 2018; **7**: 70 [PMID: 30228267 DOI: 10.1038/s41389-018-0079-x]
95 **Llosa NJ**, Cruise M, Tam A, Wicks EC, Hechenbleikner EM, Taube JM, Blosser RL, Fan H, Wang H, Luber BS, Zhang M, Papadopoulos N, Kinzler KW, Vogelstein B, Sears CL, Anders RA, Pardoll DM, Housseau F. The vigorous immune microenvironment of microsatellite instable colon cancer is balanced by multiple counter-inhibitory checkpoints. *Cancer Discov* 2015; **5**: 43-51 [PMID: 25358689 DOI: 10.1158/2159-8290.CD-14-0863]
96 **Le DT**, Uram JN, Wang H, Bartlett BR, Kemberling H, Eyring AD, Skora AD, Luber BS, Azad NS, Laheru D, Biedrzycki B, Donehower RC, Zaheer A, Fisher GA, Crocenzi TS, Lee JJ, Duffy SM, Goldberg RM, de la Chapelle A, Koshiji M, Bhaijee F, Huebner T, Hruban RH, Wood LD, Cuka N, Pardoll DM, Papadopoulos N, Kinzler KW, Zhou S, Cornish TC, Taube JM, Anders RA, Eshleman JR, Vogelstein B, Diaz LA Jr. PD-1 Blockade in Tumors with Mismatch-Repair Deficiency. *N Engl J Med* 2015; **372**: 2509-2520 [PMID: 26028255 DOI: 10.1056/NEJMoa1500596]
97 **Gupta R**, Sinha S, Paul RN. The impact of microsatellite stability status in colorectal cancer. *Curr Probl Cancer* 2018; **42**: 548-559 [PMID: 30119911 DOI: 10.1016/j.currproblcancer.2018.06.010]
98 **Rizvi NA**, Hellmann MD, Snyder A, Kvistborg P, Makarov V, Havel JJ, Lee W, Yuan J, Wong P, Ho TS, Miller ML, Rekhtman N, Moreira AL, Ibrahim F, Bruggeman C, Gasmi B, Zappasodi R, Maeda Y, Sander C, Garon EB, Merghoub T, Wolchok JD, Schumacher TN, Chan TA. Cancer immunology. Mutational landscape determines sensitivity to PD-1 blockade in non-small cell lung cancer. *Science* 2015; **348**: 124-128 [PMID: 25765070 DOI: 10.1126/science.aaa1348]
99 **Snyder A**, Makarov V, Merghoub T, Yuan J, Zaretsky JM, Desrichard A, Walsh LA, Postow MA, Wong P, Ho TS, Hollmann TJ, Bruggeman C, Kannan K, Li Y, Elipenahli C, Liu C, Harbison CT, Wang L, Ribas A, Wolchok JD, Chan TA. Genetic basis for clinical response to CTLA-4 blockade in melanoma. *N Engl J Med* 2014; **371**: 2189-2199 [PMID: 25409260 DOI: 10.1056/NEJMoa1406498]
100 **Baker K**, Zlobec I, Tornillo L, Terracciano L, Jass JR, Lugli A. Differential significance of tumour infiltrating lymphocytes in sporadic mismatch repair deficient versus proficient colorectal cancers: a potential role for dysregulation of the transforming growth factor-beta pathway. *Eur J Cancer* 2007; **43**: 624-631 [PMID: 17223543 DOI: 10.1016/j.ejca.2006.11.012]
101 **Deschoolmeester V**, Baay M, Van Marck E, Weyler J, Vermeulen P, Lardon F, Vermorken JB. Tumor infiltrating lymphocytes: an intriguing player in the survival of colorectal cancer patients. *BMC Immunol* 2010; **11**: 19 [PMID: 20385003 DOI: 10.1186/1471-2172-11-19]
102 **Liu C**, Lu Z, Xie Y, Guo Q, Geng F, Sun B, Wu H, Yu B, Wu J, Zhang H, Yu X, Kong W. Soluble PD-1-based vaccine targeting MUC1 VNTR and survivin improves anti-tumor effect. *Immunol Lett* 2018; **200**: 33-42 [PMID: 29894719 DOI: 10.1016/j.imlet.2018.06.004]
103 **Vacchelli E**, Galluzzi L, Fridman WH, Galon J, Sautès-Fridman C, Tartour E, Kroemer G. Trial watch: Chemotherapy with immunogenic cell death inducers. *Oncoimmunology* 2012; **1**: 179-188 [PMID: 22720239 DOI: 10.4161/onci.1.2.19026]
104 **Casares N**, Pequignot MO, Tesniere A, Ghiringhelli F, Roux S, Chaput N, Schmitt E, Hamai A, Hervas-Stubbs S, Obeid M, Coutant F, Métivier D, Pichard E, Aucouturier P, Pierron G, Garrido C, Zitvogel L, Kroemer G. Caspase-dependent immunogenicity of doxorubicin-induced tumor cell death. *J Exp Med* 2005; **202**: 1691-1701 [PMID: 16365148 DOI: 10.1084/jem.20050915]
105 **Schiavoni G**, Sistigu A, Valentini M, Mattei F, Sestili P, Spadaro F, Sanchez M, Lorenzi S, D'Urso MT, Belardelli F, Gabriele L, Proietti E, Bracci L. Cyclophosphamide synergizes with type I interferons through systemic dendritic cell reactivation and induction of immunogenic tumor apoptosis. *Cancer Res* 2011; **71**: 768-778 [PMID: 21156650 DOI: 10.1158/0008-5472.CAN-10-2788]
106 **Tesniere A**, Schlemmer F, Boige V, Kepp O, Martins I, Ghiringhelli F, Aymeric L, Michaud M, Apetoh L, Barault L, Mendiboure J, Pignon JP, Jooste V, van Endert P, Ducreux M, Zitvogel L, Piard F, Kroemer G. Immunogenic death of colon cancer cells treated with oxaliplatin. *Oncogene* 2010; **29**: 482-491 [PMID: 19881547 DOI: 10.1038/onc.2009.356]
107 **Warner SG**, Haddad D, Au J, Carson JS, O'Leary MP, Lewis C, Monette S, Fong Y. Oncolytic herpes simplex virus kills stem-like tumor-initiating colon cancer cells. *Mol Ther Oncolytics* 2016; **3**:

16013 [PMID: 27347556 DOI: 10.1038/mto.2016.13]
108 **Yoo SY**, Bang SY, Jeong SN, Kang DH, Heo J. A cancer-favoring oncolytic vaccinia virus shows enhanced suppression of stem-cell like colon cancer. *Oncotarget* 2016; **7**: 16479-16489 [PMID: 26918725 DOI: 10.18632/oncotarget.7660]
109 **Andtbacka RH**, Ross MI, Agarwala SS, Taylor MH, Vetto JT, Neves RI, Daud A, Khong HT, Ungerleider RS, Tanaka M, Grossmann KF. Final results of a phase Ⅱ multicenter trial of HF10, a replication-competent HSV-1 oncolytic virus, and ipilimumab combination treatment in patients with stage IIIB-IV unresectable or metastatic melanoma. *J Clin Oncol* 2017; **35**: 9510 [DOI: 10.1200/JCO.2017.35.15_suppl.9510]
110 **Chesney J**, Puzanov I, Collichio F, Singh P, Milhem MM, Glaspy J, Hamid O, Ross M, Friedlander P, Garbe C, Logan TF, Hauschild A, Lebbé C, Chen L, Kim JJ, Gansert J, Andtbacka RHI, Kaufman HL. Randomized, Open-Label Phase Ⅱ Study Evaluating the Efficacy and Safety of Talimogene Laherparepvec in Combination With Ipilimumab Versus Ipilimumab Alone in Patients With Advanced, Unresectable Melanoma. *J Clin Oncol* 2018; **36**: 1658-1667 [PMID: 28981385 DOI: 10.1200/JCO.2017.73.7379]
111 **Puzanov I**, Milhem MM, Minor D, Hamid O, Li A, Chen L, Chastain M, Gorski KS, Anderson A, Chou J, Kaufman HL, Andtbacka RH. Talimogene Laherparepvec in Combination With Ipilimumab in Previously Untreated, Unresectable Stage IIIB-IV Melanoma. *J Clin Oncol* 2016; **34**: 2619-2626 [PMID: 27298410 DOI: 10.1200/JCO.2016.67.1529]

P- Reviewer: Guo ZS, Kim TI, Wu ZQ, Sigalotti L
S- Editor: Gong ZM **L- Editor**: A **E- Editor**: Yin SY

World Journal of Gastroenterology

Submit a Manuscript: https://www.f6publishing.com

World J Gastroenterol 2018 December 28; 24(48): 5433-5438

DOI: 10.3748/wjg.v24.i48.5433

ISSN 1007-9327 (print) ISSN 2219-2840 (online)

MINIREVIEWS

Checkpoint inhibitors: What gastroenterologists need to know

Monjur Ahmed

Monjur Ahmed, Division of Gastroenterology and Hepatology, Department of Internal Medicine, Thomas Jefferson University, Philadelphia, PA 19107, United States

ORCID number: Monjur Ahmed (0000-0003-0515-9224).

Author contributions: Ahmed M finished this manuscript alone.

Conflict-of-interest statement: No conflict of interest exists.

Manuscript source: Invited manuscript

Corresponding author: Monjur Ahmed, MD, FRCP, Division of Gastroenterology and Hepatology, Department of Internal Medicine, Thomas Jefferson University, 132 South 10th Street, Suite 468, Main Building, Philadelphia, PA 19107, United States. monjur.ahmed@jefferson.edu.
Telephone: +1-215-9521493
Fax: +1-215-7551850

Received: September 28, 2018
Peer-review started: September 28, 2018
First decision: October 26, 2018
Revised: November 7, 2018
Accepted: November 16, 2018
Article in press: November 16, 2018
Published online: December 28, 2018

Abstract

Checkpoint inhibitors are increasingly being used in clinical practice. They can cause various gastrointestinal, hepatic and pancreatic side effects. As these side effects can be serious, appropriate management is essential. The different checkpoint inhibitors with their mechanisms of action and indications, as well as evaluation and management of gastrointestinal, hepatic and pancreatic side effects, are discussed in this article.

Key words: Checkpoint inhibitors; Immunotherapy; Gastrointestinal management; Hepatic and pancreatic side effects

Core tip: Checkpoint inhibitors are a kind of immunotherapy used in the treatment of various malignancies. Nevertheless, they carry the risk of causing different immune-related side effects. Physicians should be vigilant in recognizing and appropriately managing these side effects for a better outcome.

Ahmed M. Checkpoint inhibitors: what gastroenterologists need to know. *World J Gastroenterol* 2018; 24(48): 5433-5438
URL: https://www.wjgnet.com/1007-9327/full/v24/i48/5433.htm
DOI: https://dx.doi.org/10.3748/wjg.v24.i48.5433

INTRODUCTION

Checkpoint inhibitors have emerged as one of the most promising modalities of anti-cancer therapy[1]. They are monoclonal antibodies that block the checkpoint proteins either on T cells or cancer cells to enhance immune response against tumor cells[2]. Normally, when our body recognizes cancer cells or foreign bodies, our innate immune system (macrophages, dendritic cells, natural killer cells, mast cells, neutrophils, eosinophils and basophils) tries to eliminate them. Then, our adaptive immune system (B lymphocytes and T lymphocytes) starts working *via* antigen presenting cells. Checkpoint molecules are proteins that control specific cellular

processes to prevent errors. Some immune checkpoint proteins help the T cells to remain active, particularly in case of infection, whereas other immune checkpoint proteins regulate the immune system negatively by directing the T cells to switch off. Some cancer cells synthesize high levels of such immune checkpoint proteins, which can switch off the T cells and, as a result, the T cells can neither recognize nor kill the cancer cells.

Some of the common checkpoint proteins include: (1) Cytotoxic T lymphocyte-associated antigen 4 (CTLA-4) receptors on CD4 and CD8 T lymphocytes; (2) programmed cell death protein 1 (PD-1) receptors on the surface of T cells, B cells, natural killer (NK) cells, monocytes and dendritic cells; and (3) programmed cell death protein ligand 1 (PD-L1) and programmed cell death protein ligand 2 (PD-L2) proteins on healthy tissues, hematopoietic cells and tumor cells.

When interactions between the PD-1 receptors and PD-L1 (also known as B7-H1) or PD-L2 (also known as B7-H2) occurs, it promotes exhaustion of peripheral effector T cells, conversion of effector T cells to regulatory T (Treg) cells and inhibition of tumor cell apoptosis[3]. Some cancer cells are able to produce PD-L1 and PD-L2 on their surfaces to prevent any immunological attack.

CTLA-4 becomes activated by binding to B7-1 (also known as CD80) and B7-2 (also known as CD86) on antigen presenting cells (APCs), and then inhibits T cell activation at a proximal step in the immune response. On the other hand, PD-1 limits effector T cell function by linking with PD-L1 or PD-L2 in the later stages of the immune response. In the process of carcinogenesis, these immunosuppressive molecules are overexpressed[4]. Checkpoint inhibitors are monoclonal antibodies against PD-1, PD-L1 or CTLA-4 proteins. They act as a form of immunotherapy by blocking the immunosuppressive molecules that otherwise inhibit the immune system from attacking cancer cells. As a consequence, there is an immunological boost against cancer cells[5]. As they target T cells instead of cancer cells, they can be used in various malignancies[6]. A combination of checkpoint inhibitors may give a better anti-tumor response. There was a 23% response rate for metastatic non-small cell lung cancer after administration of durvalumab and tremelimumab[7].

Few checkpoint molecules have been discovered recently. These include TIM-3, LAG3, TIGIT and BTLA.

T cell immunoglobulin and mucin domain 3 (TIM-3) is present on the surface of CD4 T cells, CD8 T cells, regulatory T cells and innate immune cells (dendritic cells, macrophages and natural killer cells). TIM-3 binds to specific ligands: galectin (Gal-9), phosphatidyl serine (PtdSer), high-mobility group box-1 protein (HMGB) and carcinoembryonic antigen-related cell adhesion molecule 1 (CEACAM1). These interactions generate a variety of effects, including effector T cell apoptosis, T cell suppression, suppression of the innate immune response against tumor cells, suppression of anti-tumor activity and promotion of tumor growth[8]. TIM-3 is upregulated in patients with malignancy. In pre-clinical studies, TIM-3 monoclonal antibody monotherapy showed modest anti-tumor activities[9], but combinations of anti-TIM-3 and anti-PD-1/PD-L1 monoclonal antibodies produced significant anti-tumor responses against a variety of malignancies, including colon cancer, lung cancer, ovarian cancer, melanoma, lymphoma, acute myelogenous leukemia and sarcoma[10].

LAG-3 (lymphocyte activation gene-3 protein) is an inhibitory receptor expressed on CD4-positive T-lymphocytes, CD8-positive T-lymphocytes, NK cells and B cells, as well as on plasmacytoid dendritic cells[11-13]. LAG-3 inhibits both activation and proliferation of T cells[14,15]. Anti-LAG3 monoclonal antibodies can bind to the LAG-3 present on tumor infiltrating lymphocytes (TILs), and prevent their binding to MHC (major histocompatibility complex) class Ⅱ molecules expressed on tumor cells. This may lead to activation of antigen-specific T lymphocytes and cytotoxic T cell-mediated tumor lysis. Clinical trials were done with different types of LAG-3 monoclonal antibodies (IMP321) on various malignancies, such as metastatic renal cell cancer, breast cancer, unresectable pancreatic cancer, as well as advanced and unresectable melanoma[16].

T cell immunoreceptors with Ig and ITIM domains (TIGIT) are inhibitory immunoreceptors present on some T cells (CD4, CD8), NK cells and Treg cells that contain Ig and immunoreceptor tyrosine-based inhibitory motif (ITIM) domains. TIGIT ligands include CD155 and CD112. In certain malignancies, CD155 and CD112 are highly expressed on macrophages and dendritic cells. TIGIT ligation leads to inhibition of T cell proliferation and suppression of the cytolytic function of NK cells[17]. Anti-tumor activity is suppressed by TIGIT, primarily *via* Treg cells and not CD8-positive T cells[18]. Anti-TIGIT monoclonal antibodies as a monotherapy or in combination with anti-PD-L-1 antibodies have shown anti-tumor activity[19] in phase Ⅰ/Ⅱ trials.

BTLA (a B and T lymphocyte attenuator, also known as CD272) is an inhibitory protein functionally and structurally similar to CTLA-4 and PD-1. It is mainly expressed on immune cells, NK cells, dendritic cells and splenic macrophages. BTLA acts as a ligand for tumor necrosis factor receptor superfamily member 14 (TNFRSF-14), also known as herpes virus entry mediator (HVEM).

BTLA/HVEM complex inhibits T cell activation and proliferation[20]. BTLA is overexpressed in certain malignancies like leukemia and melanoma. In mouse models, BTLA neutralizing antibodies limited tumor growth[21]. Anti-human BTLA monoclonal antibodies are currently in development.

CURRENT CHECKPOINT INHIBITORS

Current checkpoint inhibitors, with their indications and a schematic diagram (Figure 1), are mentioned below[22-28], including CTLA-4 blockers, PD-1 inhibitors, and PD-L1

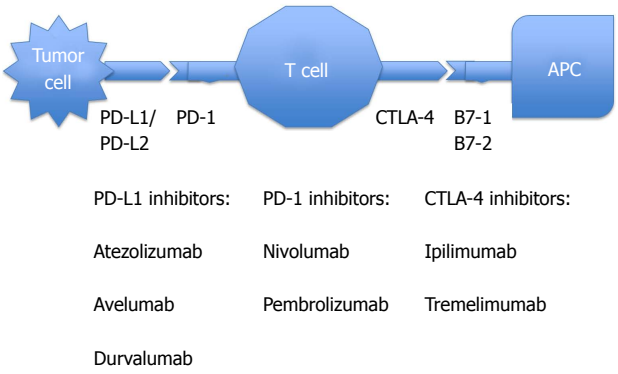

Figure 1 Schematic diagram of checkpoint inhibitors.

inhibitors.

CTLA-4 blockers

Ipilimumab: Indications include melanoma with lymph node involvement, advanced melanoma, non-small cell and small cell lung cancer, advanced renal cell cancer, and hormone refractory prostate cancer. Great success with durable clinical benefit was seen with nivolumab plus ipilimumab combination when given in DNA mismatch repair-deficient/microsatellite instability-high metastatic colorectal cancer[29].

Tremelimumab: This drug is undergoing human clinical trials for the treatment of various malignancies, but is not yet approved by the United States Food and Drug Administration (FDA).

PD-1 inhibitors

Nivolumab: Indications are melanoma with lymph node involvement, unresectable or metastatic melanoma, advanced renal cell carcinoma, advanced or metastatic urothelial cancer, metastatic non-small cell lung cancer and small cell lung cancer with progression after platinum-based chemotherapy, refractory classical Hodgkin lymphoma, recurrent or metastatic squamous cell cancer of head and neck, microsatellite instability-high or mismatch repair-deficient colorectal cancer, and hepatocellular carcinoma.

Pembrolizumab: Indications include unresectable or metastatic melanoma, metastatic non-small cell lung cancer, advanced head and neck squamous cell carcinoma, advanced or metastatic gastric or gastroesophageal junction cancer, microsatellite instability-high cancer, locally advanced or metastatic urothelial cancer, recurrent or metastatic cervical cancer, refractory classical Hodgkin lymphoma, and refractory primary mediastinal large B cell lymphoma.

PD-L1 inhibitors

Atezolizumab: Indicated for advanced or metastatic non-small cell lung cancer and advanced or metastatic urothelial cancer.

Avelumab: Indicated for advanced or metastatic urothelial cancer and metastatic Merkel cell cancer.

Durvalumab: Indicated for advanced or metastatic urothelial cancer, as well as unresectable and stage Ⅲ non-small lung cancer.

IMMUNE-RELATED ADVERSE EVENTS

Immune-related adverse events (IRAE) can occur due to the use of checkpoint inhibitors. Inflammatory side effects generally involve the skin, gastrointestinal tract, liver and endocrine glands. The cardiovascular, pulmonary, renal, hematological and musculoskeletal system are less commonly involved. IRAE are more severe following administration of CTLA-4 inhibitors in comparison to PD-1 or PD-L1 inhibitors. The time of onset of IRAE is generally 1-6 mo after administration of checkpoint inhibitors[30]. Here, we will be mainly discussing the gastrointestinal, hepatic and pancreatic side effects of checkpoint inhibitors.

Immune-related adverse events are classified according to the National Cancer Institute's Common Terminology Criteria for Adverse Events (AE), version 3.0[31]. Grade 1: Mild AE; Grade 2: Moderate AE; Grade 3: Severe AE; Grade 4: Life-threatening or disabling AE; Grade 5: Death related to AE.

Gastrointestinal

Diarrhea is the most common gastrointestinal side effect after administration of checkpoint inhibitors. Diarrhea occurs in 27%-31% of cases following CTLA-4 inhibitor therapy[32] and less than 4% of cases following anti-PD-1 and anti-PD-L1 therapy[33]. Diarrhea varies from mild to severe in intensity. Immune-mediated mild to severe colitis, colon perforation and even death can occur following checkpoint inhibitor therapy[34,35]. Severe colitis can occur in 5% of cases following CTLA-4 inhibitor therapy and less than 2% of cases following anti-PD-1 therapy. Colitis may mimic Crohn's colitis or ulcerative colitis, and can be associated with intra-abdominal abscess, anal fissure and fistula[36]. Pembrolizumab-induced collagenous colitis and lymphocytic colitis have also been reported in the literature[37,38].

Management

Mild diarrhea or grade Ⅰ diarrhea with stool frequency less than 4 times per day can be managed conservatively without discontinuing checkpoint inhibitors. Stool for ova, parasites, giardia antigen, stool culture and *C. difficile* toxin should be sent to evaluate for any underlying infection. Patient should be given adequate oral hydration and anti-diarrheal agents. If diarrhea still persists for 5-7 d or worsens, patients should be treated similar to cases of moderate diarrhea.

Moderate diarrhea or grade Ⅱ diarrhea with stool frequency between 4-6 times per day should be managed by discontinuation of checkpoint inhibitors, by ruling out

infection by sending stool samples as mentioned above, by giving adequate oral hydration and by administering empiric treatment with oral corticosteroid (prednisone 1 mg/kg per day) with close clinical follow-up[39]. Colonoscopy is not required if the patient responds to the above measures. After 2-5 d control of diarrhea, prednisone should be slowly tapered over a 1-2 mo period of time. Trimethoprim-sulfamethoxazole should be given as a prophylaxis against opportunistic infection during the tapering period[40].

If the patient does not respond to the conservative measures or if the patient has severe diarrhea, *i.e.,* grade Ⅲ or Ⅳ diarrhea, with stool frequency more than 6 times per day with severe and persistent abdominal pain, fever, rectal bleeding or ileus, intravenous hydration and intravenous steroid (methylprednisone 1-2 mg/kg per day) should be started[41]. Antidiarrheal agents like loperamide and lomotil (diphenoxylate/atropine) should be avoided. Abdominal CT (computerized axial tomography) should be done to assess the severity and complications of colitis (perforation and peritonitis). Colonoscopy or flexible sigmoidoscopy should be done not only to evaluate the severity and extent of colitis, but also to take random and targeted colon biopsies to rule out underlying cytomegalovirus (CMV) infection[35]. CMV colitis is diagnosed by characteristic histology (owl's eye intranuclear inclusion bodies), CMV biopsy PCR (polymerase chain reaction) or CMV biopsy viral culture[42]. Colonoscopic findings may include loss of vascular markings, erythema, congestion, friability, ulcerations and spontaneous bleeding. The severity of diarrhea may not correlate with the colonoscopic or histological findings.

Treatment should be continued until there is significant improvement of diarrhea, *i.e.,* grade 0-1. If there is a clinical response to corticosteroids, it is recommended to continue treatment for a month and then slowly taper. If the patient's diarrhea is refractory to steroids, or colonoscopy shows severe colitis, multiple colon ulcers or pancolitis, anti-TNF therapy like Infliximab (5 mg/kg every 2 wk) or anti-integrin therapy like Vedolizumab (300 mg 0, 2, 6 wk) should be added[43-45]. Concomitant bacterial, viral or *Clostridium difficile* infection should be treated simultaneously. Following resolution of symptoms, checkpoint inhibitors can be restarted if the benefits outweigh the risks, and if the daily dose of prednisone can be reduced to less than 10 mg per day without any other immunosuppressive medication.

Summary of diarrhea management

Diarrhea onset approximately 6 wk after checkpoint inhibitor therapy: assess severity of diarrhea and rule out infection by sending stool samples → Grade Ⅰ diarrhea: conservative treatment with oral hydration and antidiarrheal agents → Persistence of diarrhea after 5-7 d → Manage as grade Ⅱ diarrhea. Grade Ⅱ diarrhea: stop checkpoint inhibitor, start oral corticosteroid and continue oral hydration: (1) Clinical improvement → 2-5 d after control of diarrhea, start tapering corticosteroid over 1-2 mo plus trimethoprim-sulfamethoxazole as prophylaxis; (2) no clinical improvement → Manage as grade Ⅲ or Ⅳ diarrhea. Grade Ⅲ or Ⅳ diarrhea: hospitalization, parenteral hydration, parenteral corticosteroid, abdominal CT and colonoscopy: (1) Clinical response: continue steroid for a month and taper; (2) no clinical response: anti-TNF therapy.

Hepatic

Checkpoint inhibitors can cause immune-mediated hepatitis in less than 5% of cases receiving these medications[46]. Although this can occur anytime while the patient is on checkpoint inhibitor therapy, it occurs most commonly 6-7 wk after the onset of therapy[47]. Most of the time, patients remain asymptomatic with elevated serum transaminases. Sometimes, the hepatitis can be more severe, with patients presenting with fever, malaise, fatigue, hepatomegaly and hyperbilirubinemia. Acute viral hepatitis (HAV, HBV, HCV, EBV, CMV) and autoimmune hepatitis need to be excluded by serology and liver biopsy[48]. Predominant hepatic parenchymal injury with panlobular hepatitis or predominant bile duct injury with mononuclear cell infiltration around proliferated bile ductules can be seen after checkpoint inhibitor therapy[49]. It is sometimes difficult to distinguish autoimmune hepatitis from drug-induced hepatitis. In autoimmune hepatitis, intra-acinar and portal plasma cells with rosette formation and emperiopolesis are prominent, whereas neutrophilic infiltration is more commonly seen in drug-induced liver injury[50].

Management[51]

Grade 1 immune-mediated hepatitis: patient is asymptomatic or mildly symptomatic, but laboratory studies show AST/ALT: < 2.5 × ULN (upper limit of normal) and total bilirubin: < 1.5 × ULN. Treatment: continue checkpoint inhibitor therapy, but monitor LFT.

Grade 2 immune-mediated hepatitis: patient is symptomatic (fever, malaise, fatigue) and laboratory studies show AST/ALT: 2.5-5 × ULN and total bilirubin: 1.5-3 × ULN. Treatment: (1) hold checkpoint inhibitor therapy; (2) viral hepatitis (HAV, HBV, HCV, HDV, CMV, EBV, HSV, VZV), autoimmune hepatitis and drug-induced hepatitis need to be ruled out[46]; (3) prednisone 1 mg/kg per day, taper the dose when patient's symptoms improve; and (4) if symptoms do not improve after 48 h, alternate immunosuppressive agents like tacrolimus, mycophenolate mofetil or cyclophosphamide need to be considered.

Grade 3 or 4 immune-mediated hepatitis: patient is symptomatic as mentioned above, and laboratory studies show: AST/ALT: > 5 × ULN; total bilirubin: > 3 × ULN. Treatment: (1) hold checkpoint inhibitors; (2) intravenous solumedrol 2-4 mg/kg per day. Taper the dose when patient's symptoms improve; and (3) if symptoms do not improve after 5-7 d, tacrolimus 0.10-0.15 mg/kg per day should be added. Alternative agents include

mycophenolate mofetil or cyclophosphamide.

Pancreatic

Immune-mediated pancreatitis with pancreatic insufficiency has been reported a few months after initiation of checkpoint inhibitor therapy[52]. Asymptomatic elevations of amylase and lipase can occur without fulfilling the diagnostic criteria of acute pancreatitis. As the clinical significance of this lab abnormality is unknown, routine measurement of serum amylase and lipase is not recommended[53]. However, if the patient is symptomatic with abdominal pain or nausea, immune-mediated pancreatitis should be considered by checking amylase and lipase levels and performing imaging studies.

Management

Intravenous methylprednisolone (1 mg/kg per day) for a few days, followed by oral prednisone (1 mg/kg per day). Taper the dose when patient symptoms improve.

Pancreatic enzyme supplementation should be given if there is evidence of pancreatic insufficiency (fecal elastase < 15 μg/g of feces).

CONCLUSION

Checkpoint inhibitors are novel forms of immunotherapy administered by oncologists. Although they are extremely useful in various advanced and metastatic malignancies, they can cause multiple side effects. Gastroenterologists need to be aware of the various gastrointestinal, hepatic and pancreatic side effects that can be fatal if not managed early. Prompt recognition of these side effects, administration of systemic immunosuppressive therapy and supportive care could improve the clinical outcome without affecting the benefit of checkpoint inhibitors. Multidisciplinary teams should be involved in the management of these side effects. As new checkpoints are being discovered and new checkpoint inhibitors are being developed, patients will be experiencing new IRAE. Management of those IRAE will improve as we gather more experience using new checkpoint inhibitors.

REFERENCES

1 **Chen Q**, Wang C, Chen G, Hu Q, Gu Z. Delivery Strategies for Immune Checkpoint Blockade. *Adv Healthc Mater* 2018; **7**: e1800424 [PMID: 29978565 DOI: 10.1002/adhm.201800424]

2 **Trivedi MS**, Hoffner B, Winkelmann JL, Abbott ME, Hamid O, Carvajal RD. Programmed death 1 immune checkpoint inhibitors. *Clin Adv Hematol Oncol* 2015; **13**: 858-868 [PMID: 27058852]

3 **Dine J**, Gordon R, Shames Y, Kasler MK, Barton-Burke M. Immune Checkpoint Inhibitors: An Innovation in Immunotherapy for the Treatment and Management of Patients with Cancer. *Asia Pac J Oncol Nurs* 2017; **4**: 127-135 [PMID: 28503645 DOI: 10.4103/apjon.apjon_4_17]

4 **Mellman I**, Coukos G, Dranoff G. Cancer immunotherapy comes of age. *Nature* 2011; **480**: 480-489 [PMID: 22193102 DOI: 10.1038/nature10673]

5 **Oiseth SJ**, Aziz MS. Cancer immunotherapy: a brief review of the history, possibilities, and challenges ahead. *J Cancer Met Tre* 2017; **3**: 250-261 [DOI: 10.20517/2394-4722.2017.41]

6 **Assarzadegan N**, Montgomery E, Anders RA. Immune checkpoint inhibitor colitis: the flip side of the wonder drugs. *Virchows Arch* 2018; **472**: 125-133 [PMID: 29143108 DOI: 10.1007/s00428-017-2267-z]

7 **Antonia S**, Goldberg SB, Balmanoukian A, Chaft JE, Sanborn RE, Gupta A, Narwal R, Steele K, Gu Y, Karakunnel JJ, Rizvi NA. Safety and antitumour activity of durvalumab plus tremelimumab in non-small cell lung cancer: a multicentre, phase 1b study. *Lancet Oncol* 2016; **17**: 299-308 [PMID: 26858122 DOI: 10.1016/S1470-2045(15)00544-6]

8 **Liu F**, Liu Y, Chen Z. Tim-3 expression and its role in hepatocellular carcinoma. *J Hematol Oncol* 2018; **11**: 126 [PMID: 30309387 DOI: 10.1186/s13045-018-0667-4]

9 **Ngiow SF**, von Scheidt B, Akiba H, Yagita H, Teng MW, Smyth MJ. Anti-TIM3 antibody promotes T cell IFN-γ-mediated antitumor immunity and suppresses established tumors. *Cancer Res* 2011; **71**: 3540-3551 [PMID: 21430066 DOI: 10.1158/0008-5472.CAN-11-0096]

10 **Sakuishi K**, Apetoh L, Sullivan JM, Blazar BR, Kuchroo VK, Anderson AC. Targeting Tim-3 and PD-1 pathways to reverse T cell exhaustion and restore anti-tumor immunity. *J Exp Med* 2010; **207**: 2187-2194 [PMID: 20819927 DOI: 10.1084/jem.20100643]

11 **Triebel F**, Jitsukawa S, Baixeras E, Roman-Roman S, Genevee C, Viegas-Pequignot E, Hercend T. LAG-3, a novel lymphocyte activation gene closely related to CD4. *J Exp Med* 1990; **171**: 1393-1405 [PMID: 1692078]

12 **Kisielow M**, Kisielow J, Capoferri-Sollami G, Karjalainen K. Expression of lymphocyte activation gene 3 (LAG-3) on B cells is induced by T cells. *Eur J Immunol* 2005; **35**: 2081-2088 [PMID: 15971272 DOI: 10.1002/eji.200526090]

13 **Workman CJ**, Wang Y, El Kasmi KC, Pardoll DM, Murray PJ, Drake CG, Vignali DA. LAG-3 regulates plasmacytoid dendritic cell homeostasis. *J Immunol* 2009; **182**: 1885-1891 [PMID: 19201841 DOI: 10.4049/jimmunol.0800185]

14 **Blackburn SD**, Shin H, Haining WN, Zou T, Workman CJ, Polley A, Betts MR, Freeman GJ, Vignali DA, Wherry EJ. Coregulation of CD8+ T cell exhaustion by multiple inhibitory receptors during chronic viral infection. *Nat Immunol* 2009; **10**: 29-37 [PMID: 19043418 DOI: 10.1038/ni.1679]

15 **Huard B**, Prigent P, Tournier M, Bruniquel D, Triebel F. CD4/major histocompatibility complex class Ⅱ interaction analyzed with CD4- and lymphocyte activation gene-3 (LAG-3)-Ig fusion proteins. *Eur J Immunol* 1995; **25**: 2718-2721 [PMID: 7589152 DOI: 10.1002/eji.1830250949]

16 **Andrews LP**, Marciscano AE, Drake CG, Vignali DA. LAG3 (CD223) as a cancer immunotherapy target. *Immunol Rev* 2017; **276**: 80-96 [PMID: 28258692 DOI: 10.1111/imr.12519]

17 **Johnston RJ**, Comps-Agrar L, Hackney J, Yu X, Huseni M, Yang Y, Park S, Javinal V, Chiu H, Irving B, Eaton DL, Grogan JL. The immunoreceptor TIGIT regulates antitumor and antiviral CD8(+) T cell effector function. *Cancer Cell* 2014; **26**: 923-937 [PMID: 25465800 DOI: 10.1016/j.ccell.2014.10.018]

18 **Kurtulus S**, Sakuishi K, Ngiow SF, Joller N, Tan DJ, Teng MW, Smyth MJ, Kuchroo VK, Anderson AC. TIGIT predominantly regulates the immune response via regulatory T cells. *J Clin Invest* 2015; **125**: 4053-4062 [PMID: 26413872 DOI: 10.1172/JCI81187]

19 **Solomon BL**, Garrido-Laguna I. TIGIT: a novel immunotherapy target moving from bench to bedside. *Cancer Immunol Immunother* 2018; **67**: 1659-1667 [PMID: 30232519 DOI: 10.1007/s00262-018-2246-5]

20 **Zhang M**, Howard K, Winters A, Steavenson S, Anderson S, Smelt S, Doellgast G, Sheelo C, Stevens J, Kim H, Hamburger A, Sein A, Caughey DJ, Lee F, Hsu H, Siu G, Byrne FR. Monoclonal antibodies to B and T lymphocyte attenuator (BTLA) have no effect on in vitro B cell proliferation and act to inhibit in vitro T cell proliferation when presented in a cis, but not trans, format relative to the activating stimulus. *Clin Exp Immunol* 2011; **163**: 77-87 [PMID: 21078085 DOI: 10.1111/j.1365-2249.2010.04259.x]

21 **Sekar D**, Govene L, Del Río ML, Sirait-Fischer E, Fink AF, Brüne B, Rodriguez-Barbosa JI, Weigert A. Downregulation of BTLA on NKT Cells Promotes Tumor Immune Control in a Mouse Model of Mammary Carcinoma. *Int J Mol Sci* 2018; **19** [PMID: 29518903 DOI: 10.3390/ijms19030752]

22 **Postow MA**, Sidlow R, Hellmann MD. Immune-Related Adverse Events Associated with Immune Checkpoint Blockade. *N Engl J Med* 2018; **378**: 158-168 [PMID: 29320654 DOI: 10.1056/NEJMra1703481]
23 Medscape. Ipilimumab (Rx). Available from: URL: https://reference.medscape.com/drug/yervoy-ipilimumab-999636
24 Medscape. Nivolumab (Rx). Available from: URL: https://reference.medscape.com/drug/opdivo-nivolumab-999989
25 Medscape. Pembrolizumab (Rx). Available from: URL: https://reference.medscape.com/drug/keytruda-pembrolizumab-999962
26 Medscape. Atezolizumab (Rx). Available from: URL: https://reference.medscape.com/drug/tecentriq-atezolizumab-1000098
27 Medscape. Avelumab (Rx). Available from: URL: https://reference.medscape.com/drug/bavencio-avelumab-1000144
28 Medscape. Durvalumab (Rx). Available from: URL: https://reference.medscape.com/drug/imfinzi-durvalumab-1000145
29 **Overman MJ**, Lonardi S, Wong KYM, Lenz HJ, Gelsomino F, Aglietta M, Morse MA, Van Cutsem E, McDermott R, Hill A, Sawyer MB, Hendlisz A, Neyns B, Svrcek M, Moss RA, Ledeine JM, Cao ZA, Kamble S, Kopetz S, André T. Durable Clinical Benefit With Nivolumab Plus Ipilimumab in DNA Mismatch Repair-Deficient/Microsatellite Instability-High Metastatic Colorectal Cancer. *J Clin Oncol* 2018; **36**: 773-779 [PMID: 29355075 DOI: 10.1200/JCO.2017.76.9901]
30 **Eigentler TK**, Hassel JC, Berking C, Aberle J, Bachmann O, Grünwald V, Kähler KC, Loquai C, Reinmuth N, Steins M, Zimmer L, Sendl A, Gutzmer R. Diagnosis, monitoring and management of immune-related adverse drug reactions of anti-PD-1 antibody therapy. *Cancer Treat Rev* 2016; **45**: 7-18 [PMID: 26922661 DOI: 10.1016/j.ctrv.2016.02.003]
31 Cancer Therapy Evaluation Program, Common Terminology Criteria for Adverse Events, Version 3.0. Available from: URL: https://ctep.cancer.gov/protocolDevelopment/electronic_applications/ctc.htm#ctc_40
32 **Hodi FS**, O'Day SJ, McDermott DF, Weber RW, Sosman JA, Haanen JB, Gonzalez R, Robert C, Schadendorf D, Hassel JC, Akerley W, van den Eertwegh AJ, Lutzky J, Lorigan P, Vaubel JM, Linette GP, Hogg D, Ottensmeier CH, Lebbé C, Peschel C, Quirt I, Clark JI, Wolchok JD, Weber JS, Tian J, Yellin MJ, Nichol GM, Hoos A, Urba WJ. Improved survival with ipilimumab in patients with metastatic melanoma. *N Engl J Med* 2010; **363**: 711-723 [PMID: 20525992 DOI: 10.1056/NEJMoa1003466]
33 **Wang PF**, Chen Y, Song SY, Wang TJ, Ji WJ, Li SW, Liu N, Yan CX. Immune-Related Adverse Events Associated with Anti-PD-1/PD-L1 Treatment for Malignancies: A Meta-Analysis. *Front Pharmacol* 2017; **8**: 730 [PMID: 29093678 DOI: 10.3389/fphar.2017.00730]
34 **Celli R**, Kluger HM, Zhang X. Anti-PD-1 Therapy-Associated Perforating Colitis. *Case Rep Gastrointest Med* 2018; **2018**: 3406437 [PMID: 29955400 DOI: 10.1155/2018/3406437]
35 **Prieux-Klotz C**, Dior M, Damotte D, Dreanic J, Brieau B, Brezault C, Abitbol V, Chaussade S, Coriat R. Immune Checkpoint Inhibitor-Induced Colitis: Diagnosis and Management. *Target Oncol* 2017; **12**: 301-308 [PMID: 28540478 DOI: 10.1007/s11523-017-0495-4]
36 **Bertha M**, Bellaguara E, Kuzel T, Hanauer S. Checkpoint Inhibitor-Induced Colitis: A New Type of Inflammatory Bowel Disease? *ACG Case Rep J* 2017; **4**: e112 [PMID: 29043290 DOI: 10.14309/crj.2017.112]
37 **Baroudjian B**, Lourenco N, Pagès C, Chami I, Maillet M, Bertheau P, Bagot M, Gornet JM, Lebbé C, Allez M. Anti-PD1-induced collagenous colitis in a melanoma patient. *Melanoma Res* 2016; **26**: 308-311 [PMID: 26990271 DOI: 10.1097/CMR.0000000000000252]
38 **Ahmed M**, Francis G. Pembrolizumab-Induced Microscopic Colitis. *Am J Gastroenterol* 2018; **113**: 629-630 [PMID: 29610496 DOI: 10.1038/ajg.2018.8]
39 **Rudzki JD.** Management of adverse events related to checkpoint inhibition therapy. *Memo Eur Med Oncol* 2018; **11**: 132-137 [DOI: 10.1007/s12254-018-0416-y]
40 **Cooley L**, Dendle C, Wolf J, Teh BW, Chen SC, Boutlis C, Thursky KA. Consensus guidelines for diagnosis, prophylaxis and management of Pneumocystis jirovecii pneumonia in patients with haematological and solid malignancies, 2014. *Intern Med J* 2014; **44**: 1350-1363 [PMID: 25482745 DOI: 10.1111/imj.12599]
41 **Cheng R**, Cooper A, Kench J, Watson G, Bye W, McNeil C, Shackel N. Ipilimumab-induced toxicities and the gastroenterologist. *J Gastroenterol Hepatol* 2015; **30**: 657-666 [PMID: 25641691 DOI: 10.1111/jgh.12888]
42 **Goodman AL**, Murray CD, Watkins J, Griffiths PD, Webster DP. CMV in the gut: a critical review of CMV detection in the immunocompetent host with colitis. *Eur J Clin Microbiol Infect Dis* 2015; **34**: 13-18 [PMID: 25097085 DOI: 10.1007/s10096-014-2212-x]
43 **Geukes Foppen MH**, Rozeman EA, van Wilpe S, Postma C, Snaebjornsson P, van Thienen JV, van Leerdam ME, van den Heuvel M, Blank CU, van Dieren J, Haanen JBAG. Immune checkpoint inhibition-related colitis: symptoms, endoscopic features, histology and response to management. *ESMO Open* 2018; **3**: e000278 [PMID: 29387476 DOI: 10.1136/esmoopen-2017-000278]
44 **Hsieh AH**, Ferman M, Brown MP, Andrews JM. Vedolizumab: a novel treatment for ipilimumab-induced colitis. *BMJ Case Rep* 2016; **2016** [PMID: 27539137 DOI: 10.1136/bcr-2016-216641]
45 **Bergqvist V**, Hertervig E, Gedeon P, Kopljar M, Griph H, Kinhult S, Carneiro A, Marsal J. Vedolizumab treatment for immune checkpoint inhibitor-induced enterocolitis. *Cancer Immunol Immunother* 2017; **66**: 581-592 [PMID: 28204866 DOI: 10.1007/s00262-017-1962-6]
46 **Di Giacomo AM**, Biagioli M, Maio M. The emerging toxicity profiles of anti-CTLA-4 antibodies across clinical indications. *Semin Oncol* 2010; **37**: 499-507 [PMID: 21074065 DOI: 10.1053/j.seminoncol.2010.09.007]
47 **Weber JS**, Kähler KC, Hauschild A. Management of immune-related adverse events and kinetics of response with ipilimumab. *J Clin Oncol* 2012; **30**: 2691-2697 [PMID: 22614989 DOI: 10.1200/JCO.2012.41.6750]
48 **Suriawinata AA**, Thung SN. Acute and chronic hepatitis. *Semin Diagn Pathol* 2006; **23**: 132-148 [PMID: 17355087]
49 **Kim KW**, Ramaiya NH, Krajewski KM, Jagannathan JP, Tirumani SH, Srivastava A, Ibrahim N. Ipilimumab associated hepatitis: imaging and clinicopathologic findings. *Invest New Drugs* 2013; **31**: 1071-1077 [PMID: 23408334 DOI: 10.1007/s10637-013-9939-6]
50 **Suzuki A**, Brunt EM, Kleiner DE, Miquel R, Smyrk TC, Andrade RJ, Lucena MI, Castiella A, Lindor K, Björnsson E. The use of liver biopsy evaluation in discrimination of idiopathic autoimmune hepatitis versus drug-induced liver injury. *Hepatology* 2011; **54**: 931-939 [PMID: 21674554 DOI: 10.1002/hep.24481]
51 **Kumar V**, Chaudhary N, Garg M, Floudas CS, Soni P, Chandra AB. Corrigendum: Current Diagnosis and Management of Immune Related Adverse Events (irAEs) Induced by Immune Checkpoint Inhibitor Therapy. *Front Pharmacol* 2017; **8**: 311 [PMID: 28579959 DOI: 10.3389/fphar.2017.00311]
52 **Hofmann L**, Forschner A, Loquai C, Goldinger SM, Zimmer L, Ugurel S, Schmidgen MI, Gutzmer R, Utikal JS, Göppner D, Hassel JC, Meier F, Tietze JK, Thomas I, Weishaupt C, Leverkus M, Wahl R, Dietrich U, Garbe C, Kirchberger MC, Eigentler T, Berking C, Gesierich A, Krackhardt AM, Schadendorf D, Schuler G, Dummer R, Heinzerling LM. Cutaneous, gastrointestinal, hepatic, endocrine, and renal side-effects of anti-PD-1 therapy. *Eur J Cancer* 2016; **60**: 190-209 [PMID: 27085692 DOI: 10.1016/j.ejca.2016.02.025]
53 **Postow MA**. Managing immune checkpoint-blocking antibody side effects. *Am Soc Clin Oncol Educ Book* 2015; 76-83 [PMID: 25993145 DOI: 10.14694/EdBook_AM.2015.35.76]

P- Reviewer: Aykan NF, Caboclo JF, Contini S, Lin JM, Linnebacher M, Tang Y, Wakao H
S- Editor: Wang XJ **L- Editor**: Filipodia **E- Editor**: Yin SY

World Journal of Gastroenterology

Submit a Manuscript: https://www.f6publishing.com

World J Gastroenterol 2018 December 28; 24(48): 5439-5445

DOI: 10.3748/wjg.v24.i48.5439

ISSN 1007-9327 (print) ISSN 2219-2840 (online)

MINIREVIEWS

Virtual reality simulation in endoscopy training: Current evidence and future directions

Tahrin Mahmood, Michael Anthony Scaffidi, Rishad Khan, Samir Chandra Grover

Tahrin Mahmood, Michael Anthony Scaffidi, Rishad Khan, Samir Chandra Grover, Division of Gastroenterology, St. Michael's Hospital, University of Toronto, Toronto M5B 1W8, Canada

ORCID number: Tahrin Mahmood (0000-0001-9013-8166); Michael Anthony Scaffidi (0000-0003-2068-6655); Rishad Khan (0000-0002-5090-7685); Samir Chandra Grover (0000-0003-3392-1220).

Author contributions: Mahmood T, Scaffidi MA, Khan R, and Grover SC drafted the manuscript, critically appraised it for important intellectual content, and approved the final version of this manuscript.

Conflict-of-interest statement: No authors have any conflicts of interest to report of relevance to the subject matter of this manuscript.

Manuscript source: Invited manuscript

Corresponding author: Samir Chandra Grover, MD, MEd, FRCPC, Assistant Professor, Division of Gastroenterology, St. Michael's Hospital, University of Toronto, 30 Bond Street, Toronto M5B 1W8, Canada. samir.grover@utoronto.ca
Telephone: +1-416-864-5628
Fax: +1-416-864-5882

Received: September 29, 2018
Peer-review started: September 29, 2018
First decision: October 26, 2018
Revised: November 22, 2018
Accepted: November 30, 2018
Article in press: December 1, 2018
Published online: December 28, 2018

Abstract

Virtual reality simulation is becoming the standard when beginning endoscopic training. It offers various benefits including learning in a low-stakes environment, improvement of patient safety and optimization of valuable endoscopy time. This is a review of the evidence surrounding virtual reality simulation and its efficacy in teaching endoscopic techniques. There have been 21 randomized controlled trials (RCTs) that have investigated virtual reality simulation as a teaching tool in endoscopy. 10 RCTs studied virtual reality in colonoscopy, 3 in flexible sigmoidoscopy, 5 in esophagogastroduodenoscopy, and 3 in endoscopic retrograde cholangiopancreatography. RCTs reported many outcomes including distance advanced in colonoscopy, comprehensive assessment of technical and non-technical skills, and patient comfort. Generally, these RCTs reveal that trainees with virtual reality simulation based learning improve in all of these areas in the beginning of the learning process. Virtual reality simulation was not effective as a replacement of conventional teaching methods. Additionally, feedback was shown to be an essential part of the learning process. Overall, virtual reality endoscopic simulation is emerging as a necessary augment to conventional learning given the ever increasing importance of patient safety and increasingly valuable endoscopy time; although work is still needed to study the nuances surrounding its integration into curriculum.

Key words: Endoscopy; Gastrointestinal/education; Endoscopy; Gastrointestinal/standards; Simulation; Educational measurement; Clinical competence/standards; Competency-based medical education

Core tip: There is substantial evidence to support that virtual reality simulation is an excellent augment to the traditional apprenticeship model in learning endoscopic

procedures. Further work is still needed to study the nuances surrounding its integration into curriculum.

Mahmood T, Scaffidi MA, Khan R, Grover SC. Virtual reality simulation in endoscopy training: Current evidence and future directions. *World J Gastroenterol* 2018; 24(48): 5439-5445
URL: https://www.wjgnet.com/1007-9327/full/v24/i48/5439.htm
DOI: https://dx.doi.org/10.3748/wjg.v24.i48.5439

INTRODUCTION

Educators in gastroenterology are increasingly integrating simulation-based training (SBT) into endoscopy curricula. SBT allows for a learner-centered environment in which novices can engage in deliberate practice without the fear of making mistakes or harming a patient[1-4]. The application of SBT to endoscopy has manifested as a variety of model systems, including mechanical models, animal models, live *ex-vivo* models, and virtual reality (VR) computer simulators. Among these, VR simulators have become the most commonly tested model system[5,6]. In this narrative review, we explore the current state of evidence for the use of VR SBT in endoscopic training.

ENDOSCOPY TRAINING

Apprenticeship model

The apprenticeship model of learning is based on an expert endoscopist (coach) teaching a trainee (apprentice) endoscopic skills. The apprenticeship helps the trainee progress from observation to participation, and finally to independence with progressive responsibilities[7,8]. The apprenticeship model is based in situated learning theory, which holds that a skill must be learned in the authentic context where it will be applied[9]. During training, the trainee's responsibility and independence increases as he/she accumulates experience and skill (Figure 1)[3,5]. Experienced endoscopists intervene if they deem that the trainee will be unable to complete the procedure safely, and trainees are expected to demonstrate certain milestones before progressing to the next steps.

There are, however, several important disadvantages of the apprenticeship model. First, there may be an increased risk of adverse events for patients. For example, one study found that the number of complications of endoscopy are significantly increased in July or August, when the training programs start with their new trainees[10]. Similarly, a study by Matharoo *et al*[11] showed that trainee related factors resulted in as many patient safety incidents as sedation with no oxygen saturation monitor. Second, the staff endoscopist has to completely give up the control of the endoscope in order for the trainee to learn[5,12]. As the trainee does not have the experience to identify and appropriately manage the findings, the pathological findings, which are intermittent and unpredictable, maybe mismanaged[5,12]. Third, training endoscopies take longer to complete, adding to the already strained availability of the endoscopy suite[5]. Fourth, the feedback given to each trainee depends on the staff endoscopist, and therefore may vary[13,14]. Finally, there is a lack of continuity as the trainees are expected to work with different staff endoscopists, who may not understand the trainee's level of competence as a whole[8].

Simulation based training

Given these drawbacks, the endoscopy educators increasingly use SBT prior to first patient contact. SBT provides the trainee with a simulated model of reality to help the trainee understand the skills required for clinical practice[6,15]. The simulated model can be made physically (*i.e.*, bench top) or with the help of technology using VR[6,13,15]. SBT is based on the constructivist learning model, which holds that learning is constructed by the learner, rather than transferred to the learner; this renders the context of the situation not as important[16]. In endoscopic training, SBT has gained attention because it provides a way of training without the risk of adverse events to patients, and allows for standardization of feedback through the simulation[5,17,18]. Virtual reality simulators can model endoscopy by using an endoscope that is inserted into a computer-based module which displays the gastrointestinal lumen on a screen, and provides visual and tactile feedback related to the procedure[13].

CURRENT STATE OF EVIDENCE IN VIRTUAL-REALITY SBT IN ENDOSCOPY

Previous systematic reviews and meta-analyses have effectively analyzed the results of previous studies, including a report of internal validity of the existing literature[5,17,18]. Briefly, to date there have been 21 major RCTs investigating VR simulation and its role in training (Table 1). 10 of these have studies investigated VR in colonoscopy, 5 in organic gastrointestinal disease (OGD), 3 in flexible sigmoidoscopy, and 3 in endoscopic retrograde cholangiopancreatography ERCP (Table 1)[19-39].

SBT vs apprenticeship model

18 studies investigated SBT and compared it to either no training or conventional model of learning. 16 of the RCTs reported positive results for SBT, *i.e.*, improved outcomes. Of note is that in the 16 RCTs that reported positive results, SBT was either used in conjunction with conventional teaching, or the control arm did not receive any conventional teaching before the assessment period. A closer look at the two negative trials by Gerson and Sedlack reveal several reasons that can explain the results[19,20,33]. In the trial by Gerson and Dam, the SBT group had unlimited access for two weeks to didactic modules and six simulated OGD cases on a VR simulator, with no external feedback or observation, while the conventional training group completed 10 OGDs with supervision from staff endoscopists[20]. As a result, the SBT group completed fewer procedures independently

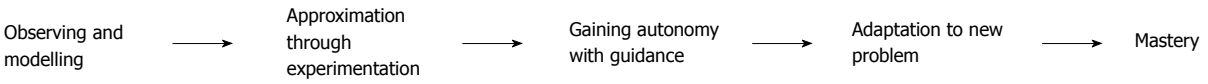

Figure 1 Progression of learning in the apprenticeship model. The apprenticeship model relies on the trainee modelling after an expert, followed by experimentation and approximation that eventually lead to increased autonomy, adaptation to new problems and eventual mastery.

compared to the conventional training group. In the trial by Sedlack, there is no clear explanation for why the SBT group did worse, however the small sample size of 8 trainees and lack of feedback must be taken into consideration[33]. In other trials by Sedlack, trainees who received VR training in combination with conventional training achieved better overall ratings of competency and patient comfort[21,22]. These studies suggest that SBT may have a role in supplementing early endoscopy training. There is, however, no strong evidence to suggest the use of SBT as a replacement for conventional training, giving the limitation of a model in mimicking real life variables and complexities. Furthermore, there is no literature comparing SBT to apprenticeship training for ERCP or other advanced procedures.

SBT with feedback vs without feedback

Feedback is essential in SBT. Recently, Mahmood and Darzi showed that without feedback on performance, SBT does not augment learning[40]. Specifically, the delivery of feedback should be given with an awareness of the trainee's cognitive load[41]. Cognitive load is the effort used in working memory and has three types: intrinsic, extraneous, and germane[41,42]. Intrinsic load relates to essential components of the learning task, *i.e.*, endoscopy, while extrinsic load relates to non-essential tasks, such as distractions related to other staff members[42]. Germane load relates to forming learning schemas to consolidate the learning, *i.e.*, compartmentalizing concepts to gain mastery[42]. Learning is thought to occur when trainees form their own cognitive schemas that they can readily access[42]. In this setting, feedback can help the trainee through negotiating goals for the current session and setting goals for future sessions. Feedback delivered during endoscopic procedures should be minimal to reduce a trainee's cognitive load and should be directive. For example, the expert endoscopist may tell or show the trainee how to change their hand position while navigating the endoscope during the session[41]. This allows the trainee to incorporate that feedback during that endoscopy and learn from the mistake. After the session, facilitative feedback, which elicits trainee's thoughts should be used to help the trainee engage in reflective learning and develop problem solving skills[41]. This is supported by previous work suggesting that delayed feedback, when compared with immediate feedback, may be advantageous in the development of cognitive schemas[41,43].

Integration of SBT in curriculum

Another area of interest in endoscopic training is whether SBT should be embedded in structured curriculum or self-directed curriculum. The benefit of self-directed curriculum is that it allows learners to set their own learning goals and pace their learning[44]. However, this is usually best suited for knowledge sharing that is meant to be sustained for a lifetime or for knowledge that is meant to be applied in varied situations after being acquired in one setting - for example, medical students learning pathophysiology that they will be expected to apply on clinical rotations[45]. Structured learning has a set goal for the trainee, and a trainer to help accomplish that goal[44]. This goal can be in a form of a certain skill or concept. Structured learning works best for teaching cognitive concepts and technical skills. Grover *et al*[30] investigated SBT as part of a structured curriculum compared to self-regulated curriculum, and found that structured curriculum led to better acquisition of technical and non-technical skills that transferred to the clinical setting. The authors concluded that when using SBT to augment the conventional teaching model, it should be through a structured curriculum that encompasses the cognitive, technical, and integrative skills needed for endoscopy.

Structured curricula can be further enhanced by incorporating educational theory-based interventions. For example, two groups applied progressive learning to endoscopy curricula, which involved challenging the learner by increasing the task difficulty and/or complexity as the learner's abilities improves[29,31]. In both studies, the authors found that training regimens in which trainees encountered progressively more difficult cases led to improved technical skills in the trainees.

FUTURE DIRECTIONS

Simulation based training through virtual-reality modalities has a role in training the novice endoscopist with no or minimal prior experience in endoscopy. SBT offers the opportunity to practice endoscopy in a risk-free environment prior to first patient contact. It is, however, necessary for trainees to undergo patient-based training with an expert endoscopist. Despite the high fidelity of simulators, it difficult to replicate all the variables that a trainee would encounter during a real patient experience, including the non-technical aspects of endoscopy that need to be mastered. As medical education moves towards a competency-based framework, one area that requires elucidation is level of expertise or competency required in the simulated setting before to moving onto a real patient. Currently, this distinction is unclear and merits further evaluation. Moreover, the use of educational constructs in SBT should be further explored. Furthermore, there is no data in the literature to date on the cost-effectiveness of VR simulation in endoscopy,

Table 1 Summary of randomized controlled trials

Ref.	Sample size	Intervention	Outcomes
Flexible Sigmoidoscopy			
Tuggy *et al*[19]	10	Group 1: VR simulation Group 2: No simulation	Group 1 performed better: Faster mean completion time (323 s *vs* 654 s), lower directional errors (1.6% *vs* 8.6%), higher % of colon visualized (79% *vs* 45%)
Gerson *et al*[20]	16	Group 1: VR simulation Group 2: Conventional teaching	Group 1 performed worse: Lower mean score (2.9 *vs* 3.8 out of 5), lower cases completed independently (29% *vs* 72%), lower retroflexion completed (56% *vs* 84%); average time, patient satisfaction did not differ
Sedlack *et al*[21]	38	Group 1: VR simulation Group 2: Conventional teaching	Group 1 performed better: Higher patient comfort; procedural skills (independence, identifying pathology, landmarks, performing biopsies, adequate visualization) did not differ
Colonoscopy			
Sedlack *et al*[22]	8	Group 1: VR simulation Group 2: No simulation	Group 1 performed better in first 30 procedures: High depth of unassisted insertion, higher % of procedures completed independently (64.1% *vs* 56.3%), high scores on other measures such as ability to insert in a safe manner, adequality visualize mucosa, identify landmarks; mean time to reach maximum insertion did not differ
Ahlberg *et al*[23]	12	Group 1: VR simulation Group 2: No simulation	Group 1 performed better: Higher rates of insertion to cecum (52% *vs* 19%), shorter procedure time (30 min *vs* 40 min), less patient discomfort
Cohen *et al*[24]	45	Group 1: VR simulation Group 2: No simulation	Group 1 performed better: Higher competence scores as judged by ability to reach the transverse colon and cecum without assistance (92.7% *vs* 90.9% by Session 10); patient comfort did not differ
Park *et al*[25]	24	Group 1: VR simulation Group 2: No simulation	Group 1 performed better: Higher global ratings (17.9 *vs* 14.8 out of 35) based on technique, use of controls, flow of procedures, advancement.
Yi *et al*[26]	11	Group 1: VR simulation Group 2: No simulation	Group 1 performed better: Higher scores during colonoscopy. Higher number of procedures completed independently (76% *vs* 43%), higher patient comfort; no difference in time or visualization of mucosa
Haycock *et al*[27]	36	Group 1: VR simulation Group 2: Conventional teaching	Group 1 performed better: Higher completion rates (95% *vs* 70%) and shorter times (407 s *vs* 743 s), higher patient comfort, higher use of correction abdominal pressure (79% *vs* 52%), lower insertion force; other variables such as number of transverse loops, correct use of variable stiffness did not differ
McIntosh *et al*[28]	18	Group 1: VR simulation Group 2: No simulation	Group 1 performed better: Less instances of requiring assistance (1.94 *vs* 3.43), greater unassisted insertion depth (43 cm *vs* 24 cm), greater rate of cecal intubation (26% *vs* 10%), high overall competence scores; patient comfort did not differ
Gomez *et al*[29]	27	Group 1: VR simulation + benchtop simulation Group 2: VR simulation Group 3: Benchtop simulation	Group 1 and 2 improved: Performed better on post-test compared to pre-test through Global Assessment of Gastrointestinal Endoscopic Skills tool (navigation, strategies, clear lumen and quality of examination)
Grover *et al*[30]	33	Group 1: Self-regulated learning with VR simulation Group 2: Structured curriculum with VR simulation	Group 1 and 2 improved; Group 2 performed better: Both groups improved on colonoscopy-specific performance; Group 2 performed better based on Joint Advisory Group on GI Endoscopy's Direct Observation of Procedural Skills Tool (JAG DOPS), had better communication rating, and better integrated global rating
Grover *et al*[31]	37	Group 1: Progressive learning with VR simulation Group 2: Non-progressive learning with benchtop simulator	Group 1 performed better: Higher JAG DOPS score, communication and integrated global rating
Esophagogastroduodenoscopy			
Di Giulio *et al*[32]	22	Group 1: VR simulation Group 2: No simulation	Group 1 performed better: Higher number of completed procedures (87.8% *vs* 70%), required less assistance (41.3% *vs* 97.9%), overall performance was better; length of time was not significantly different
Sedlack *et al*[33]	8	Group 1: VR simulation Group 2: No simulation	Group 1 performed worse: Lower patient comfort (5 *vs* 6), independence and competence scores
Shirai *et al*[34]	20	Group 1: VR simulation + Conventional teaching Group 2: Conventional teaching	Group 1 performed better: Required less direct assistance (8.6% *vs* 25.9%), higher score on 11 items scored during the procedure; no significant difference in completion time
Ferlitsch *et al*[35]	28	Group 1: VR simulation Group 2: No simulation	Group 1 performed better: Decreased total time to reach duodenum (239 s *vs* 310 s); higher technical accuracy; diagnostic accuracy did not differ
Ende *et al*[36]	29	Group 1: VR simulation + Conventional teaching Group 2: Conventional teaching Group 3: VR simulation alone	Group 1 and 2 improved: Improvement in time within group (195 s *vs* 119 s; 261 s *vs* 150 s); no significant difference in between groups All groups showed improvement in post-intervention manual skills test score. None of the other outcomes reached statistical significance, such as time to intubate esophagus
Endoscopic retrograde cholangiopancreatography (ERCP)			
Lim *et al*[37]	16	Group 1: Mechanical simulator Group 2: No simulator	Group 1 performed better: Improved cannulation rates (47.1% *vs* 69.6%), decreased total time (4.7 *vs* 10.3 mins); overall performance score not significantly different.

Liao *et al*[38]	16	Group 1: Mechanical simulator Group 2: No simulator	Group 1 performed better: Improved cannulation rates (73.25% *vs* 47.35%) and improve overall performance; benefit of single *vs* multiple simulator practices was not statistically significant.
Meng *et al*[39]	5	Group 1: Mechanical simulator Group 2: No simulator	Group 1 performed better: Improved cannulation rates (79.4% *vs* 61.5%), lower total time (19.38 min *vs* 26.31 min), and improved overall performance score.

Summary of 21 randomized controlled trials investigating endoscopic techniques, including flexible sigmoidoscopy, colonoscopy, organic gastrointestinal disease and endoscopic retrograde cholangiopancreatography, including sample size, groups in the study and summary of results. Conventional training refers to the apprenticeship model.

which can be expensive in terms of capital costs and costs associated with physician-trainers.

Feedback

During SBT, feedback is often provided by an expert that provides through verbal cues and instructions, and/or by performance metrics from the VR simulator. There are several ways to enhance the delivery of feedback. First, before each simulation session, trainees can be encouraged to document and share their objectives with the expert endoscopist, helping them form a habit of being conscious of their goals during each endoscopic procedure. This enhances learning as it provides the trainer and trainee with a specific goal to comment upon[41]. Moreover, taking the feedback from one session, the trainees can be encouraged to reflect upon what they will change in their next session, allowing them to understand how to integrate feedback into their training[41]. SBT in procedural settings allows trainees to observe how incorporating feedback into their next session can result in better outcomes, as other extraneous variables will be controlled. Feedback can be incorporated into endoscopy curricula through gamification, where similar to a game, incremental increase in difficulty and ability to achieve certain goalposts will indicate the level of skill in a trainee[46]. Second, SBT can be used to help identify trainees that are struggling early in their training and allow programs to supplement their learning. Finally, SBT allows for video-recording of procedures and for trainees to watch videos of both their own performance and expert performance. In endoscopy, watching these videos is associated with improved trainee self-assessment skills over time[47].

Non-technical skills

Non-technical components of the endoscopic procedure include communication and teamwork, judgement and decision making, leadership, and situational awareness[48]. Non-technical skills are difficult to teach, especially in a setting where the patient may be partially sedated or even awake. Soft skills in medicine are often taught through role modeling, *i.e.*, apprenticeship[49]. Similarly, non-technical skills in endoscopy are often taught in the endoscopy suite. However, using high fidelity simulation with standardized patients and actors playing the role of nursing staff to simulate integration scenarios can be used help prime trainees to the non-technical skills of endoscopy[30].

Emergencies during endoscopy

Dealing with emergencies during endoscopy can be a very stressful experience for trainees. Currently, SBT is limited to polypectomies and other routine procedures, though it may be expanded to include more emergent cases. Similar to Code Blue training, Kiesslich *et al*[50] showed that simulation training was associated with better endoscopic performance and crisis management in endoscopic emergencies. Additionally, randomized trials in Advanced Cardiac Life Support simulation revealed improved performance in the simulator-trained groups[51]. SBT allows for trainees to practice the shared mental model and crisis resource management[50]. Further studies randomized trials can explore these concepts.

Ergonomics

Recently, the importance of ergonomics in endoscopy has become evident. Studies have indicated a high prevalence of musculoskeletal disorders ranging from 37%-89% among endoscopists[52]. These injuries are thought to be due to repeated pinching or gripping, pushing, pulling and torquing of the endoscope in potentially awkward postures[53]. Currently, there are no guidelines for optimal ergonomic position due to individual differences in anthropometry. Rather than strict guidelines about positioning during procedures and endoscope handling, some general guidelines may be more valuable. For instance, for computer workstations, guidelines give users recommendations such as keeping the elbow at a right angle with the forearm, which should be parallel to the ground[54]. In endoscopy, posture while doing the procedure should be neutral without excessive bending. Trainees often tend to bend their body unconsciously when trying to get a better view on the screen. Other tips include to use the endoscope as a lever to reduce right hand torqueing, using a neutral thumb grip position, using gauze with right-hand grip to reduce pressure, and using the left-hand pinky grip technique to reduce right-hand strain in difficult or tight endoscope positions[55]. SBT can be used to teach these skills to the trainees by helping them practice posturing with a model that mimics the physical aspects of the endoscope workstation. Studies assessing the effectiveness of SBT to teach ergonomics are lacking.

CONCLUSION

SBT is an important supplement to conventional training

to help facilitate learning of endoscopy with no risk to patients. There is, however, insufficient evidence to advocate for SBT as a replacement for conventional training due to its limitation in mimicking real life. Current simulation training curricula may be enhanced with additional focus on the delivery of feedback and the integration of educational theory based strategies. Future studies should broaden the context in which SBT is studied or utilized.

REFERENCES

1 **Ziv A**, Ben-David S, Ziv M. Simulation based medical education: an opportunity to learn from errors. *Med Teach* 2005; **27**: 193-199 [PMID: 16011941 DOI: 10.1080/01421590500126718]
2 Simulation-Based Learning. Available from: URL: https://www.learning-theories.org/doku.php?id=instructional_design:simulation-based_learning
3 **Al-Elq AH**. Simulation-based medical teaching and learning. *J Family Community Med* 2010; **17**: 35-40 [PMID: 22022669 DOI: 10.4103/1319-1683.68787]
4 **Cook DA**, Hatala R, Brydges R, Zendejas B, Szostek JH, Wang AT, Erwin PJ, Hamstra SJ. Technology-enhanced simulation for health professions education: a systematic review and meta-analysis. *JAMA* 2011; **306**: 978-988 [PMID: 21900138 DOI: 10.1001/jama.2011.1234]
5 **Walsh CM**, Sherlock ME, Ling SC, Carnahan H. Virtual reality simulation training for health professions trainees in gastrointestinal endoscopy. *Cochrane Database Syst Rev* 2012; CD008237 [PMID: 22696375 DOI: 10.1002/14651858.CD008237.pub2]
6 **Triantafyllou K**, Lazaridis LD, Dimitriadis GD. Virtual reality simulators for gastrointestinal endoscopy training. *World J Gastrointest Endosc* 2014; **6**: 6-12 [PMID: 24527175 DOI: 10.4253/wjge.v6.i1.6]
7 Cognitive Apprenticeship. Available from: URL: https://www.learning-theories.org/doku.php?id=instructional_design:cognitive_apprenticeship
8 **Rassie K**. The apprenticeship model of clinical medical education: time for structural change. *N Z Med J* 2017; **130**: 66-72 [PMID: 28859068]
9 **Ataizi M**. Situated Learning. In: Seel NM. Encyclopedia of the Sciences of Learning. Boston, Springer 2012
10 **Bini EJ**, Firoozi B, Choung RJ, Ali EM, Osman M, Weinshel EH. Systematic evaluation of complications related to endoscopy in a training setting: A prospective 30-day outcomes study. *Gastrointest Endosc* 2003; **57**: 8-16 [PMID: 12518123 DOI: 10.1067/mge.2003.15]
11 **Matharoo M**, Haycock A, Sevdalis N, Thomas-Gibson S. A prospective study of patient safety incidents in gastrointestinal endoscopy. *Endosc Int Open* 2017; **5**: E83-E89 [PMID: 28191498 DOI: 10.1055/s-0042-117219]
12 **Dunkin BJ**. Flexible endoscopy simulators. *Semin Laparosc Surg* 2003; **10**: 29-35 [PMID: 12695807]
13 **Sedlack RE**. The state of simulation in endoscopy education: continuing to advance toward our goals. *Gastroenterology* 2013; **144**: 9-12 [PMID: 23149221 DOI: 10.1053/j.gastro.2012.11.007]
14 **Kim JS**, Kim BW. Training in Endoscopy: Esophagogastroduodenoscopy. *Clin Endosc* 2017; **50**: 318-321 [PMID: 28783922 DOI: 10.5946/ce.2017.096]
15 **Desilets DJ**, Banerjee S, Barth BA, Kaul V, Kethu SR, Pedrosa MC, Pfau PR, Tokar JL, Varadarajulu S, Wang A, Wong Kee Song LM, Rodriguez SA; ASGE Technology Committee. Endoscopic simulators. *Gastrointest Endosc* 2011; **73**: 861-867 [PMID: 21521562 DOI: 10.1016/j.gie.2011.01.063]
16 **Riegler A**. Constructivism. In: L'Abate L. Paradigms in theory construction. New York: Springer, 2012: 235-256
17 **Singh S**, Sedlack RE, Cook DA. Effects of simulation-based training in gastrointestinal endoscopy: a systematic review and meta-analysis. *Clin Gastroenterol Hepatol* 2014; **12**: 1611-1623.e4 [PMID: 24509241 DOI: 10.1016/j.cgh.2014.01.037]
18 **Khan R**, Plahouras J, Johnston BC, Scaffidi MA, Grover SC, Walsh CM. Virtual reality simulation training for health professions trainees in gastrointestinal endoscopy. *Cochrane Database Syst Rev* 2018; **8**: CD008237 [PMID: 30117156 DOI: 10.1002/14651858.CD008237.pub3]
19 **Tuggy ML**. Virtual reality flexible sigmoidoscopy simulator training: impact on resident performance. *J Am Board Fam Pract* 1998; **11**: 426-433 [PMID: 9875997]
20 **Gerson LB**, Van Dam J. A prospective randomized trial comparing a virtual reality simulator to bedside teaching for training in sigmoidoscopy. *Endoscopy* 2003; **35**: 569-575 [PMID: 12822091 DOI: 10.1055/s-2003-40243]
21 **Sedlack RE**, Kolars JC, Alexander JA. Computer simulation training enhances patient comfort during endoscopy. *Clin Gastroenterol Hepatol* 2004; **2**: 348-352 [PMID: 15067632]
22 **Sedlack RE**, Kolars JC. Computer simulator training enhances the competency of gastroenterology fellows at colonoscopy: results of a pilot study. *Am J Gastroenterol* 2004; **99**: 33-37 [PMID: 14687137]
23 **Ahlberg G**, Hultcrantz R, Jaramillo E, Lindblom A, Arvidsson D. Virtual reality colonoscopy simulation: A compulsory practice for the future colonoscopist? *Endoscopy* 2005; **37**: 1198-204
24 **Cohen J**, Cohen SA, Vora KC, Xue X, Burdick JS, Bank S, Bini EJ, Bodenheimer H, Cerulli M, Gerdes H, Greenwald D, Gress F, Grosman I, Hawes R, Mullin G, Schnoll-Sussman F, Starpoli A, Stevens P, Tenner S, Villanueva G. Multicenter, randomized, controlled trial of virtual-reality simulator training in acquisition of competency in colonoscopy. *Gastrointest Endosc* 2006; **64**: 361-368 [PMID: 16923483 DOI: 10.1016/j.gie.2005.11.062]
25 **Park J**, MacRae H, Musselman LJ, Rossos P, Hamstra SJ, Wolman S, Reznick RK. Randomized controlled trial of virtual reality simulator training: transfer to live patients. *Am J Surg* 2007; **194**: 205-211 [PMID: 17618805 DOI: 10.1016/j.amjsurg.2006.11.032]
26 **Yi SY**, Ryu KH, Na YJ, Woo HS, Ahn W, Kim WS, Lee DY. Improvement of colonoscopy skills through simulation-based training. *Stud Health Technol Inform* 2008; **132**: 565-567 [PMID: 18391369]
27 **Haycock A**, Koch AD, Familiari P, van Delft F, Dekker E, Petruzziello L, Haringsma J, Thomas-Gibson S. Training and transfer of colonoscopy skills: a multinational, randomized, blinded, controlled trial of simulator versus bedside training. *Gastrointest Endosc* 2010; **71**: 298-307 [PMID: 19889408 DOI: 10.1016/j.gie.2009.07.017]
28 **McIntosh KS**, Gregor JC, Khanna NV. Computer-based virtual reality colonoscopy simulation improves patient-based colonoscopy performance. *Can J Gastroenterol Hepatol* 2014; **28**: 203-206 [PMID: 24729994]
29 **Gomez PP**, Willis RE, Van Sickle K. Evaluation of two flexible colonoscopy simulators and transfer of skills into clinical practice. *J Surg Educ* 2015; **72**: 220-227 [PMID: 25239553 DOI: 10.1016/j.jsurg.2014.08.010]
30 **Grover SC**, Garg A, Scaffidi MA, Yu JJ, Plener IS, Yong E, Cino M, Grantcharov TP, Walsh CM. Impact of a simulation training curriculum on technical and nontechnical skills in colonoscopy: a randomized trial. *Gastrointest Endosc* 2015; **82**: 1072-1079 [PMID: 26007221 DOI: 10.1016/j.gie.2015.04.008]
31 **Grover SC**, Scaffidi MA, Khan R, Garg A, Al-Mazroui A, Alomani T, Yu JJ, Plener IS, Al-Awamy M, Yong EL, Cino M, Ravindran NC, Zasowski M, Grantcharov TP, Walsh CM. Progressive learning in endoscopy simulation training improves clinical performance: a blinded randomized trial. *Gastrointest Endosc* 2017; **86**: 881-889 [PMID: 28366440 DOI: 10.1016/j.gie.2017.03.1529]
32 **Di Giulio E**, Fregonese D, Casetti T, Cestari R, Chilovi F, D'Ambra G, Di Matteo G, Ficano L, Delle Fave G. Training with a computer-based simulator achieves basic manual skills required for upper endoscopy: a randomized controlled trial. *Gastrointest Endosc* 2004; **60**: 196-200 [PMID: 15278044]
33 **Sedlack RE**. Validation of computer simulation training for esophagogastroduodenoscopy: Pilot study. *J Gastroenterol Hepatol* 2007; **22**: 1214-1219 [PMID: 17559386 DOI: 10.1111/j.1440-1746.2007.04841.x]
34 **Shirai Y**, Yoshida T, Shiraishi R, Okamoto T, Nakamura H, Harada T, Nishikawa J, Sakaida I. Prospective randomized study on the use of a computer-based endoscopic simulator for training in esophagogastroduodenoscopy. *J Gastroenterol Hepatol* 2008; **23**: 1046-1050 [PMID: 18554236 DOI: 10.1111/j.1440-1746.2008.05457.

x]
35 **Ferlitsch A**, Schoefl R, Puespoek A, Miehsler W, Schoeniger-Hekele M, Hofer H, Gangl A, Homoncik M. Effect of virtual endoscopy simulator training on performance of upper gastrointestinal endoscopy in patients: a randomized controlled trial. *Endoscopy* 2010; **42**: 1049-1056 [PMID: 20972956 DOI: 10.1055/s-0030-1255818]
36 **Ende A**, Zopf Y, Konturek P, Naegel A, Hahn EG, Matthes K, Maiss J. Strategies for training in diagnostic upper endoscopy: a prospective, randomized trial. *Gastrointest Endosc* 2012; **75**: 254-260 [PMID: 22153875 DOI: 10.1016/j.gie.2011.07.063]
37 **Lim BS**, Leung JW, Lee J, Yen D, Beckett L, Tancredi D, Leung FW. Effect of ERCP mechanical simulator (EMS) practice on trainees' ERCP performance in the early learning period: US multicenter randomized controlled trial. *Am J Gastroenterol* 2011; **106**: 300-306 [PMID: 20978485 DOI: 10.1038/ajg.2010.411]
38 **Liao WC**, Leung JW, Wang HP, Chang WH, Chu CH, Lin JT, Wilson RE, Lim BS, Leung FW. Coached practice using ERCP mechanical simulator improves trainees' ERCP performance: a randomized controlled trial. *Endoscopy* 2013; **45**: 799-805 [PMID: 23897401 DOI: 10.1055/s-0033-1344224]
39 **Meng W**, Leung JW, Yue P, Wang Z, Wang X, Wang H. Practice with ercp mechanical simulator (EMS) improves basic ercp skills of novice surgical trainees. *Gastrointest Endosc* 2016; **83**: AB267-AB268 [DOI: 10.1016/j.gie.2016.03.397]
40 **Mahmood T**, Darzi A. The learning curve for a colonoscopy simulator in the absence of any feedback: no feedback, no learning. *Surg Endosc* 2004; **18**: 1224-1230 [PMID: 15457382 DOI: 10.1007/s00464-003-9143-4]
41 **Dilly CK**, Sewell JL. How to Give Feedback During Endoscopy Training. *Gastroenterology* 2017; **153**: 632-636 [PMID: 28757268 DOI: 10.1053/j.gastro.2017.07.023]
42 **Leppink J**, van den Heuvel A. The evolution of cognitive load theory and its application to medical education. *Perspect Med Educ* 2015; **4**: 119-127 [PMID: 26016429 DOI: 10.1007/s40037-015-0192-x]
43 **Walsh CM**, Ling SC, Wang CS, Carnahan H. Concurrent versus terminal feedback: it may be better to wait. *Acad Med* 2009; **84**: S54-S57 [PMID: 19907387 DOI: 10.1097/ACM.0b013e3181b38daf]
44 Structured Learning *vs* Self-Directed Learning. Available from: URL: https://eimf.eu/structured-learning-vs-self-directed-learning/
45 **Hung W**, Jonassen DH, Liu R. Problem-Based Learning. *Handb Res Educ Commun Technol* 2008; **3**: 485-506
46 **Burke B**. Gamification 2020: What Is the Future of Gamification? Available from: URL: https://www.gartner.com/doc/2226015/gamification--future-gamification
47 **Khan R**, Scaffidi MA, Parker C, Al-Mazroui A, Tsui C, Iqbal S. Sa1089 The Influence of Video-Based Feedback on Self-Assessment Accuracy of Procedural Skills. *Gastrointest Endosc* 2017; **85**: AB186 [DOI: 10.1016/j.gie.2017.03.408]
48 **Haycock A**. Framework for observing and rating Endoscopic Non-Technical Skills. Available from: URL: https://www.thejag.org.uk/downloads/JAG training information/ENTS handbook v2.pdf
49 **Dyche L**. Interpersonal skill in medicine: the essential partner of verbal communication. *J Gen Intern Med* 2007; **22**: 1035-1039 [PMID: 17437144 DOI: 10.1007/s11606-007-0153-0]
50 **Kiesslich R**, Moenk S, Reinhardt K, Kanzler S, Schilling D, Jakobs R, Denzer U, Neumann M, Vollmer J, Schütz M, Heinrichs W, Neurath MF, Galle PR. [Combined simulation training: a new concept and workshop is useful for crisis management in gastrointestinal endoscopy]. *Z Gastroenterol* 2005; **43**: 1031-1039 [PMID: 16142611 DOI: 10.1055/s-2005-858542]
51 **Sahu S**, Lata I. Simulation in resuscitation teaching and training, an evidence based practice review. *J Emerg Trauma Shock* 2010; **3**: 378-384 [PMID: 21063561 DOI: 10.4103/0974-2700.70758]
52 **Shergill AK**, McQuaid KR, Rempel D. Ergonomics and GI endoscopy. *Gastrointest Endosc* 2009; **70**: 145-153 [PMID: 19559836 DOI: 10.1016/j.gie.2008.12.235]
53 **ASGE Technology Committee.**, Pedrosa MC, Farraye FA, Shergill AK, Banerjee S, Desilets D, Diehl DL, Kaul V, Kwon RS, Mamula P, Rodriguez SA, Varadarajulu S, Song LM, Tierney WM. Minimizing occupational hazards in endoscopy: personal protective equipment, radiation safety, and ergonomics. *Gastrointest Endosc* 2010; **72**: 227-235 [PMID: 20537638 DOI: 10.1016/j.gie.2010.01.071]
54 **Wahlström J**. Ergonomics, musculoskeletal disorders and computer work. *Occup Med* (Lond) 2005; **55**: 168-176 [PMID: 15857896 DOI: 10.1093/occmed/kqi083]
55 **Chang MA**, Mitchell J, Abbas Fehmi SM. Optimizing ergonomics during endoscopy. *VideoGIE* 2017; **2**: 170 [PMID: 29905300 DOI: 10.1016/j.vgie.2017.03.005]

P- Reviewer: Eleftheriadis NP, Hosoe N **S- Editor**: Wang XJ
L- Editor: A **E- Editor**: Yin SY

World Journal of Gastroenterology

Submit a Manuscript: https://www.f6publishing.com

World J Gastroenterol 2018 December 28; 24(48): 5446-5453

DOI: 10.3748/wjg.v24.i48.5446

ISSN 1007-9327 (print) ISSN 2219-2840 (online)

MINIREVIEWS

Quality of life in patients with minimal hepatic encephalopathy

Lorenzo Ridola, Silvia Nardelli, Stefania Gioia, Oliviero Riggio

Lorenzo Ridola, Department of Medico-Surgical Sciences and Biotechnologies, Sapienza University of Rome, Latina 04100, Italy

Silvia Nardelli, Stefania Gioia, Oliviero Riggio, Department of Clinical Medicine, Sapienza University of Rome, Rome 00185, Italy

ORCID number: Lorenzo Ridola (0000-0002-8596-2609); Silvia Nardelli (0000-0002-8596-2609); Stefania Gioia (0000-0002-8596-2609); Oliviero Riggio (0000-0002-8596-2609).

Author contributions: Ridola L contributed to conception and design, analysis and interpretation of the data, drafting of the article, critical revision of the article for important intellectual content and final approval of the article; Nardelli S and Gioia S contributed to acquisition of data and critical revision of the article; Riggio O contributed to critical revision of the article for important intellectual content and final approval of the article.

Conflict-of-interest statement: The authors have declared no conflicts of interest.

Manuscript source: Invited manuscript

Corresponding author: Lorenzo Ridola, MD, PhD, Department of Medico-Surgical Sciences and Biotechnologies, Sapienza University of Rome, Corso della Repubblica, Latina 04110 Italy.
lorenzo.ridola@uniroma1.it
Telephone: +39-773-6556155
Fax: +39-773-6556155

Received: October 5, 2018
Peer-review started: October 5, 2018
First decision: November 1, 2018
Revised: November 8, 2018
Accepted: November 9, 2018
Article in press: November 9, 2018

Published online: December 28, 2018

Abstract

Minimal hepatic encephalopathy (MHE) represents the mildest type of hepatic encephalopathy (HE). This condition alters the performance of psychometric tests by impairing attention, working memory, psychomotor speed, and visuospatial ability, as well as electrophysiological and other functional brain measures. MHE is a frequent complication of liver disease, affecting up to 80% of tested patients, depending of the diagnostic tools used for the diagnosis. MHE is related to falls, to an impairment in fitness to drive and the development of overt HE, MHE severely affects the lives of patients and caregivers by altering their quality of life (QoL) and their socioeconomic status. MHE is detected in clinically asymptomatic patients through appropriate psychometric tests and neurophysiological methods which highlight neuropsychological alterations such as video-spatial orientation deficits, attention disorders, memory, reaction times, electroencephalogram slowing, prolongation of latency evoked cognitive potentials and reduction in the critical flicker frequency. Several treatments have been proposed for MHE treatment such as non-absorbable disaccharides, poorly absorbable antibiotics such rifaximin, probiotics and branched chain amino acids. However, because of the multiple diagnosis methods, the various endpoints of treatment trials and the variety of agents used in trials, to date the treatment of MHE is not routinely recommended apart from on a case-by-case basis. Aim of this review is analyze the burden of MHE on QoL of patients and provide a brief summary of therapeutic approaches.

Key words: Cirrhosis; Minimal hepatic encephalopathy; Covert hepatic encephalopathy; Health related quality of life

Core tip: Minimal hepatic encephalopathy (MHE) being related to falls, an impairment in fitness to drive and the development of overt hepatic encephalopathy (HE), severely affects the lives of patients and caregivers by altering their quality of life (QoL) and their socioeconomic status. The aim of this review is to analyze the burden of MHE on QoL of patients and provide a brief summary of therapeutic approaches.

Ridola L, Nardelli S, Gioia S, Riggio O. Quality of life in patients with minimal hepatic encephalopathy. *World J Gastroenterol* 2018; 24(48): 5446-5453
URL: https://www.wjgnet.com/1007-9327/full/v24/i48/5446.htm
DOI: https://dx.doi.org/10.3748/wjg.v24.i48.5446

INTRODUCTION

Hepatic encephalopathy (HE) is a complex neurological syndrome, typical of liver advanced liver disease, which determines a wide and complex spectrum of nonspecific neurological and psychiatric manifestations[1]. In its mild expression, minimal HE (MHE)[2,3], this condition impairs the performance of psychometric tests, such as working memory, psychomotor speed, and visuospatial ability, as well as electrophysiological and other functional brain measures, without, however, any evidence of apparent and classical clinical manifestations[4,5]. MHE is a frequent complication of liver disease and is considered as one of the worsts manifestations, severely affecting the life of patients and caregivers. Moreover, the cognitive impairment results in the use of more healthcare resources than other liver diseases[6-11]. Depending on the population studied and the diagnostic tool used, MHE incidence may vary, ranging between 20% and 80% of patients with cirrhosis[12-17]. A full overview of the different diagnostic modalities of MHE has been recently published[18]. MHE, involves the areas of attention, alertness, response inhibition, and executive functions[19-22] reducing the safety and quality of life (QoL), both of patients and caregivers. Moreover, those patients show also sleep disorders[23-26] and deficits in specific activities such as driving, which are dangerous for themselves and for others. As low-grade HE (grade Ⅰ) is difficult to diagnose, the term "covert" has been recently introduced combining MHE and Grade Ⅰ HE[27]. The term "covert" has been debated since the condition is simply not overt, obvious and severe or clinically unquestionable, but is not really unapparent (latent, subclinical, minimal). Finally, MHE and covert hepatic encephalopathy (CHE) are well known risk factors for the development of overt hepatic encephalopathy (OHE). In fact, the risk for a first episode of OHE range from 5% and 25% within 5 years after cirrhosis diagnosis, depending on risk factors, such as other complications related to cirrhosis (MHE or CHE, infections, variceal bleeding, or ascites) and possibly diabetes and hepatitis C[28-33]. Under this light, it appears clear that the presence of MHE has a detrimental role on the QoL of patient and, at this regard, a survey of the American Association for the Study of Liver Diseases of 2007[34], showed that most clinicians believe MHE to be a significant problem, remaining unfortunately under investigated. In fact, only 50% of clinicians had screened their patients for MHE, and 38% had never studied their patients with liver cirrhosis using psychometric assessment. MHE impairs patients' QoL, increases the occurrence of disability, and has a negative effect on their daily activities. The impact of the perception of the disease, in the form of a "Sickness Impact Profile (SIP)", has been investigated in patients with cirrhosis to assess QoL indicators, *i.e.,* sleep, rest, eating, work, home management, recreation, walking, daily care, movement and emotional behavior. These conditions resulted significantly altered in patients with MHE compared to individuals without MHE[35]. In addition, in the presence of MHE, QoL indicators, such as the capacity to drive a car, and the incidence of sleep disorders were impaired[36]. Aim of this review is analyze the burden of MHE on quality of life of patients and provide a summary of the proposed therapeutic approaches.

IMPACT OF MHE ON QOL

Although liver cirrhosis presents a poor prognosis, recent findings in diagnosis, therapeutic strategies and general management of this disease have significantly improved survival rates. Several studies have shown that liver diseases severely worsen the health-related QoL (HRQoL)[37-39], especially in relation to hospitalizations, severity of the disease, and its complications such as recurrent HE or OHE, as well as the coexistence of sleep disorders[40]. Recent evidence suggests that OHE leads to persistent cognitive impairment even after its resolution.

In accordance with the growing interest in the central role of perception in a patient's state of health, the evaluation of HRQoL is acquiring importance in clinical practice as well as in planning therapeutic strategies. It has in fact already been shown that "quality" and "disability" of daily life have a stronger impact than "longevity" on patients' expectation of life[41]. A series of evidences show that HRQoL may appear to be influenced by the coexistence of MHE[10,35,36,42-45]. These findings have enhanced the interest to verify whether the specific treatment of these condition could lead to a consequent improvement in HRQoL. In decompensated cirrhosis, MHE worsens the domains of activity, emotional function and global scoring on the chronic liver disease questionnaire (CLDQ). MHE also alters appetite in cirrhosis and, consequently the liver function impairment, a condition of malnutrition occurs adversely impacting quality of life[46]. Prasad *et al*[10] showed more than 10 years ago that lactulose treatment of MHE patients significantly improved not only psychometric performance, but also their HRQoL. In 75% of patients with MHE resolution, a significant improvement in the "SIP" and a correlation between improvement in psychometric performance and QoL were observed[43].

Furthermore, Sanyal *et al*[47] demonstrated that the chronic administration of rifaximin in patients without OHE at enrollment, but with a history of recurring HE, significantly improved HRQoL.

Strongly related with QoL is, in our opinion, the relationship between MHE and falls. In fact, patients with liver cirrhosis are at risk of fractures due to osteoporosis secondary to malnutrition, hypogonadism and liver failure[48-50]. The injuries, especially fractures and subsequent surgical sequelae, and related hospitalizations, determine morbidity and mortality in patients with cirrhosis[51] and therefore can be considered well related with QoL. The falls and subsequent fractures also have a serious impact on the patient's family and community and have a high economic impact[52,53]. Román *et al*[54] have shown that, because of falls, the need for healthcare (8.8% *vs* 0%, P = 0.004), whereas hospitalization (6.6% *vs* 2.3%, P = NS) was greater in patients with MHE than in cirrhotic patients without MHE. Multivariate analysis identified MHE [odds ratio (OR) = 2.91, 95% confidence interval (CI): 1.13-7.48, P = 0.02], in addition to a previous history of OHE (OR = 2.87, 95%CI: 1.10-7.50, P = 0.03) and taking psychoactive drugs (OR = 3.91, 95%CI: 0.96-15.9, P = 0.05), as factors independently associated with falls. These findings were subsequently confirmed by Soriano *et al*[55] in a larger patient cohort. The authors were able to conclude, using multivariate analysis, that the presence of cognitive impairment, or the presence of MHE diagnosed by an abnormal Psychometric Hepatic Encephalopathy Score (PHES) were the only independent factors predictive of a fall (OR = 10.2 95%CI: 3.4-30.4, P < 0.001). Moreover, the probability of a fall in one year was found to be significantly higher in patients with MHE (52% *vs* 6.5%, P < 0.0001) compared to those without MHE. Urios *et al*[56] demonstrated that patients with MHE show an altered balance, mainly if evaluated on an unstable surface with eyes open, with longer reaction and confinement times and lower success in stability test limits, than patients free from MHE. Finally, patients with MHE may experience also sleep disorders, severely affecting quality of life. Singh *et al*[57] evaluated sleep disorders in MHE and assess the effect of lactulose on sleep disturbances and HRQoL, concluding that excessive sleepiness on day time and an impairment in sleep quality are common in patients with MHE. The administration of lactulose also leads to improvement in MHE as well as sleep disturbances and HRQoL.

MHE AND HRQOL ASSESSMENT

There is no single optimal measure to assess the presence of MHE. In fact, none of the methods proposed cover all aspects of HE, appropriate norms are needed for a good sensitivity and specificity in identifying patients at risk of overt HE, the rate of pathological results in patient groups without overt HE differs markedly and finally the results of the various methods are not consistent. However, with a significant negative impact on the daily lives of patients and caregivers, MHE is still likely to be ignored by most clinicians if standards of neuropsychological testing are not followed while testing a patient for MHE. Magnetic resonance imaging has recently proposed with promising results to assess the presence of MHE[58,59]. A comprehensive review on the diagnostic modalities was previously published by our group[18].

SIP

The SIP questionnaire (Medical Outcome Trust, Boston, MA) was used to assess the influence of disease and treatment on daily functioning. The questionnaire is based on 136 items grouped into 12 scales (sleep and rest, eating, work, home management, recreation and pastimes, ambulation, mobility, body care and movement, social interaction, alertness, emotional behavior, and communication)[60]. The SIP provides the opportunity to calculate a total score, ranging from 0 (best) to 100 (worst), and patients mark only items that relate to their health at that time. Change in the total SIP score after a predetermined period of time of treatment or follow-up could be a measure of change in overall HRQoL.

CLDQ

The CLDQ is a validated tool for evaluating quality of life in subjects with chronic liver disease[61]. The CLDQ contains 29 items grouped in six domains: abdominal symptoms (three items), fatigue (five items), systemic symptoms (five items), activity (three items), emotional function (eight items) and worry (five items). For each question patients were ranked on a 7-point scale, with higher scores indicating better HRQoL. Data are presented by domain, overall and by items.

Short Form-36

Short Form-36 (SF-36) is a paper-pencil test corrected for age, education and occupation of a healthy Italian population sample[62], which investigates the full range of the patient's health status by 36 multiple-choice questions. The test measures eight domains, four in the area of "physical health" (physical functioning, role limitation-physical, bodily pain, general health) and four in the area of "mental health" (role limitation-emotional, vitality, mental health and social functioning). Each domain is scored between 0 and 100 points, when higher scores indicate a better HRQoL. It includes a final question on the patient's perception of changes in his/her health condition in the previous 12 mo. The physical component summary (PCS) and the mental component summary (MCS) may also be computed. The SF-36 has a strength limitation, it is validated only in italian population.

THE ROLE OF MHE TREATMENT ON QOL

MHE and CHE can alter severely patient's daily life, and in certain cases (*e.g.*, impairment of driving skills or work performance, poor QoL, or cognitive complaints) the

Table 1 Published studies aimed to assess the role of treatment on quality of life of patients with minimal hepatic hencephalopathy

Author	Year	Study type	MHE/CHE diagnosis	Active treatment (s)	Patients treated	Weeks of treatment	Objectives	Main results
Prasad *et al*[10]	2007	Original, randomized	NCT A, NCT B, FCT A, FCT B, PC, BDT	Lactulose	45 (25)	12	Psychometry, QoL	Significant improvement in psychometry: $P < 0001$; and QoL: $P < 0.002$. Improvement in HRQoL was related to the improvement in psychometry.
Sidhu *et al*[43]	2011	Original, randomized	NCT A, FCT A, Digit Symbol test, BDT, PC	Rifaximin	94 (49)	8	MHE reversal, QoL	MHE reversal in 37/49 *vs* 9/45. Improvement in QoL. Improvement in HRQoL correlated with improvement in psychometry
Sidhu *et al*[65]	2016	Original, randomized	NCT A, FCT A, Digit Symbol test, BDT, PC	Lactulose *vs* Rifaximin	112 (55/57)	12	MHE reversal, QoL	MHE reversal in 38/55 and in 42/57; HRQoL was significantly improved in both groups
Mittal *et al*[68]	2011	Original, randomized	NCT A, NCT B, FCT A, FCT B, PC, BDT	Lactulose or Probiotics or LOLA	160 (40/40/40)	12	Psychometry, ammonia, QoL	MHE reversal in 19/40 *vs* 14/40 *vs* 14/40 *vs* 4/40. Improvement in QoL.
Bajaj *et al*[72]	2008	Original, randomized	NCT A, Digit Symbol Test, BDT	Probiotic yogurt	25 (17)	8	MHE reversal, OHE development, QoL, ammonia, cytokines	MHE reversal in 71% *vs* 0%; OHE development in 0% *vs* 25%; no differences in QoL and cytokine Levels. Excellent adherence in cirrhotics after probiotic yogurt supplementation with potential for long-term adherence
Bajaj *et al*[81]	2011	Original, randomized	NCT A, NCT B, Digit Symbol test, BDT, ICT	Rifaximin	42 (21)	8	Psychometry, QoL, driving ability, anti-inflammatory interleukins	Improvement in psychometry, driving performance and QoL
Malaguarnera *et al*[76]	2018	Original, Observational	NCT-A, NCT-B, LTT, SDT, DST	Resveratrol	35 (35)	Variable	QoL, ammonia levels	Resveratrol showed efficacy in the treatment of depression, anxiety, and ammonia serum levels, and improved the quality of life Of MHE patients.
Malaguarnera *et al*[77]	2011	Randomized, double-blind, placebo-controlled study.	TMT-A, TMT-B	Acetyl-L-carnitine twice a day	33 (34)	13	Clinical and laboratory assessments, psychometric tests and automated electroencephalogram (EEG) analysis and QoL evaluations	treatment is associated with significant improvement in patient energy levels, general functioning and well-being. The improvement of quality of life is associated with reduction of anxiety and depression.
Zhang *et al*[82]	2015	Original	NCT A, NCT B, Digit Symbol test	Rifaximin	26 (26)	1	Psychometry, ammonia, SIBO	MHE reversal in 15/26; reduction in SIBO and ammonia levels
Bajaj *et al*[83]	2014	Original, randomized	NCT A NCT B, Digit Symbol test, BDT	Probiotics	30 (14)	8	Psychometry, ammonia, inflammatory markers, QoL	Reduction in endotoxin and TNF-α but not in cytokines. No effects on psychometric performance
Luo *et al*[84]	2011	Meta-analysis	Different diagnostic tools	Lactulose	434	Variable	Psychometry, ammonia levels, QoL, progression to OHE	Lactulose superior to placebo on all outcomes (psychometry: RR = 0.52, 95%CI: 0.44-0.62, $P < 0.00001$)

MHE: Minimal hepatic encephalopathy; OHE: Overt hepatic encephalopathy: HRQoL: Health related quality of life; NCT-A: Number connection test-A; NCT-B: Number connection test-B; BDT: Block design test; SDT: Serial dotting test; DST: Digit symbol test; LTT: Line tracing test; PHES: Psychometric hepatic encephalopathy score; ICT: Inhibitory control test; CFF: Critical flicker frequency; EEG: Electroencephalogram; ICT: Inhibitory control test; BCAA; Branched chain amino acids; SIBO: Small intestine bacterial overgrowt; CEP: Cognitive evoked potentials; TNF: Tumor necrosis factor.

indication to adopt any given pharmacological treatment may prevail. However, because of various methods used to assess the presence of MHE and CHE, the varying and multiple endpoints, the short-term treatment trials, and differing agents used in trials to date, recently published guidelines state that treatment of MHE and CHE is not routinely recommended apart from on a case-by-case basis[63]. Table 1 provides a complete overview of the studies of MHE treatment in the specific setting of QoL.

Concerning specific treatments, rifaximin is an oral non-systemic broad-spectrum antibiotic, similar to rifampin. Rifaximin, after concentrating in the gut, is able to modulate the intestinal to reduce intestinal ammonia and toxin formation. Bajaj *et al*[64] demonstrated that patients with MHE treated with rifaximin for an 8-wk period showed significantly greater improvements in the psychosocial dimension of the SIP and in driving and cognitive performance than patients treated with placebo. These results were confirmed in another randomized controlled trial (RCT), in which the authors demonstrated that rifaximin is significantly able to improve both cognitive functions and HRQoL in patients with MHE[43]. Recently, an RCT comparing rifaximin with lactulose for MHE reversal and HRQoL amelioration failed to demonstrate significant differences between groups[65].

Lactulose or lactitol are non-absorbable disaccharides used widely in the management of OHE. Lactulose is fermented in the colon, being metabolized to acetic and lactic acid, acidifying intestinal contents and conversion of ammonia (NH_3) to ammonium (NH_4^+) that is not systemically absorbed and is excreted in stool. Moreover, lactulose also has a cathartic effect, increasing nitrogen excretion fourfold. Although Prasad *et al*[10] concluded that lactulose treatment improves both cognitive function and HRQoL in MHE patients, most subsequent studies have not provided strong evidence confirming the efficacy of non-absorbable disaccharides in MHE treatment[43,66-69]. A meta-analysis evaluating the role of pharmacological treatment with non-absorbable disaccharides in patients with MHE failed to show clear evidence that any treatment played a convincing role in improving cognitive function and HRQoL[70].

Probiotics are live microorganisms and synbiotics are probiotics with the addition of fermentable fiber able to change the balance of intestinal microflora. The supposed mechanism of action is that, reducing intestinal bacterial urease activity, these drugs decrease the absorption of ammonia and other gut-derived toxins potentially involved in the pathogenesis of (M)HE. Seven recently published RCTs were aimed to evaluate the role of probiotic treatment/supplementation in treating MHE. Unfortunately, the results do not support the evidence on the efficacy in MHE reversal of a treatment with probiotics alone or in addition to other drugs[67-69,71-74]. In fact, no significant difference in the improvement of QoL, MHE, hospitalization rates, or progression to OHE has been reported when probiotics were compared with lactulose[75]. Carnitine a resveratrol have also been proposed with encouraging results in MHE treatments[76,77], as well as polyethylene glycol[78]; or nitazoxanide[79], actually proposed for OHE treatment, could be considered for future studies for MHE treatment. Finally, recently published European Association of Liver disease Clinical Practice Guidelines on Nutrition in chronic liver disease highlight to avoid protein restriction in patients with HE[80].

CONCLUSION

MHE and CHE represent a broad spectrum of neuropsychological manifestations of liver disease in which the detection of risk thresholds for the occurrence of OHE, impairment in daily life activities and in QoL has unfortunately not yet been well defined. Studies specifically aimed at establishing whether a treatment of MHE is able to affect clinically relevant endpoints are still needed[27]. The presence of minimal or CHE should be assessed following objective and universal modalities. Following this direction, only changes of psychometric tests should not be chosen as the main endpoint of the study; being only used as a criterion to include comparable patients. The sample size should be assessed according to clinically relevant endpoints, such as the quality of life or the occurrence of OHE during the follow up. For the assessment of the efficacy of a treatment in patients with MHE, the organization of large multicenter studies is considered mandatory, as well as a parallel design with a placebo or a no-treatment arm should be considered necessary. In this specific setting, the majority of studies enrolled patients with MHE diagnosed with different modality and studies have been designed with a different aim. Therefore, these evidences cannot be comparable, and we cannot draw unequivocal conclusions. Moreover, because MHE is a chronic condition, the tested drug should be administered for a very long period of time without significant side-effects. Among the emerging drugs, modulators of the intestinal bacterial flora should be the first candidates to be tested in this field. Future studies should fill the gaps in our knowledge.

REFERENCES

1 **Ferenci P**, Lockwood A, Mullen K, Tarter R, Weissenborn K, Blei AT. Hepatic encephalopathy--definition, nomenclature, diagnosis, and quantification: final report of the working party at the 11th World Congresses of Gastroenterology, Vienna, 1998. *Hepatology* 2002; **35**: 716-721 [PMID: 11870389 DOI: 10.1053/jhep.2002.31250]

2 **Gitlin N**, Lewis DC, Hinkley L. The diagnosis and prevalence of subclinical hepatic encephalopathy in apparently healthy, ambulant, non-shunted patients with cirrhosis. *J Hepatol* 1986; **3**: 75-82 [PMID: 3745889]

3 **Lockwood AH**. "What's in a name?" Improving the care of cirrhotics. *J Hepatol* 2000; **32**: 859-861 [PMID: 10845675]

4 **Amodio P**, Montagnese S, Gatta A, Morgan MY. Characteristics of minimal hepatic encephalopathy. *Metab Brain Dis* 2004; **19**: 253-267 [PMID: 15554421]

5 **McCrea M**, Cordoba J, Vessey G, Blei AT, Randolph C. Neuropsychological characterization and detection of subclinical hepatic encephalopathy. *Arch Neurol* 1996; **53**: 758-763 [PMID: 8759982]

6 **Rakoski MO**, McCammon RJ, Piette JD, Iwashyna TJ, Marrero

JA, Lok AS, Langa KM, Volk ML. Burden of cirrhosis on older Americans and their families: analysis of the health and retirement study. *Hepatology* 2012; **55**: 184-191 [PMID: 21858847 DOI: 10.1002/hep.24616]
7 **Kappus MR**, Bajaj JS. Covert hepatic encephalopathy: not as minimal as you might think. *Clin Gastroenterol Hepatol* 2012; **10**: 1208-1219 [PMID: 22728384 DOI: 10.1016/j.cgh.2012.05.026]
8 **Bajaj JS**, Riggio O, Allampati S, Prakash R, Gioia S, Onori E, Piazza N, Noble NA, White MB, Mullen KD. Cognitive dysfunction is associated with poor socioeconomic status in patients with cirrhosis: an international multicenter study. *Clin Gastroenterol Hepatol* 2013; **11**: 1511-1516 [PMID: 23707462 DOI: 10.1016/j.cgh.2013.05.010]
9 **Bajaj JS**, Hafeezullah M, Hoffmann RG, Varma RR, Franco J, Binion DG, Hammeke TA, Saeian K. Navigation skill impairment: Another dimension of the driving difficulties in minimal hepatic encephalopathy. *Hepatology* 2008; **47**: 596-604 [PMID: 18000989 DOI: 10.1002/hep.22032]
10 **Prasad S**, Dhiman RK, Duseja A, Chawla YK, Sharma A, Agarwal R. Lactulose improves cognitive functions and health-related quality of life in patients with cirrhosis who have minimal hepatic encephalopathy. *Hepatology* 2007; **45**: 549-559 [PMID: 17326150 DOI: 10.1002/hep.21533]
11 **Bajaj JS**, Wade JB, Gibson DP, Heuman DM, Thacker LR, Sterling RK, Stravitz RT, Luketic V, Fuchs M, White MB, Bell DE, Gilles H, Morton K, Noble N, Puri P, Sanyal AJ. The multi-dimensional burden of cirrhosis and hepatic encephalopathy on patients and caregivers. *Am J Gastroenterol* 2011; **106**: 1646-1653 [PMID: 21556040 DOI: 10.1038/ajg.2011.157]
12 **Groeneweg M**, Moerland W, Quero JC, Hop WC, Krabbe PF, Schalm SW. Screening of subclinical hepatic encephalopathy. *J Hepatol* 2000; **32**: 748-753 [PMID: 10845661]
13 **Saxena N**, Bhatia M, Joshi YK, Garg PK, Tandon RK. Auditory P300 event-related potentials and number connection test for evaluation of subclinical hepatic encephalopathy in patients with cirrhosis of the liver: a follow-up study. *J Gastroenterol Hepatol* 2001; **16**: 322-327 [PMID: 11339425]
14 **Schomerus H**, Hamster W. Quality of life in cirrhotics with minimal hepatic encephalopathy. *Metab Brain Dis* 2001; **16**: 37-41 [PMID: 11726087]
15 **Sharma P**, Sharma BC, Puri V, Sarin SK. Critical flicker frequency: diagnostic tool for minimal hepatic encephalopathy. *J Hepatol* 2007; **47**: 67-73 [PMID: 17459511 DOI: 10.1016/j.jhep.2007.02.022]
16 **Bajaj JS**. Management options for minimal hepatic encephalopathy. *Expert Rev Gastroenterol Hepatol* 2008; **2**: 785-790 [PMID: 19090738 DOI: 10.1586/17474124.2.6.785]
17 **Romero-Gómez M**, Córdoba J, Jover R, del Olmo JA, Ramírez M, Rey R, de Madaria E, Montoliu C, Nuñez D, Flavia M, Compañy L, Rodrigo JM, Felipo V. Value of the critical flicker frequency in patients with minimal hepatic encephalopathy. *Hepatology* 2007; **45**: 879-885 [PMID: 17393525 DOI: 10.1002/hep.21586]
18 **Ridola L**, Cardinale V, Riggio O. The burden of minimal hepatic encephalopathy: from diagnosis to therapeutic strategies. *Ann Gastroenterol* 2018; **31**: 151-164 [PMID: 29507462 DOI: 10.20524/aog.2018.0232]
19 **Bajaj JS**, Saeian K, Verber MD, Hischke D, Hoffmann RG, Franco J, Varma RR, Rao SM. Inhibitory control test is a simple method to diagnose minimal hepatic encephalopathy and predict development of overt hepatic encephalopathy. *Am J Gastroenterol* 2007; **102**: 754-760 [PMID: 17222319 DOI: 10.1111/j.1572-0241.2007.01048.x]
20 **Ford JM**, Gray M, Whitfield SL, Turken AU, Glover G, Faustman WO, Mathalon DH. Acquiring and inhibiting prepotent responses in schizophrenia: event-related brain potentials and functional magnetic resonance imaging. *Arch Gen Psychiatry* 2004; **61**: 119-129 [PMID: 14757588 DOI: 10.1001/archpsyc.61.2.119]
21 **Schiff S**, Vallesi A, Mapelli D, Orsato R, Pellegrini A, Umiltà C, Gatta A, Amodio P. Impairment of response inhibition precedes motor alteration in the early stage of liver cirrhosis: a behavioral and electrophysiological study. *Metab Brain Dis* 2005; **20**: 381-392 [PMID: 16382348 DOI: 10.1007/s11011-005-7922-4]
22 **Weissenborn K**, Ennen JC, Schomerus H, Rückert N, Hecker H. Neuropsychological characterization of hepatic encephalopathy. *J Hepatol* 2001; **34**: 768-773 [PMID: 11434627]
23 **Córdoba J**, Cabrera J, Lataif L, Penev P, Zee P, Blei AT. High prevalence of sleep disturbance in cirrhosis. *Hepatology* 1998; **27**: 339-345 [PMID: 9462628 DOI: 10.1002/hep.510270204]
24 **Franco RA**, Ashwathnarayan R, Deshpandee A, Knox J, Daniel J, Eastwood D, Franco J, Saeian K. The high prevalence of restless legs syndrome symptoms in liver disease in an academic-based hepatology practice. *J Clin Sleep Med* 2008; **4**: 45-49 [PMID: 18350962]
25 **Martino ME**, Romero-Vives M, Fernández-Lorente J, De Vicente E, Bárcena R, Gaztelu JM. Sleep electroencephalogram alterations disclose initial stage of encephalopathy. *Methods Find Exp Clin Pharmacol* 2002; **24** Suppl D: 119-122 [PMID: 12575478]
26 **Mostacci B**, Ferlisi M, Baldi Antognini A, Sama C, Morelli C, Mondini S, Cirignotta F. Sleep disturbance and daytime sleepiness in patients with cirrhosis: a case control study. *Neurol Sci* 2008; **29**: 237-240 [PMID: 18810597 DOI: 10.1007/s10072-008-0973-7]
27 **Ridola L,** Nardelli S, Gioia S, Riggio O. How to design a multicenter clinical trial in Hepatic Encephalopathy. JCEH 2018 in press [DOI: 10.1016/j.jceh.2018.02.007]
28 **Bustamante J**, Rimola A, Ventura PJ, Navasa M, Cirera I, Reggiardo V, Rodés J. Prognostic significance of hepatic encephalopathy in patients with cirrhosis. *J Hepatol* 1999; **30**: 890-895 [PMID: 10365817]
29 **Hartmann IJ**, Groeneweg M, Quero JC, Beijeman SJ, de Man RA, Hop WC, Schalm SW. The prognostic significance of subclinical hepatic encephalopathy. *Am J Gastroenterol* 2000; **95**: 2029-2034 [PMID: 10950053 DOI: 10.1111/j.1572-0241.2000.02265.x]
30 **Gentilini P**, Laffi G, La Villa G, Romanelli RG, Buzzelli G, Casini-Raggi V, Melani L, Mazzanti R, Riccardi D, Pinzani M, Zignego AL. Long course and prognostic factors of virus-induced cirrhosis of the liver. *Am J Gastroenterol* 1997; **92**: 66-72 [PMID: 8995940]
31 **Benvegnù L**, Gios M, Boccato S, Alberti A. Natural history of compensated viral cirrhosis: a prospective study on the incidence and hierarchy of major complications. *Gut* 2004; **53**: 744-749 [PMID: 15082595]
32 **Watson H**, Jepsen P, Wong F, Ginès P, Córdoba J, Vilstrup H. Satavaptan treatment for ascites in patients with cirrhosis: a meta-analysis of effect on hepatic encephalopathy development. *Metab Brain Dis* 2013; **28**: 301-305 [PMID: 23463488 DOI: 10.1007/s11011-013-9384-4]
33 **Amodio P**, Del Piccolo F, Marchetti P, Angeli P, Iemmolo R, Caregaro L, Merkel C, Gerunda G, Gatta A. Clinical features and survivial of cirrhotic patients with subclinical cognitive alterations detected by the number connection test and computerized psychometric tests. *Hepatology* 1999; **29**: 1662-1667 [PMID: 10347105 DOI: 10.1002/hep.510290619]
34 **Bajaj JS**, Etemadian A, Hafeezullah M, Saeian K. Testing for minimal hepatic encephalopathy in the United States: An AASLD survey. *Hepatology* 2007; **45**: 833-834 [PMID: 17326210 DOI: 10.1002/hep.21515]
35 **Groeneweg M**, Quero JC, De Bruijn I, Hartmann IJ, Essink-bot ML, Hop WC, Schalm SW. Subclinical hepatic encephalopathy impairs daily functioning. *Hepatology* 1998; **28**: 45-49 [PMID: 9657095 DOI: 10.1002/hep.510280108]
36 **Arguedas MR**, DeLawrence TG, McGuire BM. Influence of hepatic encephalopathy on health-related quality of life in patients with cirrhosis. *Dig Dis Sci* 2003; **48**: 1622-1626 [PMID: 12924658]
37 **Saab S**, Ibrahim AB, Shpaner A, Younossi ZM, Lee C, Durazo F, Han S, Esrason K, Wu V, Hiatt J, Farmer DG, Ghobrial RM, Holt C, Yersiz H, Goldstein LI, Tong MJ, Busuttil RW. MELD fails to measure quality of life in liver transplant candidates. *Liver Transpl* 2005; **11**: 218-223 [PMID: 15666392 DOI: 10.1002/lt.20345]
38 **Younossi ZM**, Boparai N, Price LL, Kiwi ML, McCormick M, Guyatt G. Health-related quality of life in chronic liver disease: the impact of type and severity of disease. *Am J Gastroenterol* 2001; **96**: 2199-2205 [PMID: 11467653 DOI: 10.1111/j.1572-0241.2001.03956.x]
39 **Younossi ZM**, McCormick M, Price LL, Boparai N, Farquhar L, Henderson JM, Guyatt G. Impact of liver transplantation on health-related quality of life. *Liver Transpl* 2000; **6**: 779-783 [PMID:

11084068 DOI: 10.1053/jlts.2000.18499]
40 **Labenz C**, Baron JS, Toenges G, Schattenberg JM, Nagel M, Sprinzl MF, Nguyen-Tat M, Zimmermann T, Huber Y, Marquardt JU, Galle PR, Wörns MA. Prospective evaluation of the impact of covert hepatic encephalopathy on quality of life and sleep in cirrhotic patients. *Aliment Pharmacol Ther* 2018; **48**: 313-321 [PMID: 29863286 DOI: 10.1111/apt.14824]
41 **McNeil BJ**, Weichselbaum R, Pauker SG. Speech and survival: tradeoffs between quality and quantity of life in laryngeal cancer. *N Engl J Med* 1981; **305**: 982-987 [PMID: 7278922 DOI: 10.1056/NEJM198110223051704]
42 **Bao ZJ**, Qiu DK, Ma X, Fan ZP, Zhang GS, Huang YQ, Yu XF, Zeng MD. Assessment of health-related quality of life in Chinese patients with minimal hepatic encephalopathy. *World J Gastroenterol* 2007; **13**: 3003-3008 [PMID: 17589955]
43 **Sidhu SS**, Goyal O, Mishra BP, Sood A, Chhina RS, Soni RK. Rifaximin improves psychometric performance and health-related quality of life in patients with minimal hepatic encephalopathy (the RIME Trial). *Am J Gastroenterol* 2011; **106**: 307-316 [PMID: 21157444 DOI: 10.1038/ajg.2010.455]
44 **Marchesini G**, Bianchi G, Amodio P, Salerno F, Merli M, Panella C, Loguercio C, Apolone G, Niero M, Abbiati R; Italian Study Group for quality of life in cirrhosis. Factors associated with poor health-related quality of life of patients with cirrhosis. *Gastroenterology* 2001; **120**: 170-178 [PMID: 11208726]
45 **Kim WR**, Brown RS Jr, Terrault NA, El-Serag H. Burden of liver disease in the United States: summary of a workshop. *Hepatology* 2002; **36**: 227-242 [PMID: 12085369 DOI: 10.1053/jhep.2002.34734]
46 **Mina A**, Moran S, Ortiz-Olvera N, Mera R, Uribe M. Prevalence of minimal hepatic encephalopathy and quality of life in patients with decompensated cirrhosis. *Hepatol Res* 2014; **44**: E92-E99 [PMID: 24033755 DOI: 10.1111/hepr.12227]
47 **Sanyal A**, Younossi ZM, Bass NM, Mullen KD, Poordad F, Brown RS, Vemuru RP, Mazen Jamal M, Huang S, Merchant K, Bortey E, Forbes WP. Randomised clinical trial: rifaximin improves health-related quality of life in cirrhotic patients with hepatic encephalopathy - a double-blind placebo-controlled study. *Aliment Pharmacol Ther* 2011; **34**: 853-861 [PMID: 21848797 DOI: 10.1111/j.1365-2036.2011.04808.x]
48 **Collier J**. Bone disorders in chronic liver disease. *Hepatology* 2007; **46**: 1271-1278 [PMID: 17886334 DOI: 10.1002/hep.21852]
49 **Guañabens N**, Parés A, Ros I, Caballería L, Pons F, Vidal S, Monegal A, Peris P, Rodés J. Severity of cholestasis and advanced histological stage but not menopausal status are the major risk factors for osteoporosis in primary biliary cirrhosis. *J Hepatol* 2005; **42**: 573-577 [PMID: 15763344 DOI: 10.1016/j.jhep.2004.11.035]
50 **Diamond T**, Stiel D, Lunzer M, Wilkinson M, Roche J, Posen S. Osteoporosis and skeletal fractures in chronic liver disease. *Gut* 1990; **31**: 82-87 [PMID: 2318434]
51 **Cohen SM**, Te HS, Levitsky J. Operative risk of total hip and knee arthroplasty in cirrhotic patients. *J Arthroplasty* 2005; **20**: 460-466 [PMID: 16124961 DOI: 10.1016/j.arth.2004.05.004]
52 **Ström O**, Borgstrom F, Zethraeus N, Johnell O, Lidgren L, Ponzer S, Svensson O, Abdon P, Ornstein E, Ceder L, Thorngren KG, Sernbo I, Jonsson B. Long-term cost and effect on quality of life of osteoporosis-related fractures in Sweden. *Acta Orthop* 2008; **79**: 269-280 [PMID: 18484255 DOI: 10.1080/17453670710015094]
53 **Pike C**, Birnbaum HG, Schiller M, Sharma H, Burge R, Edgell ET. Direct and indirect costs of non-vertebral fracture patients with osteoporosis in the US. *Pharmacoeconomics* 2010; **28**: 395-409 [PMID: 20402541 DOI: 10.2165/11531040-000000000-00000]
54 **Román E**, Córdoba J, Torrens M, Torras X, Villanueva C, Vargas V, Guarner C, Soriano G. Minimal hepatic encephalopathy is associated with falls. *Am J Gastroenterol* 2011; **106**: 476-482 [PMID: 20978484 DOI: 10.1038/ajg.2010.413]
55 **Soriano G**, Román E, Córdoba J, Torrens M, Poca M, Torras X, Villanueva C, Gich IJ, Vargas V, Guarner C. Cognitive dysfunction in cirrhosis is associated with falls: a prospective study. *Hepatology* 2012; **55**: 1922-1930 [PMID: 22213000 DOI: 10.1002/hep.25554]
56 **Urios A**, Mangas-Losada A, Gimenez-Garzó C, González-López O, Giner-Durán R, Serra MA, Noe E, Felipo V, Montoliu C. Altered postural control and stability in cirrhotic patients with minimal hepatic encephalopathy correlate with cognitive deficits. *Liver Int* 2017; **37**: 1013-1022 [PMID: 27988985 DOI: 10.1111/liv.13345]
57 **Singh J**, Sharma BC, Puri V, Sachdeva S, Srivastava S. Sleep disturbances in patients of liver cirrhosis with minimal hepatic encephalopathy before and after lactulose therapy. *Metab Brain Dis* 2017; **32**: 595-605 [PMID: 28070704 DOI: 10.1007/s11011-016-9944-5]
58 **Razek AA**, Abdalla A, Ezzat A, Megahed A, Barakat T. Minimal hepatic encephalopathy in children with liver cirrhosis: diffusion-weighted MR imaging and proton MR spectroscopy of the brain. *Neuroradiology* 2014; **56**: 885-891 [PMID: 25060166 DOI: 10.1007/s00234-014-1409-0]
59 **El-mewafy Z**, Abdel Razek AAK, El-Eshmawy M, Abo El-Eneen N, EL-Biaomy A. Magnetic resonance spectroscopy of the frontal region in patients with metabolic syndrome: correlation with anthropometric measurement. *Pol J Radiol* 2018; **83**: e215-e219 [DOI: 10.5114/pjr.2018.76024]
60 **Bergner M**, Bobbitt RA, Carter WB, Gilson BS. The Sickness Impact Profile: development and final revision of a health status measure. *Med Care* 1981; **19**: 787-805 [PMID: 7278416]
61 **Younossi ZM**, Guyatt G, Kiwi M, Boparai N, King D. Development of a disease specific questionnaire to measure health related quality of life in patients with chronic liver disease. *Gut* 1999; **45**: 295-300 [PMID: 10403745]
62 **Apolone G**, Mosconi P. The Italian SF-36 Health Survey: translation, validation and norming. *J Clin Epidemiol* 1998; **51**: 1025-1036 [PMID: 9817120]
63 **Vilstrup H**, Amodio P, Bajaj J, Cordoba J, Ferenci P, Mullen KD, Weissenborn K, Wong P. Hepatic encephalopathy in chronic liver disease: 2014 Practice Guideline by the American Association for the Study of Liver Diseases and the European Association for the Study of the Liver. *Hepatology* 2014; **60**: 715-735 [PMID: 25042402 DOI: 10.1002/hep.27210]
64 **Bajaj JS**, Heuman DM, Wade JB, Gibson DP, Saeian K, Wegelin JA, Hafeezullah M, Bell DE, Sterling RK, Stravitz RT, Fuchs M, Luketic V, Sanyal AJ. Rifaximin improves driving simulator performance in a randomized trial of patients with minimal hepatic encephalopathy. *Gastroenterology* 2011; **140**: 478-487.e1 [PMID: 20849805 DOI: 10.1053/j.gastro.2010.08.061]
65 **Sidhu SS**, Goyal O, Parker RA, Kishore H, Sood A. Rifaximin vs. lactulose in treatment of minimal hepatic encephalopathy. *Liver Int* 2016; **36**: 378-385 [PMID: 26201713 DOI: 10.1111/liv.12921]
66 **Schulz C**, Schütte K, Kropf S, Schmitt FC, Vasapolli R, Kliegis LM, Riegger A, Malfertheiner P. RiMINI - the influence of rifaximin on minimal hepatic encephalopathy (MHE) and on the intestinal microbiome in patients with liver cirrhosis: study protocol for a randomized controlled trial. *Trials* 2016; **17**: 111 [PMID: 26926775 DOI: 10.1186/s13063-016-1205-8]
67 **Lunia MK**, Sharma BC, Sharma P, Sachdeva S, Srivastava S. Probiotics prevent hepatic encephalopathy in patients with cirrhosis: a randomized controlled trial. *Clin Gastroenterol Hepatol* 2014; **12**: 1003-8.e1 [PMID: 24246768 DOI: 10.1016/j.cgh.2013.11.006]
68 **Mittal VV**, Sharma BC, Sharma P, Sarin SK. A randomized controlled trial comparing lactulose, probiotics, and L-ornithine L-aspartate in treatment of minimal hepatic encephalopathy. *Eur J Gastroenterol Hepatol* 2011; **23**: 725-732 [PMID: 21646910 DOI: 10.1097/MEG.0b013e32834696f5]
69 **Sharma P**, Sharma BC, Puri V, Sarin SK. An open-label randomized controlled trial of lactulose and probiotics in the treatment of minimal hepatic encephalopathy. *Eur J Gastroenterol Hepatol* 2008; **20**: 506-511 [PMID: 18467909 DOI: 10.1097/MEG.0b013e3282f3e6f5]
70 **Gluud LL**, Vilstrup H, Morgan MY. Non-absorbable disaccharides versus placebo/no intervention and lactulose versus lactitol for the prevention and treatment of hepatic encephalopathy in people with cirrhosis. *Cochrane Database Syst Rev* 2016; **5**: CD003044 [PMID: 27153247 DOI: 10.1002/14651858.CD003044.pub4]
71 **Malaguarnera M**, Greco F, Barone G, Gargante MP, Malaguarnera M, Toscano MA. Bifidobacterium longum with fructo-oligosaccharide

(FOS) treatment in minimal hepatic encephalopathy: a randomized, double-blind, placebo-controlled study. *Dig Dis Sci* 2007; **52**: 3259-3265 [PMID: 17393330 DOI: 10.1007/s10620-006-9687-y]

72 **Bajaj JS**, Saeian K, Christensen KM, Hafeezullah M, Varma RR, Franco J, Pleuss JA, Krakower G, Hoffmann RG, Binion DG. Probiotic yogurt for the treatment of minimal hepatic encephalopathy. *Am J Gastroenterol* 2008; **103**: 1707-1715 [PMID: 18691193 DOI: 10.1111/j.1572-0241.2008.01861.x]

73 **Saji S**, Kumar S, Thomas V. A randomized double blind placebo controlled trial of probiotics in minimal hepatic encephalopathy. *Trop Gastroenterol* 2011; **32**: 128-132 [PMID: 21922877]

74 **Sharma K**, Pant S, Misra S, Dwivedi M, Misra A, Narang S, Tewari R, Bhadoria AS. Effect of rifaximin, probiotics, and l-ornithine l-aspartate on minimal hepatic encephalopathy: a randomized controlled trial. *Saudi J Gastroenterol* 2014; **20**: 225-232 [PMID: 25038208 DOI: 10.4103/1319-3767.136975]

75 **Dalal R**, McGee RG, Riordan SM, Webster AC. Probiotics for people with hepatic encephalopathy. *Cochrane Database Syst Rev* 2017; **2**: CD008716 [PMID: 28230908 DOI: 10.1002/14651858.CD008716.pub3]

76 **Malaguarnera G**, Pennisi M, Bertino G, Motta M, Borzì AM, Vicari E, Bella R, Drago F, Malaguarnera M. Resveratrol in Patients with Minimal Hepatic Encephalopathy. *Nutrients* 2018; **10**: [PMID: 29522439 DOI: 10.3390/nu10030329]

77 **Malaguarnera M**, Bella R, Vacante M, Giordano M, Malaguarnera G, Gargante MP, Motta M, Mistretta A, Rampello L, Pennisi G. Acetyl-L-carnitine reduces depression and improves quality of life in patients with minimal hepatic encephalopathy. *Scand J Gastroenterol* 2011; **46**: 750-759 [PMID: 21443422 DOI: 10.3109/00365521.2011.565067]

78 **Rahimi RS**, Singal AG, Cuthbert JA, Rockey DC. Lactulose vs polyethylene glycol 3350--electrolyte solution for treatment of overt hepatic encephalopathy: the HELP randomized clinical trial. *JAMA Intern Med* 2014; **174**: 1727-1733 [PMID: 25243839 DOI: 10.1001/jamainternmed.2014.4746]

79 **Abd-Elsalam S**, El-Kalla F, Elwan N, Badawi R, Hawash N, Soliman S, Soliman S, Elkhalawany W, ElSawaf MA, Elfert A. A Randomized Controlled Trial Comparing Nitazoxanide Plus Lactulose With Lactulose Alone in Treatment of Overt Hepatic Encephalopathy. *J Clin Gastroenterol* 2018 Epub ahead of print [PMID: 29668561 DOI: 10.1097/MCG.0000000000001040]

80 **European Association for the Study of the Liver**, European Association for the Study of the Liver. EASL Clinical Practice Guidelines on nutrition in chronic liver disease. *J Hepatol* 2018; Epub ahead of print [PMID: 30144956 DOI: 10.1016/j.jhep.2018.06.024]

81 **Bajaj JS**, Saeian K, Hafeezullah M, Hoffmann RG, Hammeke TA. Patients with minimal hepatic encephalopathy have poor insight into their driving skills. *Clin Gastroenterol Hepatol* 2008; **6**: 1135-9; quiz 1065 [PMID: 18928938 DOI: 10.1016/j.cgh.2008.05.025]

82 **Zhang Y**, Feng Y, Cao B, Tian Q. Effects of SIBO and rifaximin therapy on MHE caused by hepatic cirrhosis. *Int J Clin Exp Med* 2015; **8**: 2954-2957 [PMID: 25932262]

83 **Bajaj JS**, Heuman DM, Hylemon PB, Sanyal AJ, Puri P, Sterling RK, Luketic V, Stravitz RT, Siddiqui MS, Fuchs M, Thacker LR, Wade JB, Daita K, Sistrun S, White MB, Noble NA, Thorpe C, Kakiyama G, Pandak WM, Sikaroodi M, Gillevet PM. Randomised clinical trial: Lactobacillus GG modulates gut microbiome, metabolome and endotoxemia in patients with cirrhosis. *Aliment Pharmacol Ther* 2014; **39**: 1113-1125 [PMID: 24628464 DOI: 10.1111/apt.12695]

84 **Luo M**, Li L, Lu CZ, Cao WK. Clinical efficacy and safety of lactulose for minimal hepatic encephalopathy: a meta-analysis. *Eur J Gastroenterol Hepatol* 2011; **23**: 1250-1257 [PMID: 21971378 DOI: 10.1097/MEG.0b013e32834d1938]

P- Reviewer: Abd-Elsalam S, Malaguarnera M, Razek AAKA
S- Editor: Ma RY **L- Editor**: A **E- Editor**: Yin SY

World Journal of Gastroenterology

Submit a Manuscript: https://www.f6publishing.com

World J Gastroenterol 2018 December 28; 24(48): 5454-5461

DOI: 10.3748/wjg.v24.i48.5454

ISSN 1007-9327 (print) ISSN 2219-2840 (online)

MINIREVIEWS

Post-translational modifications of prostaglandin-endoperoxide synthase 2 in colorectal cancer: An update

Rafael I Jaén, Patricia Prieto, Marta Casado, Paloma Martín-Sanz, Lisardo Boscá

Rafael I Jaén, Patricia Prieto, Lisardo Boscá, Department of Metabolism and Physiopathology of Inflammatory Diseases, Instituto de Investigaciones Biomédicas Alberto Sols (CSIC-UAM), Madrid 28029, Spain

Marta Casado, Department of Biomedicine, Instituto de Biomedicina de Valencia (CSIC), Valencia 46010, Spain

Marta Casado, Paloma Martín-Sanz, Lisardo Boscá, Centro de Investigación Biomédica en Red de Enfermedades Cardiovasculares, y Hepáticas y Digestivas, ISCIII, Madrid 28029, Spain

Paloma Martín-Sanz, Lisardo Boscá, Unidad Asociada IIBM-ULPGC, Universidad de las Palmas de Gran Canaria (ULPGC), Las Palmas de Gran Canaria 35001, Spain

ORCID number: Rafael I Jaén (0000-0002-7298-2125); Patricia Prieto (0000-0001-6943-7663); Marta Casado (0000-0001-6457-4650); Paloma Martín-Sanz (0000-0002-0758-9749); Lisardo Boscá (0000-0002-0253-5469).

Author contributions: Jaén RI and Prieto P contributed equally to the discussion of the minireview and provided key information on the glycosylation of prostaglandin-endoperoxide synthase 2 in colorectal cancer samples. Casado M, Martín-Sanz P and Boscá L revised the literature, organized the content of the minireview and prepared the figures of the manuscript.

Supported by Ministerio de Ciencia Innovación y Universidades, No. SAF2017-82436R and SAF2016-75004R; Comunidad de Madrid, No. S2017/BMD-3686; Fundación Ramón Areces, No. 2016/CIVP18A3864; and Instituto de Salud Carlos Ⅲ and by Fondos FEDER, No. Cibercv and Ciberehd.

Conflict-of-interest statement: The authors have declared no conflicts of interest.

Manuscript source: Invited manuscript

Corresponding author: Lisardo Boscá, BM, BCh, PhD, Senior Research Fellow, Department of Metabolism and Physiopathology of Inflammatory Diseases, Instituto de Investigaciones Biomédicas Alberto Sols, Arturo Duperier 4, Madrid 28029, Spain. lbosca@iib.uam.es.
Telephone: +34-91-4972747
Fax: +34-91-4972747

Received: October 7, 2018
Peer-review started: October 7, 2018
First decision: November 7, 2018
Revised: November 13, 2018
Accepted: November 13, 2018
Article in press: November 16, 2018
Published online: December 28, 2018

Abstract

The biosynthesis of prostanoids is involved in both physiological and pathological processes. The expression of prostaglandin-endoperoxide synthase 2 (PTGS2; also known as COX-2) has been traditionally associated to the onset of several pathologies, from inflammation to cardiovascular, gastrointestinal and oncologic events. For this reason, the search of selective PTGS2 inhibitors has been a focus for therapeutic interventions. In addition to the classic non-steroidal anti-inflammatory drugs, selective and specific PTGS2 inhibitors, termed coxibs, have been generated and widely used. PTGS2 activity is less restrictive in terms of substrate specificity than the homeostatic counterpart PTGS1, and it accounts for the elevated prostanoid synthesis that accompanies several pathologies. The main regulation of PTGS2 occurs at the transcription level. In addition to this, the stability of the mRNA is finely regulated through the interaction with several cytoplasmic elements, ranging from specific

microRNAs to proteins that control mRNA degradation. Moreover, the protein has been recognized to be the substrate for several post-translational modifications that affect both the enzyme activity and the targeting for degradation *via* proteasomal and non-proteasomal mechanisms. Among these modifications, phosphorylation, glycosylation and covalent modifications by reactive lipidic intermediates and by free radicals associated to the pro-inflammatory condition appear to be the main changes. Identification of these post-translational modifications is relevant to better understand the role of PTGS2 in several pathologies and to establish a correct analysis of the potential function of this protein in diseases progress. Finally, these modifications can be used as biomarkers to establish correlations with other parameters, including the immunomodulation dependent on molecular pathological epidemiology determinants, which may provide a better frame for potential therapeutic interventions.

Key words: Prostaglandins; Prostaglandin-endoperoxide synthase 2; Post-translational modifications; Glycosylation; Colorectal cancer; Inflammation

Core tip: The post-translational modifications of prostaglandin-endoperoxide synthase 2 (PTGS2) appear to be specific signatures of this enzyme in human colorectal cancer (CRC). Glycosylations of PTGS2 that alter the electrophoretic mobility of the protein are mainly observed in the tumor samples but are absent in the non-tumor samples obtained from these patients. These modifications not only may play a pathophysiological role in the progression of CRC but also may provide new biomarkers to develop specific therapeutic interventions.

Jaén RI, Prieto P, Casado M, Martín-Sanz P, Boscá L. Post-translational modifications of prostaglandin-endoperoxide synthase 2 in colorectal cancer: An update. *World J Gastroenterol* 2018; 24(48): 5454-5461
URL: https://www.wjgnet.com/1007-9327/full/v24/i48/5454.htm
DOI: https://dx.doi.org/10.3748/wjg.v24.i48.5454

INTRODUCTION

The role of prostaglandin-endoperoxide synthase 2 (PTGS2) in physiology and pathophysiology has been addressed in different studies since this enzyme is induced under several circumstances, including inflammation, tumor progression and cell survival[1-6]. Two PTGSs are present in mammalian cells: PTGS1, which is constitutively expressed in almost all tissues at low levels, playing a homeostatic role; and PTGS2, which is considered as an immediate early gene that is expressed in response to a wide array of cell challenges and stressors[7-10]. Both enzymes catalyze the same reaction, which constitutes the rate-limiting step in the biosynthesis of different prostanoids, such as several prostaglandins, *via* tissue specific prostaglandin synthases, thromboxane A2 and other eicosanoids[11,12]. Provision of arachidonic acid as substrate is dependent on the activation of phospholipase A2, which in turn, responds to different cell stressors connecting phospholipid hydrolysis to prostanoid synthesis[10,11,13,14] (Figure 1). Both PTGS isoforms are conserved among mammals and weight 70-75 kDa. They share more than 60% sequence homology in mammalian species and retain more than 85% identity when comparing orthologues from different species, displaying conserved regulatory and catalytic domains as depicted in Figure 2. Structural studies show that the isoleucine located at position 523 in PTGS1 is substituted by valine in PTGS2 (position 509) and this difference in hydrophobicity and size constitutes the basis for the design of selective, isoenzyme-specific hydrophobic inhibitors, such as the coxibs[15-17]. Regarding the conserved protein motifs, they include an epidermal growth factor-like domain followed by a membrane-binding region that allows positioning of the different PTGS in cytoplasmic microambiances. The catalytic site of the enzyme involves two independent activities: the deoxygenation of arachidonic acid and an additional site responsible for the subsequent reduction *via* the peroxidase activity[18]. These domains are relevant for the subcellular localization of PTGS allowing the protein to interact with the luminal space of the endoplasmic reticulum and with the nuclear membrane. This is important to understand the activity of the enzyme since phospholipases and their targets, the phospholipids required to release arachidonic acid, are located in biological membranes[19-23]. Additionally, other free fatty acids, such as eicosanepentaenoic acid[24], docosahexaenoic acid[23], α-and γ-linolenic acid or linoleic acid can be metabolized by PTGS2 leading to molecules involved in the control of inflammation[25,26] (Figure 3). Several works described selective distribution of both PTGS isoforms in the cell, with a preferred positioning of PTGS2 near the nuclear structure. This is also pertinent for the fate of the products of the enzymes[10]. These prostanoids can be released to the extracellular milieu and exert their autocrine or paracrine actions either by the specific G protein-coupled receptor (GPCR)-coupled prostaglandin E_2 (PGE_2) receptor (EP) receptors[27], by diffusion or through the interaction with several transporters (*i.e.*, the prostaglandin transporter system, the ABC cassettes, or the scavenger lipid receptor CD36[28-30]). In addition to GPCR-mediated early signaling, prostanoids may alter gene transcription after interaction with several nuclear receptors, such as the peroxisomal proliferator activated receptors (PPARs)[31-33].

PTGS2 EXPRESSION IN COLORECTAL CANCER TUMORIGENESIS

The role of PTGS2 expression in the initiation and progress of colorectal cancer (CRC) still remains a matter

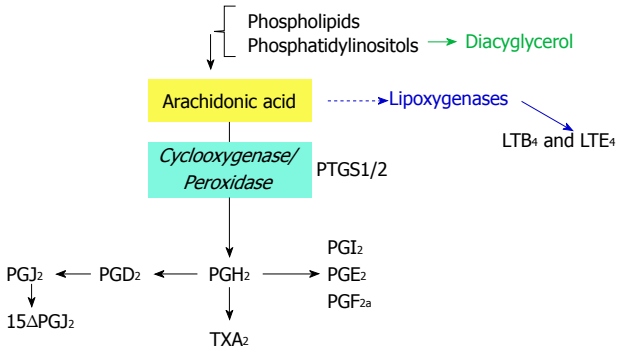

Figure 1 Biochemical reactions catalyzed by prostaglandin-endoperoxide synthase using arachidonic acid as substrate. Phospholipids are cleaved by phospholipases to render arachidonic acid. Prostaglandin-endoperoxide synthase activity generates the precursor prostaglandin H2 that is converted in the different prostaglandins (PGs) by prostaglandin synthases and thromboxane A2, by thromboxane synthase. PG: Prostaglandin; PTGS: Prostaglandin-endoperoxide synthase.

of debate. On one hand, epidemiological studies using broad (aspirin, indomethacin) or selective inhibitors of the PTGS isoforms at least suggest that under these conditions, prevention occurs in the development of CRC[1,16,31,34,35]. However, direct measurement of PGE_2 levels in samples from adenomatous *vs* healthy tissue fails to show a clear cut-off supporting tumor growth and survival. In addition to this, the use of selective inhibitors of the EP receptors also contributes to the suggestion that autocrine signaling is perhaps critical in the commitment of the tumor cells to proliferate and invade the tissue *via* activation of mitogenic and metastatic pathways[6,27,31,34,36,37]. In addition to this, it is well known the capacity of PGE_2 to favor angiogenesis of epithelial cells, contributing to the spreading and survival of the tumor. Moreover, due to the immunosuppressive activity of extracellular prostanoids, the anti-tumor role of the immune system is compromised, favoring the survival of the transformed cells in this microenvironment[3,33]. Not only the released products of PTGS2 have this capacity to alter cell fate, but at the intracellular level, prostaglandins itself or as result of oxidation due to increased oxidative stress may contribute to activate nuclear receptors, such as PPARs, that oppose to the pro-inflammatory defense mechanism favoring oncogenic progression[31,32]. Thus, the amount and fate of the products released by PTGS2 activity have different functions in the onset of CRC. Moreover, several authors have considered the possibility that, at least for PTGS1, it may exert "moonlighting" functions whose biological relevance remains to be established[38,39]. Additionally, the PTGS products can be modified by another series of enzymes, the 15PGDHs, which are transcriptionally regulated and determine the prostanoid levels coming from the PTGS activity, contributing in this way to the fine tuning of the activity of these lipid mediators and their involvement on the pathophysiology of CRC tumorigenesis[40,41]. Indeed, agreement exists in the opposite regulation of PTGS2 and 15PGDH in the sense that elevated PTGS2 levels repress 15PGDH expression and *vice versa*, elevated 15PGDH use to repress PTGS levels through different complementary mechanisms, involving destabilization of the PTGS2 mRNA *via* specific interaction with microRNAs[8,14,42]. Finally, the interplay between different contributors to CRC is moving towards a new integrative view that considers the immunological modulation due to several agents, including vitamin D, polyunsaturated fatty acids, diets with specific content in omega-3/-6, and pharmacological treatment with broad (aspirin) or selective PTGS2 inhibitors (coxibs). Together, these factors determine the immune modulation of what is defined as the immunomodulatory molecular pathological epidemiology (PME), as an integrated view of the environment-tumor-immune interactions, that may establish efficient protocols for immunoprevention and immunotherapy, leading to a better precision medicine[43,44].

PTGS2 is mainly regulated at the transcription level. The promoter region of *PTGS2* contains several regulatory elements conferring response to transcription factors such as activating protein-2 (AP-2), nuclear factor kappa B (NF-κB), cAMP response element (CRE), E-box and Sp1, with various sites with impact on the promoter activity[35,45-47] (Figure 2). Despite this presence of canonical conserved transcription regulatory elements, preliminary data from our group show that the activity of the promoter has specific signatures when comparing its activity in rodent *vs* human cells, at least in the response to the engagement of NF-AT sites. Indeed, NF-AT inhibition with cyclosporine A or tacrolimus results in the repression of the pro-inflammatory transcriptional regulation in human cells, but not in the rodent counterparts, suggesting a specific fine-tuning of the promoter activity of this gene, at least in myeloid and hepatic cell lines (Figure 4). Moreover, PTGS2 expression is controlled also at post-transcriptional level; from a gene containing 10 exons and producing at least three products ranging from 4.6 to 2.8 kb, a regulatory site, positioned in the last exon that contains the 3'-UTR encoding sequences, is responsible for RNA instability[48]. As a result of this complex regulation, the levels of prostaglandins may vary significantly among several pathological situations, due to the availability of different substrates for the enzyme, the post-translational modifications occurring in a given tissue and/or the capacity to export and degrade the PTGS products (15PGDH; lipoxygenases, *etc.*). Indeed, it has been proposed a role for PGE_2 in the CRC stem cell expansion and metastasis, at least in mice models of the disease[34]. Nevertheless, consensus exists regarding the fact that PTGS2 expression is associated with various pathophysiological events, ranging from inflammatory diseases to different cancers. The main problem encountered by researchers in the field is the frequent lack of correlation between mRNA and protein levels of PTGS2 and the corresponding biosynthesis of prostanoids, mainly PGE_2. This is due to

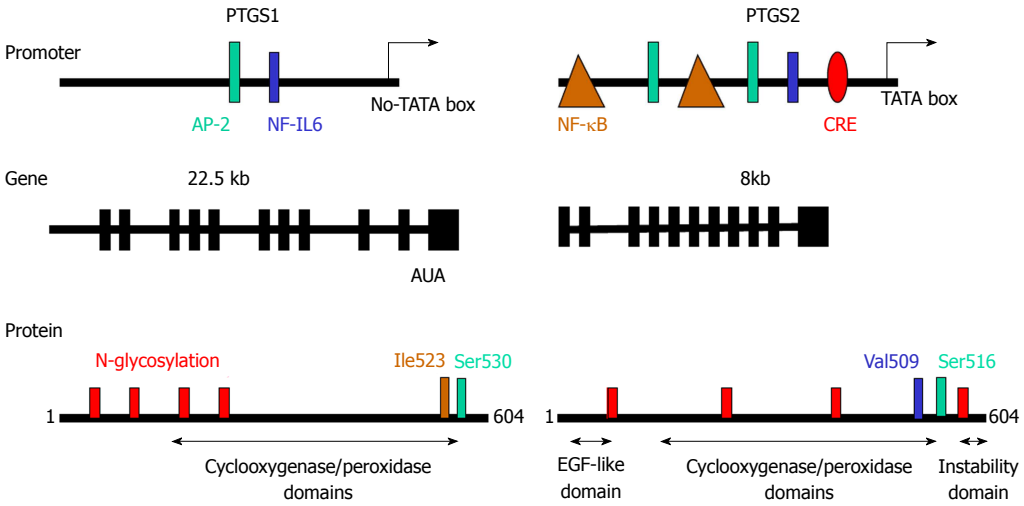

Figure 2 Comparison of the promoter region, gene structure and protein sequence of consensus prostaglandin-endoperoxide synthase 1 and 2. The scheme shows the main transcription factors involved in the transcriptional control of prostaglandin-endoperoxide synthase (PTGS), the structure of the mRNA and the structural motifs present in the protein and relevant for the activity of the enzyme. The glycosylation of PTGS has effects on the activity and fate of the protein, protecting PTGS2 from proteasomal degradation. In addition to this, the electrophoretic mobility of the protein is altered by the glycosylation status of the protein. PTGS: Prostaglandin-endoperoxide synthase; AP-2: Activating protein 2; CRE: cAMP response element; NF-κB: Nuclear factor kappa B.

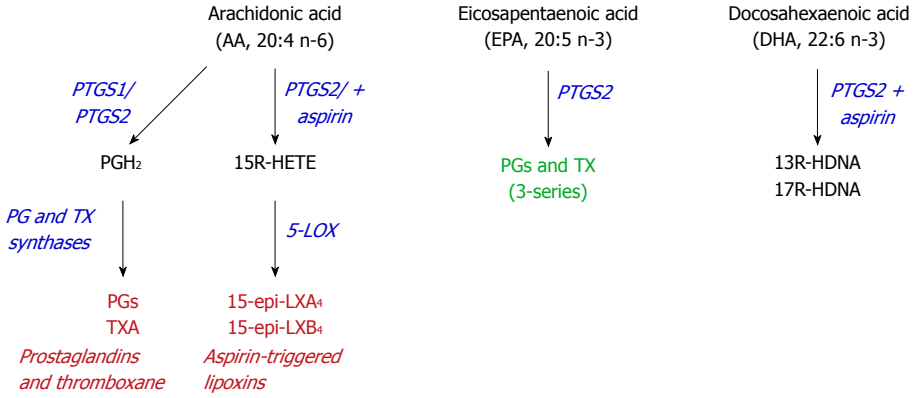

Figure 3 Alternative use of polyunsaturated fatty acids. Aspirin may alter the activity of prostaglandin-endoperoxide synthase (PTGS) since it inhibits PTGS1, but retains the cyclooxygenase activity from PTGS2, leading to the synthesis of 15R-hydroxyeicosatetraenoic acid, from arachidonic acid, or 13- or 17R-hydroxy-docosahexaenoic acid, from docosahexaenoic acid. PTGS: Prostaglandin-endoperoxide synthase; HETE: Hydroxyeicosatetraenoic acid; HDHA: Hydroxy-docosahexaenoic acid.

the exquisite control on the transcription of the gene; the existence of sequences that destabilize the mRNA and the posttranslational modifications that alter not only the catalytic activity of the enzyme, but also the stability of the protein, usually favoring proteasomal and non-proteasomal degradation[49-51]. Indeed, some suggestion of a 'moonlighting' effect for the protein has been reported for PTGS, an aspect of growing interest in the cancer field[38,39,52]. Finally, more than 40 clinical trials on the use of coxibs in CRC have been registered (ClinicalTrials.gov). Despite the controversy on the use of selective (coxibs) *vs* less specific PTGS2 inhibitors (NSAIDS) the main problems coming from these studies of chemoprevention are associated to the lack of specific biomarkers on the progress of the disease[53] and the existence of side effects that, at the end, represent a serious bias in the establishment of the critical parameters associated to the onset of the pathology[16,34,54].

PATHOPHYSIOLOGICAL RELEVANCE OF THE POST-TRANSLATIONAL REGULATION OF PTGS2

Apart from the classic pharmacological acetylation by aspirin on Ser530 in PTGS1 and Ser516 in PTGS2[55], that prevents the full activity of the enzyme [PTGS2 retains the ability to generate 15R-hydroxyeicosatetraenoic acid (HETE) from arachidonic acid], other physiological post-translational modifications have been described for the PTGS isoenzymes. These modifications have an impact on the catalytic activity, on the subcellular localization, and on the targeting of the protein for degradation *via* proteasomal or non-proteasomal (endoplasmic reticulum-dependent pathways) pathways[51]. Overall, these modifi-

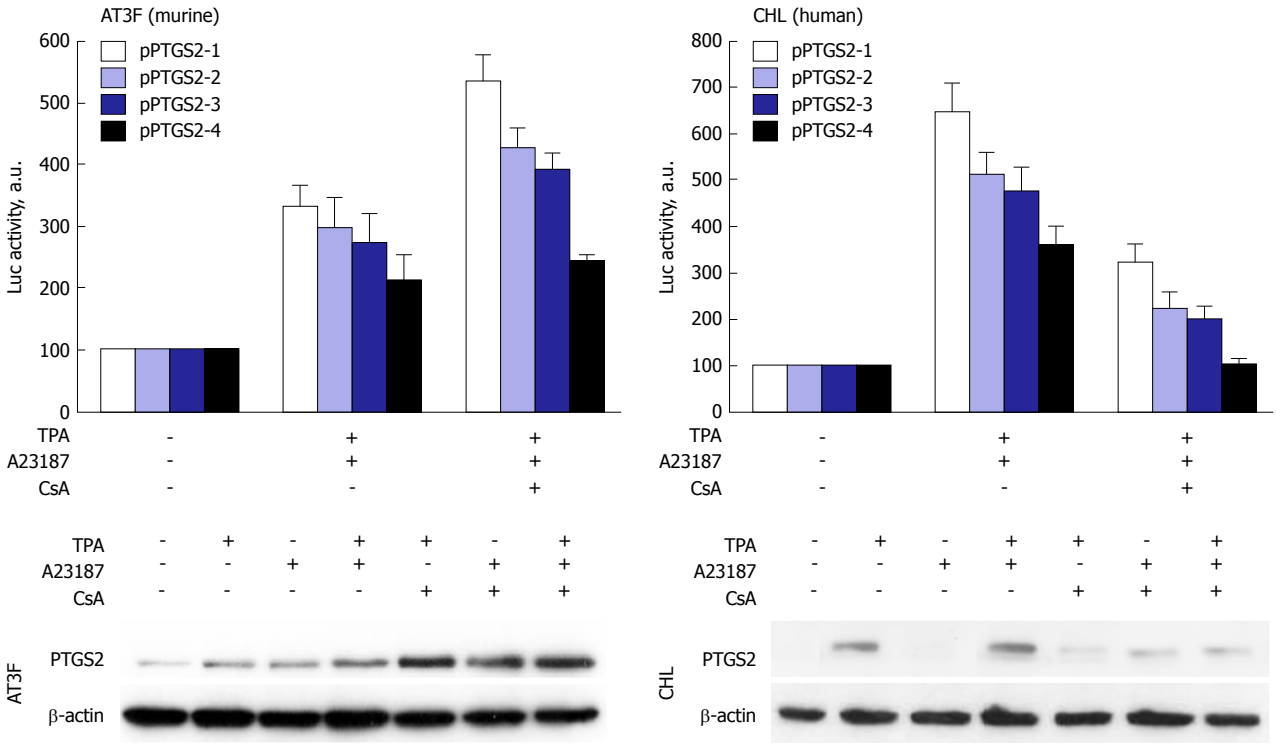

Figure 4 Prostaglandin-endoperoxide synthase 2 exhibits species-specific transcriptional control. Despite the broad conservation of the transcription factor motifs in the prostaglandin-endoperoxide synthase 2 promoter, the activity of the promoter in response to the NF-AT inhibitor cyclosporine A (CsA) is repressed in human hepatic cell lines, but enhanced in murine hepatic counterparts. To confirm this effect, murine AT3F hepatic cells and human CHL hepatic cells were transfected with different constructions of the promoter linked to a luciferase reporter gene (see[46] for details). The protein levels and the luciferase activity were determined at 24h after treatment with the indicated stimuli: tetradecanoylphorbol acetate 100 nmol/L, Ca^{2+}-ionophore A23187 1 μmol/L; CsA 100 nmol/L. TPA: Tetradecanoylphorbol acetate; CsA: Cyclosporine A; PTGS: Prostaglandin-endoperoxide synthase.

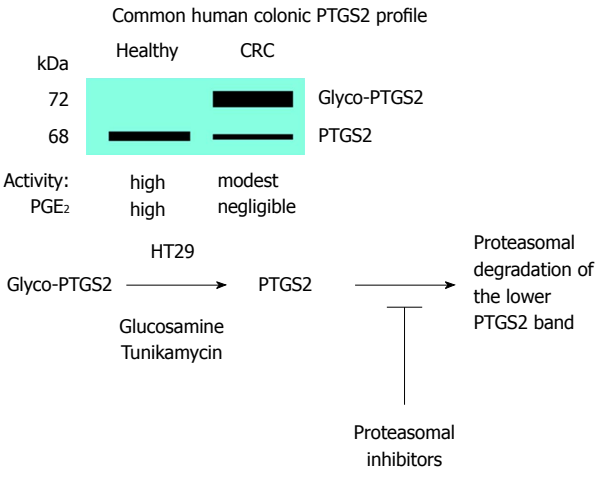

Figure 5 Glycosylation of prostaglandin-endoperoxide synthase 2 in colorectal cancer. The main form in colorectal cancer tissues is the glycosylated 72 kDa protein. This glycosylated prostaglandin-endoperoxide synthase 2 (PTGS2) is also expressed in several tumor colonic cell lines and can be deglycosylated after incubation of the cells with glucosamine or tunikamycin. After this treatment, PTGS2 is rapidly degraded *via* proteasomal activity. CRC: Colorectal cancer; PTGS: Prostaglandin-endoperoxide synthase.

cations are in the basis of most of the pathophysiological responses associated to the different conditions in which PTGS2 is expressed.

Since the catalytic activity of PTGS requires a functional heme group in the protein and this can be modified by different oxidants, such as nitric oxide and other free radicals interacting with the prosthetic group, the enzymatic activity can be altered in this way[56]. This is especially relevant in situations in which the high throughput nitric oxide synthase (NOS-2) is expressed and a high synthesis of NO occurs; however, this cannot exclude other NOS isoenzymes that, although releasing lesser NO, because of the proximity to PTGS may selectively affect its activity, although discrepancies in the literature exist describing either inhibition or activation by NO. In fact, a complex crosstalk between the NOS and the PTGS systems has been reported in spheroid cultures of CRC: NO inhibits PTGS activity through different pathways, including S-nitrosylation by peroxynitrite[57].

Western blot analysis of PTGS2 in samples of CRC patients and in tumor colonic cell lines have evidenced the presence of several immunodetected bands corresponding to PTGS2. The change in electrophoretic mobility of the proteins is due to the presence of glycosylated motifs in the protein as confirmed by biochemical and proteomic studies. Indeed, proteomic analysis of PTGS2 characterized the main glycosylated aminoacidic residues[58]. Both N-and O-linked glycosylation in asparagine and serine/threonine are possible. This glycosylated form is prevalent in CRC samples and in tumor colonic cell lines, but is usually absent in samples of healthy colonic tissue when PTGS2 is expressed[21,59-61]. Indeed, this glycosylated PTGS2 is more resistant to

proteolytic degradation than the non-glycosylated counterpart; however, we have been unable to identify the specific glycosylation(s) of this PTGS2 by using proteomic approaches. In fact, this is surprising since previous work identified the N-glycosylation at Asn580/594 as a condition favoring its proteolysis through the ER-dependent pathway[51]. However, the absence of glycosyl marks in the protein, after treatment with glucosamine that reverts the glycosylated band to the non-glycosylated form, targets the protein for a rapid degradation, as reflected by the absence of changes in the mRNA levels, but inducing a significant decrease in the protein levels of HT29 cells treated with glucosamine[61]. Moreover, inhibitors of the proteasome prevent the degradation of PTGS2 in colonic cell lines treated with glucosamine. In addition to this, the catalytic activity of glycosylated PTGS2 is lesser than the corresponding to the non-glycosylated form[59,61]. Finally, additional work is required to address the effect of PTGS2 glycosylation on the response to the classic inhibitors of the enzyme, a condition of pharmacologic and therapeutic interest in the regulation of the catalytic activity of the enzyme[62]. Figure 5 summarizes the effect of glycosylation on PTGS2 activity and fate.

Another issue no completely resolved in the post-translational modifications of PTGS2 is the phosphorylation in tyrosine and serine/threonine residues. In fact, PTGS2 contains consensus motifs for the phosphorylation by protein tyrosine kinases, such as FYN. However, direct proofs for the occurring of such phosphorylations have failed to provide sufficient evidence. The same happens for the PKC phosphorylation motifs present in the protein. However, it appears that specific tyrosine phosphorylation is required for the functional glycosylation of PTGS2, suggesting the convergence of different pathways in the final post-translational modifications of the enzyme, with relevance not only for the enzymatic activity but also for the targeting and degradation[9].

CONCLUSION

Understanding the pathophysiological role of the post-translational modifications of PTGS2 remains a subject of research in the area of oncology. Assessment of the role of prostanoids in CRC initiation and progression may contribute to a better management of the patients and in the proposal of therapeutic interventions intended to regulate colonic PTGS2 activity. Finally, the possibility exists to use PTGS2 post-translational modifications in biopsies as an additional predictive biomarker in CRC evaluation, and a better integration in the immunomodulatory-molecular pathological epidemiology[43].

REFERENCES

1 **Benelli R**, Venè R, Ferrari N. Prostaglandin-endoperoxide synthase 2 (cyclooxygenase-2), a complex target for colorectal cancer prevention and therapy. *Transl Res* 2018; **196**: 42-61 [PMID: 29421522 DOI: 10.1016/j.trsl.2018.01.003]

2 **Kawamura M**, Inaoka H, Obata S, Harada Y. Why do a wide variety of animals retain multiple isoforms of cyclooxygenase? *Prostaglandins Other Lipid Mediat* 2014; **109-111**: 14-22 [PMID: 24721150 DOI: 10.1016/j.prostaglandins.2014.03.002]

3 **Kobayashi K**, Omori K, Murata T. Role of prostaglandins in tumor microenvironment. *Cancer Metastasis Rev* 2018 Epub ahead of print [PMID: 29926309 DOI: 10.1007/s10555-018-9740-2]

4 **Mitchell JA**, Kirkby NS. Eicosanoids, prostacyclin and cyclooxygenase in the cardiovascular system. *Br J Pharmacol* 2018 Epub ahead of print [PMID: 29468666 DOI: 10.1111/bph.14167]

5 **Su CW**, Zhang Y, Zhu YT. Stromal COX-2 signaling are correlated with colorectal cancer: A review. *Crit Rev Oncol Hematol* 2016; **107**: 33-38 [PMID: 27823649 DOI: 10.1016/j.critrevonc.2016.08.010]

6 **Vosooghi M**, Amini M. The discovery and development of cyclooxygenase-2 inhibitors as potential anticancer therapies. *Expert Opin Drug Discov* 2014; **9**: 255-267 [PMID: 24483845 DOI: 10.1517/17460441.2014.883377]

7 **Chen SF**, Wu CH, Lee YM, Tam K, Tsai YC, Liou JY, Shyue SK. Caveolin-1 interacts with Derlin-1 and promotes ubiquitination and degradation of cyclooxygenase-2 via collaboration with p97 complex. *J Biol Chem* 2013; **288**: 33462-33469 [PMID: 24089527 DOI: 10.1074/jbc.M113.521799]

8 **Kangwan N**, Kim YJ, Han YM, Jeong M, Park JM, Hahm KB. Concerted actions of ameliorated colitis, aberrant crypt foci inhibition and 15-hydroxyprostaglandin dehydrogenase induction by sonic hedgehog inhibitor led to prevention of colitis-associated cancer. *Int J Cancer* 2016; **138**: 1482-1493 [PMID: 26476372 DOI: 10.1002/ijc.29892]

9 **Yu SM**, Kim SJ. Protein phosphorylation on tyrosine restores expression and glycosylation of cyclooxygenase-2 by 2-deoxy-D-glucose-caused endoplasmic reticulum stress in rabbit articular chondrocyte. *BMB Rep* 2012; **45**: 317-322 [PMID: 22617457 DOI: 10.5483/BMBRep.2012.45.5.317]

10 **Yuan C**, Smith WL. A cyclooxygenase-2-dependent prostaglandin E2 biosynthetic system in the Golgi apparatus. *J Biol Chem* 2015; **290**: 5606-5620 [PMID: 25548276 DOI: 10.1074/jbc.M114.632463]

11 **Martín-Sanz P**, Casado M, Boscá L. Cyclooxygenase 2 in liver dysfunction and carcinogenesis: Facts and perspectives. *World J Gastroenterol* 2017; **23**: 3572-3580 [PMID: 28611510 DOI: 10.3748/wjg.v23.i20.3572]

12 **Martín-Sanz P**, Mayoral R, Casado M, Boscá L. COX-2 in liver, from regeneration to hepatocarcinogenesis: what we have learned from animal models? *World J Gastroenterol* 2010; **16**: 1430-1435 [PMID: 20333781 DOI: 10.3748/wjg.v16.i12.1430]

13 **Backshall A**, Alferez D, Teichert F, Wilson ID, Wilkinson RW, Goodlad RA, Keun HC. Detection of metabolic alterations in non-tumor gastrointestinal tissue of the Apc(Min/+) mouse by (1)H MAS NMR spectroscopy. *J Proteome Res* 2009; **8**: 1423-1430 [PMID: 19159281 DOI: 10.1021/pr800793w]

14 **Castro-Sánchez L**, Agra N, Llorente Izquierdo C, Motiño O, Casado M, Boscá L, Martín-Sanz P. Regulation of 15-hydroxyprostaglandin dehydrogenase expression in hepatocellular carcinoma. *Int J Biochem Cell Biol* 2013; **45**: 2501-2511 [PMID: 23954207 DOI: 10.1016/j.biocel.2013.08.005]

15 **Consalvi S**, Biava M, Poce G. COX inhibitors: a patent review (2011 - 2014). *Expert Opin Ther Pat* 2015; **25**: 1357-1371 [PMID: 26566186 DOI: 10.1517/13543776.2015.1090973]

16 **Garcia Rodriguez LA**, Cea-Soriano L, Tacconelli S, Patrignani P. Coxibs: pharmacology, toxicity and efficacy in cancer clinical trials. *Recent Results Cancer Res* 2013; **191**: 67-93 [PMID: 22893200 DOI: 10.1007/978-3-642-30331-9_4]

17 **Rouzer CA**, Marnett LJ. Cyclooxygenases: structural and functional insights. *J Lipid Res* 2009; **50** Suppl: S29-S34 [PMID: 18952571 DOI: 10.1194/jlr.R800042-JLR200]

18 **Wang P**, Bai HW, Zhu BT. Structural basis for certain naturally occurring bioflavonoids to function as reducing co-substrates of cyclooxygenase I and II. *PLoS One* 2010; **5**: e12316 [PMID: 20808785 DOI: 10.1371/journal.pone.0012316]

19 **Alexanian A**, Sorokin A. Cyclooxygenase 2: protein-protein interactions and posttranslational modifications. *Physiol*

Genomics 2017; **49**: 667-681 [PMID: 28939645 DOI: 10.1152/physiolgenomics.00086.2017]
20 **Hu Y**, Suarez J, Fricovsky E, Wang H, Scott BT, Trauger SA, Han W, Hu Y, Oyeleye MO, Dillmann WH. Increased enzymatic O-GlcNAcylation of mitochondrial proteins impairs mitochondrial function in cardiac myocytes exposed to high glucose. *J Biol Chem* 2009; **284**: 547-555 [PMID: 19004814 DOI: 10.1074/jbc.M808518200]
21 **Jang BC**, Sung SH, Park JG, Park JW, Bae JH, Shin DH, Park GY, Han SB, Suh SI. Glucosamine hydrochloride specifically inhibits COX-2 by preventing COX-2 N-glycosylation and by increasing COX-2 protein turnover in a proteasome-dependent manner. *J Biol Chem* 2007; **282**: 27622-27632 [PMID: 17635918 DOI: 10.1074/jbc.M610778200]
22 **Kassassir H**, Siewiera K, Talar M, Stec-Martyna E, Pawlowska Z, Watala C. Non-enzymatic modifications of prostaglandin H synthase 1 affect bifunctional enzyme activity - Implications for the sensitivity of blood platelets to acetylsalicylic acid. *Chem Biol Interact* 2016; **253**: 78-92 [PMID: 27083140 DOI: 10.1016/j.cbi.2016.04.021]
23 **Raman P**, Madhavpeddi L, Gonzales RJ. Palmitate induces glycosylation of cyclooxygenase-2 in primary human vascular smooth muscle cells. *Am J Physiol Cell Physiol* 2018; **314**: C545-C553 [PMID: 29384693 DOI: 10.1152/ajpcell.00254.2017]
24 **Fauvelle F**, Boccard J, Cavarec F, Depaulis A, Deransart C. Assessing Susceptibility to Epilepsy in Three Rat Strains Using Brain Metabolic Profiling Based on HRMAS NMR Spectroscopy and Chemometrics. *J Proteome Res* 2015; **14**: 2177-2189 [PMID: 25761974 DOI: 10.1021/pr501309b]
25 **Kozak KR**, Crews BC, Ray JL, Tai HH, Morrow JD, Marnett LJ. Metabolism of prostaglandin glycerol esters and prostaglandin ethanolamides in vitro and in vivo. *J Biol Chem* 2001; **276**: 36993-36998 [PMID: 11447235 DOI: 10.1074/jbc.M105854200]
26 **Prieto P**, Rosales-Mendoza CE, Terrón V, Toledano V, Cuadrado A, López-Collazo E, Bannenberg G, Martín-Sanz P, Fernández-Velasco M, Boscá L. Activation of autophagy in macrophages by pro-resolving lipid mediators. *Autophagy* 2015; **11**: 1729-1744 [PMID: 26506892 DOI: 10.1080/15548627.2015.1078958]
27 **O'Callaghan G**, Houston A. Prostaglandin E2 and the EP receptors in malignancy: possible therapeutic targets? *Br J Pharmacol* 2015; **172**: 5239-5250 [PMID: 26377664 DOI: 10.1111/bph.13331]
28 **Shirasaka Y**, Shichiri M, Kasai T, Ohno Y, Nakanishi T, Hayashi K, Nishiura A, Tamai I. A role of prostaglandin transporter in regulating PGE_2 release from human bronchial epithelial BEAS-2B cells in response to LPS. *J Endocrinol* 2013; **217**: 265-274 [PMID: 23528477 DOI: 10.1530/JOE-12-0339]
29 **Jay AG**, Hamilton JA. The enigmatic membrane fatty acid transporter CD36: New insights into fatty acid binding and their effects on uptake of oxidized LDL. *Prostaglandins Leukot Essent Fatty Acids* 2018; **138**: 64-70 [PMID: 27288302 DOI: 10.1016/j.plefa.2016.05.005]
30 **Glatz JF**. Lipids and lipid binding proteins: a perfect match. *Prostaglandins Leukot Essent Fatty Acids* 2015; **93**: 45-49 [PMID: 25154384 DOI: 10.1016/j.plefa.2014.07.011]
31 **Dixon DA**, Blanco FF, Bruno A, Patrignani P. Mechanistic aspects of COX-2 expression in colorectal neoplasia. *Recent Results Cancer Res* 2013; **191**: 7-37 [PMID: 22893198 DOI: 10.1007/978-3-642-30331-9_2]
32 **Marion-Letellier R**, Savoye G, Ghosh S. Fatty acids, eicosanoids and PPAR gamma. *Eur J Pharmacol* 2016; **785**: 44-49 [PMID: 26632493 DOI: 10.1016/j.ejphar.2015.11.004]
33 **Salvado MD**, Alfranca A, Haeggström JZ, Redondo JM. Prostanoids in tumor angiogenesis: therapeutic intervention beyond COX-2. *Trends Mol Med* 2012; **18**: 233-243 [PMID: 22425675 DOI: 10.1016/j.molmed.2012.02.002]
34 **Wang D**, Fu L, Sun H, Guo L, DuBois RN. Prostaglandin E2 Promotes Colorectal Cancer Stem Cell Expansion and Metastasis in Mice. *Gastroenterology* 2015; **149**: 1884-1895.e4 [PMID: 26261008 DOI: 10.1053/j.gastro.2015.07.064]
35 **Cebola I**, Custodio J, Muñoz M, Díez-Villanueva A, Paré L, Prieto P, Aussó S, Coll-Mulet L, Boscá L, Moreno V, Peinado MA. Epigenetics override pro-inflammatory PTGS transcriptomic signature towards selective hyperactivation of PGE2 in colorectal cancer. *Clin Epigenetics* 2015; **7**: 74 [PMID: 26207152 DOI: 10.1186/s13148-015-0110-4]
36 **Valverde A**, Peñarando J, Cañas A, López-Sánchez LM, Conde F, Hernández V, Peralbo E, López-Pedrera C, de la Haba-Rodríguez J, Aranda E, Rodríguez-Ariza A. Simultaneous inhibition of EGFR/VEGFR and cyclooxygenase-2 targets stemness-related pathways in colorectal cancer cells. *PLoS One* 2015; **10**: e0131363 [PMID: 26107817 DOI: 10.1371/journal.pone.0131363]
37 **Venè R**, Tosetti F, Minghelli S, Poggi A, Ferrari N, Benelli R. Celecoxib increases EGF signaling in colon tumor associated fibroblasts, modulating EGFR expression and degradation. *Oncotarget* 2015; **6**: 12310-12325 [PMID: 25987127 DOI: 10.18632/oncotarget.3678]
38 **Boukouris AE**, Zervopoulos SD, Michelakis ED. Metabolic Enzymes Moonlighting in the Nucleus: Metabolic Regulation of Gene Transcription. *Trends Biochem Sci*2016; **41**: 712-730 [PMID: 27345518 DOI: 10.1016/j.tibs.2016.05.013]
39 **Min KW**, Lee SH, Baek SJ. Moonlighting proteins in cancer. *Cancer Lett* 2016; **370**: 108-116 [PMID: 26499805 DOI: 10.1016/j.canlet.2015.09.022]
40 **Na HK**, Park JM, Lee HG, Lee HN, Myung SJ, Surh YJ. 15-Hydroxyprostaglandin dehydrogenase as a novel molecular target for cancer chemoprevention and therapy. *Biochem Pharmacol* 2011; **82**: 1352-1360 [PMID: 21856294 DOI: 10.1016/j.bcp.2011.08.005]
41 **Ramanan M**, Doble M. Transcriptional Regulation of mPGES1 in Cancer: An Alternative Approach to Drug Discovery? *Curr Drug Targets* 2017; **18**: 119-131 [PMID: 27570080 DOI: 10.2174/1389450117666160826093137]
42 **Agra Andrieu N**, Motiño O, Mayoral R, Llorente Izquierdo C, Fernández-Alvarez A, Boscá L, Casado M, Martín-Sanz P. Cyclooxygenase-2 is a target of microRNA-16 in human hepatoma cells. *PLoS One* 2012; **7**: e50935 [PMID: 23226427 DOI: 10.1371/journal.pone.0050935]
43 **Ogino S**, Nowak JA, Hamada T, Milner DA Jr., Nishihara R. Insights into Pathogenic Interactions Among Environment, Host, and Tumor at the Crossroads of Molecular Pathology and Epidemiology. *Annu Rev Pathol* 2018 Epub ahead of print [PMID: 30125150 DOI: 10.1146/annurev-pathmechdis-012418-012818]
44 **Ogino S**, Nowak JA, Hamada T, Phipps AI, Peters U, Milner DA Jr, Giovannucci EL, Nishihara R, Giannakis M, Garrett WS, Song M. Integrative analysis of exogenous, endogenous, tumour and immune factors for precision medicine. *Gut* 2018; **67**: 1168-1180 [PMID: 29437869 DOI: 10.1136/gutjnl-2017-315537]
45 **Schumacher Y**, Aparicio T, Ourabah S, Baraille F, Martin A, Wind P, Dentin R, Postic C, Guilmeau S. Dysregulated CRTC1 activity is a novel component of PGE2 signaling that contributes to colon cancer growth. *Oncogene* 2016; **35**: 2602-2614 [PMID: 26300003 DOI: 10.1038/onc.2015.283]
46 **Callejas NA**, Boscá L, Williams CS, DuBOIS RN, Martín-Sanz P. Regulation of cyclooxygenase 2 expression in hepatocytes by CCAAT/enhancer-binding proteins. *Gastroenterology* 2000; **119**: 493-501 [PMID: 10930384 DOI: 10.1053/gast.2000.9374]
47 **Callejas NA**, Fernández-Martínez A, Castrillo A, Boscá L, Martín-Sanz P. Selective inhibitors of cyclooxygenase-2 delay the activation of nuclear factor kappa B and attenuate the expression of inflammatory genes in murine macrophages treated with lipopolysaccharide. *Mol Pharmacol* 2003; **63**: 671-677 [PMID: 12606776 DOI: 10.1124/mol.63.3.671]
48 **Appleby SB**, Ristimäki A, Neilson K, Narko K, Hla T. Structure of the human cyclo-oxygenase-2 gene. *Biochem J* 1994; **302** (Pt 3): 723-727 [PMID: 7945196 DOI: 10.1042/bj3020723]
49 **Mbonye UR**, Wada M, Rieke CJ, Tang HY, Dewitt DL, Smith WL. The 19-amino acid cassette of cyclooxygenase-2 mediates entry of the protein into the endoplasmic reticulum-associated degradation system. *J Biol Chem* 2006; **281**: 35770-35778 [PMID: 17001073 DOI: 10.1074/jbc.M608281200]
50 **Mbonye UR**, Yuan C, Harris CE, Sidhu RS, Song I, Arakawa T, Smith WL. Two distinct pathways for cyclooxygenase-2 protein degradation. *J Biol Chem* 2008; **283**: 8611-8623 [PMID: 18203712 DOI: 10.1074/

jbc.M710137200]
51 **Wada M**, Saunders TL, Morrow J, Milne GL, Walker KP, Dey SK, Brock TG, Opp MR, Aronoff DM, Smith WL. Two pathways for cyclooxygenase-2 protein degradation in vivo. *J Biol Chem* 2009; **284**: 30742-30753 [PMID: 19758985 DOI: 10.1074/jbc.M109.052415]
52 **Ho MY**, Tang SJ, Ng WV, Yang W, Leu SJ, Lin YC, Feng CK, Sung JS, Sun KH. Nucleotide-binding domain of phosphoglycerate kinase 1 reduces tumor growth by suppressing COX-2 expression. *Cancer Sci* 2010; **101**: 2411-2416 [PMID: 20731664 DOI: 10.1111/j.1349-7006.2010.01691.x]
53 **Chisanga D**, Keerthikumar S, Pathan M, Ariyaratne D, Kalra H, Boukouris S, Mathew NA, Al Saffar H, Gangoda L, Ang CS, Sieber OM, Mariadason JM, Dasgupta R, Chilamkurti N, Mathivanan S. Colorectal cancer atlas: An integrative resource for genomic and proteomic annotations from colorectal cancer cell lines and tissues. *Nucleic Acids Res* 2016; **44**: D969-D974 [PMID: 26496946 DOI: 10.1093/nar/gkv1097]
54 **Wright JM**. The double-edged sword of COX-2 selective NSAIDs. *CMAJ* 2002; **167**: 1131-1137 [PMID: 12427705]
55 **Lucido MJ**, Orlando BJ, Vecchio AJ, Malkowski MG. Crystal Structure of Aspirin-Acetylated Human Cyclooxygenase-2: Insight into the Formation of Products with Reversed Stereochemistry. *Biochemistry* 2016; **55**: 1226-1238 [PMID: 26859324 DOI: 10.1021/acs.biochem.5b01378]
56 **Sorokin A**. Nitric Oxide Synthase and Cyclooxygenase Pathways: A Complex Interplay in Cellular Signaling. *Curr Med Chem* 2016; **23**: 2559-2578 [PMID: 27480213 DOI: 10.2174/0929867323666160729105312]
57 **Paduch R**, Kandefer-Szerszeń M. Nitric Oxide (NO) and Cyclooxygenase-2 (COX-2) Cross-Talk in Co-Cultures of Tumor Spheroids with Normal Cells. *Cancer Microenviron* 2011; **4**: 187-198 [PMID: 21909878 DOI: 10.1007/s12307-011-0063-x]
58 **Nemeth JF**, Hochgesang GP Jr, Marnett LJ, Caprioli RM. Characterization of the glycosylation sites in cyclooxygenase-2 using mass spectrometry. *Biochemistry* 2001; **40**: 3109-3116 [PMID: 11258925 DOI: 10.1021/bi002313c]
59 **Cao C**, Gao R, Zhang M, Amelio AL, Fallahi M, Chen Z, Gu Y, Hu C, Welsh EA, Engel BE, Haura EB, Cress WD, Wu L, Zajac-Kaye M, Kaye FJ. Role of LKB1-CRTC1 on glycosylated COX-2 and response to COX-2 inhibition in lung cancer. *J Natl Cancer Inst* 2014; **107**: 358 [PMID: 25465874 DOI: 10.1093/jnci/dju358]
60 **Park SH**, Hong H, Han YM, Kangwan N, Kim SJ, Kim EH, Hahm KB. Nonsteroidal anti-inflammatory drugs (NSAID) sparing effects of glucosamine hydrochloride through N-glycosylation inhibition; strategy to rescue stomach from NSAID damage. *J Physiol Pharmacol* 2013; **64**: 157-165 [PMID: 23756390]
61 **Prieto P**, Jaén RI, Calle D, Nú-ez E, Gómez M. HRMAS and proteomic analysis of new biomarkers in colorectal cancer: the paradigm of posttranslational modifications of COX-2. Submitted 2018
62 **Sevigny MB**, Graham K, Ponce E, Louie MC, Mitchell K. Glycosylation of human cyclooxygenase-2 (COX-2) decreases the efficacy of certain COX-2 inhibitors. *Pharmacol Res* 2012; **65**: 445-450 [PMID: 22245433 DOI: 10.1016/j.phrs.2012.01.001]

P- Reviewer: Chan AT **S- Editor**: Ma RY **L- Editor**: A
E- Editor: Yin SY

World Journal of Gastroenterology

Submit a Manuscript: https://www.f6publishing.com

World J Gastroenterol 2018 December 28; 24(48): 5462-5476

DOI: 10.3748/wjg.v24.i48.5462

ISSN 1007-9327 (print) ISSN 2219-2840 (online)

ORIGINAL ARTICLE

Basic Study

Counteraction of perforated cecum lesions in rats: Effects of pentadecapeptide BPC 157, L-NAME and L-arginine

Domagoj Drmic, Mariam Samara, Tinka Vidovic, Dominik Malekinusic, Marko Antunovic, Borna Vrdoljak, Jelena Ruzman, Marija Milkovic Perisa, Katarina Horvat Pavlov, Jerusha Jeyakumar, Sven Seiwerth, Predrag Sikiric

Domagoj Drmic, Mariam Samara, Tinka Vidovic, Dominik Malekinusic, Marko Antunovic, Borna Vrdoljak, Jelena Ruzman, Marija Milkovic Perisa, Katarina Horvat Pavlov, Jerusha Jeyakumar, Sven Seiwerth, Predrag Sikiric, Departments of Pharmacology and Pathology, Medical Faculty University of Zagreb, Zagreb 10000, Croatia

ORCID number: Domagoj Drmic (0000-0002-1081-7175); Mariam Samara (0000-0003-2384-273X); Tinka Vidovic (0000-0003-0092-9365); Dominik Malekinusic (0000-0001-6258-5647); Marko Antunovic (0000-0002-3801-5481); Borna Vrdoljak (0000-0003-2306-8799); Jelena Ruzman (0000-0002-9807-7270); Marija Milkovic Perisa (0000-0002-9530-9208); Katarina Horvat Pavlov (0000-0002-2661-7346); Jerusha Jeyakumar (0000-0003-4883-3899); Sven Seiwerth (0000-0002-5894-419X); Predrag Sikiric (0000-0002-7952-2252).

Author contributions: Drmic D, Seiwerth S and Sikiric P designed the research. Drmic D, Samara M, Vidovic T, Malekinusic D, Antunovic M, Vrdoljak B, Ruzman J, Milkovic Perisa M, Horvat Pavlov K, Jeyakumar J, Seiwerth S and Sikiric P performed the research. Seiwerth S and Sikiric P contributed reagents and analytic tools. Drmic D, Samara M, Vidovic T, Malekinusic D, Antunovic M, Vrdoljak B, Ruzman J, Milkovic Perisa M, Horvat Pavlov K, Jeyakumar J, Seiwerth S and Sikiric P analyzed the data. Drmic D, Seiwerth S and Sikiric P wrote the paper.

Institutional review board statement: The study was reviewed and approved by the Department of Veterinary, Ministry of Agriculture, Republic of Croatia, No: UP/I 322-01/07-01/210.

Conflict-of-interest statement: The authors state that they have no conflicts of interest.

Data sharing statement: No additional data are available.

Manuscript source: Invited manuscript

Corresponding author: Predrag Sikiric, MD, PhD, Professor, Department of Pharmacology, School of Medicine, University of Zagreb, Salata 11, POB 916, Zagreb 10000, Croatia. sikiric@mef.hr
Telephone: +385-1-4566833
Fax: +385-1-4920050

Received: August 20, 2018
Peer-review started: August 20, 2018
First decision: October 8, 2018
Revised: December 5, 2018
Accepted: December 19, 2018
Article in press: December 19, 2018
Published online: December 28, 2018

Abstract

AIM

To study the counteraction of perforated cecum lesion using BPC 157 and nitric oxide (NO) system agents.

METHODS

Alongside with the agents' application (after 1 min, medication (/kg, 10 mL/2 min bath/rat) includes: BPC 157 (10 μg), L-NAME (5 mg), L-arginine (100mg) alone or combined, and saline baths (controls)) on the rat perforate cecum injury, we continuously assessed the gross reappearance of the vessels (USB microcamera) quickly propagating toward the defect at the cecum surface, defect contraction, bleeding attenuation, MDA-

and NO-levels in cecum tissue at 15 min, and severity of cecum lesions and adhesions at 1 and 7 d.

RESULTS

Post-injury, during/after a saline bath, the number of vessels was significantly reduced, the defect was slightly narrowed, bleeding was significant and MDA-levels increased and NO-levels decreased. BPC 157 bath: the vessel presentation was markedly increased, the defect was noticeably narrowed, the bleeding time was shortened and MDA- and NO-levels remained normal. L-NAME: reduced vessel presentation but not more than the control, did not change defect and shortened bleeding. L-arginine: exhibited less vessel reduction, did not change the defect and prolonged bleeding. In combination, mutual counteraction occurred (L-NAME + L-arginine) or the presentation was similar to that of BPC 157 rats (BPC 157 + L-NAME; BPC 157 + L-arginine; BPC 157 + L-NAME + L-arginine), except the defect did not change. Thereby at day 1 and 7, saline, L-NAME, L-arginine and L-NAME + L-arginine failed (defect was still open and large adhesions present).

CONCLUSION

The therapeutic effect was achieved with BPC 157 alone or in combination with L-NAME and L-arginine as it was able to consolidate the stimulating and inhibiting effects of the NO-system towards more effective healing recruiting vessels.

Key words: BPC 157; Perforated cecum; L-arginine; L-NAME; Vessels; Rats

Core tip: In rats, the cecum was exposed, and a perforation (5-mm diameter) was made at the ventral face of the basal region of the cecum close to the largest curvature. After 1 min, a bath (1 mL/rat) containing BPC 157, L-NAME, L-arginine, saline (controls) was directly applied to the perforated cecum, alone or in combination. Previously, BPC 157 rapidly activated the collateral circulation from existing vessels in ischemic colitis or inferior caval vein occlusion (by passing through the arcade vessels or the left ovarian vein and other veins) to reestablish blood flow and exert its free radical scavenger effect in both ischemia and reperfusion.

Drmic D, Samara M, Vidovic T, Malekinusic D, Antunovic M, Vrdoljak B, Ruzman J, Milkovic Perisa M, Horvat Pavlov K, Jeyakumar J, Seiwerth S, Sikiric P. Counteraction of perforated cecum lesions in rats: Effects of pentadecapeptide BPC 157, L-NAME and L-arginine. *World J Gastroenterol* 2018; 24(48): 5462-5476

URL: https://www.wjgnet.com/1007-9327/full/v24/i48/5462.htm

DOI: https://dx.doi.org/10.3748/wjg.v24.i48.5462

INTRODUCTION

In cecum perforation studies[1-3] the immediate post-perforation threat is rarely studied, particularly regarding: the rapid disappearance of blood vessels in the cecum serosa that are instantly emptied and thereby "disappear", perforation defect enlargement, bleeding and fluid leakage, increased oxidative stress and disturbed nitric oxide (NO) levels in cecum tissue. Likewise, the possible effect of cytoprotective agents, known to act as a class on endothelium maintenance in the gastrointestinal tract (and, thereby, mucosal maintenance)[4-9], especially the stable gastric pentadecapeptide BPC 157 as a cytoprotective agent rapidly acting on endothelium integrity maintenance[10-19], has been not investigated.

We focused on a perforated cecum, the stable gastric pentadecapeptide BPC 157, the NOS-blocker L-NAME, and the NOS-substrate L-arginine, as well as on the initial post-perforation period, rapid disappearance of blood vessels at the cecum serosa (emptied/disappeared), a large immediate defect, bleeding, leakage of fluid, increased oxidative stress and disturbed NO levels in cecum tissue. The rationale was the beneficial effects in rats with ischemic colitis and inferior caval vein occlusion syndrome[20,21] and the particular effect of BPC 157 on blood vessels[20,21]. Namely, we recently demonstrated that BPC 157 rapidly activated the collateral circulation from existing vessels in rats with ischemic colitis or inferior caval vein occlusion[20,21]. In ischemic colitis (*i.e.*, segment of the left colic artery and vein excluded by two ligations) we proved effectiveness by passing through arcade vessels[20]. Antagonizing the syndrome of inferior caval vein infrarenal occlusion, we evidenced by passing through the left ovarian vein and other veins[21]. These accentuated the specific action of BPC 157 to reestablish blood flow, and exert its free radical scavenger effect in both ischemia and reperfusion[20,21].

In addition, BPC 157, as a novel mediator of Robert's cytoprotection[4,10-19], also affects several other molecular pathways[21-27]. It is native and stable in human gastric juice and maintains gastrointestinal mucosal integrity[10-19], and it represents a prototype of a more effective class of cytoprotective agents with both prophylactic and therapeutic abilities[5,17] (unlike standard cytoprotective agents that exhibit only prophylactic effectiveness (shared limitation of activity))[4-9]. BPC 157 (used in ulcerative colitis and now in multiple sclerosis trials) also counteracts colitis (in various models of colitis)[20,28-33] and its complications, such as fistulas[34-38], failed healing of anastomoses[28,29,39,40] and other gastrointestinal lesions[10-19], given parenterally or orally. Furthermore, BPC 157 is known to counteract thrombosis, not only after abdominal aorta anastomosis[41] or inferior caval vein ligation[21], but also after bleeding prolongation upon amputation and the administration of anticoagulants and aspirin[42,43] or inferior caval vein ligation[21]. This

effect is related to its endothelial maintenance[21,41-43] and its interaction with the NO system, which provides the counteraction of both the opposite effects of L-NAME (prothrombotic) and L-arginine (antithrombotic) application[43]. Otherwise, bleeding from the perforated lesion and perforated lesion outcome might be complicated with these innate L-NAME and NOS substrate L-arginine effects[43].

In practice, as described previously[20,21], our approach to cure a perforated cecum begins with the original understanding of stomach cytoprotection (a very rapid protection of the stomach endothelium and epithelium against diverse direct injuries; endothelium maintenance → epithelium maintenance), regularly shown with cytoprotective agents[4-9]. This was further perceived as an extended cytoprotection background[20,21] (endothelium maintenance → epithelium maintenance = blood vessel recruitment and activation towards the site of injury), also described as "bypassing" occlusion via alternative ways, as demonstrated with BPC 157[20,21], which can likely cure rats with a perforated cecum and thereafter. Furthermore, antagonization of two distinct detrimental obstructive events (*i.e.*, left colic artery and vein ligation-colitis and inferior caval vein-infrarenal ligation-full syndrome)[20,21] appears. Likewise, positive outcome matching also appears, providing a special effect: blood vessel recruitment to organize bypassing of vessel occlusions and reestablishment of blood flow by BPC 157 therapy[20,21]. Thus, we can make the argument that, under analogous or more severe conditions (*i.e.*, perforated cecum), a similar positive outcome will appear. If this occurs, we can attenuate cecum perforation syndrome; in BPC 157-treated rats, therapy may lead to attenuation and reversal of the consequent tissue damage. Specifically, a reversal of vessel disappearance by vessels "running" toward the defect (vessels filled/reappeared), transition of defect enlargement to defect narrowing (note, fistula defects healing)[34-38], change from prolonged bleeding to bleeding attenuation[21,42,43], induced reduction of increased MDA values and normalization of NO values in cecum tissue[20,21]. In subsequent days and weeks, this may lead to a closed cecum defect and attenuation of adhesion formation.

For further clarification and to demonstrate a direct beneficial effect, medication (BPC 157, L-NAME, and L-arginine, alone and/or together) was applied directly to the injury[20,21] once during surgery, as a bath to the perforated cecum, the solution then spread throughout the abdominal cavity. Consequently, the beneficial effects are directly related to the reversal of perforated injury outcome consequences, in both the early and later periods. These effects may be triggered shortly after injury initiation, or reverse an already advanced injury course.

MATERIALS AND METHODS

Animals

Male Albino Wistar rats, 200 g b.w., were randomly assigned (7 rats per group) and used for the experiments, which were approved by the local ethics committee. The perforation procedure was performed in rats that had food and water ad libitum before the procedure and until the end of the experiment.

Drugs

Pentadecapeptide Gly-Glu-Pro-Pro-Pro-Gly-Lys-Pro-Ala-Asp-Asp-Ala-Gly-Leu-Val, M.W. 1419, named BPC 157, a part of the sequence of human gastric juice protein encoded by BPC, freely soluble in water at pH 7.0 and in saline, was prepared (Diagen, Ljubljana, Slovenia) as described previously[10-21]. The peptide with 99% high-pressure liquid chromatography (HPLC) purity, 1-des-Gly peptide as a biologically inactive impurity, was used[10-21]. L-NAME and L-arginine were commercially purchased (Sigma, United States).

Perforated defect creation, medication, assessment

In deeply anaesthetized rats (thiopental (Rotexmedica, Germany) 40 mg/kg ip, apaurin (Krka, Slovenia) 10 mg/kg ip), the cecum was exposed, and a perforation (5-mm diameter) was made at the ventral aspect of the basal region of the cecum close to the largest curvature; the rats were monitored for the next 15 min.

After 1 min, a bath (1 mL/rat) containing BPC 157 (0.01 mg/kg), NOS blocker L-NAME (5 mg/kg), or NOS substrate L-arginine (100 mg/kg) was directly applied to the perforated cecum, alone or combined, and spread through the abdominal cavity, whereas controls accordingly received a saline bath of equal volume. Using a USB microscope camera (Veho discovery VMS-004D-400x USB microscope; Veho®, United Kingdom), from the point immediately before therapy, we recorded and assessed the blood vessels (emptied/disappeared; refilled/reappeared) (total % of cecum vessel augmentation/reduction from proximal to distal end = [number of blood vessels (10 vessels assessed) /100] × %] in terms of augmentation/reduction of each vasa recta (0 as the point immediately before therapy) and defect closing or widening (as % of presentation immediately before therapy) and at particular time points: A-after perforation (1 min), B-during application (2 min), C-period after application (2 min), D-next 5 min period and E-period until the end of observation (15 min). The bleeding time (s) throughout that period was also assessed; at 15 min, oxidative stress was measured by quantifying thiobarbituric acid (TBA) reactivity as malondialdehyde (MDA) equivalents, and nitric oxide determination in cecum tissue was also carried out.

At day 1 and day 7, rats were relaparotimiezed, and we assessed the serosal/mucosal defect (longest lesion diameter, mm) and adhesion severity scoring (adhesions of the abdominal wall-1 point; adhesions of the intestine-1 point; adhesions of the cecal area: ventral side-1 point/dorsal side-1 point; adhesions involving both the intestine and colon-3 points) (resulting in a total maximum score of 7). Representative tissue sections were processed for further histological analysis as described previously[10-21].

Oxidative stress in cecum tissue

At 15 min post-injury, oxidative stress in the tissue samples (1 cm^2 around the defect) was assessed by quantifying thiobarbituric acid (TBA) reactivity as malondialdehyde (MDA) equivalents. Trichloroacetic acid (TCA) was added to homogenize the tissue samples, which were then centrifuged (3000 rpm, 5 min), and the supernatant was collected. Thereafter, 1% TBA was added, and the samples were boiled (95 ℃, 60 min). The tubes were kept on ice for 10 min, and the absorbance was determined at the wavelengths of 532 and 570 nm. The concentration of MDA was read from a standard calibration curve plotted using 1,1,3,3'-tetra-ethoxy propane (TEP). The extent of lipid peroxidation was expressed as MDA using a molar extinction coefficient for MDA of 1.56×10^5 mol/(L•cm). The results are expressed in nmol/mg of protein[20,21].

Nitric oxide determination in cecum tissue

At 15 min post-injury, we determined the nitric oxide (NO) levels in cecum tissue samples using the Griess reaction (Griess Reagent System, Promega, United States). Sulfanilamide was then incubated with the homogenized tissue, and then, N-1-naphthylethylenediamine dihydrochloride was added. The Griess reaction is based on a diazotization reaction in which acidified nitrite reacts with diazonium ions and, in a further step, are coupled to N-1-naphthylethylenediamine dihydrochloride, forming a chromophoric azo derivate. The absorbance was measured at 540 nm using sodium nitrite solution as the standard. NO levels are reported in μmol/mg protein. The protein concentrations were determined using a commercial kit (BioRad Protein DR Assay Reagent Kit, United States)[20,21].

Statistical analysis

Statistical analysis was performed by parametric one-way ANOVA with the post-hoc Newman-Keuls test and non-parametric Kruskal-Wallis and subsequent Mann-Whitney *U*-tests to compare the groups. The values are represented as means ± SD and minimum/median/maximum. The results with $P < 0.05$ were considered significant.

RESULTS

After direct administration of the agents to the site of injury one minute after cecum perforation, the results obtained can clearly describe the ongoing events. Of note, after the administration of the drug directly to the lesion, the solution spread through the abdominal cavity; however, its effect can still be directly correlated with the injury course (aggravated, regular, reversed), particularly in the earliest period, and then, the final outcome is seen at one week after surgery and medication application.

The numerous negative changes [*i.e.,* initial course: vessel presentation (Figure 1), defect closing or widening (Figure 2), bleeding time (Figure 3), NO-cecum level (Figure 4), MDA-cecum level (Figure 5); and final course of the injury: cecum defect and adhesions at 1 or 7 days (Table 1)] are significant in several respects.

Depending on the agent applied, the initial defensive response confers blood vessel presentation (emptied/disappeared; refilled/reappeared) and augmentation/reduction (Figures 1, 6 and 7), defect closing or widening (Figure 2) and bleeding prolongation or shortening (Figures 3 and 7). MDA oxidative stress (Figure 5) and NO levels (Figure 4) were determined in the cecum tissue as well. They permit combining of initial response to the final response (cecum defect and adhesions at 1 or 7 days (Table 1)].

Initial course, blood vessel presentation, bleeding, and defect contraction

Controls: In rats that received a saline bath, the initial course was progressive vessel disappearance and very poor vessel branching, which occurred during application (Figures 1 and 6). Thereafter, the defect only had a small initial contraction (Figure 2) and then continuous widening. Additionally, there was a significant bleeding period (Figures 3 and 7).

BPC 157 therapy: Rats with a perforated cecum that underwent a BPC 157 bath exhibited progressive vessel presentation toward the injury (*i.e.*, a network of small vessels branching around the injury) (Figures 1 and 6). The defect contracted during application (Figure 2) and the bleeding period was significantly shortened thereafter (Figure 3).

L-arginine therapy: After application of L-arginine, rats with a perforated cecum exhibited less vessel disappearance (Figure 1). We noted counteracted defect widening (Figure 2), and the bleeding period was significantly prolonged (Figure 3).

L-NAME therapy: After application of L-NAME, rats with a perforated cecum exhibited vessel disappearance similar to controls (Figure 1). There was counteraction of defect widening (Figure 2), and the bleeding period was shortened (Figure 3).

Combination therapy of L-arginine and L-NAME: After application of L-arginine and L-NAME, rats with a perforated cecum exhibited a combined effect, with less vessel disappearance (Figure 1), counteracted defect widening (Figure 2) and a bleeding period in the range of that for the control animals (Figure 3).

Combined therapy of L-arginine and/or L-NAME with BPC 157: After application of BPC 157 with L-arginine and/or L-NAME, rats with a perforated cecum that underwent combined BPC 157 therapy (L-NAME + BPC 157; L-arginine + BPC 157; L-NAME + L-arginine + BPC 157) regularly exhibited progressive vessel presentation (Figure 1) and a shortened bleeding time (Figure 3),

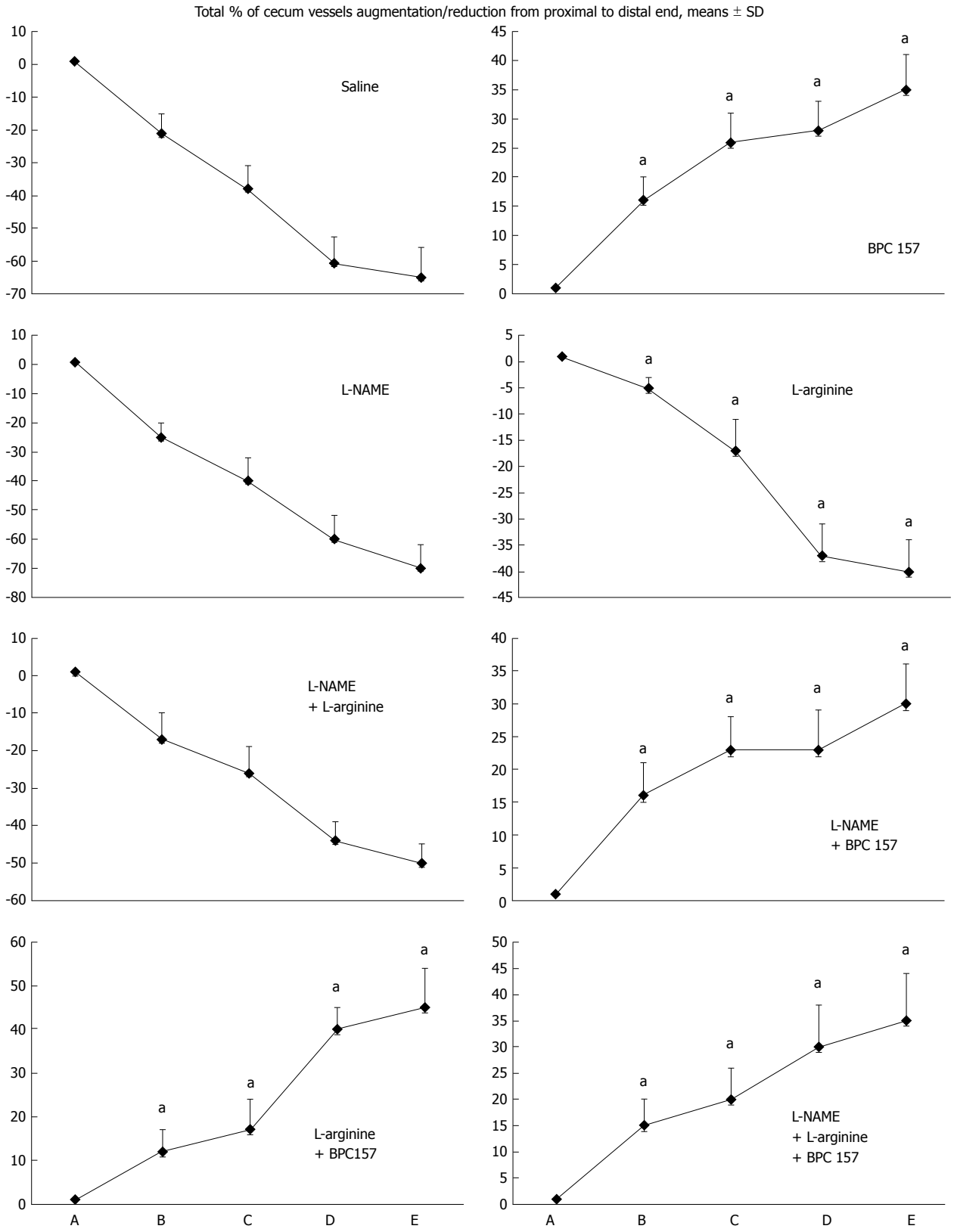

Figure 1 Blood vessels, filled/appearance or cleared out/disappearance (assessed with a USB microscope camera, Veho discovery VMS-004D-400x USB microscope), as [total % of cecum vessels augmentation/reduction from proximal to distal end = [number of blood vessels (10 vessels assessed) /100] x % of augmentation/reducing of each vasa recta (0 as point immediately before therapy) (A)]. A: after perforation (1 min); B: during application (2 min); C: the period after application (2 min); D: the subsequent 5-min period; E: the period until the end of the observation (15 min). At 1 min post-injury, medication (/kg, 10 mL/2 min bath/rat) administered at the perforated (5 mm diameter) cecum lesion and cecum (M-mucosa; S-serosa), including BPC 157 (10 μg), NOS blocker L-NAME (5 mg), NOS substrate L-arginine (100 mg) alone or combined, and saline bath of equal volume (controls). Rats were then left after abdominal closure undisturbed until sacrifice, at day 1 or day 7. [a]*P* < 0.05 *vs* control.

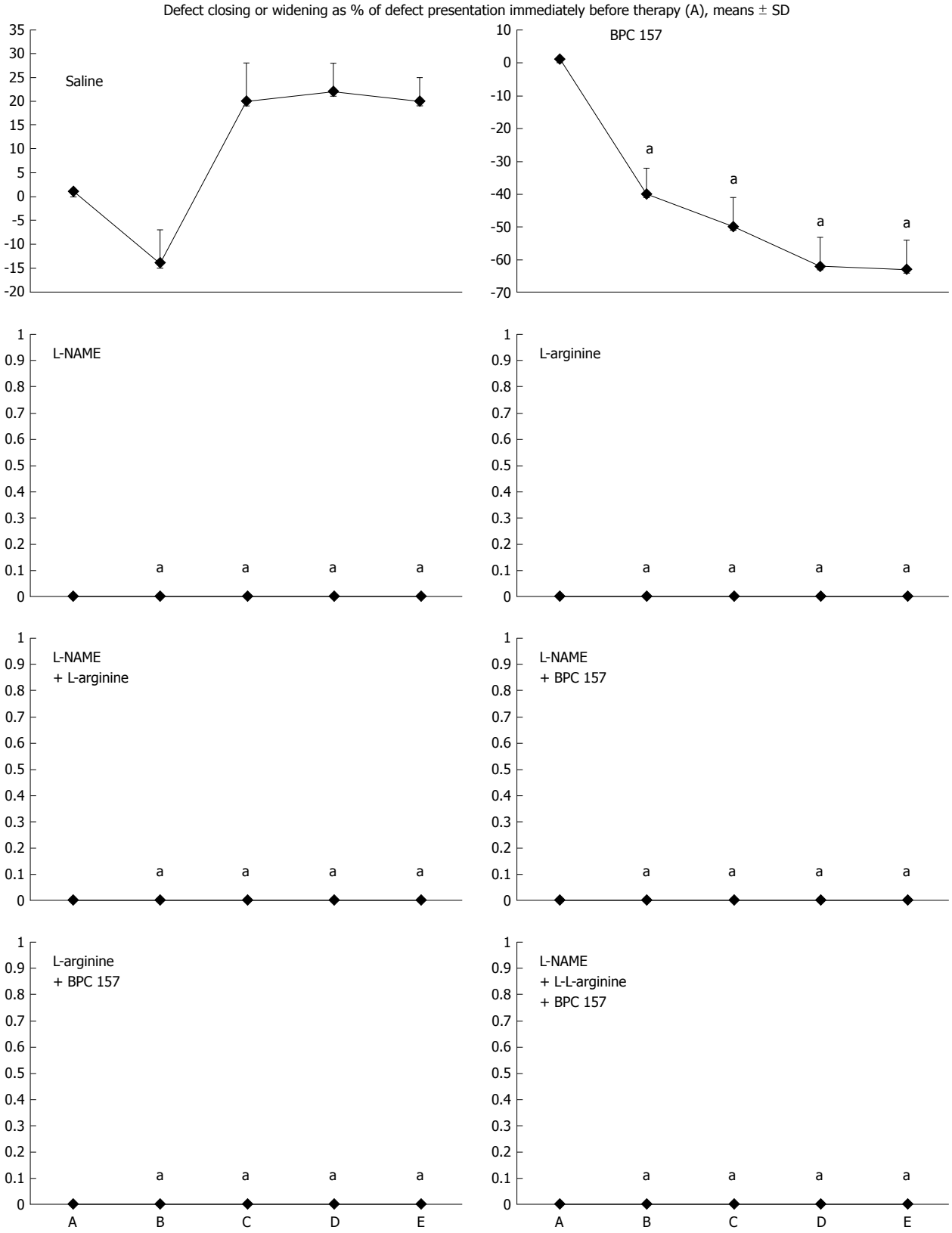

Figure 2 Defect closing or widening [both as % of presentation immediately before therapy (A)]; bleeding time (s); A: after perforation (1 min); B: during application (2 min); C: the period after application (2 min); D: the subsequent 5-min period; E: the period until the end of the observation (15 min). At 1 min post-injury, administration of medication (/kg, 10 mL/2 min bath/rat) at the perforated (5 mm diameter) cecum lesion and cecum (M-mucosa; S-serosa), including BPC 157 (10 μg), NOS blocker L-NAME (5 mg), NOS substrate L-arginine (100 mg) alone or combined, and a saline bath equal volume (controls). Rats were then left after abdominal closure undisturbed until sacrifice, at day 1 or day 7. $^{a}P < 0.05$ at least *vs* control.

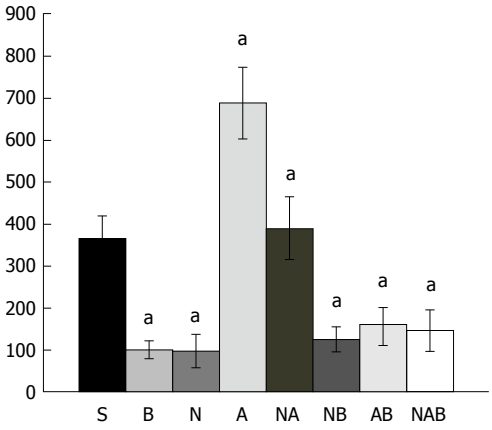

Figure 3 Bleeding time after perforation. At 1 min post-injury, administration of medication (/kg, 10 mL/2 min bath/rat) at the perforated (5 mm diameter) cecum lesion and cecum includes BPC 157 (10 μg) (B), NOS blocker L-NAME (5 mg) (N), NOS substrate L-arginine (100 mg) (A) alone or combined, and a saline bath of equal volume (controls) (S). Rats were then left after abdominal closure undisturbed until sacrifice, at day 1 or day 7. $^{a}P < 0.05$ at least *vs* control (S).

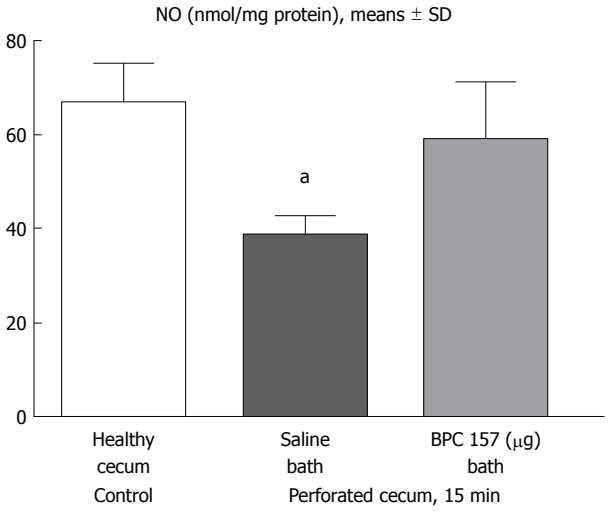

Figure 4 15 min post-injury, we determined nitric oxide in cecum tissue samples using the Griess reaction. Administration of medication (/kg, 10 mL/2 min bath/rat) at the perforated (5 mm diameter) cecum lesion and cecum was BPC 157 (10 μg) or a saline bath equal volume (controls). Minimum $^{a}P < 0.05$ *vs* control.

similar to the rats that received BPC 157 alone. All rats exhibited counteraction of defect widening (Figure 2).

Final course, defect and adhesion presentation at one day and one week of follow up

Controls: Regularly, after one day or one week, rats that underwent cecum perforation presented with a significant defect (Table 1, Figure 8) that remained open and showed significant adhesions (Table 1).

BPC 157 therapy: Rats with a perforated cecum that underwent a BPC 157 bath exhibited an attenuated defect and finally, no gross defect (Table 1, Figure 8), and markedly fewer adhesions were present.

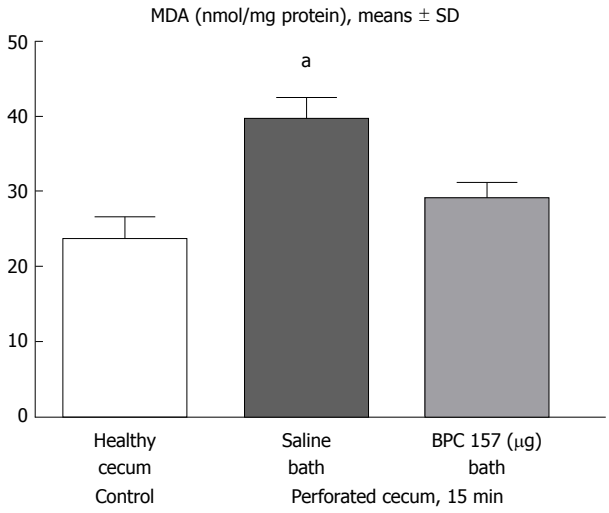

Figure 5 At 15 min post-injury, oxidative stress in tissue samples was assessed by quantifying thiobarbituric acid reactivity as malondialdehyde equivalents. Administration of medication (/kg, 10 mL/2 min bath/rat) at the perforated (5 mm diameter) cecum lesion and cecum was BPC 157 (10 μg) or a saline bath of equal volume (controls). Minimum $^{a}P < 0.05$ *vs* control. MDA: Malondialdehyde equivalents.

L-arginine therapy: Rats with a perforated cecum that underwent an L-arginine bath initially exhibited an open defect larger than in the controls, and markedly more adhesions were present (Table 1).

L-NAME therapy: Rats with a perforated cecum that underwent an L-NAME bath exhibited an open defect larger than that in the controls, and markedly more adhesions were present (Table 1).

Combined therapy of L-arginine and L-NAME: Rats with a perforated cecum that underwent this combined therapy exhibited an open defect that was found to be larger than that in the controls, and markedly more adhesions were present (Table 1).

Combined therapy of L-arginine and/or L-NAME with BPC 157: BPC 157 with L-arginine and/or L-NAME (L-NAME+BPC 157; L-arginine+BPC 157; L-NAME+L-arginine+BPC 157) led to defect attenuation and eventually no defect grossly present with fewer adhesions, similar to the rats that received BPC 157 alone (Table 1).

NO level

In the early term, NO level assessment demonstrated a reduction in the levels in rats that underwent cecum perforation, but the NO values in rats with a perforated cecum that underwent BPC 157 medication were similar to those in healthy rats (Figure 4).

Lipid peroxidation

In the early stages, lipid peroxidation assessment demonstrated a huge increase in rats that underwent cecum perforation but no MDA oxidative stress in rats with a perforate cecum that underwent BPC 157 medication (Figure 5).

Table 1 Assessed cecum lesion (sum of longest diameters, mm, at mucosal site (M) and serosal site (S), means ± SD) and adhesion severity (score 0-7, Min/Med/Max)

Medication (/kg, 10 ml/2 min bath/rat)	Assessed cecum lesion (sum of longest diameters, mm, means ± SD) and adhesion severity (score 0-9, Min/Med/Max)			
	Day 1		Day 7	
	Perforated cecum lesion	Adhesion severity	Perforated cecum lesion	Adhesion severity
0.9%NaCl (control)	5.0 ± 0.5 (M) 5.0 ± 0.5 (S)	3/3/3	5.0 ± 0.5 (M) 6.0 ± 0.5 (S)	3/4/4
BPC 157 (10 μg)	3.0 ± 0.0 (M)[a] 3.0 ± 0.0 (S)[a]	1/1/1[a]	0.0 ± 0.0 (M)[a] 0.0 ± 0.0 (S)[a]	1/1/2[a]
L-NAME 5 mg	7.5 ± 0.4 (M)[a] 7.5 ± 0.5 (S)[a]	5/6/6[a]	8.0 ± 0.4 (M)[a] 8.8 ± 0.5 (S)[a]	6/6/6[a]
L-arginine 100 mg	7.0 ± 0.0 (M)[a] 7.0 ± 0.0 (S)	4/5/5[a]	7.5 ± 0.3 (M)[a] 8.0 ± 0.4 (S)[a]	5/6/6[a]
L-NAME 5 mg + L-arginine 100 mg	7.3 ± 0.5 (M) 7.3 ± 0.5 (S)	5/6/6[a]	8.0 ± 0.3 (M) 8.2 ± 0.5 (S)	5/6/6[a]
L-NAME 5 mg + BPC 157 10 μg	3.0 ± 0.0 (M)[a] 3.0 ± 0.0 (S)[a]	1/1/1[a]	0.0 ± 0.0 (M)[a] 0.0 ± 0.0 (S)[a]	1/1/2[a]
L-arginine 100 mg + BPC 157 10 μg	3.0 ± 0.0 (M)[a] 3.0 ± 0.0 (S)[a]	1/1/1[a]	0.0 ± 0.0 (M)[a] 0.0 ± 0.0 (S)[a]	1/1/2[a]
L-NAME 5 mg + L-arginine 100 mg + BPC 157 10 μg	3.0 ± 0.0 (M)[a] 3.0 ± 0.0 (S)[a]	0/1/1[a]	0.0 ± 0.0 (M)[a] 0.0 ± 0.0 (S)[a]	1/1/2[a]

At 1 min post-injury, administration of medication (/kg, 10 mL/2 min bath/rat) at the perforated (5 mm diameter) lesion and cecum, includes BPC 157 (10 μg), NOS-blocker L-NAME (5 mg), NOS-substrate L-arginine (100 mg) alone or combined, a saline bath of equal volume (controls), and rats were left after abdominal closure undisturbed till the sacrifice, at day 1 or day 7. Minimum [a]$P < 0.05$ *vs* control.

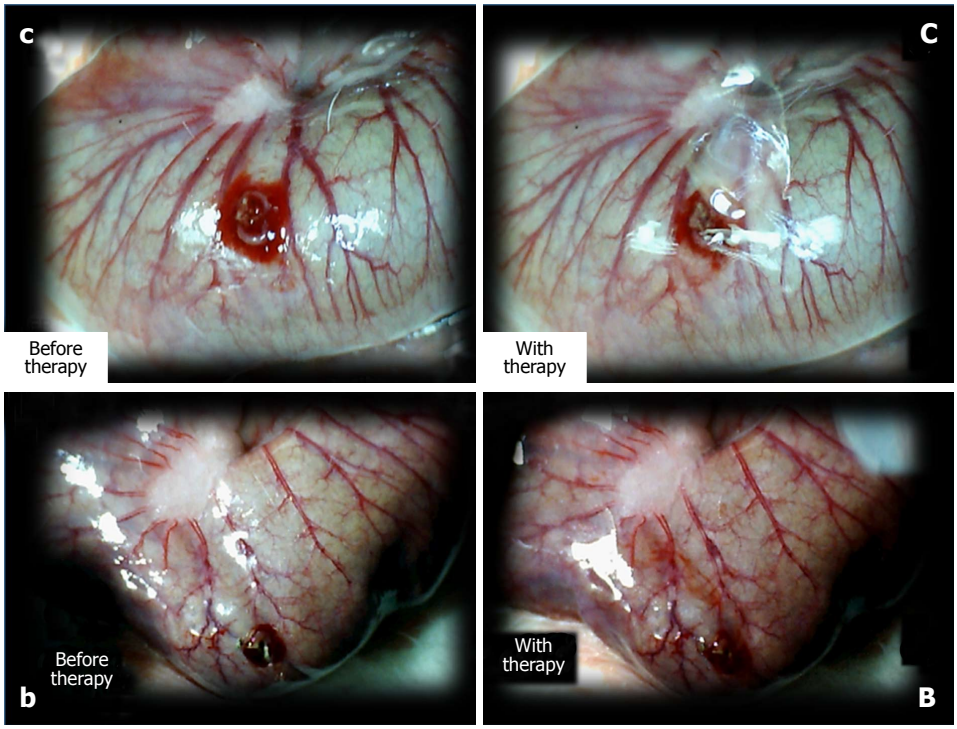

Figure 6 The perforated cecum. Perforate lesions, before therapy (c, b) (left). Perforate lesions with therapy [control, saline (C), BPC 157 (B)] (right). Illustrative distinctive effect of medication administration (saline bath (right, upper, control (C) *vs* BPC 157 bath [right, low, BPC 157 (B)]. Regular failing effect of saline bath application on vessels presentation [right, upper, control (C)] *vs* the immediate recruitment effect of BPC 157 bath administration on the blood vessels presentation toward the perforated injury [right, low, BPC 157 (B)]. Note the initial recovery of blood vessels that appear alongside with the BPC 157 bath, a network raising toward the perforated defect.

Microscopy

At the first day post-injury, controls exhibited intensive edema, loss of glands in the vicinity of the perforation, scarce inflammation, and neutrophils. By contrast, BPC 157-treated animals had much less edema, intensive inflammation (mixed neutro and mono) and a fibrin cloth attached to the defect ('holding' the edges) (Figure 9).

In control animals, after 7 d, the perforation showed

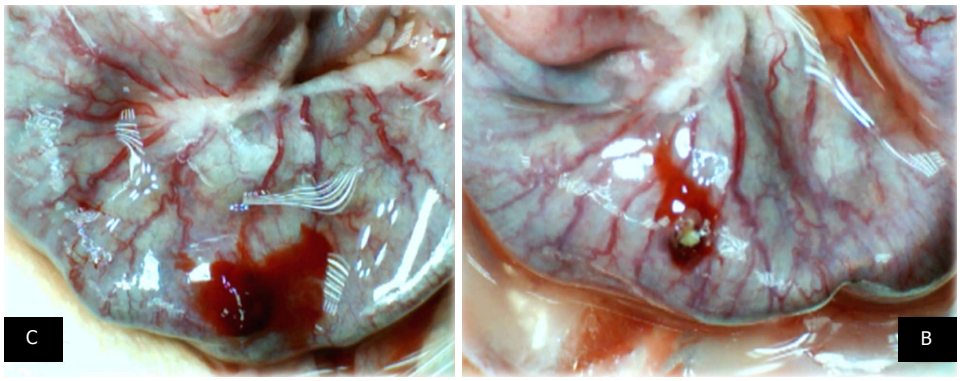

Figure 7 At 10 min, in the perforated cecum, the illustrative effect of medication administration [saline bath (left, control (C)] and BPC 157 bath [right, BPC 157 (B)]. In the damaged cecum, the regular effect of saline bath application on vessels presentation [left, control (C)] *vs* the immediate effect of BPC 157 bath administration on the blood vessels presentation toward the perforated injury [right, BPC 157 (B)].

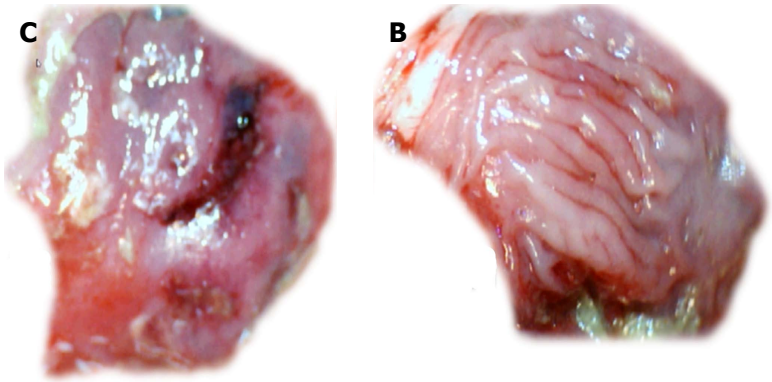

Figure 8 Gross presentation of the area of perforation [left, control (C); right, BPC 157 (B)] and perforated injury [left, control (C)]. Presentation at day 7. Veho discovery VMS-004D-400x USB microscope. Control, 7 d, left, C. Gross lesion shown upon cecum opening before sacrifice. BPC 157, 7 d, mucosa presentation without a grossly visible defect (right, BPC 157 (B)).

communication between the lumen and peritoneal cavity that was partly closed by a loose clot with much debris and many inflammatory cells (Figure 10). In treated animals, the defect was sealed with well-formed granulation tissue. The surrounding mucosa in controls was edematous, and the epithelium showed practically no regenerative activity. However, in treated animals, the edema was much less pronounced, and the surface epithelium began to migrate over the defect.

However, no lethal outcome was noted during the experiment.

DISCUSSION

Major disturbances in an immediate post-injury period also entails the possible injury reversal in studies of ischemic colitis and inferior caval vein occlusion[20,21]. Thus, to reverse the immediate post-perforation threat in the cecum (and, therefore, the complete downhill course) we focused on the immediate post-perforation period. We also addressed the novel aspect of vascular rescue through the application of cytoprotective agents, known, as a class, to function in endothelium maintenance in the gastrointestinal tract (and, thus, mucosal maintenance)[4-9]. Instant application of the stable gastric pentadecapeptide BPC 157 was used as a prototype agent rapidly acting on endothelium integrity maintenance[10-19], which is known to be of therapeutic value in rats with ischemic colitis and inferior caval vein ligation[20,21].

Of note, the whole initial syndrome (in particular, instantly emptied blood vessels at the cecum serosa and thus the rapid "disappearance" of existing vessels and failure of vessel function upon injury) and, consequently, perforation defect enlargement and fluid leakage, profuse bleeding, increased oxidative stress and disturbed NO levels in cecum tissue were accordingly affected.

We suggest that this effect should be seen, based on evidence of BPC 157 rapidly activating the collateral circulation from existing vessels in rats with ischemic colitis[20] or inferior caval vein occlusion[21]. Thus, the essential findings (*i.e.*, cecum perforation syndrome occurring in BPC 157-treated rats shows attenuation and reversal of the consequent tissue damages) indicate the rapidly activated bypassing loops (*i.e.*, through arcade vessels or the left ovarian vein and other veins)[20,21], corresponding to the prompt reperfusion seen after perforation. Reperfusion may be observed by vessels "running" toward the defect (vessels filled/reappeared), and a small-vessel network appearing around the perforated

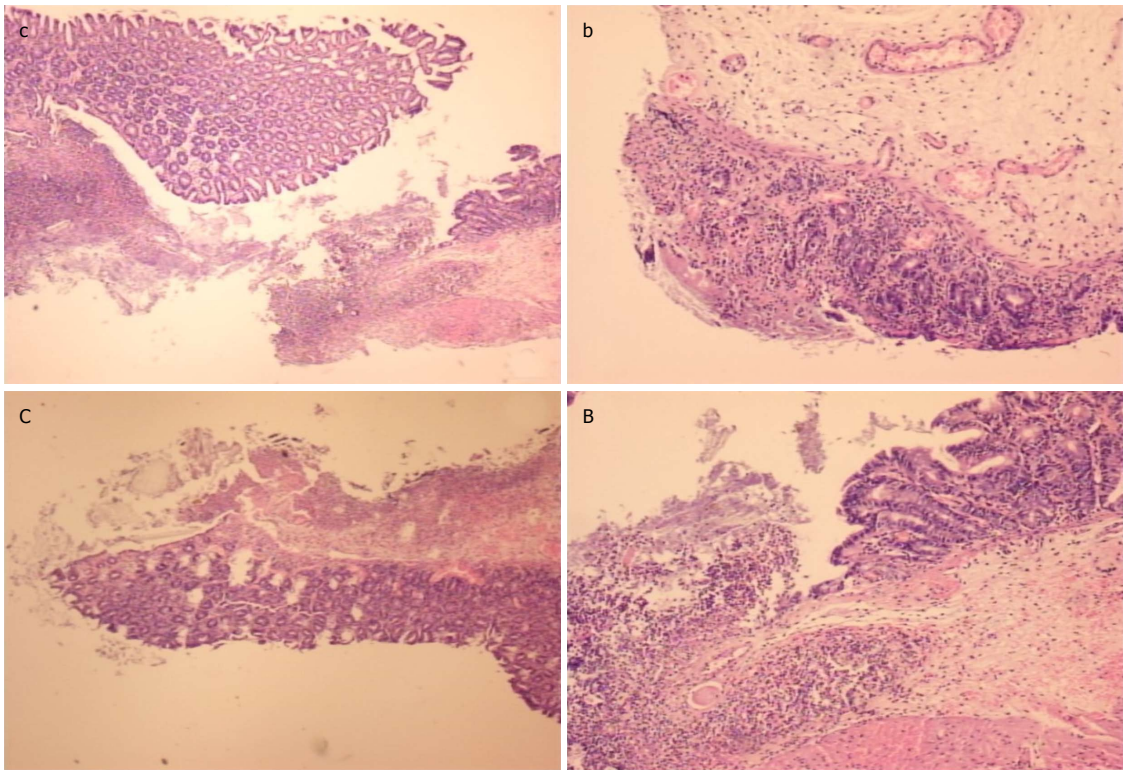

Figure 9 At the first day post-injury, controls (c, C) exhibited intensive edema, loss of glands in the vicinity of the perforation, not possible to obtain a complete defect (due to edema, the tissue is disintegrating), scarce inflammation, and neutrophils [c, HE x 4; C, HE x 10 (control)]. In rats treated with BPC 157 (b, B), we noted much less edema and intensive inflammation (mixed-neutro and mono). Fibrin cloth attached to defect ("holding" the edges) (b, HEx4; B, HEx10 (BPC 157)).

defect with BPC 157 bath administration. Each considered a break of blood flow, this suggests that the therapy resolving the defect (*i.e.*, cecum defect enlargement reversed to defect contraction in BPC 157-treated rats) may be a result of the reestablishment of blood flow. The bleeding time from the perforated cecum is thereby shortened, as demonstrated in rats with amputation, anticoagulant application, or vein obstruction[21,42,43]. Furthermore, defect closing corresponds to the closing of various fistula defects, which were surgically made by particular defect creations in corresponding organs[34-38].

In addition, the free radical scavenger effect and normalization of NO tissue values noted in rats with ischemic colitis or inferior vein obstruction in colon and venous tissues in both ischemia and reperfusion[20,21] correspond to the reduction in increased MDA values and normalization of NO values in cecum tissue in perforation studies. Heavy loss of endothelium cells from the vascular wall and, therefore, less eNOS NO production ability[44] would explain increased MDA values and decreased NO levels, which were regularly found in the cecum. Additionally, various free radical-induced lesions in other organs were counteracted by BPC 157 administration[20,21,45-48].

The importance of these beneficial effects was verified by the final complete closing of the defect, both grossly and microscopically, with the surface epithelium beginning to migrate over the defect and a lower adhesion severity score. It may also be that BPC 157 exhibits an additional beneficial effect because it counteracts peritonitis and adhesion formation along with beneficial effects in diverse intestinal lesion models[34-36,39,40].

Thus, it may be generally observed, that BPC 157 promptly facilitates and extends the cytoprotection background (endothelium maintenance → epithelium maintenance = blood vessel recruitment and activation toward injury, providing also described "bypassing" of occlusion through alternative ways)[20,21]; thus, all chains of events were accordingly and promptly involved to rapidly initiate and achieve a full healing effect.

This specific level of healing (initial and final) can be not obtained from the effect of NOS-blockade (L-NAME) or NOS-substrate (L-arginine), two pharmacologically distinct mechanisms with opposite effects on the same signaling NO-pathway[13]. Initially, L-arginine reduced vessel disappearance and counteracted defect widening, and prolonged the bleeding period. With L-NAME, vessel disappearance was similar to that in the controls; however, there was counteraction of defect widening, and the bleeding period was shortened. These would both be inadequate, though NO-specific, responses [given together, L-NAME+L-arginine regularly reversed each other's initial responses, being not different from the controls, with a bleeding period similar to the controls (L-NAME+L-arginine)]. Namely, they both eventually aggravated perforated lesions in the cecum, a non-NO-specific effect (given together, they did not reverse

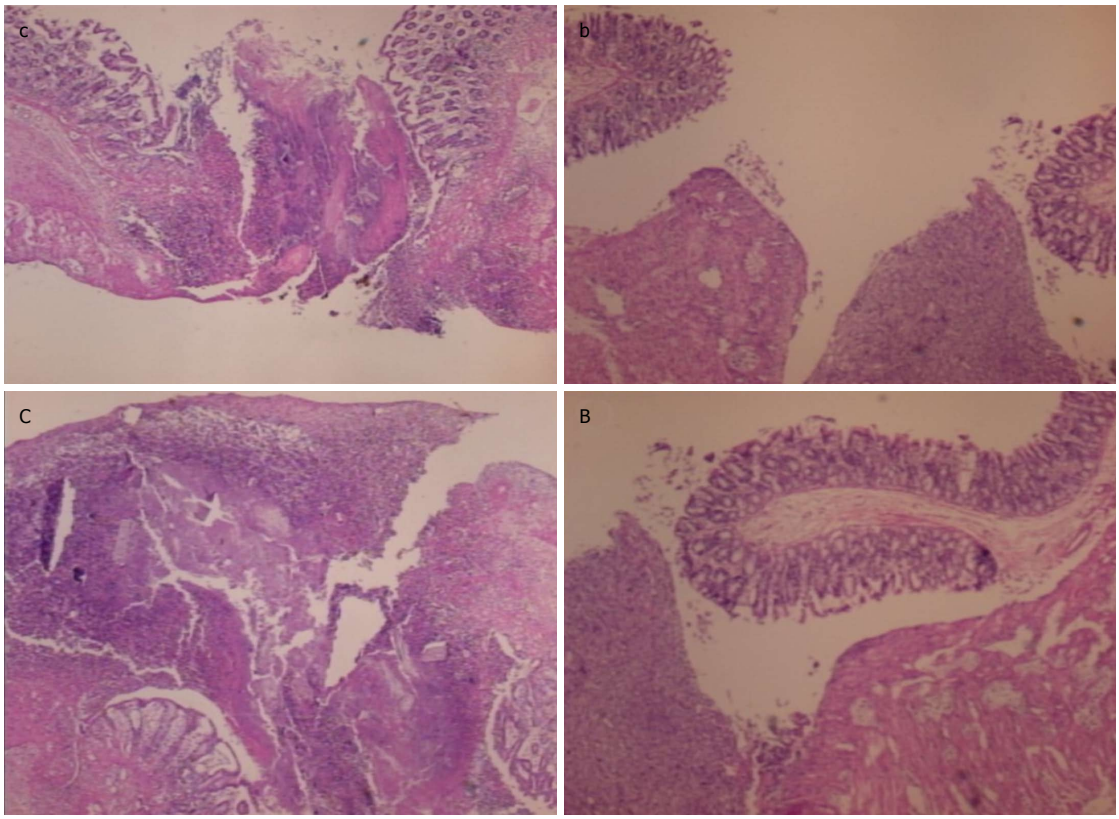

Figure 10 In control animals (c, C), the perforation after 7 d shows a communication between the lumen and peritoneal cavity, partly closed by a loose cloth with many debris and inflammatory cells [c, HE x 4; C, HE x 10 (control)]. In rats treated with BPC 157 (b, B), the defect was sealed with well-formed granulation tissue. The surrounding mucosa in controls was edematous, and the epithelium shows practically no regenerative activity, while in treated animals, the edema was much less pronounced and the surface epithelium started to migrate over the defect [b, HE x 4; B, HE x 10 (BPC 157)].

each other's final responses: L-NAME+L-arginine rats still had an open defect larger than that in the controls with adhesions of higher score). By contrast, as a proof of concept regarding the beneficial effects of BPC 157, rats in experiments with perforated cecum and colitis syndromes[20] showed the counteraction of the worsening of the course of injury after L-NAME and L-arginine application as individual agents (L-NAME rats; L-arginine rats → L-NAME+BPC 157 rats, L-arginine+BPC 157 rats ≈ BPC 157 rats) . When given together, the counteraction of the remaining extensive pathology was observed regardless of whether L-NAME and L-arginine reversed each other's worsening responses (L-NAME + L-arginine rats → L-NAME + L-arginine + BPC 157 rats ≈ BPC 157 rats)[20].

In conclusion, the remaining extensive pathology in the L-NAME+L-arginine animals (both in early and final terms) means that other systems (*i.e*., the BPC 157 system) may function along with the NO system (previously supposed to be immobilized by the mutual actions of combined L-NAME and L-arginine)[13]. In the case of the effectiveness of BPC 157, the normalized MDA values and NO levels (always with progressive vessel presentation, a shortened bleeding time, closure of the defect, surface epithelium migration over the defect and fewer adhesions) indicated effectiveness over the background of the NO-system, whether immobilized (L-NAME + L-arginine), overstimulated (L-arginine) or blocked (L-NAME)[13]. Thus, BPC 157 could consolidate the NO system's stimulating and inhibiting effects toward more effective healing (*i.e.*, revascularization (vessel "running" toward the defect and small vessel network around the perforated defect) appearing with BPC 157 bath administration)[13]. Furthermore, this additional rapid cytoprotective vascular recovery and presentation leads to a consequent strong angiogenic effect in subsequent days[12,18,23-27,49,50], more profound than the angiogenesis of standard anti-ulcer agents[50] because of its interaction with several molecular pathways[21-27]. Illustratively, in other studies, BPC 157 induced an acceleration of blood flow recovery and vessel number within days in rats with hind limb ischemia[25].

Additionally, in practice, this means distinct endpoints should be overwhelmed to achieve the presentation seen in rats that underwent BPC 157 application. Finally, in addition to counteracting the parallel (worsening) effect of L-NAME/L-arginine on ischemic colitis and cecum perforation syndromes[21], BPC 157 counteracts the common parallel L-NAME/L-arginine activity points in other assays (*i.e*., magnesium intoxication and miosis/mydriasis)[51,52]. Notably, BPC 157 instantly prevents and reverses L-NAME-induced hypertension and L-NAME-induced thrombocytopenia as well as L-arginine-induced hypotension and L-arginine-induced prolonged bleeding

and thrombocytopenia[13].

Therefore, BPC 157, with certain vascular effects[20,21] and NO-effect[13] can be used in perforated cecum and bleeding therapy.

ARTICLE HIGHLIGHTS

Research background

To illustrate the background, present status, and significance of the study we should emphasize that in cecum perforation studies the immediate post-perforation threat is rarely studied. On the other hand, we recently claimed that treatment with the prototype cytoprotective agent, stable gastric pentadecapeptide BPC 157, induces bypassing of occlusions in rats that underwent vessel occlusions through the rapid presentation of collaterals, and exert its free radical scavenger effect in both ischemia and reperfusion. As a consequence, in this study, we focused on the resolving of the cecum perforation lesion, particularly the rapid disappearance of blood vessels in the cecum serosa that are instantly emptied and thereby "disappear", perforation defect enlargement, bleeding and fluid leakage, increased oxidative stress and disturbed NO levels in cecum tissue.

Research motivation

The main topics, the key problems to be solved, and the significance of solving these problems for further research are related to reverse the immediate post-perforation threat in the cecum (and, therefore, the complete downhill course). We focused on perforated cecum, the stable gastric pentadecapeptide BPC 157, the NOS-blocker L-NAME, and the NOS-substrate L-arginine, as well as on the initial post-perforation period, rapid disappearance of blood vessels at the cecum serosa (emptied/disappeared), a large immediate defect, bleeding, leakage of fluid, increased oxidative stress and disturbed NO levels in cecum tissue. The rationale was that BPC 157 rapidly activated the collateral circulation from the existing vessels in rats with ischemic colitis or inferior caval vein occlusion. This was further perceived as an extended cytoprotection background (endothelium maintenance → epithelium maintenance = blood vessel recruitment and activation toward injury), also described as "bypassing" occlusion via alternative ways, as demonstrated with BPC 157, which, in principle, can likely cure rats with perforated cecum and thereafter.

Research objectives

The main objectives, the objectives that were realized, and the significance of these objectives for future research could be summarized as follows. In practice, as described previously, our approach to cure perforated cecum begins with the original understanding of stomach cytoprotection (a very rapid protection of the stomach endothelium and epithelium against diverse direct injuries; endothelium maintenance → epithelium maintenance), as "bypassing" occlusion via alternative ways, as demonstrated with BPC 157. Furthermore, we used these findings as the general argument that under analogous or even worse conditions (*i.e*., perforated cecum) a similar positive outcome can appear. Consequently, BPC 157 can attenuate cecum perforation syndrome; in BPC 157-treated rats, therapy may lead to attenuation and reversal of the consequent tissue damage. Especially, reversal of vessel disappearance to vessel "running" toward the defect (vessel filled/reappeared), reversal of defect enlargement to defect narrowing, reversal of prolonged bleeding to bleeding attenuation can induce reduction in the increased MDA values and normalization of NO values in cecum tissue. In subsequent days and weeks, this may lead to a closed cecum defect and attenuation of adhesion formation.

Research methods

As an advantageous principle, methodology includes direct monitoring of the events occurring in rats during perforation of the cecum and immediately thereafter with the application of the stable gastric pentadecapeptide BPC 157, as a cytoprotective agent, and NO-agents, L-NAME and L-arginine. In deeply anaesthetized rats the cecum was exposed, and a perforation (5-mm diameter) was made at the ventral face of the basal region of the cecum close to the largest curvature; the rats were monitored for the next 15 min. The agents' application (after 1 minute, medication (/kg, 10 mL/2min bath/rat) includes: BPC 157 (10 μg), L-NAME (5 mg), L-arginine (100 mg) alone or combined, and saline baths (controls)) on the rat perforate caecum injury. Alongside with the agents' application, we continuously assessed the gross reappearance of the vessels (USB microcamera) quickly propagating toward the defect at the caecum surface, defect contraction, bleeding attenuation, MDA- and NO-levels in colon tissue at 15 min, and, in repalaratomized rats severity of colon lesions and adhesions at 1 and 7 days.

Research results

The study of the counteraction of perforated cecum lesions in rats and the effects of pentadecapeptide BPC 157, L-NAME and L-arginine merits several emphasizes to summarize the research findings, their contribution to the research in the field, and the problems that remain to be solved. First, as an issue so far not fully addressed, to reverse the immediate post-perforation threat in the cecum (and, therefore, the complete downhill course) we focused on this immediate post-perforation period. We also addressed the novel aspect of vascular rescue through the application of cytoprotective agents, known, as a class, to function in endothelium maintenance in the gastrointestinal tract (and, thus, mucosal maintenance). Of note, with applied BPC 157 therapy, the whole initial syndrome (in particular, instantly emptied blood vessels at the cecum serosa (thus rapid "disappearance" of the existing vessels and vessel function failure upon injury)) and, consequently, perforation defect enlargement and fluid leakage, profuse bleeding, increased oxidative stress and disturbed NO levels in cecum tissue were accordingly affected. This specific level of healing (initial and final) can be not obtained from the effect of NOS-blockade (L-NAME) or NOS-substrate (L-arginine).

Research conclusions

As the new findings, we suggest that this recovering of the perforated cecum should be an activity much like an activity seen when BPC 157 rapidly activated the collateral circulation from existing vessels in rats with ischemic colitis or inferior caval vein occlusion. Thus, the essential findings (*i.e.*, cecum perforation syndrome occurs in BPC 157-treated rats with attenuation and reversal of the consequent tissue damages) indicate the rapidly activated bypassing loops (*i.e.*, through arcade vessels or the left ovarian vein and other veins, corresponding to the prompt particular vascular rescue seen after perforation). Vascular rescue may be vessels "running" toward the defect (vessel filled/reappeared), and a small-vessel network appears around the perforated defect with BPC 157 bath administration. Each considered a break of blood flow, suggests that the therapy resolving the defect (*i.e.*, cecum defect enlargement reversed to defect contraction in BPC 157-treated rats) may be reestablishing blood flow. That explanation represents the newest theoretical extension of cytoprotection theory background (endothelium maintenance → epithelium maintenance = blood vessel recruitment and activation toward injury, providing also described "bypassing" of occlusion through alternative ways). Since all chains of events could be accordingly and promptly involved to rapidly initiate and achieve a full healing effect. The bleeding time from the perforated cecum is thereby shortened, as previously demonstrated in rats with amputation, anticoagulant application, or vein obstruction. Furthermore, defect closing corresponds to the previously demonstrated closing of various fistula defects, which were surgically made by particular defect creations in corresponding organs. The implications of this study for clinical practice in the future can be that BPC 157, with certain vascular effects and NO-effect, can be used in the perforated cecum and bleeding therapy.

Research perspectives

The main experiences and lessons that can be learnt from this study may be the evidence that BPC 157 promptly facilitates and extends the cytoprotection background (endothelium maintenance → epithelium maintenance = blood vessel recruitment and activation toward injury, providing also described "bypassing" of occlusion through alternative ways). Thus, the evidence was obtained that all chains of events were accordingly and promptly involved to rapidly initiate and achieve a full healing effect, and with the respect to the corresponding positive effects in two other studies (ischemic/reperfusion colitis; inferior caval vein occlusion), the beneficial effect in rats with perforated cecum may be generally observed. Thereby, the future research should be related to the similar and/or even worse condition, to verify full significance of the presented beneficial findings seen in rats after cecum perforation and BPC 157 therapy application.

REFERENCES

1 **Aslan MK**, Boybeyi O, Soyer T, Senyücel MF, Ayva S, Kısa U, Cesur

O, Cakmak M. Evaluation of omental inflammatory response with P-/E-selectin levels and histopathologic findings in experimental model. *J Pediatr Surg* 2012; **47**: 2050-2054 [PMID: 23163997 DOI: 10.1016/j.jpedsurg.2012.06.024]

2 **Liu J**, Shi B, Shi K, Ma G, Zhang H, Lou X, Liu H, Wan S, Liang D. Ghrelin upregulates PepT1 activity in the small intestine epithelium of rats with sepsis. *Biomed Pharmacother* 2017; **86**: 669-676 [PMID: 28038428 DOI: 10.1016/j.biopha.2016.12.026]

3 **Santiago MB**, Vieira AA, Giusti-Paiva A. Impaired chemoreflex sensitivity during septic shock induced by cecal ligation and perforation. *Can J Physiol Pharmacol* 2013; **91**: 1107-1111 [PMID: 24289082 DOI: 10.1139/cjpp-2013-0219]

4 **Robert A**. Cytoprotection by prostaglandins. *Gastroenterology* 1979; **77**: 761-767 [PMID: 38173]

5 **Sikiric P**, Seiwerth S, Grabarevic Z, Petek M, Rucman R, Turkovic B, Rotkvic I, Jagic V, Duvnjak M, Mise S, Djacic S, Separovic J, Veljaca M, Sallmani A, Banic M, Brkic T. The beneficial effect of BPC 157, a 15 amino acid peptide BPC fragment, on gastric and duodenal lesions induced by restraint stress, cysteamine and 96% ethanol in rats. A comparative study with H2 receptor antagonists, dopamine promotors and gut peptides. *Life Sci* 1994; **54**: PL63-68 [PMID: 7904712 DOI: 10.1016/0024-3205(94)00796-9]

6 **Szabo S.** Gastric Cytoprotection [Internet]. 1. st. Boston, MA: Springer US; 1989. Available from: URL: http://link.springer.com/10.1007/978-1-4684-5697-4

7 **Szabo S**, Trier JS, Brown A, Schnoor J. Early vascular injury and increased vascular permeability in gastric mucosal injury caused by ethanol in the rat. *Gastroenterology* 1985; **88**: 228-236 [PMID: 3871087]

8 **Szabo S**, Trier J. Pathogenesis of acute gastric mucosal injury: Sulfhydrils as a protector, adrenal cortex as a modulator, and vascular endothelium as a target. In: Allen A, Flemstrom G, Garner A, Silen W, Turnberg L. Mechanism of mucosal protection in the upper gastrointestinal tract. New York: Raven; 1984: 387-393

9 **Trier JS**, Szabo S, Allan CH. Ethanol-induced damage to mucosal capillaries of rat stomach. Ultrastructural features and effects of prostaglandin F2 beta and cysteamine. *Gastroenterology* 1987; **92**: 13-22 [PMID: 3781180]

10 **Sikiric P**, Seiwerth S, Rucman R, Drmic D, Stupnisek M, Kokot A, Sever M, Zoricic I, Zoricic Z, Batelja L, Ziger T, Luetic K, Vlainic J, Rasic Z, Bencic ML. Stress in gastrointestinal tract and stable gastric pentadecapeptide BPC 157. Finally, do we have a solution? *Curr Pharm Des* 2017; **23**: 4012-4028 [PMID: 28228068 DOI: 10.2174/1381612823666170220163219]

11 **Sikiric P**, Seiwerth S, Rucman R, Kolenc D, Vuletic LB, Drmic D, Grgic T, Strbe S, Zukanovic G, Crvenkovic D, Madzarac G, Rukavina I, Sucic M, Baric M, Starcevic N, Krstonijevic Z, Bencic ML, Filipcic I, Rokotov DS, Vlainic J. Brain-gut axis and pentadecapeptide BPC 157: Theoretical and practical implications. *Curr Neuropharmacol* 2016; **14**: 857-865 [PMID: 27138887]

12 **Seiwerth S**, Brcic L, Vuletic LB, Kolenc D, Aralica G, Misic M, Zenko A, Drmic D, Rucman R, Sikiric P. BPC 157 and blood vessels. *Curr Pharm Des* 2014; **20**: 1121-1125 [PMID: 23782145 DOI: 10.2174/13816128113199990421]

13 **Sikiric P**, Seiwerth S, Rucman R, Turkovic B, Rokotov DS, Brcic L, Sever M, Klicek R, Radic B, Drmic D, Ilic S, Kolenc D, Aralica G, Stupnisek M, Suran J, Barisic I, Dzidic S, Vrcic H, Sebecic B. Stable gastric pentadecapeptide BPC 157-NO-system relation. *Curr Pharm Des* 2014; **20**: 1126-1135 [PMID: 23755725]

14 **Sikiric P**, Seiwerth S, Rucman R, Turkovic B, Rokotov DS, Brcic L, Sever M, Klicek R, Radic B, Drmic D, Ilic S, Kolenc D, Aralica G, Safic H, Suran J, Rak D, Dzidic S, Vrcic H, Sebecic B. Toxicity by NSAIDs. Counteraction by stable gastric pentadecapeptide BPC 157. *Curr Pharm Des* 2013; **19**: 76-83 [PMID: 22950504]

15 **Sikiric P**, Seiwerth S, Rucman R, Turkovic B, Rokotov DS, Brcic L, Sever M, Klicek R, Radic B, Drmic D, Ilic S, Kolenc D, Stambolija V, Zoricic Z, Vrcic H, Sebecic B. Focus on ulcerative colitis: Stable gastric pentadecapeptide BPC 157. *Curr Med Chem* 2012; **19**: 126-132 [PMID: 22300085]

16 **Sikiric P**, Seiwerth S, Rucman R, Turkovic B, Rokotov DS, Brcic L, Sever M, Klicek R, Radic B, Drmic D, Ilic S, Kolenc D, Vrcic H, Sebecic B. Stable gastric pentadecapeptide BPC 157: novel therapy in gastrointestinal tract. *Curr Pharm Des* 2011; **17**: 1612-1632 [PMID: 21548867 DOI: 10.2174/138161211796196954]

17 **Sikiric P**, Seiwerth S, Brcic L, Sever M, Klicek R, Radic B, Drmic D, Ilic S, Kolenc D. Revised Robert's cytoprotection and adaptive cytoprotection and stable gastric pentadecapeptide BPC 157. Possible significance and implications for novel mediator. *Curr Pharm Des* 2010; **16**: 1224-1234 [PMID: 20166993]

18 **Sikiric P**, Seiwerth S, Brcic L, Blagaic AB, Zoricic I, Sever M, Klicek R, Radic B, Keller N, Sipos K, Jakir A, Udovicic M, Tonkic A, Kokic N, Turkovic B, Mise S, Anic T. Stable gastric pentadecapeptide BPC 157 in trials for inflammatory bowel disease (PL-10, PLD-116, PL 14736, Pliva, Croatia). Full and distended stomach, and vascular response. *Inflammopharmacology* 2006; **14**: 214-221 [PMID: 17186181 DOI: 10.1007/s10787-006-1531-7]

19 **Sikirić P**, Petek M, Rucman R, Seiwerth S, Grabarević Z, Rotković I, Turković B, Jagić V, Mildner B, Duvnjak M. A new gastric juice peptide, BPC. An overview of the stomach-stress-organoprotection hypothesis and beneficial effects of BPC. *J Physiol Paris* 1993; **87**: 313-327 [PMID: 8298609 DOI: 10.1016/0928-4257(93)90038-U]

20 **Duzel A**, Vlainic J, Antunovic M, Malekinusic D, Vrdoljak B, Samara M, Gojkovic S, Krezic I, Vidovic T, Bilic Z, Knezevic M, Sever M, Lojo N, Kokot A, Kolovrat M, Drmic D, Vukojevic J, Kralj T, Kasnik K, Siroglavic M, Seiwerth S, Sikiric P. Stable gastric pentadecapeptide BPC 157 in the treatment of colitis and ischemia and reperfusion in rats: New insights. *World J Gastroenterol* 2017; **23**: 8465-8488 [PMID: 29358856 DOI: 10.3748/wjg.v23.i48.8465]

21 **Vukojević J**, Siroglavić M, Kašnik K, Kralj T, Stanćić D, Kokot A, Kolarić D, Drmić D, Sever AZ, Barišić I, Šuran J, Bojić D, Patrlj MH, Sjekavica I, Pavlov KH, Vidović T, Vlainić J, Stupnišek M, Seiwerth S, Sikirić P. Rat inferior caval vein (ICV) ligature and particular new insights with the stable gastric pentadecapeptide BPC 157. *Vascul Pharmacol* 2018; **106**: 54-66 [PMID: 29510201 DOI: 10.1016/j.vph.2018.02.010]

22 **Cesarec V**, Becejac T, Misic M, Djakovic Z, Olujic D, Drmic D, Brcic L, Rokotov DS, Seiwerth S, Sikiric P. Pentadecapeptide BPC 157 and the esophagocutaneous fistula healing therapy. *Eur J Pharmacol* 2013; **701**: 203-212 [PMID: 23220707 DOI: 10.1016/j.ejphar.2012.11.055]

23 **Chang CH**, Tsai WC, Lin MS, Hsu YH, Pang JH. The promoting effect of pentadecapeptide BPC 157 on tendon healing involves tendon outgrowth, cell survival, and cell migration. *J Appl Physiol* (1985) 2011; **110**: 774-780 [PMID: 21030672 DOI: 10.1152/japplphysiol.00945.2010]

24 **Chang CH**, Tsai WC, Hsu YH, Pang JH. Pentadecapeptide BPC 157 enhances the growth hormone receptor expression in tendon fibroblasts. *Molecules* 2014; **19**: 19066-19077 [PMID: 25415472 DOI: 10.3390/molecules191119066]

25 **Hsieh MJ**, Liu HT, Wang CN, Huang HY, Lin Y, Ko YS, Wang JS, Chang VH, Pang JS. Therapeutic potential of pro-angiogenic BPC157 is associated with VEGFR2 activation and up-regulation. *J Mol Med* (Berl) 2017; **95**: 323-333 [PMID: 27847966 DOI: 10.1007/s00109-016-1488-y]

26 **Huang T**, Zhang K, Sun L, Xue X, Zhang C, Shu Z, Mu N, Gu J, Zhang W, Wang Y, Zhang Y, Zhang W. Body protective compound-157 enhances alkali-burn wound healing in vivo and promotes proliferation, migration, and angiogenesis in vitro. *Drug Des Devel Ther* 2015; **9**: 2485-2499 [PMID: 25995620 DOI: 10.2147/DDDT.S82030]

27 **Tkalcević VI**, Cuzić S, Brajsa K, Mildner B, Bokulić A, Situm K, Perović D, Glojnarić I, Parnham MJ. Enhancement by PL 14736 of granulation and collagen organization in healing wounds and the potential role of egr-1 expression. *Eur J Pharmacol* 2007; **570**: 212-221 [PMID: 17628536 DOI: 10.1016/j.ejphar.2007.05.072]

28 **Klicek R**, Kolenc D, Suran J, Drmic D, Brcic L, Aralica G, Sever M, Holjevac J, Radic B, Turudic T, Kokot A, Patrlj L, Rucman R, Seiwerth S, Sikiric P. Stable gastric pentadecapeptide BPC 157 heals cysteamine-colitis and colon-colon-anastomosis and counteracts cuprizone brain injuries and motor disability. *J Physiol Pharmacol* 2013; **64**: 597-612 [PMID: 24304574]

29 **Lojo N**, Rasic Z, Zenko Sever A, Kolenc D, Vukusic D, Drmic D, Zoricic I, Sever M, Seiwerth S, Sikiric P. Effects of diclofenac, L-NAME, L-arginine, and pentadecapeptide BPC 157 on gastrointestinal, liver, and brain lesions, failed anastomosis, and intestinal adaptation deterioration in 24 hour-short-bowel rats. *PLoS One* 2016; **11**: e0162590 [PMID: 27627764 DOI: 10.1371/journal.pone.0162590]

30 **Sandor Z,** Vincze A, Jadus M, Dohoczky C, Erceg D, Brajsa K, Kolega M, Szabo S. The protective effect of newly isolated peptide PL-10 in the iodoacetamide colitis model in rats. *Gastroenterology* 1997; **112**: A400

31 **Sikiric P**, Seiwerth S, Grabarevic Z, Balen I, Aralica G, Gjurasin M, Komericki L, Perovic D, Ziger T, Anic T, Prkacin I, Separovic J, Stancic-Rokotov D, Lovric-Bencic M, Mikus D, Staresinic M, Aralica J, DiBiaggio N, Simec Z, Turkovic B, Rotkvic I, Mise S, Rucman R, Petek M, Sebecic B, Ivasovic Z, Boban-Blagaic A, Sjekavica I. Cysteamine-colon and cysteamine-duodenum lesions in rats. Attenuation by gastric pentadecapeptide BPC 157, cimetidine, ranitidine, atropine, omeprazole, sulphasalazine and methylprednisolone. *J Physiol Paris* 2001; **95**: 261-270 [PMID: 11595448 DOI: 10.1016/S0928-4257(01)00036-5]

32 **Sikiric P**, Seiwerth S, Aralica G, Perovic D, Staresinic M, Anic T, Gjurasin M, Prkacin I, Separovic J, Stancic-Rokotov D, Lovric-Bencic M, Mikus D, Turkovic B, Rotkvic I, Mise S, Rucman R, Petek M, Ziger T, Sebecic B, Ivasovic Z, Jagic V, Komericki L, Balen I, Boban-Blagaic A, Sjekavica I. Therapy effect of antiulcer agents on new chronic cysteamine colon lesion in rat. *J Physiol Paris* 2001; **95**: 283-288 [PMID: 11595451 DOI: 10.1016/S0928-4257(01)00039-0]

33 **Veljaca M**, Lesch C, Sanchez B, Low J, Guglietta A. Protection of BPC-15 on TNBS-induced colitis in rats: possible mechanisms of action. *Gastroenterology* 1995; **108**: 936

34 **Baric M**, Sever AZ, Vuletic LB, Rasic Z, Sever M, Drmic D, Pavelic-Turudic T, Sucic M, Vrcic H, Seiwerth S, Sikiric P. Stable gastric pentadecapeptide BPC 157 heals rectovaginal fistula in rats. *Life Sci* 2016; **148**: 63-70 [PMID: 26872976 DOI: 10.1016/j.lfs.2016.02.029]

35 **Grgic T**, Grgic D, Drmic D, Sever AZ, Petrovic I, Sucic M, Kokot A, Klicek R, Sever M, Seiwerth S, Sikiric P. Stable gastric pentadecapeptide BPC 157 heals rat colovesical fistula. *Eur J Pharmacol* 2016; **780**: 1-7 [PMID: 26875638 DOI: 10.1016/j.ejphar.2016.02.038]

36 **Klicek R**, Sever M, Radic B, Drmic D, Kocman I, Zoricic I, Vuksic T, Ivica M, Barisic I, Ilic S, Berkopic L, Vrcic H, Brcic L, Blagaic AB, Coric M, Brcic I, Rokotov DS, Anic T, Seiwerth S, Sikiric P. Pentadecapeptide BPC 157, in clinical trials as a therapy for inflammatory bowel disease (PL14736), is effective in the healing of colocutaneous fistulas in rats: role of the nitric oxide-system. *J Pharmacol Sci* 2008; **108**: 7-17 [PMID: 18818478]

37 **Skorjanec S**, Kokot A, Drmic D, Radic B, Sever M, Klicek R, Kolenc D, Zenko A, Lovric Bencic M, Belosic Halle Z, Situm A, Zivanovic Posilovic G, Masnec S, Suran J, Aralica G, Seiwerth S, Sikiric P. Duodenocutaneous fistula in rats as a model for "wound healing-therapy" in ulcer healing: the effect of pentadecapeptide BPC 157, L-nitro-arginine methyl ester and L-arginine. *J Physiol Pharmacol* 2015; **66**: 581-590 [PMID: 26348082]

38 **Skorjanec S**, Dolovski Z, Kocman I, Brcic L, Blagaic Boban A, Batelja L, Coric M, Sever M, Klicek R, Berkopic L, Radic B, Drmic D, Kolenc D, Ilic S, Cesarec V, Tonkic A, Zoricic I, Mise S, Staresinic M, Ivica M, Lovric Bencic M, Anic T, Seiwerth S, Sikiric P. Therapy for unhealed gastrocutaneous fistulas in rats as a model for analogous healing of persistent skin wounds and persistent gastric ulcers: stable gastric pentadecapeptide BPC 157, atropine, ranitidine, and omeprazole. *Dig Dis Sci* 2009; **54**: 46-56 [PMID: 18649140 DOI: 10.1007/s10620-008-0332-9]

39 **Sever M**, Klicek R, Radic B, Brcic L, Zoricic I, Drmic D, Ivica M, Barisic I, Ilic S, Berkopic L, Blagaic AB, Coric M, Kolenc D, Vrcic H, Anic T, Seiwerth S, Sikiric P. Gastric pentadecapeptide BPC 157 and short bowel syndrome in rats. *Dig Dis Sci* 2009; **54**: 2070-2083 [PMID: 19093208 DOI: 10.1007/s10620-008-0598-y]

40 **Vuksic T**, Zoricic I, Brcic L, Sever M, Klicek R, Radic B, Cesarec V, Berkopic L, Keller N, Blagaic AB, Kokic N, Jelic I, Geber J, Anic T, Seiwerth S, Sikiric P. Stable gastric pentadecapeptide BPC 157 in trials for inflammatory bowel disease (PL-10, PLD-116, PL14736, Pliva, Croatia) heals ileoileal anastomosis in the rat. *Surg Today* 2007; **37**: 768-777 [PMID: 17713731 DOI: 10.1007/s00595-006-3498-9]

41 **Hrelec M**, Klicek R, Brcic L, Brcic I, Cvjetko I, Seiwerth S, Sikiric P. Abdominal aorta anastomosis in rats and stable gastric pentadecapeptide BPC 157, prophylaxis and therapy. *J Physiol Pharmacol* 2009; **60** Suppl 7: 161-165 [PMID: 20388960]

42 **Stupnisek M**, Franjic S, Drmic D, Hrelec M, Kolenc D, Radic B, Bojic D, Vcev A, Seiwerth S, Sikiric P. Pentadecapeptide BPC 157 reduces bleeding time and thrombocytopenia after amputation in rats treated with heparin, warfarin or aspirin. *Thromb Res* 2012; **129**: 652-659 [PMID: 21840572 DOI: 10.1016/j.thromres.2011.07.035]

43 **Stupnisek M**, Kokot A, Drmic D, Hrelec Patrlj M, Zenko Sever A, Kolenc D, Radic B, Suran J, Bojic D, Vcev A, Seiwerth S, Sikiric P. Pentadecapeptide BPC 157 reduces bleeding and thrombocytopenia after amputation in rats treated with heparin, warfarin, L-NAME and L-arginine. *PLoS One* 2015; **10**: e0123454 [PMID: 25897838 DOI: 10.1371/journal.pone.0123454]

44 **Berra-Romani R**, Avelino-Cruz JE, Raqeeb A, Della Corte A, Cinelli M, Montagnani S, Guerra G, Moccia F, Tanzi F. Ca^{2+}-dependent nitric oxide release in the injured endothelium of excised rat aorta: a promising mechanism applying in vascular prosthetic devices in aging patients. *BMC Surg* 2013; **13** Suppl 2: S40 [PMID: 24266895 DOI: 10.1186/1471-2482-13-S2-S40]

45 **Belosic Halle Z**, Vlainic J, Drmic D, Strinic D, Luetic K, Sucic M, Medvidovic-Grubisic M, Pavelic Turudic T, Petrovic I, Seiwerth S, Sikiric P. Class side effects: decreased pressure in the lower oesophageal and the pyloric sphincters after the administration of dopamine antagonists, neuroleptics, anti-emetics, L-NAME, pentadecapeptide BPC 157 and L-arginine. *Inflammopharmacology* 2017; Epub ahead of print [PMID: 28516373 DOI: 10.1007/s10787-017-0358-8]

46 **Ilic S**, Drmic D, Zarkovic K, Kolenc D, Coric M, Brcic L, Klicek R, Radic B, Sever M, Djuzel V, Ivica M, Boban Blagaic A, Zoricic Z, Anic T, Zoricic I, Djidic S, Romic Z, Seiwerth S, Sikiric P. High hepatotoxic dose of paracetamol produces generalized convulsions and brain damage in rats. A counteraction with the stable gastric pentadecapeptide BPC 157 (PL 14736). *J Physiol Pharmacol* 2010; **61**: 241-250 [PMID: 20436226]

47 **Luetic K**, Sucic M, Vlainic J, Halle ZB, Strinic D, Vidovic T, Luetic F, Marusic M, Gulic S, Pavelic TT, Kokot A, Seiwerth RS, Drmic D, Batelja L, Seiwerth S, Sikiric P. Cyclophosphamide induced stomach and duodenal lesions as a NO-system disturbance in rats: L-NAME, L-arginine, stable gastric pentadecapeptide BPC 157. *Inflammopharmacology* 2017; **25**: 255-264 [PMID: 28255738 DOI: 10.1007/s10787-017-0330-7]

48 **Sikiric P**, Seiwerth S, Grabarevic Z, Rucman R, Petek M, Rotkvic I, Turkovic B, Jagic V, Mildner B, Duvnjak M. Hepatoprotective effect of BPC 157, a 15-amino acid peptide, on liver lesions induced by either restraint stress or bile duct and hepatic artery ligation or CCl4 administration. A comparative study with dopamine agonists and somatostatin. *Life Sci* 1993; **53**: PL291-PL296 [PMID: 7901724]

49 **Brcic L**, Brcic I, Staresinic M, Novinscak T, Sikiric P, Seiwerth S. Modulatory effect of gastric pentadecapeptide BPC 157 on angiogenesis in muscle and tendon healing. *J Physiol Pharmacol* 2009; **60** Suppl 7: 191-196 [PMID: 20388964]

50 **Sikiric P**, Separovic J, Anic T, Buljat G, Mikus D, Seiwerth S, Grabarevic Z, Stancic-Rokotov D, Pigac B, Hanzevacki M, Marovic A, Rucman R, Petek M, Zoricic I, Ziger T, Aralica G, Konjevoda P, Prkacin I, Gjurasin M, Miklic P, Artukovic B, Tisljar M, Bratulic M, Mise S, Rotkvic I. The effect of pentadecapeptide BPC 157, H2-blockers, omeprazole and sucralfate on new vessels and new granulation tissue formation. *J Physiol Paris* 1999; **93**: 479-485 [PMID: 10672992]

51 **Medvidovic-Grubisic M**, Stambolija V, Kolenc D, Katancic J, Murselovic T, Plestina-Borjan I, Strbe S, Drmic D, Barisic I, Sindic A, Seiwerth S, Sikiric P. Hypermagnesemia disturbances in rats, NO-related: pentadecapeptide BPC 157 abrogates, L-NAME and L-arginine worsen. *Inflammopharmacology* 2017; **25**: 439-449 [PMID: 28210905 DOI: 10.1007/s10787-017-0323-6]

52 **Kokot A**, Zlatar M, Stupnisek M, Drmic D, Radic R, Vcev A, Seiwerth S, Sikiric P. NO system dependence of atropine-induced mydriasis and L-NAME- and L-arginine-induced miosis: Reversal by the pentadecapeptide BPC 157 in rats and guinea pigs. *Eur J Pharmacol* 2016; **771**: 211-219 [PMID: 26698393 DOI: 10.1016/j.ejphar.2015.12.016]

P- Reviewer: Николаевич YN, Ricci G **S- Editor**: Gong ZM
L- Editor: A **E- Editor**: Yin SY

World Journal of Gastroenterology

Submit a Manuscript: https://www.f6publishing.com

World J Gastroenterol 2018 December 28; 24(48): 5477-5490

DOI: 10.3748/wjg.v24.i48.5477

ISSN 1007-9327 (print) ISSN 2219-2840 (online)

ORIGINAL ARTICLE

Basic Study

Mismatched effects of receptor interacting protein kinase-3 on hepatic steatosis and inflammation in non-alcoholic fatty liver disease

Waqar Khalid Saeed, Dae Won Jun, Kiseok Jang, Sang Bong Ahn, Ju Hee Oh, Yeon Ji Chae, Jai Sun Lee, Hyeon Tae Kang

Waqar Khalid Saeed, Dae Won Jun, Department of Gastroenterology, Hanyang University College of Medicine, Seoul 04763, South Korea

Kiseok Jang, Department of Pathology, Hanyang University College of Medicine, Seoul 04763, South Korea

Sang Bong Ahn, Department of Internal Medicine, Eulji University, Daejeon 34824, South Korea

Ju Hee Oh, Yeon Ji Chae, Jai Sun Lee, Hyeon Tae Kang, Department of Translational Medicine, Hanyang University College of Medicine, Seoul 04763, South Korea

ORCID number: Waqar Khalid Saeed (0000-0002-7888-9108); Dae Won Jun (0000-0002-2875-6139); Kiseok Jang (0000-0002-6585-3990); Sang Bong Ahn (0000-0001-7419-5259); Ju Hee Oh (0000-0003-3031-0272); Yeon Ji Chae (0000-0001-7126-1070); Jai Sun Lee (0000-0002-1673-8777); Hyeon Tae Kang (0000-0002-0595-3025).

Author contributions: Saeed WK drafted the manuscript; Jun DW designed the research and supervised the project; Oh JH, Chae YJ, Lee JS, and Kang HT collected the data; Lee JS analyzed the data; Jang K analyzed the histology data; Ahn SB supervised and revised the manuscript.

Supported by National Research Foundation of Korea (NRF), funded by the South Korean Government, No. NRF-2017M3A9C8028794.

Institutional animal care and use committee statement: All the experimental procedures were approved by the Hanyang University Institutional Animal Care and Use Committee of (HY-IACUC-16-0075).

Conflict-of-interest statement: The authors have declared no conflicts of interest.

Data sharing statement: No additional data is available.

Manuscript source: Unsolicited manuscript

Corresponding author: Dae Won Jun, MD, PhD, Professor, Department of Internal Medicine, Hanyang University College of Medicine, 222-1 Wangsimni-ro, Seongdong-gu, Seoul 04763, South Korea. noshin@hanyang.ac.kr
Telephone: +82-2-22908338
Fax: +82-2-9720068

Received: August 27, 2018
Peer-review started: August 27, 2018
First decision: October 24, 2018
Revised: November 8, 2018
Accepted: November 13, 2018
Article in press: November 13, 2018
Published online: December 28, 2018

Abstract

AIM

To validate the effects of receptor interacting protein kinase-3 (RIP3) deletion in non-alcoholic fatty liver disease (NAFLD) and to clarify the mechanism of action.

METHODS

Wild-type (WT) and RIP3 knockout (KO) mice were

fed normal chow and high fat (HF) diets for 12 wk. The body weight was assessed once weekly. After 12 wk, the liver and serum samples were extracted. The liver tissue expression levels of RIP3, microsomal triglyceride transfer protein, protein disulfide isomerase, apolipoprotein-B, X-box binding protein-1, sterol regulatory element-binding protein-1c, fatty acid synthase, cluster of differentiation-36, diglyceride acyltransferase, peroxisome proliferator-activated receptor alpha, tumor necrosis factor-alpha (TNF-α), and interleukin-6 were assessed. Oleic acid treated primary hepatocytes from WT and RIP3KO mice were stained with Nile red. The expression of inflammatory cytokines, including chemokine (C-X-C motif) ligand (CXCL) 1, CXCL2, and TNF-α, in monocytes was evaluated.

RESULTS

RIP3KO HF diet fed mice showed a significant gain in body weight, and liver weight, liver to body weight ratio, and liver triglycerides were increased in HF diet fed RIP3KO mice compared to HF diet fed WT mice. RIP3KO primary hepatocytes also had increased intracellular fat droplets compared to WT primary hepatocytes after oleic acid treatment. RIP3 overexpression decreased hepatic fat content. Quantitative real-time polymerase chain reaction analysis showed that the expression of very-low-density lipoproteins secretion markers (microsomal triglyceride transfer protein, protein disulfide isomerase, and apolipoprotein-B) was significantly suppressed in RIP3KO mice. The overall NAFLD Activity Score was the same between WT and RIP3KO mice; however, RIP3KO mice had increased fatty change and decreased lobular inflammation compared to WT mice. Inflammatory signals (CXCL1/2, TNF-α, and interleukin-6) increased after lipopolysaccharide and pan-caspase inhibitor (necroptotic condition) treatment in monocytes. Neutrophil chemokines (CXCL1, and CXCL2) were decreased, and TNF-α was increased after RIP3 inhibitor treatment in monocytes.

CONCLUSION

RIP3 deletion exacerbates steatosis, and partially inhibits inflammation in the HF diet induced NAFLD model.

Key words: Necroptosis; Receptor interacting protein kinase-3; Mixed lineage kinase domain-like protein; Non-alcoholic fatty liver disease; Steatosis

Core tip: Receptor interacting protein kinase-3 (RIP3) deletion was associated with increased fatty change, hepatic tissue triglycerides, body weight, and serum aspartate aminotransferase and alanine aminotransferase levels. Very-low-density lipoproteins secretion markers, including apolipoprotein-B, microsomal triglyceride transfer protein, and protein disulfide isomerase, were suppressed with RIP3 deletion. High fat diet fed RIP3KO mice had reduced expressions of tumor necrosis factor alpha and neutrophil chemokines [Chemokine (C-X-C motif) ligands: CXCL1, and CXCL2] compared to high fat diet fed wild-type mice. *In vitro* analysis suggests that necroptotic stimulation [lipopolysaccharide + N-Benzyloxycarbonyl-Val-Ala-Asp(O-Me) fluoromethyl ketone] increased CXCL1/2 expression in monocytes. Treatment with RIP3 inhibitor (GSK'843) decreased the expression of CXCL1/2 as well as interleukin-6.

Saeed WK, Jun DW, Jang K, Ahn SB, Oh JH, Chae YJ, Lee JS, Kang HT. Mismatched effects of receptor interacting protein kinase-3 on hepatic steatosis and inflammation in non-alcoholic fatty liver disease. *World J Gastroenterol* 2018; 24(48): 5477-5490
URL: https://www.wjgnet.com/1007-9327/full/v24/i48/5477.htm
DOI: https://dx.doi.org/10.3748/wjg.v24.i48.5477

INTRODUCTION

Non-alcoholic fatty liver disease (NAFLD) comprises one of the major liver disease burden in the developed world. In the United States, the prevalence of NAFLD is up to 25%[1]. NAFLD, the hepatic component of metabolic syndrome, is a multifactorial wide spectrum disease ranging from simple steatosis to steatohepatitis and further progressing to fibrosis and hepatocellular carcinoma. In NAFLD, increased lipid accumulation in hepatocytes leads to steatosis, inflammation, and fibrosis. NAFLD could also be hinting towards decreasing heart function[2]. In younger patients, NAFLD is also associated with decreased sleep, decreased quality and frequency of food intake, and a sedentary life-style[3]. The lifestyle modifications directed towards reduced steatosis in NAFLD would not only improve NAFLD but also cardiac function[2]. Although the prevalence of NAFLD is increasing, there are still numerous diagnostic and treatment issues associated with NAFLD. For instance, liver biopsy remains the gold standard method for NAFLD diagnosis, but currently no diagnostic method can correctly distinguish between simple steatosis and steatohepatitis. Moreover, there is still a lack of a satisfactory treatment strategy for NAFLD[4].

In NAFLD, the 'first hit' comprises of accumulation of fatty acids in hepatocytes facilitated by increased fatty acid synthesis and increased insulin resistance. Later, the multiple 'parallel hits' mainly comprising of endoplasmic reticulum stress, mitochondrial dysfunction, oxidative stress, and inflammatory cytokines further facilitate hepatocyte dysfunction and death[5]. Cell death is the fundamental step leading to steatohepatitis from benign steatosis. The increased steatosis and inflammation can trigger hepatocyte death by either apoptosis or necrosis[6-8]. Recently, the significance of inhibiting alternate cell death pathways including necroptosis has been extensively reported[9].

Necroptosis, which is a receptor interacting protein kinase 1 and 3 (RIP1/RIP3) and mixed lineage kinase domain like pseudokinase (MLKL) dependent, apoptosis alternative, and necrosis like cell death pathway, has been evaluated in various hepatic pathologies[10-17]. The increased expression of RIP3 and MLKL observed in human NASH, type II diabetes, and obese patients[11-13] highlights the significance of necroptosis in human metabolic disease conditions. Moreover, human metabolic disease serum markers, including HbA1c and insulin, are also correlated with RIP3 and *p*-MLKL expression[13].

Previously, several studies reported varying results on necroptosis inhibition in animal NAFLD models[11-13,18]. To evaluate the role of necroptosis inhibition, the studies utilized methionine choline deficient (MCD) diet, high fat (HF) diet, and choline-deficient HF diet (CD-HFD) induced-NAFLD models[11-13,18]. In the HF diet-induced NAFLD model, RIP3 inhibition led to increased steatosis and glucose intolerance[13,18]. The global RIP3 deletion led to increased body weight and hepatic steatosis in the HF diet-induced NAFLD model, while in the MCD diet-induced NAFLD model, RIP3 deletion showed protective effects on both hepatic steatosis and inflammation[11,12]. Interestingly, HF diet fed RIP3KO mice also had increased hepatic apoptosis, inflammation, and fibrosis[18]. Moreover, adipose tissue apoptosis and inflammation were also increased in RIP3KO mice compared to WT mice[13,18]. An additional *in vivo* signaling pathway was suspected which led to increased steatosis[13,18], adipocyte apoptosis, and inflammation[13]. On contrary, in the MCD diet-induced NAFLD model, RIP3KO mice had decreased inflammation, steatosis, and fibrosis compared to WT mice[11,12]. Although the previous studies evaluated the effect of RIP3 deletion in the HF diet-induced NAFLD model, the detailed mechanism of increased steatosis associated with RIP3 deletion was not clear.

Therefore, by using HF diet-induced NAFLD in RIP3KO mice, we aimed to validate and evaluate the precise underlying mechanism of steatosis and inflammation in hepatocytes and inflammatory cells.

MATERIALS AND METHODS

Animal experiments

C57BL/6 wild-type (WT) (8-9 wk old) and RIP3-KO mice (8-9 wk old) were randomly divided into following groups (n = 8); WT- normal chow (NC), WT-HF, RIP3KO-NC, and RIP3KO-HF. To evaluate the effects of RIP3 inhibition on HF diet-induced NAFLD development, NC and HF (60% kcal) diets were fed for 12 wk to the assigned groups. Four animals were kept per cage and animals were maintained in a temperature-controlled room (22 ℃) on a 12:12 h light-dark cycle. The body weight was recorded once weekly. After 12 wk, the animals were sacrificed. The liver weight and liver to body weight ratio were measured. All the experimental procedures were approved by the Hanyang University Institutional Animal Care and Use Committee of (HY-IACUC-16-0075). RIP3-KO animals were generously provided by Newton *et al*[19] Genentech (San Francisco, CA, United States).

Histological assessment of liver biopsy samples

For histological assessment, paraformaldehyde fixed, paraffin embedded liver tissue samples were sectioned (4 μm) and stained with hematoxylin & eosin. The stained liver biopsy samples were analyzed by a single pathologist. The NASH clinical research network scoring system was used to histologically grade the NAFLD in mice liver[20]. Briefly, steatosis degree, hepatocyte ballooning, and lobular inflammation were graded semi-quantitatively. The NAFLD Activity Score (NAS) was assessed by a combination of each score. Based on the NAS score, the commutative score of (0-2), control; (3-4), NAFLD; and (> 5), NASH was assigned.

Triglyceride quantification

To quantify liver triglycerides (TG) content, a TG quantification kit (Abcam, Cambridge, MA, United States) was used. Briefly, snap-frozen livers tissues (50–100 mg) were homogenized in 5% NP-40, and then slowly heated to 80 ℃ for 5 min and cooled down. The process was repeated twice. The samples were then centrifuged for 5 min, and supernatants were diluted 20-fold with distilled water and analyzed calorimetrically according to manufacturer's instructions.

HepG2 cells culture and maintenance

HepG2 cells were seeded on 6-well plate using Dulbecco's modified Eagle's medium (DMEM; Gibco, Grand Island, NY, United States) containing 10% fetal bovine serum (FBS) and 1% penicillin/streptomycin (P/S). After 24 h, the media was removed, and the cells were washed with Dulbecco's phosphate-buffered saline (DPBS) followed by treatment with oleic acid (OA; 400 μmol/L; Sigma-Aldrich, St Louis, MO, United States), palmitic acid (PA; 400 μmol/L; Sigma-Aldrich), and GSK' 843 (5 μmol/L; AOBIOUS INC, Gloucester, MA, United States). After 24 h, the RNA was isolated using the RNeasy mini kit (Qiagen, Hilden, Germany) according to manufacturer's instructions.

Primary hepatocytes isolation and culture

Primary hepatocytes from WT and RIP3-KO mice were isolated by a two-step collagenase perfusion method as described previously[21]. Briefly, mice were anesthetized using Zoletil and Rompun 1:1. The liver was perfused using calcium and magnesium-free Hanks' Balanced Salt Solution (HBSS; Welgene, Gyeongsan, South Korea) supplemented with 25 mmol/L, 4-(2-hydroxyethyl)-1-piperazine ethanesulfonic acid (HEPES; Amresco, Solon, OH, United States) and 0.5 mmol/L, ethylene-

glycol-bis-(β-aminoethylene)-N,N,N′,N′-tetraacetic acid (EGTA; Sigma-Aldrich), followed by perfusion with low glucose DMEM supplemented with 15 mmol/L HEPES and Collagenase Type IV (100 U/mL; Worthington Biochemical Corporation, Lakewood, NJ, United States) (pH 7.4, 37 ℃). After perfusion, the liver was carefully removed and gently minced in 20 mL ice-cold William' s E medium (Gibco) supplemented with 10% heat-inactivated FBS, 10 mL/L insulin-transferrin-selenium (ITS; Gibco), and 10 mL/L P/S. The homogenized liver suspension was filtered using a 70 μm cell strainer. The cell suspension was centrifuged at 50 × *g* for 5 min. The pellet was re-suspended in 10 mL William's Medium supplemented with 10% FBS, ITS (10 mL/L), P/S (10 mL/L), and 10 mL buffered Percoll (Sigma-Aldrich). The resultant cell suspension was centrifuged at 50 × *g* for 5 min, and the pellet re-suspended in William's E medium supplemented with 10% FBS, ITS (10 mL/L), and 1 μmol/L dexamethasone and P/S (10 mL/L). The cell viability was determined using the Trypan Blue exclusion method and was generally > 85%. After isolation, primary hepatocytes were plated on rat-tail collagen I (Corning Inc., Corning, NY, United States) coated culture dishes (Thermo Fisher Scientific Inc., Waltham, MA, United States) at 3 × 10^5 cells/mL. The hepatocytes were maintained at 37 ℃ in a humidified atmosphere of 5% CO_2 for 4 h. After 4 h, the media were removed, and cells were treated with OA (400 μmol/L) in serum-free William's E medium containing ITS (10 mL/L), 1 μmol/L dexamethasone, and P/S (10 mL/L). The control group was treated with equal volumes of dimethyl sulfoxide (DMSO). After 24 h, the hepatocytes were processed as per experimental protocols.

Macrophage cell culture and maintenance

The macrophage U937 cell line was used. The cells were seeded on 6-well plates using DMEM supplemented with 10% FBS and 1% P/S. After 24 h, the media were removed, and the cells were washed with DPBS followed by incubation with tumor necrosis factor alpha (TNF-α) (10 ng/mL; R&D Systems, Minneapolis, MN, United States), N-benzyloxycarbonyl-Val-Ala-Asp(O-Me) fluoromethyl ketone (zVAD) (30 μmol/L, R&D Systems), lipopolysaccharide (LPS) (25 ng/mL; Sigma-Aldrich), and GSK'843 (5 μmol/L). After 24 h, the RNA was isolated using the RNeasy mini kit (Qiagen) according to manufactures instructions.

Serum biochemical analysis

The whole blood samples collected in Becton Dickinson serum separation tubes (Franklin Lakes, NJ, United States) were centrifuged at 3000 rpm at 4 ℃ for 10 min. The serum samples were collected and stored at -80 ℃ until analysis. Serum alanine aminotransferase (ALT), aspartate aminotransferase (AST), and TG were measured with an automatic chemical analyzer (Hitachi-747; Hitachi, Tokyo, Japan).

Nile red staining

For lipid droplet staining, primary hepatocytes and HepG2 cells were seeded on a coverslip and maintained for 4 and 24 h, respectively. After adherence, the media were removed and cells were co-treated with OA (400 μmol/L) and GSK'843 (5 μmol/L). The control groups were treated with equal volumes of DMSO. After 24 h, the media were removed, and the cells were washed twice with DPBS, fixed with 4% paraformaldehyde in PBS for 30 min at room temperature, rinsed twice with DPBS, and incubated with fluorescence dye Nile red (0.5 mg/mL in acetone). The confocal imaging was performed using a Leica TCS SP5 confocal microscope (Leica Microsystems, Wetzlar, Germany).

RIP3 non-viral vector construction

The human RIP3 (NM_006871) coding regions were amplified by polymerase chain reaction (PCR) using TrueORF cDNA Clones (Origene, Rockville, MD, United States) for genes. The fragments were cloned into the pECFP (enhanced green fluorescent protein)-C1 vector (Clontech, Palo Alto, CA, United States). Later, RIP3 PCR products were subcloned into the pGEM-T easy vector (Promega, Madison, WI, United States) and then cloned into the EcoRI - BamHI sites of the pECFP-C1 vector.

RIP3 overexpression in primary hepatocytes

The primary hepatocytes were isolated and maintained as previously described. RIP3 was overexpressed in primary hepatocytes using JetPEI DNA transfection reagent (Polyplus-transfection SA, Illkirch, France) according to the manufacturer's instructions. Briefly, 1 × 10^5/mL primary hepatocytes were seeded on collagen-coated cover slides in 24-well plates. After 4 h, the media were replaced with fresh culture media supplemented with 10% FBS. RIP3 DNA (3 μg/well) was diluted in 100 μL NaCl (150 mmol/L) and was gently vortexed and spun down. Six microliters per well JetPEI reagent was diluted in 100 μL NaCl (150 mmol/L) and was gently vortexed and spun down. The diluted reagent was mixed and vortexed with diluted DNA and incubated for 30 min at room temperature. After 30 min, 50 μL JetPEI/DNA mix was added to each well of a 24-well plate. After 12 h, the transfection was confirmed by visualizing green fluorescence of EGFP-C1 using a Leica DMI 14000B inverted microscope (Leica Microsystems).

RNA isolation and quantitative real-time PCR

Total liver RNA was isolated from liver tissue using the TRIzol Reagent (Invitrogen, Carlsbad, CA, United States) according to the manufacturer's instructions. The isolated RNA samples were converted to cDNA using reverse transcriptase (SuperScript III; Invitrogen) and oligo (dT) primers. All PCR reactions were performed on the LightCycler 480 system (Roche Diagnostics, Mannheim, Germany) using LightCycler480

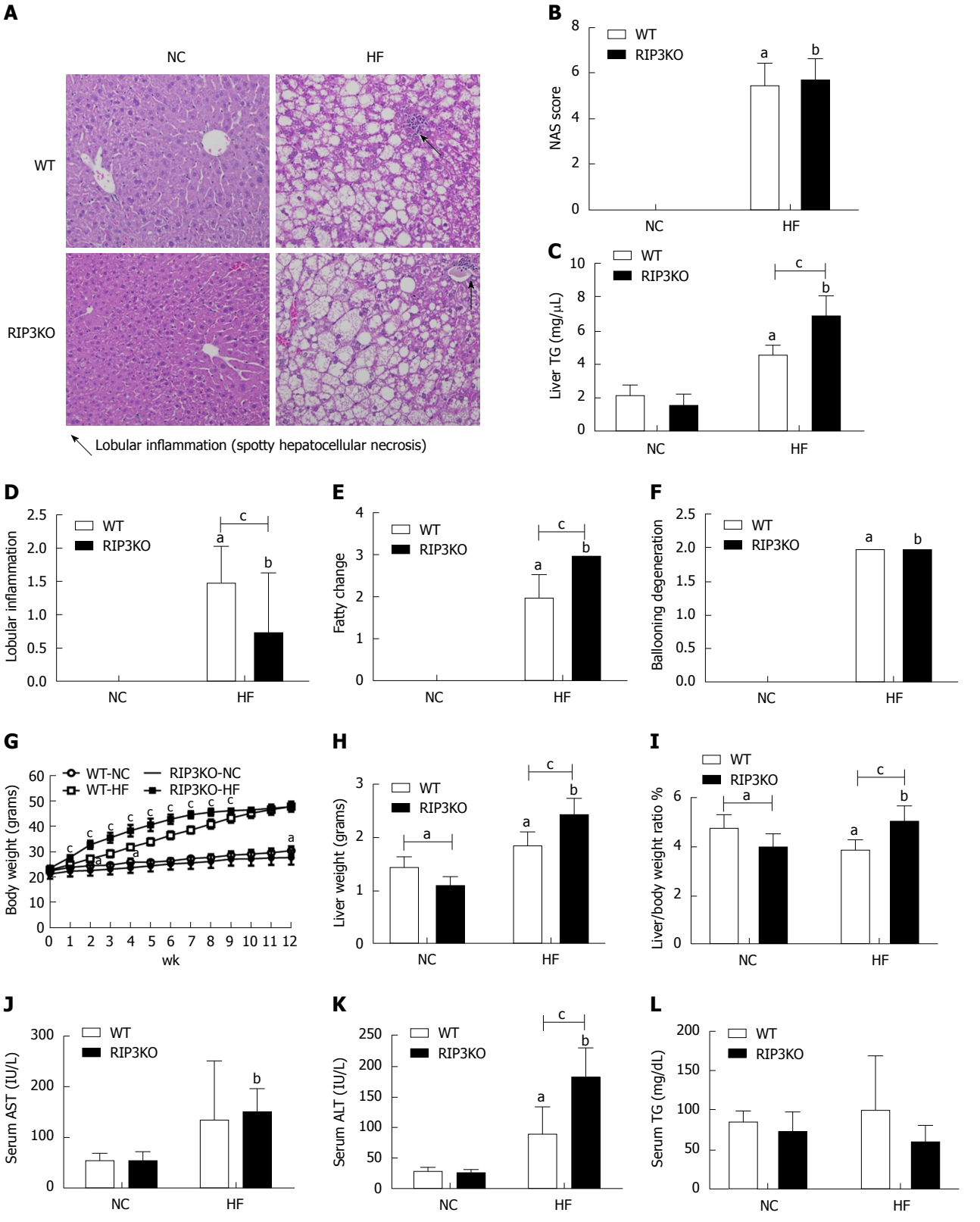

Figure 1 Receptor interacting protein kinase-3 deletion exacerbates HF diet induced steatosis. A: Following 12-wk HF diet, the liver tissue hematoxylin & eosin staining showed increased steatosis in RIP3KO-HF group compared to WT-HF group. B-F: Liver TG contents were significantly increased in the RIP3KO-HF group compared to the WT-HF group. RIP3KO-HF group had increased steatosis and decreased lobular inflammation. G-L: HF diet fed RIP3KO mice had increased liver weight and liver/body weight ratio compared to HF diet fed WT mice. The RIP3KO-HF group had increased serum AST and ALT but decreased serum TG compared to the WT-HF group. [a]*P* < 0.05 by Mann-Whitney *U* test, compared to NC diet fed WT group; [b]*P* < 0.05 by Mann-Whitney *U* test, compared to NC diet fed RIP3-KO group; [c]*P* < 0.05 by Mann-Whitney *U* test, compared to HF diet fed WT group. HF: High fat; NC: Normal chow; WT: Wild-type; KO: Knockout; RIP3: Receptor interacting protein kinase-3; AST: Aspartate aminotransferase; ALT: Alanine aminotransferase; TG: Triglycerides.

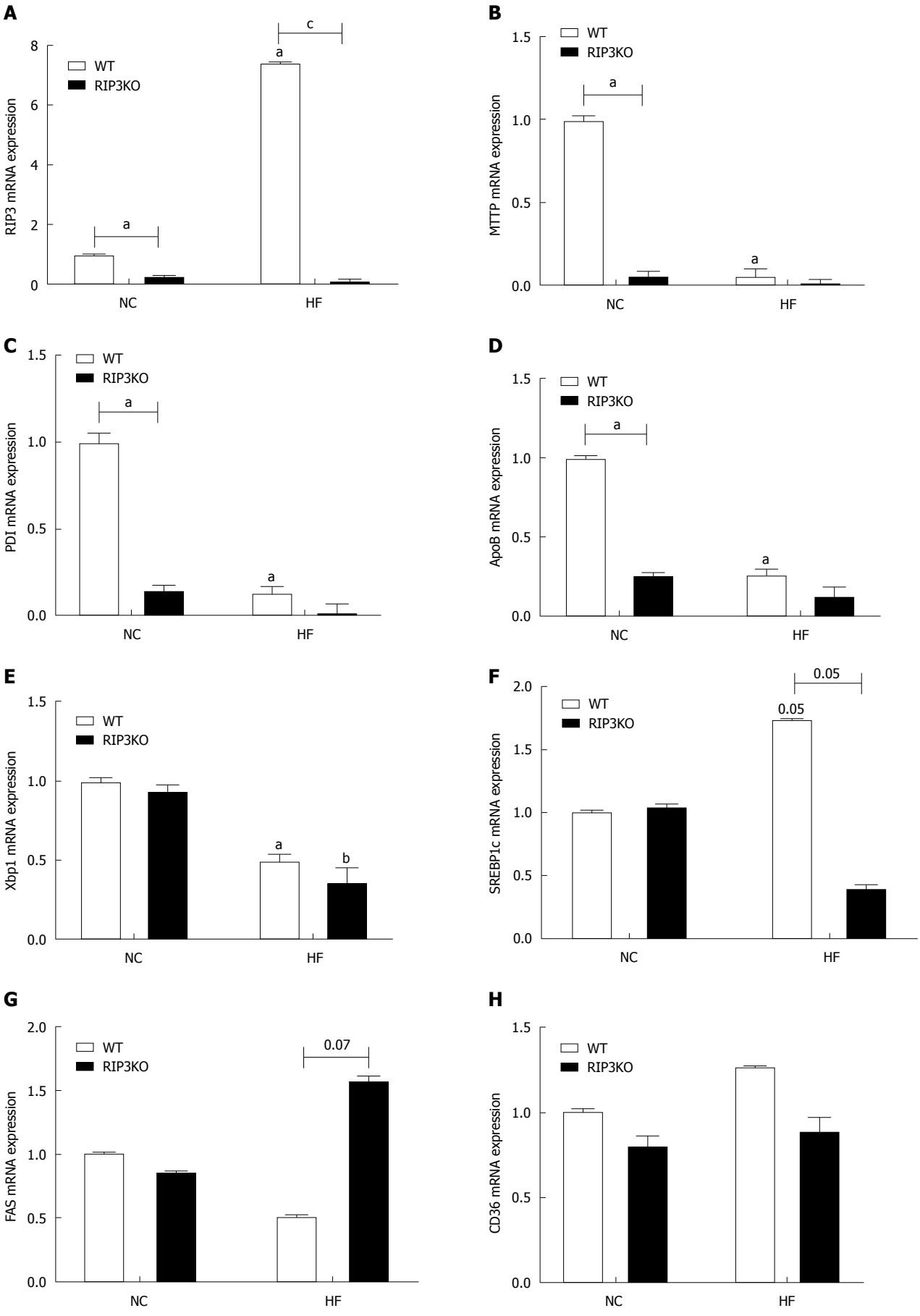
A
RIP3 mRNA expression
WT
RIP3KO
a
a
c
NC
HF
B
MTTP mRNA expression
WT
RIP3KO
a
a
NC
HF
C
PDI mRNA expression
WT
RIP3KO
a
a
NC
HF
D
ApoB mRNA expression
WT
RIP3KO
a
a
NC
HF
E
Xbp1 mRNA expression
WT
RIP3KO
a
b
NC
HF
F
SREBP1c mRNA expression
WT
RIP3KO
0.05
0.05
NC
HF
G
FAS mRNA expression
WT
RIP3KO
0.07
NC
HF
H
CD36 mRNA expression
WT
RIP3KO
NC
HF

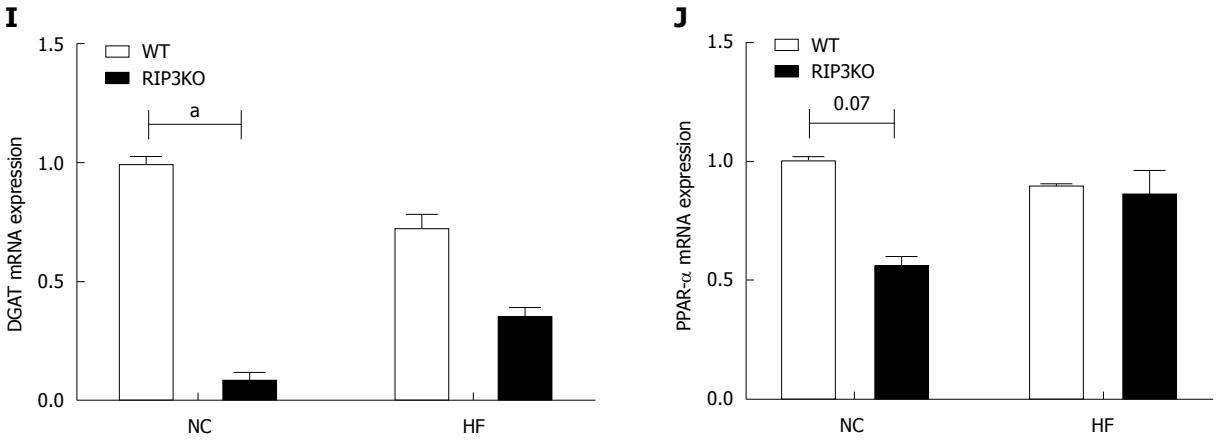

Figure 2 Effect of receptor interacting protein kinase-3 deletion on fat synthesis. A-J: Quantitative real-time PCR analysis showed an increased expression of RIP3 the WT-HF group after HF diet feeding. Interestingly, very-low-density lipoprotein secretion markers including apolipoprotein-B, microsomal triglyceride transfer protein, protein disulfide isomerase, and X-box binding protein-1 were decreased in the RIP3KO-HF group compared to the WT-HF group. The differences in SREBP1c, FAS, CD36, DGAT, and PPAR-α were not definite. [a]*P* < 0.05 by Mann-Whitney *U* test, compared to NC diet fed WT group; [b]*P* < 0.05 by Mann-Whitney *U* test, compared to NC diet fed RIP3-KO group; [c]*P* < 0.05 by Mann-Whitney *U* test, compared to HF diet fed WT group. HF: High fat; KO: Knockout; NC: Normal chow; WT: Wild-type; RIP3: Receptor interacting protein kinase-3; VLDL: Very-low-density lipoproteins; ApoB: Apolipoprotein-B; MTTP: Microsomal triglyceride transfer protein; PDI: Protein disulfide isomerase; XBP1: X-box binding protein-1; SREBP1c: Sterol regulatory element-binding protein-1c; FAS: Fatty acid synthase; CD36: Cluster of differentiation-36; DGAT: Diglyceride acyltransferase; PPAR-α: Peroxisome proliferator-activated receptor alpha.

SYBRGreen I Mastermix (Roche Diagnostics) in standard 10 μL reaction volumes as follows: 4 μL (100 ng) cDNA, 0.5 μL of 10 pmol/L sense primer, 0.5 μL of 10 pmol/L antisense primer, and 5 μL LightCycler 480 SYBRGreen I Mastermix (Roche Diagnostics). To guarantee the reliability of the obtained results, all samples were processed in triplicate and performed using a negative control. The values obtained were normalized to the control and expressed as fold changes.

Statistical analysis

The values are expressed as mean ± standard deviation. Statistical analysis was performed using SPSS for Windows version 21.0 (IBM Corp., Armonk, NY, United States). All experiments were performed three times. One-way analysis of variance and the Mann-Whitney *U* test were performed to compare the mean of different groups, and a *P*-value < 0.05 was considered significant.

RESULTS

Exacerbated intrahepatic fat amount but attenuated hepatic inflammation in HF diet fed RIP3KO mice

RIP3KO mice showed increased hepatic fat deposition on histological and hepatic tissue TG contents analysis compared to WT mice (4.58 nm/μL *vs* 6.92 nm/μL, *P* = 0.000) when fed with 60% HF but not with normal chow diet (Figure 1A and C). Body weight was significantly increased in HF diet fed RIP3KO mice compared to WT mice. Overall, NAS score was not significantly different between the both WT-HF and RIP3KO-HF groups; however, fatty change was significantly increased (2 *vs* 3, *P* = 0.000) and lobular inflammation was decreased (1.5 *vs* 0.75, *P* = 0.007) in HF fed RIP3KO mice (Figure 1B, D-F). Liver weight (1.87 g *vs* 2.43 g, *P* = 0.001) and liver to body weight ratio (5.09 *vs* 3.91, *P* = 0.000) were also increased in HF diet fed RIP3KO mice compared to WT mice (Figure 1H and I). Serum ALT was increased in HF diet fed RIP3KO mice (Figure 1K).

Effect of RIP3 ablation on hepatic fat regulation

RIP3 expression increased with the HF diet (Figure 2A), as previously observed[18]. The expression of other genes involved in lipid homeostasis, including those for sterol regulatory element-binding protein-1c, fatty acid synthase, cluster of differentiation-36, diglyceride acyltransferase, and peroxisome proliferator-activated receptor alpha, were not definite (Figure 2F-J). The genes involved in very-low-density lipoprotein (VLDL) secretion were analyzed to evaluate increased hepatic tissue TG contents. The mRNA analysis showed that RIP3KO mice had significantly decreased VLDL secretion markers, including microsomal triglyceride transfer protein (MTTP), protein disulfide isomerase (PDI), and apolipoprotein-B (ApoB). VLDL secretion markers were further suppressed in HF diet fed RIP3KO animals (Figure 2B-D).

Next, to confirm whether the effect of RIP3 deletion could also be observed *in vitro*, primary hepatocytes from WT and RIP3KO mice were isolated. Following treatment with OA, Nile red staining was increased in both WT and RIP3KO primary hepatocytes. However, OA treated RIP3KO primary hepatocytes had increased Nile red staining compared to WT primary hepatocytes (Figure 3A). Next, to confirm further, RIP3 was overexpressed in primary hepatocytes using an RIP3 overexpression system. If RIP3 ablation exacerbates hepatic lipid storage, then RIP3 overexpression should decrease lipid storage. As expected, RIP3 overexpressed

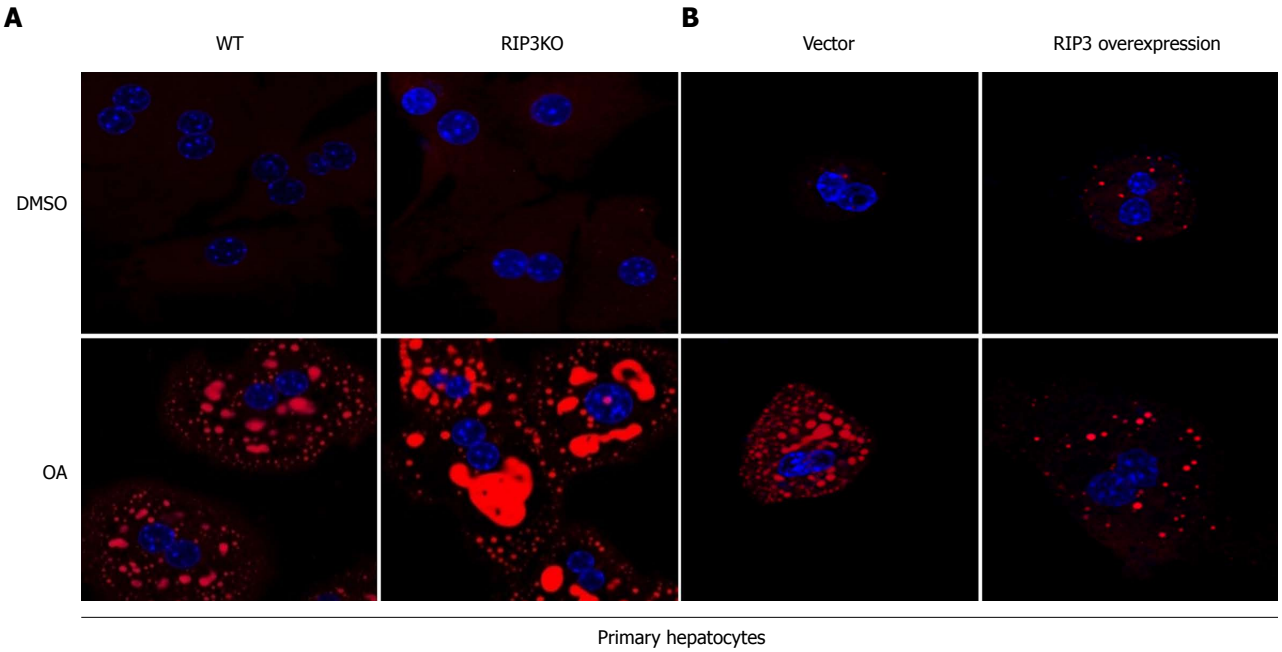
A
WT
RIP3KO
DMSO
OA
B
Vector
RIP3 overexpression
Primary hepatocytes

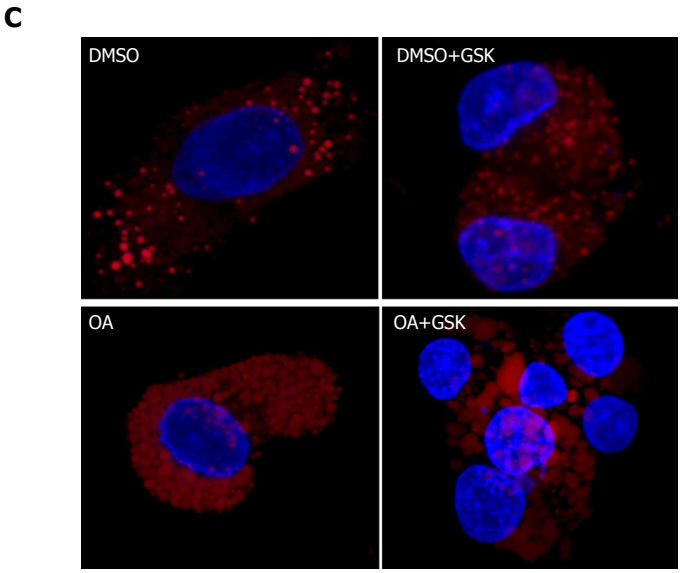
C
DMSO
DMSO+GSK
OA
OA+GSK

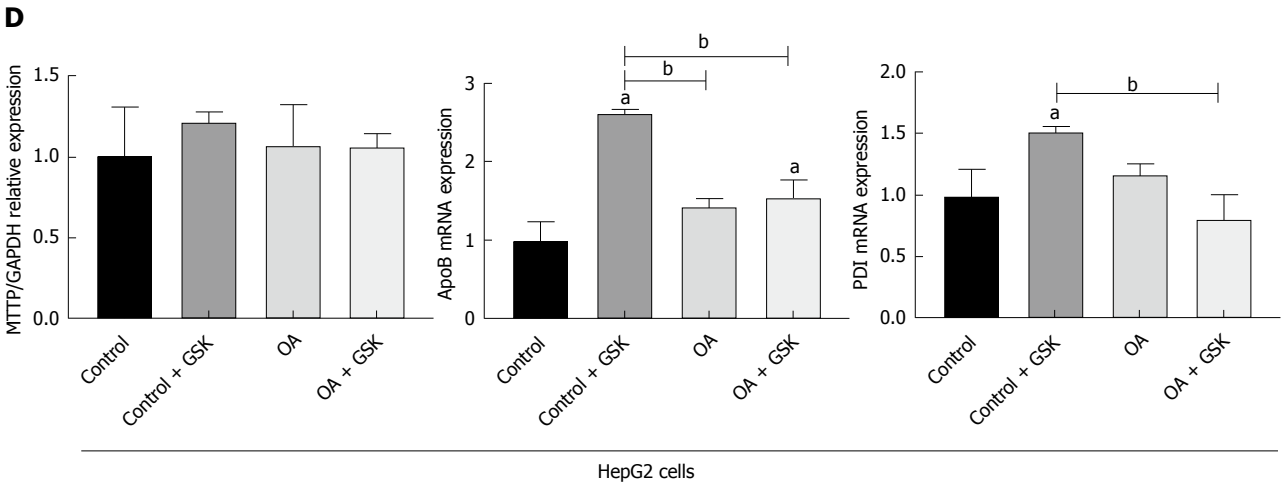
D
MTTP/GAPDH relative expression
1.5
1.0
0.5
0.0
Control
Control + GSK
OA
OA + GSK
ApoB mRNA expression
3
2
1
0
a
b
PDI mRNA expression
2.0
1.5
1.0
0.5
0.0
HepG2 cells

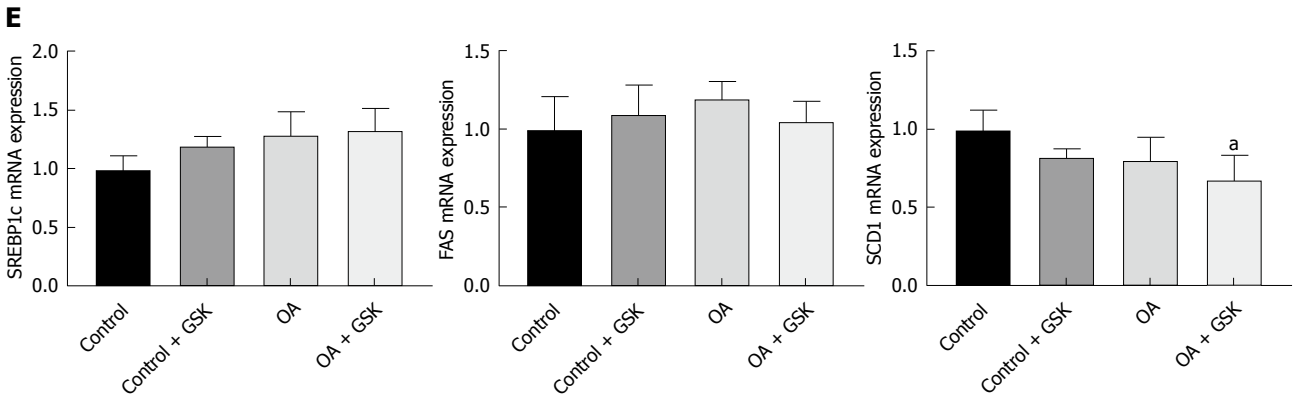

Figure 3 RIP3 deletion increases hepatic fat storage. A and B: The primary hepatocytes from WT and RIP3KO mice were treated with DMSO and OA. The RIP3KO primary hepatocytes had increased Nile red staining compared to WT primary hepatocytes. RIP3 overexpression decreased Nile red staining compared to the vector group treated with OA. C and D: HepG2 cells treated with GSK'843 did not show increase Nile red staining. The expression of MTTP, PDI, and ApoB was also not decreased in GSK'843 treated HepG2 cells. E: GSK'843 treatment did not increase the expression of SREBP1c, FAS, and SCD-1 in HepG2 cells. [a]*P* < 0.05 by ANOVA, Duncan post hoc analysis, compared to control; [b]*P* < 0.05 by ANOVA, Duncan post hoc analysis. WT: Wild-type; RIP3: Receptor interacting protein kinase-3; KO: Knockout; DMSO: Dimethyl sulfoxide; OA: Oleic acid; ApoB: Apolipoprotein-B; MTTP: Microsomal triglyceride transfer protein; PDI: Protein disulfide isomerase; XBP1: X-box binding protein-1; SREBP1c: Sterol regulatory element-binding protein-1c; FAS: Fatty acid synthase; SCD-1: Stearyl-CoA desaturase-1; ANOVA, Analysis of variance.

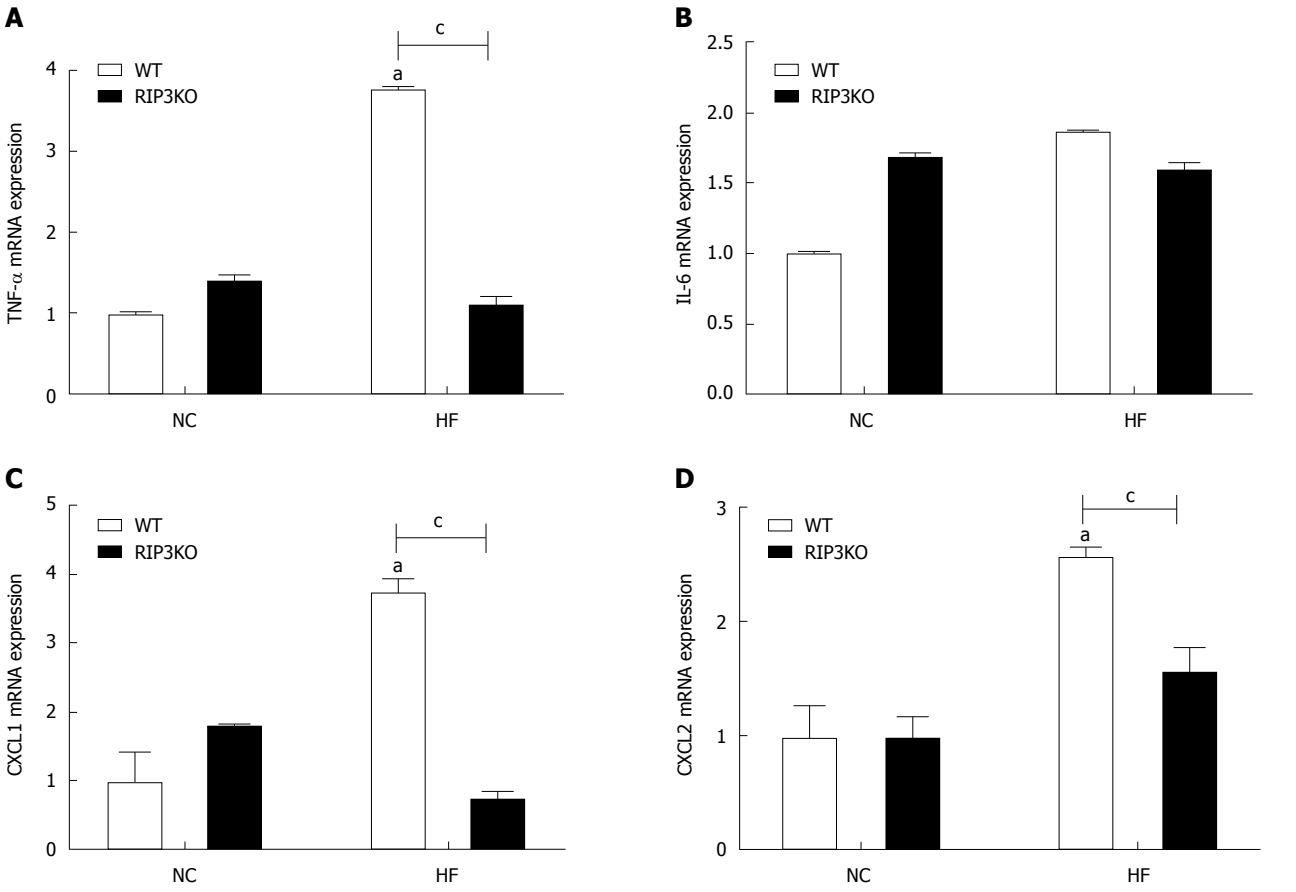

Figure 4 RIP3 reduces inflammation in liver tissue. Following HF diet feeding, RIP3KO mice had reduced expression of TNF-α, CXCL1, and CXCL2 compared to HF diet fed WT mice. [a]*P* < 0.05 by Mann-Whitney *U* test, compared to NC diet fed WT group; [c]*P* < 0.05 by Mann-Whitney *U* test, compared to HF diet fed WT group. HF: High fat; KO: Knockout; WT: Wild-type; NC: Normal chow; RIP3: Receptor interacting protein kinase-3; TNF-α: Tumor necrosis factor alpha; CXCL1: Chemokine (C-X-C motif) ligand-1; CXCL2: Chemokine (C-X-C motif) ligand-2.

primary hepatocytes had decreased Nile red staining compared to control (Figure 3B). Next, we evaluated whether RIP3 inhibition using GSK'843 would also yield similar results in HepG2 cells. However, GSK'843 treated HepG2 cells did not show an increase in Nile red staining, a decrease in MTTP, PDI, and ApoB expression (Figure 3C and D), and changes in sterol regulatory element-binding protein-1c, fatty acid synthase, and

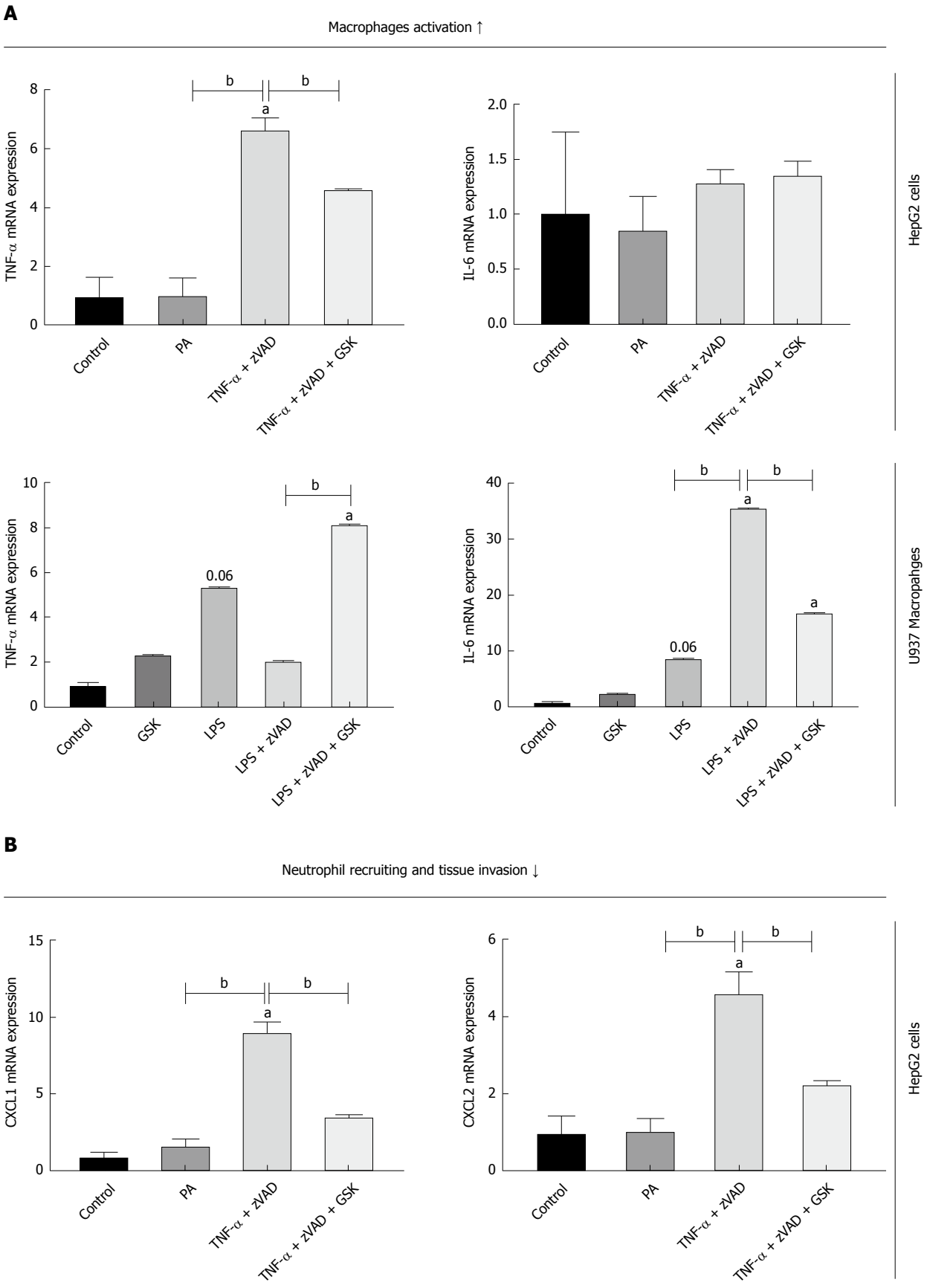
A
Macrophages activation ↑
TNF-α mRNA expression
IL-6 mRNA expression
Control
PA
TNF-α + zVAD
TNF-α + zVAD + GSK
HepG2 cells
GSK
LPS
LPS + zVAD
LPS + zVAD + GSK
U937 Macropahges
B
Neutrophil recruiting and tissue invasion ↓
CXCL1 mRNA expression
CXCL2 mRNA expression
HepG2 cells

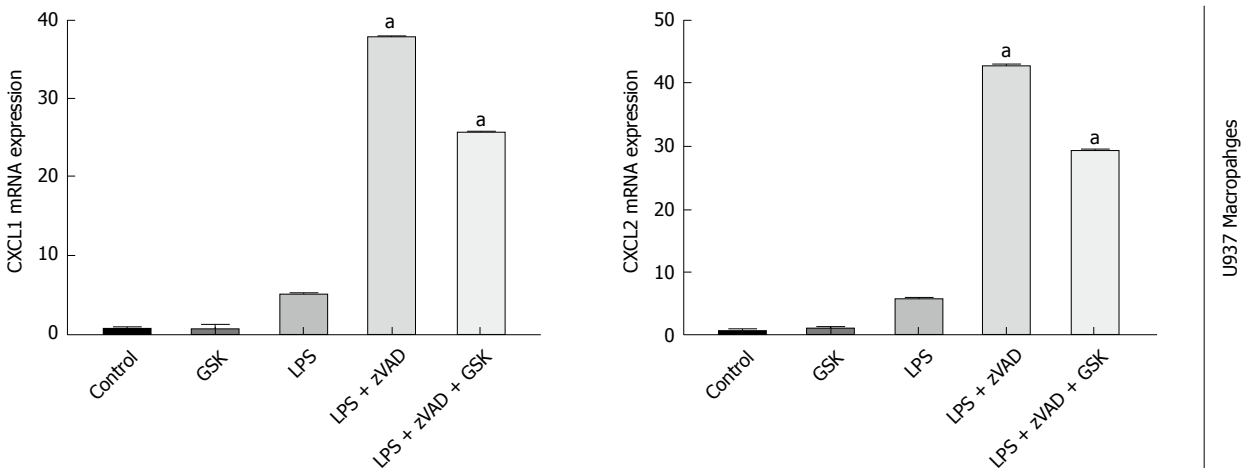

Figure 5 Effect of RIP3 on inflammatory markers. A and B: TNF-α/LPS + zVAD induced increase in TNF-α expression was exacerbated with GSK'843 treatment. TNF-α/LPS + zVAD induced increased expression of CXCL1 and CXCL2 was decreased with GSK'843 treatment. [a]*P* < 0.05 by ANOVA, Duncan post hoc analysis, compared to control; [b]*P* < 0.05 by ANOVA, Duncan post hoc analysis. TNF-α: Tumor necrosis factor alpha; LPS: Lipopolysaccharide; zVAD: N-Benzyloxycarbonyl-Val-Ala-Asp(O-Me) fluoromethyl ketone; CXCL1: Chemokine (C-X-C motif) ligand-1; CXCL2: Chemokine (C-X-C motif) ligand-2; ANOVA, Analysis of variance.

stearyl-CoA desaturase (SCD-1) expression (Figure 3E).

RIP3 partially regulated macrophage activation

HF diet fed RIP3KO mice had reduced expression of TNF-α, CXCL1, and CXCL2 compared to HF diet fed WT mice (Figure 4A-D). *In vitro* analysis suggested that necroptotic stimulation (LPS + zVAD) increased CXCL1/2 expression in monocytes. RIP3 inhibitor (GSK' 843) decreased the expression of CXCL1/2 as well as IL-6, but GSK'843 did not reduce TNF-α expression. The levels of neutrophil chemokines (CXCL1, and CXCL2) were decreased with GSK'843 (Figure 5A and B).

DISCUSSION

Our results suggest that RIP3 inhibition is associated with suppression of VLDL secretion markers and partial inhibition of macrophage activation *via* inhibiting CXCL1 and 2 expressions.

Previously, varying results of RIP3 inhibition in HF and MCD diet-induced animal NAFLD models were observed. In HF diet-induced NAFLD model[18], RIP3 deletion was associated with increased fatty change, hepatic tissue TG, body weight, and serum AST and ALT. Another study, however, reported that in the MCD diet-induced NAFLD model, RIP3 deletion did not affect lipidosis score in the early phase (2-wk) but did decrease it in the late phase (8 wk)[11]. The MCD diet-induced NAFLD studies did not extensively evaluate for hepatic steatosis[11,12]. None of the previous studies examined the precise mechanism of hepatic fat accumulation and the interaction with hepatocytes pathways of lipid *de novo* synthesis, transportation, and metabolism. Our results also showed that VLDL secretion markers, including ApoB, MTTP, and PDI, were suppressed with RIP3 deletion (Figure 2). The primary hepatocytes isolated from WT and RIP3KO mice were treated with DMSO and OA. Similar to increased hepatic TG contents in RIP3KO mice, OA treated RIP3KO primary hepatocytes had increased Nile red staining compared to OA treated WT primary hepatocytes. Correspondingly, primary hepatocytes overexpressing RIP3 also showed decreased Nile red staining compared to control (Figure 3). However, we did not observe a decrease in the expression of MTTP, PDI, and ApoB following treatment with GSK'843 in HepG2 cells.

Similar to previous findings[13], our results showed that the overall NAS score was the same between HF diet fed WT and RIP3KO mice; however, lobular inflammation was decreased in our study. Moreover, in contrast to the MCD diet-induced NAFLD model, RIP3 deletion associated reductions in serum AST and ALT were not observed in our study. On the contrary, in HF diet-induced NAFLD model, RIP3 induction was thought to protect hepatocytes against further steatosis and, thus, the RIP3 deletion might have led to more deleterious effects[18]. Moreover, RIP3 deletion was also associated with exacerbated inflammation in the HF diet-induced NAFLD[18]. Interestingly, RIP3 deletion reduced ethanol induced steatosis[22]. In our study, following HF diet feeding, CXCL1/2 expression increased in liver tissue. The expressions of CXCL1/2 were reduced in RIP3KO mice compared to corresponding controls. *In vitro*, TNFα/LPS + zVAD induced CXCL1/2 expressions. GSK'843 treatment reduced CXCL1 and CXCL2 expression in U937 macrophages and HepG2 cells, but TNF-α expression was not reduced (Figures 5 and 6).

Our study has the following limitations. First, we did not evaluate the long-term effects of RIP3 deletion on the exacerbated response in HF diet-induced NAFLD model. Moreover, we did not evaluate the previously highlighted contribution of increased hepatic and adipose tissue apoptosis associated with RIP3 deletion

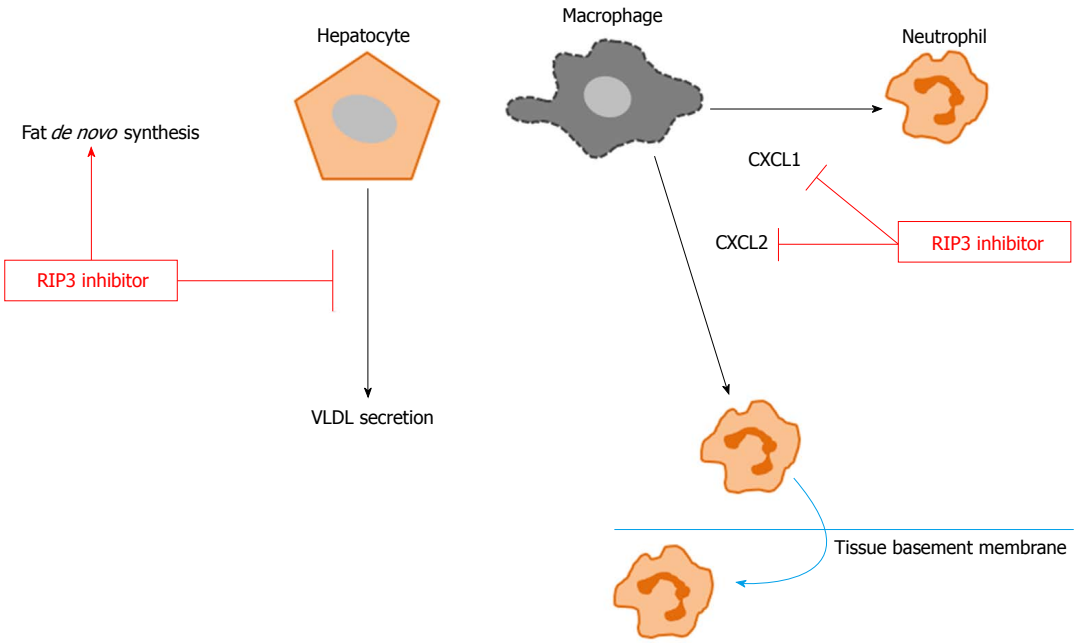

Figure 6 Conceptual diagram. GSK'843 treatment decreases neutrophil recruitment markers, including CXCL1 and CXCL2, thereby reducing neutrophil recruitment to the tissue. However, RIP3 inhibition increases *de novo* fat synthesis while decreasing VLDL secretion. RIP3: Receptor interacting protein kinase-3; CXCL1: Chemokine (C-X-C motif) ligand-1; CXCL2: Chemokine (C-X-C motif) ligand-2; VLDL: Very-low-density lipoproteins.

in NAFLD. RIP3 ablation in adipose tissue leads to the metabolic phenotype in RIP3KO mice. Moreover, RIP3 has a role in maintaining white adipose tissue homeostasis and systemic RIP3 ablation leads to insulin resistance and glucose intolerance. RIP3 overexpression is thought to balance caspase-8 mediated increase in apoptosis. Following RIP3 deletion, a switch towards increased apoptosis in both liver and adipose tissues was observed, and increased adipocytes apoptosis was thought to mediate the systemic effects[13]. Therefore, to elaborate the detailed mechanism of additional *in vivo* signaling, a further in depth analysis is needed. Second, examination of hepatocyte specific RIP3 knockout and RIP3 kinase dead mice would be useful to understand HF diet-induced NAFLD. The pathogenic context, initiating stimulus, and compartment specific RIP3 regulation[12,13] might reveal why such diverse results of RIP3 deletion are observed in the NAFLD models. Other studies also reported that the expression of regulated necrosis molecules could be different according to the trigger, disease pathogenesis, organs involved, and species[23]. Moreover, studies have also suggested that different cell types could be responding differentially to necroptosis stimuli[13].

In conclusion, our results show that RIP3 deletion aggravates hepatic steatosis in the HF diet-induced NAFLD model. RIP3 deletion was also associated with suppression of VLDL secretion from hepatocytes. Moreover, targeting RIP3 could have deleterious systemic consequences. Future research should consider the diverse and unwanted systemic consequences of RIP3 deletion in NAFLD. The role of RIP3 could be a double-edged sword in NAFLD. Although RIP3 has a crucial role in necroptosis, RIP3 showed diverse effects in metabolic disease. Therefore, careful attention and more extensive studies are needed to further elaborate the interactions between RIP3 and NAFLD associated signaling pathways.

ARTICLE HIGHLIGHTS

Research background

The receptor interacting protein kinase-3 (RIP3) inhibition in various non-alcoholic fatty liver disease (NAFLD) models has shown varied results. The underlying mechanism associated with these diverse outcomes is still not clear. The evaluation of necroptosis signaling molecules in NAFLD might provide a useful therapeutic target.

Research motivation

Previous studies report that in high fat (HF)-induced NAFLD, RIP3 deletion exacerbated fatty change, inflammation, fibrosis, and apoptosis. However, in the methionine choline deficient diet-induced NAFLD model, these changes were not observed. The reason for the varied results associated with RIP3 deletion in different NAFLD models is unknown.

Research objective

To validate the effects of RIP3 deletion in NAFLD and to clarify the mechanism of action.

Research methods

Wild-type and RIP3 knockout mice were fed HF and normal chow diets for 12 wk. The body weight was assessed weekly. After 12 wk, the liver and serum samples were analyzed for changes. Hematoxylin & eosin staining, NAFLD Activity Score evaluation, and triglyceride quantification were performed. The changes in very-low-density lipoproteins (VLDL) secretion and inflammation markers were recorded. Primary hepatocytes were evaluated for lipid contents. HepG2 cells and U937 cells were evaluated for changes in inflammatory

markers.

Research results

Our results show that RIP3 deletion is associated with exacerbated hepatic lipid contents, suppressed VLDL secretion markers, and partially suppressed inflammation.

Research conclusion

In HF diet-induced NAFLD, RIP3 deletion is associated with increased hepatic steatosis and partially suppressed inflammation

Research perspective

Necroptosis signaling molecules, especially mixed lineage kinase domain-like proteins, should be further explored for its therapeutic potential in NAFLD.

REFERENCES

1 **Fingas CD,** Best J, Sowa J-P, Canbay A. Epidemiology of nonalcoholic steatohepatitis and hepatocellular carcinoma. *Clinical Liver Disease* 2016; **8:** 119-122 [DOI: 10.1002/cld.585]

2 **Trovato FM**, Martines GF, Catalano D, Musumeci G, Pirri C, Trovato GM. Echocardiography and NAFLD (non-alcoholic fatty liver disease). *Int J Cardiol* 2016; **221**: 275-279 [PMID: 27404689 DOI: 10.1016/j.ijcard.2016.06.180]

3 **Trovato FM**, Martines GF, Brischetto D, Catalano D, Musumeci G, Trovato GM. Fatty liver disease and lifestyle in youngsters: diet, food intake frequency, exercise, sleep shortage and fashion. *Liver Int* 2016; **36**: 427-433 [PMID: 26346413 DOI: 10.1111/liv.12957]

4 **Oh H**, Jun DW, Saeed WK, Nguyen MH. Non-alcoholic fatty liver diseases: update on the challenge of diagnosis and treatment. *Clin Mol Hepatol* 2016; **22**: 327-335 [PMID: 27729634 DOI: 10.3350/cmh.2016.0049]

5 **Bessone F**, Razori MV, Roma MG. Molecular pathways of nonalcoholic fatty liver disease development and progression. *Cell Mol Life Sci* 2018 Epub ahead of print [PMID: 30343320 DOI: 10.1007/s00018-018-2947-0]

6 **Ipsen DH**, Lykkesfeldt J, Tveden-Nyborg P. Molecular mechanisms of hepatic lipid accumulation in non-alcoholic fatty liver disease. *Cell Mol Life Sci* 2018; **75**: 3313-3327 [PMID: 29936596 DOI: 10.1007/s00018-018-2860-6]

7 **Atay K**, Canbakan B, Koroglu E, Hatemi I, Canbakan M, Kepil N, Tuncer M, Senturk H. Apoptosis and Disease Severity is Associated with Insulin Resistance in Non-alcoholic Fatty Liver Disease. *Acta Gastroenterol Belg* 2017; **80**: 271-277 [PMID: 29560693]

8 **Farrell GC**, Haczeyni F, Chitturi S. Pathogenesis of NASH: How Metabolic Complications of Overnutrition Favour Lipotoxicity and Pro-Inflammatory Fatty Liver Disease. *Adv Exp Med Biol* 2018; **1061**: 19-44 [PMID: 29956204 DOI: 10.1007/978-981-10-8684-7_3]

9 **Galluzzi L**, Bravo-San Pedro JM, Vitale I, Aaronson SA, Abrams JM, Adam D, Alnemri ES, Altucci L, Andrews D, Annicchiarico-Petruzzelli M, Baehrecke EH, Bazan NG, Bertrand MJ, Bianchi K, Blagosklonny MV, Blomgren K, Borner C, Bredesen DE, Brenner C, Campanella M, Candi E, Cecconi F, Chan FK, Chandel NS, Cheng EH, Chipuk JE, Cidlowski JA, Ciechanover A, Dawson TM, Dawson VL, De Laurenzi V, De Maria R, Debatin KM, Di Daniele N, Dixit VM, Dynlacht BD, El-Deiry WS, Fimia GM, Flavell RA, Fulda S, Garrido C, Gougeon ML, Green DR, Gronemeyer H, Hajnoczky G, Hardwick JM, Hengartner MO, Ichijo H, Joseph B, Jost PJ, Kaufmann T, Kepp O, Klionsky DJ, Knight RA, Kumar S, Lemasters JJ, Levine B, Linkermann A, Lipton SA, Lockshin RA, López-Otín C, Lugli E, Madeo F, Malorni W, Marine JC, Martin SJ, Martinou JC, Medema JP, Meier P, Melino S, Mizushima N, Moll U, Muñoz-Pinedo C, Nuñez G, Oberst A, Panaretakis T, Penninger JM, Peter ME, Piacentini M, Pinton P, Prehn JH, Puthalakath H, Rabinovich GA, Ravichandran KS, Rizzuto R, Rodrigues CM, Rubinsztein DC, Rudel T, Shi Y, Simon HU, Stockwell BR, Szabadkai G, Tait SW, Tang HL, Tavernarakis N, Tsujimoto Y, Vanden Berghe T, Vandenabeele P, Villunger A, Wagner EF, Walczak H, White E, Wood WG, Yuan J, Zakeri Z, Zhivotovsky B, Melino G, Kroemer G. Essential versus accessory aspects of cell death: recommendations of the NCCD 2015. *Cell Death Differ* 2015; **22**: 58-73 [PMID: 25236395 DOI: 10.1038/cdd.2014.137]

10 **Saeed WK**, Jun DW. Necroptosis: an emerging type of cell death in liver diseases. *World J Gastroenterol* 2014; **20**: 12526-12532 [PMID: 25253954 DOI: 10.3748/wjg.v20.i35.12526]

11 **Afonso MB**, Rodrigues PM, Carvalho T, Caridade M, Borralho P, Cortez-Pinto H, Castro RE, Rodrigues CM. Necroptosis is a key pathogenic event in human and experimental murine models of non-alcoholic steatohepatitis. *Clin Sci* (Lond) 2015; **129**: 721-739 [PMID: 26201023 DOI: 10.1042/CS20140732]

12 **Gautheron J**, Vucur M, Reisinger F, Cardenas DV, Roderburg C, Koppe C, Kreggenwinkel K, Schneider AT, Bartneck M, Neumann UP, Canbay A, Reeves HL, Luedde M, Tacke F, Trautwein C, Heikenwalder M, Luedde T. A positive feedback loop between RIP3 and JNK controls non-alcoholic steatohepatitis. *EMBO Mol Med* 2014; **6**: 1062-1074 [PMID: 24963148 DOI: 10.15252/emmm.201403856]

13 **Gautheron J**, Vucur M, Schneider AT, Severi I, Roderburg C, Roy S, Bartneck M, Schrammen P, Diaz MB, Ehling J, Gremse F, Heymann F, Koppe C, Lammers T, Kiessling F, Van Best N, Pabst O, Courtois G, Linkermann A, Krautwald S, Neumann UP, Tacke F, Trautwein C, Green DR, Longerich T, Frey N, Luedde M, Bluher M, Herzig S, Heikenwalder M, Luedde T. The necroptosis-inducing kinase RIPK3 dampens adipose tissue inflammation and glucose intolerance. *Nat Commun* 2016; **7**: 11869 [PMID: 27323669 DOI: 10.1038/ncomms11869]

14 **Afonso MB**, Rodrigues PM, Simão AL, Ofengeim D, Carvalho T, Amaral JD, Gaspar MM, Cortez-Pinto H, Castro RE, Yuan J, Rodrigues CM. Activation of necroptosis in human and experimental cholestasis. *Cell Death Dis* 2016; **7**: e2390 [PMID: 27685634 DOI: 10.1038/cddis.2016.280]

15 **Dara L**, Johnson H, Suda J, Win S, Gaarde W, Han D, Kaplowitz N. Receptor interacting protein kinase 1 mediates murine acetaminophen toxicity independent of the necrosome and not through necroptosis. *Hepatology* 2015; **62**: 1847-1857 [PMID: 26077809 DOI: 10.1002/hep.27939]

16 **Deutsch M**, Graffeo CS, Rokosh R, Pansari M, Ochi A, Levie EM, Van Heerden E, Tippens DM, Greco S, Barilla R, Tomkötter L, Zambirinis CP, Avanzi N, Gulati R, Pachter HL, Torres-Hernandez A, Eisenthal A, Daley D, Miller G. Divergent effects of RIP1 or RIP3 blockade in murine models of acute liver injury. *Cell Death Dis* 2015; **6**: e1759 [PMID: 25950489 DOI: 10.1038/cddis.2015.126]

17 **Saeed WK**, Jun DW, Jang K, Chae YJ, Lee JS, Kang HT. Does necroptosis have a crucial role in hepatic ischemia-reperfusion injury? *PLoS One* 2017; **12**: e0184752 [PMID: 28957350 DOI: 10.1371/journal.pone.0184752]

18 **Roychowdhury S**, McCullough RL, Sanz-Garcia C, Saikia P, Alkhouri N, Matloob A, Pollard KA, McMullen MR, Croniger CM, Nagy LE. Receptor interacting protein 3 protects mice from high-fat diet-induced liver injury. *Hepatology* 2016; **64**: 1518-1533 [PMID: 27301788 DOI: 10.1002/hep.28676]

19 **Newton K**, Sun X, Dixit VM. Kinase RIP3 is dispensable for normal NF-kappa Bs, signaling by the B-cell and T-cell receptors, tumor necrosis factor receptor 1, and Toll-like receptors 2 and 4. *Mol Cell Biol* 2004; **24**: 1464-1469 [PMID: 14749364]

20 **Kleiner DE**, Brunt EM, Van Natta M, Behling C, Contos MJ, Cummings OW, Ferrell LD, Liu YC, Torbenson MS, Unalp-Arida A, Yeh M, McCullough AJ, Sanyal AJ; Nonalcoholic Steatohepatitis Clinical Research Network. Design and validation of a histological scoring system for nonalcoholic fatty liver disease. *Hepatology* 2005; **41**: 1313-1321 [PMID: 15915461 DOI: 10.1002/hep.20701]

21 **Riccalton-Banks L**, Bhandari R, Fry J, Shakesheff KM. A simple method for the simultaneous isolation of stellate cells and

hepatocytes from rat liver tissue. *Mol Cell Biochem* 2003; **248**: 97-102 [PMID: 12870660]

22 **Roychowdhury S**, McMullen MR, Pisano SG, Liu X, Nagy LE. Absence of receptor interacting protein kinase 3 prevents ethanol-induced liver injury. *Hepatology* 2013; **57**: 1773-1783 [PMID: 23319235 DOI: 10.1002/hep.26200]

23 **Honarpisheh M**, Desai J, Marschner JA, Weidenbusch M, Lech M, Vielhauer V, Anders HJ, Mulay SR. Regulated necrosis-related molecule mRNA expression in humans and mice and in murine acute tissue injury and systemic autoimmunity leading to progressive organ damage, and progressive fibrosis. *Biosci Rep* 2016; **36**: [PMID: 27811014 DOI: 10.1042/bsr20160336]

P- Reviewer: Kanda T, Musumeci G **S- Editor**: Ma RY
L- Editor: Filipodia **E- Editor**: Huang Y

World Journal of Gastroenterology

Submit a Manuscript: https://www.f6publishing.com

World J Gastroenterol 2018 December 28; 24(48): 5491-5504

DOI: 10.3748/wjg.v24.i48.5491

ISSN 1007-9327 (print) ISSN 2219-2840 (online)

ORIGINAL ARTICLE

Basic Study

Near-infrared photoimmunotherapy of pancreatic cancer using an indocyanine green-labeled anti-tissue factor antibody

Winn Aung, Atsushi B Tsuji, Aya Sugyo, Hiroki Takashima, Masahiro Yasunaga, Yasuhiro Matsumura, Tatsuya Higashi

Winn Aung, Atsushi B Tsuji, Aya Sugyo, Tatsuya Higashi, Department of Molecular Imaging and Theranostics, National Institute of Radiological Sciences, National Institutes for Quantum and Radiological Science and Technology (QST-NIRS), Chiba 263-8555, Japan

Hiroki Takashima, Masahiro Yasunaga, Yasuhiro Matsumura, Division of Developmental Therapeutics, Exploratory Oncology Research and Clinical Trial Center, National Cancer Center, Chiba 277-8577, Japan

ORCID number: Winn Aung (0000-0002-0896-7158); Atsushi B Tsuji (0000-0003-2726-288X); Aya Sugyo (0000-0002-5174-4478); Hiroki Takashima (0000-0001- 6487-7344); Masahiro Yasunaga (0000-0002-5712-9847); Yasuhiro Matsumura (0000-0003-4331-8177); Tatsuya Higashi (0000-0002-8338-4737).

Author contributions: Aung W designed the research, performed the majority of experiments and analyzed the data; Takashima H, Yasunaga M and Matsumura Y provided the anti-TF antibody; Sugyo A participated in the animal experiments; Tsuji AB and Higashi T coordinated the research and helped for the manuscript preparation; Aung W wrote the manuscript; All authors revised and endorsed the final draft.

Supported by a Grant-in-Aid for Scientific Research (C) from the Ministry of Education, Culture, Sports, Science, and Technology, Japan, No. 17K10460 (to Aung W).

Institutional review board statement: This study was reviewed and approved by the Institutional review board of National Institute of Radiological Sciences. No patients and patient derived samples were involved in this study.

Institutional animal care and use committee statement: All procedures involving animals were reviewed and approved by the Institutional Animal Care and Use Committee of National Institute of Radiological Sciences. (Protocol No: 13-1022-6).

Conflict-of-interest statement: The authors declare no potential conflicts of interest relevant to this article.

Data sharing statement: All relevant data were presented in the manuscript. Further information is available from the corresponding author at winn.aung@qst.go.jp.

ARRIVE guidelines statement: ARRIVE Guidelines have been adopted and authors uploaded the PDF version of the completed ARRIVE checklist to the system.

Manuscript source: Unsolicited manuscript

Corresponding author: Winn Aung, MBBS, PhD, Senior Researcher, Department of Molecular Imaging and Theranostics, National Institute of Radiological Sciences, National Institutes for Quantum and Radiological Science and Technology, 4-9-1 Anagawa, Inage-ku, Chiba 263-8555, Japan. winn.aung@qst.go.jp
Telephone: +81-43-3823706
Fax: +81-43-2060818

Received: October 2, 2018
Peer-review started: October 2, 2018
First decision: November 1, 2018
Revised: November 7, 2018
Accepted: November 16, 2018
Article in press: November 16, 2018

Published online: December 28, 2018

Abstract

AIM

To investigate near-infrared photoimmunotherapeutic effect mediated by an anti-tissue factor (TF) antibody conjugated to indocyanine green (ICG) in a pancreatic cancer model.

METHODS

Near-infrared photoimmunotherapy (NIR-PIT) is a highly selective tumor treatment that utilizes an antibody-photosensitizer conjugate administration, followed by NIR light exposure. Anti-TF antibody 1849-ICG conjugate was synthesized by labeling of rat IgG_{2b} anti-TF monoclonal antibody 1849 (anti-TF 1849) to a NIR photosensitizer, ICG. The expression levels of TF in two human pancreatic cancer cell lines were examined by western blotting. Specific binding of the 1849-ICG to TF-expressing BxPC-3 cells was examined by fluorescence microscopy. NIR-PIT-induced cell death was determined by cell viability imaging assay. *In vivo* longitudinal fluorescence imaging was used to explore the accumulation of 1849-ICG conjugate in xenograft tumors. To examine the effect of NIR-PIT, tumor-bearing mice were separated into 5 groups: (1) 100 μg of 1849-ICG i.v. administration followed by NIR light exposure (50 J/cm^2) on two consecutive days (Days 1 and 2); (2) NIR light exposure (50 J/cm^2) only on two consecutive days (Days 1 and 2); (3) 100 μg of 1849-ICG i.v. administration; (4) 100 μg of unlabeled anti-TF 1849 i.v. administration; and (5) the untreated control. Semiweekly tumor volume measurements, accompanied with histological and immunohistochemical (IHC) analyses of tumors, were performed 3 d after the 2nd irradiation with NIR light to monitor the effect of treatments.

RESULTS

High TF expression in BxPC-3 cells was observed *via* western blot analysis, concordant with the observed preferential binding with intracellular localization of 1849-ICG *via* fluorescence microscopy. NIR-PIT-induced cell death was observed by performing cell viability imaging assay. In contrast to the other test groups, tumor growth was significantly inhibited by NIR-PIT with a statistically significant difference in relative tumor volumes for 27 d after the treatment start date [2.83 ± 0.38 (NIR-PIT) *vs* 5.42 ± 1.61 (Untreated), *vs* 4.90 ± 0.87 (NIR), *vs* 4.28 ± 1.87 (1849-ICG), *vs* 4.35 ± 1.42 (anti-TF 1849), at Day 27, $P < 0.05$]. Tumors that received NIR-PIT showed evidence of necrotic cell death-associated features upon hematoxylin-eosin staining accompanied by a decrease in Ki-67-positive cells (a cell proliferation marker) by IHC examination.

CONCLUSION

The TF-targeted NIR-PIT with the 1849-ICG conjugate can potentially open a new platform for treatment of TF-expressing pancreatic cancer.

Key words: Pancreatic cancer; Anti-tissue factor antibody; Indocyanine green; Photoimmunotherapy; Near-infrared

Core tip: We examined whether anti-tissue factor (TF) antibody 1849-indocyanine green (ICG) conjugate (1849-ICG) induced the photoimmunotherapeutic effect in a pancreatic cancer xenograft. There was no report about employing 1849-ICG conjugate which selectively binds the target antigen TF for near-infrared photoimmunotherapy (NIR-PIT) of tumor, though some studies have suggested the usefulness of anti-TF 1849 in cancer imaging and therapy. Our study proposes for the first time that 1849-ICG conjugate is a desirable candidate for new treatment modality NIR-PIT of pancreatic cancer after evaluating its cytotoxic and antitumor effects *via in vitro* and *in vivo* studies in mouse model of pancreatic cancer.

Aung W, Tsuji AB, Sugyo A, Takashima H, Yasunaga M, Matsumura Y, Higashi T. Near-infrared photoimmunotherapy of pancreatic cancer using an indocyanine green-labeled anti-tissue factor antibody. *World J Gastroenterol* 2018; 24(48): 5491-5504
URL: https://www.wjgnet.com/1007-9327/full/v24/i48/5491.htm
DOI: https://dx.doi.org/10.3748/wjg.v24.i48.5491

INTRODUCTION

Pancreatic cancer is one of the most devastating health issues that has caused 411600 deaths, globally, in 2015 for all ages and both sexes[1]. In 2018, in the United States, it is the fourth and ninth leading cancer type for estimated cancer death and new cancer case, respectively[2]. Pancreatic cancer has the lowest 5-year survival rate of 8%, for all stages combined[2]. The major reasons of poor prognosis are late diagnosis and lack of effective therapy. Therefore, for achieving early diagnosis and new treatment options, the efficacious antibody based molecular-targeting therapeutic approaches are currently gaining attention in preclinical and clinical research. Conventional immunotherapy itself as well as using certain antibodies, antibody-drug conjugate (ADC) therapy, radioimmunotherapy (RIT), and photoimmunotherapy (PIT) are being investigated substantially. Meanwhile, the effort to explore a novel target molecule and a suitable theranostic agent is still imperative.

Tissue factor (TF) is a 47-kDa single chain transmembrane glycoprotein belonging to the cytokine receptor family group 2, composed of 263 amino acid residues. TF mediates a variety of physiologically- and pathophysiologically-relevant functions and its overexpression is linked to thrombogenicity, tumor angiogenesis, cell signaling, tumor cell proliferation, and metastasis[3-5]. Various malignant entities including pancreatic cancer has shown the expression of TF[6,7]. Moreover, in contrast

to normal pancreas with low TF expression, a high TF expression in pancreatic cancer correlates with tumor grade, extent, metastasis and invasion[6,8,9]. Haas and co-workers have previously analyzed the expression of TF in eight human pancreatic cancer cell lines including BxPC-3 and reported presence of TF expression, at RNA and protein level. Corresponding to the TF expression in cell lines, they also demonstrated that most of the tissue specimens of pancreatic cancer patients have highly variable TF expression, as determined by immunofluorescence staining[10]. Previously, we suggested that TF may be a promising target for cancer diagnostic imaging or therapy, developed several anti-TF antibodies, and showed that a rat IgG_{2b} anti-TF monoclonal antibody 1849 has high affinity against TF[11,12]. We reported the development of Alexa Flour-647-labeled anti-TF antibody 1849 probe for fluorescence imaging in a TF-overexpressing human pancreatic cancer xenograft model[11] and an ^{111}In-labeled anti-TF antibody 1849 probe for immuno- single-photon emission computed tomography (SPECT) imaging in glioma model[13] and pancreatic cancer models (manuscript under preparation). Cai *et al*[14,15] have successfully developed a radiotracer for immuno-PET (positron emission computed tomography) imaging of *in vivo* TF expression in pancreatic cancer and breast cancer models[16]. Wang *et al*[17] labeled anti-TF antibody with ^{90}Y and reported its radiotherapeutic effect on human xenograft NSCLC tumors in nude mice. These studies that considered TF as a molecular target encourage us to use anti-TF antibody 1849 in near-infrared PIT (NIR-PIT).

NIR-PIT is a modified version of the conventional photodynamic therapy (PDT) or photothermal therapy (PTT). NIR-PIT exerts a target cell specific cancer treatment that enables highly selective cell death after systemic administration of a photosensitizer-conjugated antibody against tumor-associated antigens, and accompanying exposure with NIR light. The light of a specific wavelength activates the relevant photosensitizer, and this interaction induces a cytotoxic reaction. An antibody which binds a cancer specific antigen expressing on the cellular membrane, is desirable for selective targeting of cancer cells. Over recent decades, a wide variety of available monoclonal antibodies that bind to the various molecular targets, have been considered and used with NIR-PIT in preclinical studies by several research groups. Among them, NIR-PIT using anti-epidermal growth factor receptor (EGFR) antibody (cetuximab) conjugated to a photosensitizer, phthalocyanine dye IRDye® 700DX NHS Ester (IR700DX), has been widely studied and is currently in its Phase Ⅰ/Ⅱ clinical study (study of RM-1929 and PIT in patients with recurrent head and neck cancer: NCT02422979).

In the present study, we conjugate an anti-TF monoclonal antibody 1849 with a photosensitizer, indocyanine green (ICG), and demonstrate the potential of the generated 1849-ICG conjugate as a desirable candidate for NIR-PIT of pancreatic cancer, after evaluating its cytotoxic and antitumor effects *via in vitro* and *in vivo* studies in a mouse model of pancreatic cancer.

MATERIALS AND METHODS

Cell lines

The human pancreatic cancer cell lines, BxPC-3 and SUIT-2, were purchased from the ATCC (Manassas, VA, United States). BxPC-3 cells were maintained in RPMI 1640 medium (Sigma-Aldrich, St. Louis, MO, United States) supplemented with 10% fetal bovine serum (FBS) (Nichirei Biosciences, Tokyo, Japan), 100 U/mL penicillin-G sodium, and 100 mg/mL streptomycin sulfate (Invitrogen, Carlsbad, CA, United States) at 37 ℃ under a humidified atmosphere containing 5% CO_2. SUIT-2 cells were maintained in high glucose Dulbecco's modified Eagle's medium (DMEM) (Wako, Osaka, Japan) supplemented with 10% FBS, 100 U/mL penicillin, and 100 μg/mL streptomycin.

Western blot analysis

Western blotting was performed to analyze TF expression in cultured cells. Whole-cell lysates were prepared using radioimmunoprecipitation assay buffer (Wako Pure Chemical Industries, Osaka, Japan) supplemented with a protease inhibitor cocktail (Sigma-Aldrich). Total protein concentration was measured using a NanoDrop One spectrophotometer (Thermo Fisher Scientific, Wilmington, DE, United States). Protein samples (35 μg) were separated on a 4%-20% polyacrylamide gel (ATTO Corporation, Tokyo, Japan) and transferred on to Immobilon-P membrane (Millipore, Billerica, MA, United States). As primary antibodies, anti-TF 1849 (generated by us) and a commercially available goat anti-human actin (C-11) antibody (Santa Cruz Biotechnology, Santa Cruz, CA, United States), were used. A horseradish peroxidase (HRP)-linked anti-rabbit IgG antibody and anti-rat IgG antibody (GE Healthcare, Little Chalfont, United Kingdom) were used as the secondary antibodies. Immunoreactive bands were visualized using the Enhanced Chemiluminescence Plus Western blotting detection system (GE Healthcare).

Photosensitizer labeling of anti TF-antibody

The rat IgG_{2b} anti-TF monoclonal antibody 1849 which reacts with human TF antigen was developed as previously described[12]. An ICG Labeling kit-NH2 was purchased from Dojindo Molecular Technologies, Inc. (Rockville, MD, United States). Labeling of antibody with ICG was performed according to the manufacturer's manual. A component of this kit, NH_2-reactive ICG, has a succinimidyl ester group and can easily form a covalent bond with an amino group of the antibody. Briefly, NH_2-reactive dyes were added to anti-TF antibody (130 μg) solution on the membrane of a filtration tube and incubated at 37 ℃ for 10 min. The buffer solution was then added to the mixture and centrifuged. The conjugate was recovered by pipetting with phosphate-buffered saline (PBS). The concentration of the conjugates was determined

by Bradford protein assay using a BioRad microplate reader (Bio-Rad Laboratrories, Inc., Hercules, CA, United States). The absorbance of ICG was measured at 800 nm with the Synergy HT multi-mode microplate reader (BioTek Instrument, Inc., Winooski, VT, United States), and the number of fluorophore molecules conjugated to each antibody was calculated. The ratio of ICG to antibody was 0.4.

Fluorescence microscopy studies

Fluorescence microscopy was employed to observe the localization of 1849-ICG and the cytotoxic effect of PIT. BxPC-3 or SUIT-2 cells were plated on a Lab-Tek Chamber slide (Thermo Fisher Scientific, Frederick, MD, United States) and incubated for 18 h. Subsequently, culture media were discarded, and the cells were immediately stained after fixation with cold methanol for 5 min at -20 ℃. Nonspecific binding of the antibody was blocked by incubating with Block-Ace reagent (Dainippon Pharmaceutical, Osaka, Japan) solution containing 10% goat serum for 30 min at room temperature. Subsequently, the cells were incubated with the 1849-ICG diluted (1:100) in antibody diluent buffer (Dako, Glostrup, Denmark) or without antibody, at 4 ℃. After 18 h, cells were washed with Tris-buffered saline (TBS), and the nuclei were stained with 4,6-diamidino-2-phenylindole Fluoromount-G (SourthenBiotech, Birmingham, AL, United States). The cells were visualized under a Keyence BZ-X700 microscope (Keyence Japan Co, Ltd, Osaka, Japan) equipped with the following filter sets: excitation wavelength 675 to 750 nm, emission wavelength 760 to 860 nm and dichroic mirror wavelength 760 nm for ICG. To compare BxPC-3 and SUIT-2 cells, images were acquired using the same settings of exposure time and black balance. Phase-contrast images were also acquired.

Cell viability imaging assay after PIT

BxPC-3 cells (2×10^5/well) were seeded in a chamber slide. After 6 h, the culture medium was changed to fresh medium containing 1849-ICG (2.5 μg/mL medium) or not. After an overnight incubation, the culture medium was replaced with phenol red free medium and the cells were subsequently irradiated with NIR light from an Infrared Diode Laser system (Laser Create Co., Tokyo, Japan) at a wavelength of 808 ± 3 nm and a power density of 50 J/cm^2 (1 W/cm^2 for 50 s). The irradiation dose was measured with a thermal laser power sensor and an optical power meter, Starlite (OPHIR Japan, Saitama, Japan). Two hours later, two color staining assay using ReadyProbes™ Cell Viability Imaging kit (Thermo Fisher Scientific) was performed. As per manufacturer's instruction, nuclei of all viable cells were stained with NucBlue® Live reagent, while only the nuclei of dead cells were stained with NucGreen® Dead reagent. The cells were imaged under a Keyence BZ-X700 microscope (Keyence Japan Co, Ltd) equipped with appropriate filter sets for DAPI (excitation/emission maxima: 360/460 nm), GFP (green) filter set (excitation/emission maxima: 470/525 nm) and ICG (excitation/emission maxima: 710/810 nm).

Animal and tumor model

A single-cell suspension of 5×10^6 BxPC-3 cells in 100 μL RPMI medium was mixed with BD Matrigel matrix (BD Biosciences, Bedford, MA, United States) and subcutaneously inoculated into both thighs of 7-wk-old male, BALB/cA Jcl-nu/nu nude mice (CLEA, Shizuoka, Japan) for *in vivo* imaging and NIR-PIT studies. During the experimental procedure, mice were anesthetized with isoflurane. All animal experiments were conducted in compliance with the guidelines for animal experimentation approved by the Animal Care and Use Committee of our institution, National Institute of Radiological Sciences.

In vivo NIR fluorescence imaging

Tumor-bearing mice were injected intravenously with 1849-ICG (100 μg) *via* a tail vein. The mice were anesthetized by inhalation of 2.5% isoflurane, and spectral fluorescence images at dorsal position were obtained using the Maestro *In-vivo* Imaging system (CRi, Woburn, MA, United States) with the ICG filter sets (excitation, 700–770 nm and emission, 790 nm long pass) at pre-injection, followed by various time points post-injection (24, 48, 72, and 144 h). The tunable filter was automatically stepped up in 10-nm increments from 780 to 950 nm for the ICG filter setting, while the camera sequentially captured images at each wavelength interval. With the commercial Maestro software (CRi), subtractions of background and baseline intensities, followed by un-mixing of spectral fluorescence images were performed a step by step. By setting the auto calculate threshold, the region of interest on entire tumors of the ICG spectrum image were determined and the tumor fluorescence signal intensities (FI) were measured. The constant exposure time was set to compare the FI of the serial images. Overlaid image of ICG spectrum image and white light image was acquired by using Photoshop software (Adobe, San Jose, CA, United States).

In vivo PIT of tumor

When the subcutaneous BxPC-3 tumors in mice reached approximately 10 mm at the longest diameter, the tumor-bearing mice were randomly assigned to one of the 5 groups (n = 6 for each group) for the treatment study conducted as per the shown scheme (Figure 1). Mice were initially injected 1849-ICG (100 μg) intravenously. On day 1 and day 2, the tumor was irradiated with NIR light from an Infrared Diode Laser system (Laser Create Co.) at a wavelength of 808 ± 3 nm and a power density of 50 J/cm^2 (1 W/cm^2 for 50 s), as measured with a StarLite Laser Power meter (OPHIR Japan Ltd.). During irradiation, the surrounding areas of tumors were shielded from light using aluminum foil. Briefly, group (1) received 1849-ICG i.v. administration followed by two doses of irradiation on two consecutive days, group (2)

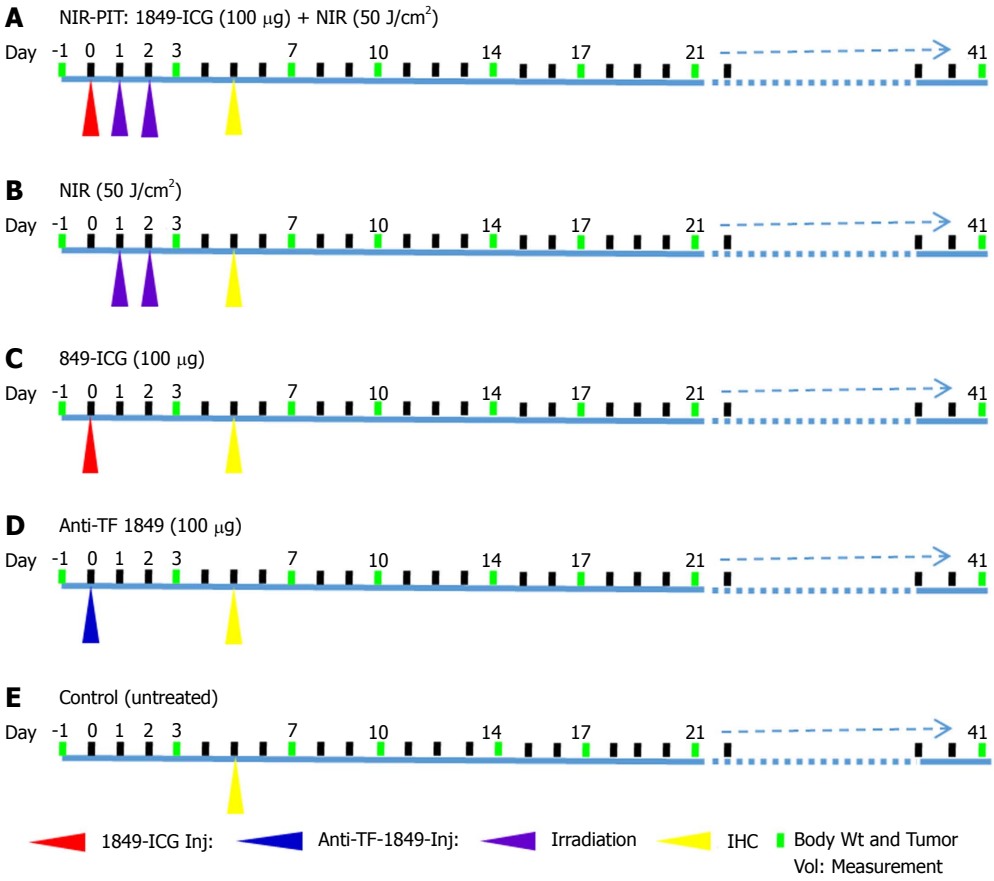

Figure 1 Experimental treatment scheme. A: Near-infrared photoimmunotherapy (NIR-PIT); B: NIR light alone; C: Indocyanine green-labeled antibody 1849 conjugate alone; D: Anti-tissue factor antibody 1849 alone; E: Control (untreated). Anti-TF 1849: Anti-tissue factor antibody 1849; 1849-ICG: Indocyanine green-labeled anti-tissue factor antibody 1849; NIR: Near-infrared; NIR-PIT: Near-infrared photoimmunotherapy.

received two doses of irradiation only on two consecutive days, group (3) received 1849-ICG i.v administration only, group (4) received unlabeled anti-TF 1849 i.v. administration, and group (5) received no treatment. To determine the tumor response, tumors of mice (n = 12 for each group except n = 11 in anti-TF 1849 group) were measured twice a week throughout the experiment using calipers, and volumes were approximated using the formula: volume (mm^3) = [length (mm)] × [width (mm)]^2 × 0.5. Relative tumor volume was calculated as the volume on the indicated day divided by the starting volume on the day prior to the treatment. Body weight of mice was also measured twice a week; general health conditions and local skin condition at the irradiated area of mice were monitored daily.

Histological and immunohistochemical analysis

At 72 h after 2nd irradiation of NIR-PIT, 2 mice from each group (n = 2) were euthanized by cervical dislocation under anesthesia (isoflurane). Tumors were excised from these mice, fixed in 4% paraformaldehyde, and embedded in paraffin. To observe the histologic changes, paraffin-embedded tissues were cut into 5-μm slice, serial sections were fixed on glass slides and stained with hematoxylin and eosin (H&E) staining. To perform immunohistochemical (IHC) analysis, tissue sections were rehydrated, and subjected to antigen retrieval. The sections were stained for Ki-67, a cell proliferation marker[18], using an anti-human Ki-67 polyclonal antibody (Dako Denmark, Glostrup, Denmark), as previously described[19]. Slides were analyzed using the Olympus BX43 microscope system (Olympus, Tokyo, Japan).

Statistical analysis

All results were expressed as mean ± SD. Significant differences between groups were determined by Student's t-test (Excel, Microsoft, Redmond, WA, United States). Two-tailed unpaired t-test was used for comparisons of relative tumor volume. The probability of survival based on relative tumor volume (3.1-fold increase of individual tumor volume from the initial volume) was estimated in each group with a Kaplan-Meier survival curve analysis, and the results were compared with use of the Gehan-Breslow-Wilcoxon test. P-values < 0.05 were considered significant.

RESULTS

Expression of TF in human pancreatic cancer cell lines

Expression of human TF protein in BxPC-3 and SUIT-2 pancreatic cancer cells was determined through western blot analysis and fluorescence microscopy. In western

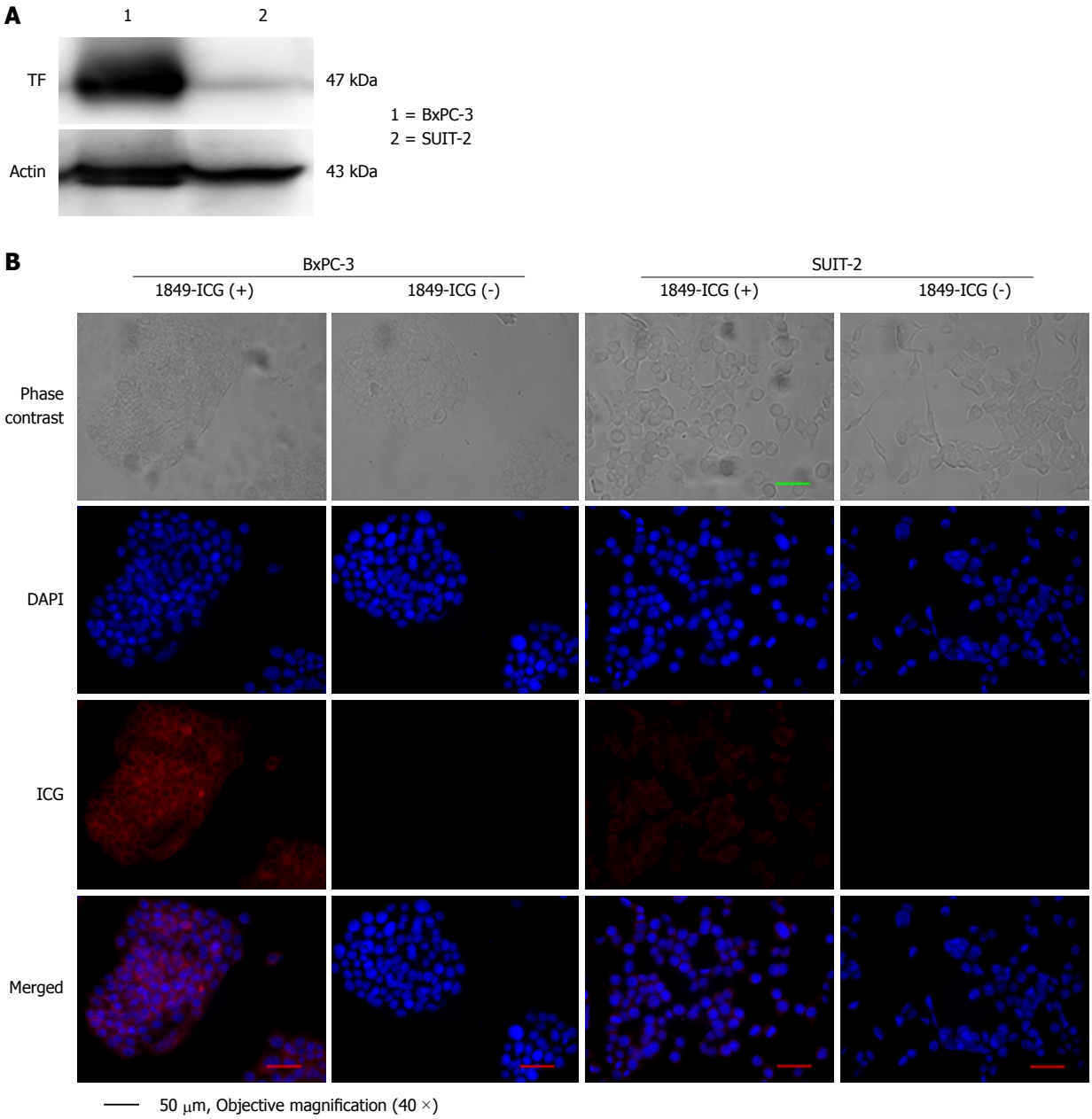

Figure 2 Tissue factor expression in human pancreatic cancer cell lines. A: Tissue factor (TF) expression in the cell lines BxPC-3 (lane 1) and SUIT-2 (lane 2) was examined by western blotting; B: Both cell lines were incubated with or without indocyanine green-labeled anti-TF antibody 1849 (1849-ICG) for 18 h and examined under a fluorescent microscope. Intracellular localization of intense fluorescent signals indicated substantial binding and internalization of 1849-ICG within BxPC-3, but very rarely in SUIT-2 cells (Scale bar = 50 μm, 40 × objective magnification). DAPI: 4,6-diamidino-2-phenylindole; 1849-ICG: Indocyanine green-labeled anti-tissue factor antibody 1849; TF: Tissue factor.

blot analysis of cell lysate, TF expression was found to be much higher in BxPC-3 cells than in SUIT-2 cells (Figure 2A). Moreover, fluorescence microscopy after overnight incubation with 1849-ICG revealed that the preferential binding with intracellular localization of 1849-ICG was higher in BxPC-3 cells than SUIT-2 cells (Figure 2B). Taken together, our data indicated the specific binding of the 1849-ICG conjugate antibody to the highly-expressed TF in BxPC-3 pancreatic cancer cells.

Phototoxic cell death in response to TF-ICG mediated PIT

PIT induced rapid cell death, and numerous dead cells stained with NucGreen® Dead reagent were visualized (Figure 3). Meanwhile, there was no significant cytotoxicity associated with exposure of 1849-ICG or NIR light exposure alone, in the absence of each other (Figure 3).

In vivo tumor visualization by NIR fluorescence imaging

Mice with subcutaneous BxPC-3 tumors were intravenously injected with 1849-ICG, followed by NIR fluorescence imaging at the indicated time points (24, 48, 72, 96 and 144 h after injection). In the untreated group, tumors showed highest FI 24 h after injection and fairly retained the FI until 144 h, our last observation time

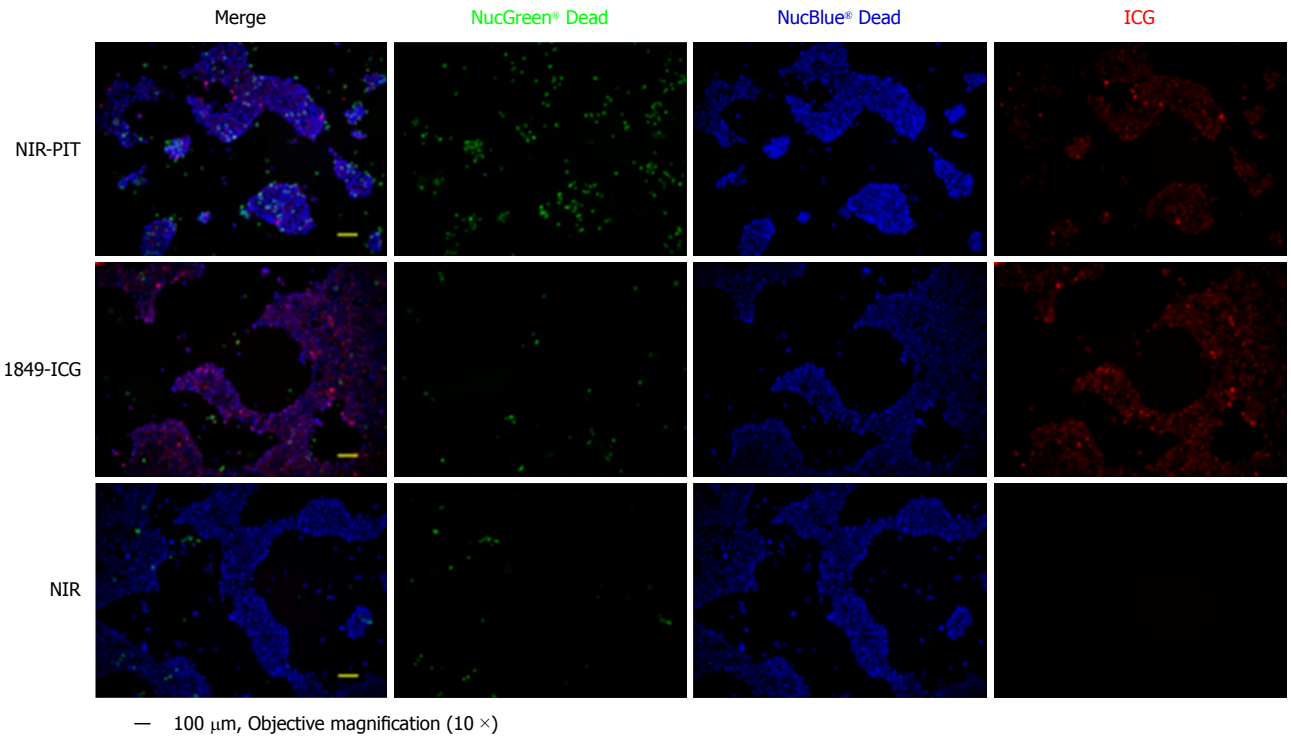

Figure 3 Phototoxic cell death after photoimmunotherapy. Two hours after photoimmunotherapy (PIT) treatment, the cells were stained using the Cell viability imaging kit. The nuclei of dead cells were stained with NucGreen® Dead reagent (green), while the viable cell nuclei were stained with NucBlue® Live reagent (blue). Near-infrared (NIR)-PIT induced rapid cell death and numerous dead cells were markedly visible. There was no significant cytotoxicity associated with exposure to indocyanine green-labeled anti-tissue factor antibody 1849 or NIR light only. (Scale bar = 100 μm, 10 × objective magnification). 1849-ICG: Indocyanine green-labeled anti-tissue factor antibody 1849; NIR: Near-infrared; PIT: Photoimmunotherapy.

point, even though FI of tumor decreased gradually over time in longitudinal imaging (Figure 4A). In contrast, the FI of tumors in the PIT group decreased immediately after receiving the irradiation but it increased again in 24 h (Figure 4B).

PIT effects on the tumor growth in nude mice

Tumor growth was significantly inhibited by NIR-PIT with statistically significant differences in the relative tumor volumes for 27 d after the treatment onset when compared to the other groups (no treatment, 1849-ICG only, anti-TF 1849 only and NIR irradiation only) ($P < 0.05$) (Figure 5A). No significant therapeutic effect was observed in the control groups. A significantly prolonged survival was observed in the NIR-PIT group ($P < 0.05$ *vs* the other groups) (Figure 5B). No body weight change (Figure 5C), skin damage, or abnormal general condition were observed in these mice.

Evaluation of the PIT effects with histological and IHC analysis

According to our histological examination and some previous studies, the cells in BxPC-3 tumors have been observed to form a nest pattern, surrounded by stromal tissues in BxPC-3 tumors[20]. However, H&E-stained sections of tumors treated with PIT revealed necrotic death-associated features, such as loss of tumor cells and the nest pattern, scattering of damaged and hypertrophic tumor cells, and marked interstitial fibrosis (Figure 6). On the other hand, no obvious damage was observed in the tumors of the control groups: receiving only 1849-ICG but no NIR irradiation, receiving only NIR irradiation, receiving only unconjugated anti-TF 1849, and receiving no treatment (Figure 6). As per the IHC examination, the numbers of Ki-67-positive tumor cells, indicating active proliferation, decreased noticeably in the tumor tissues of mice treated with PIT, when compared with the other groups (Figure 7).

DISCUSSION

For cancer therapy, conventional PDT has been suggested as one of the treatment modalities[21]. In PDT, tumor targeting of photosensitizers depends primarily upon the passive enhanced permeability and retention (EPR) effect[22]. However, EPR-based tumor targeting alone faces intrinsic limitations in its specificity and efficacy[23]. To overcome this ambiguity, active targeting strategies using special molecules (antibodies, ligands, *etc.*), which bind to tumor antigens specifically, have been exploited and are preferred as a drug delivery system. Recently, Mitsunaga *et al*[24] and others recommended cancer cell-selective NIR-PIT to overcome the limitation of conventional PDT. Their studies revealed that NIR-PIT induces reliable cytotoxic and antitumor effects in several tumors and derived cell lines[25-32]. Researchers labeled the different types of tumor-specific antibodies such as anti-EGFR mAb[25,26], anti-CD20 mAb[27], anti-

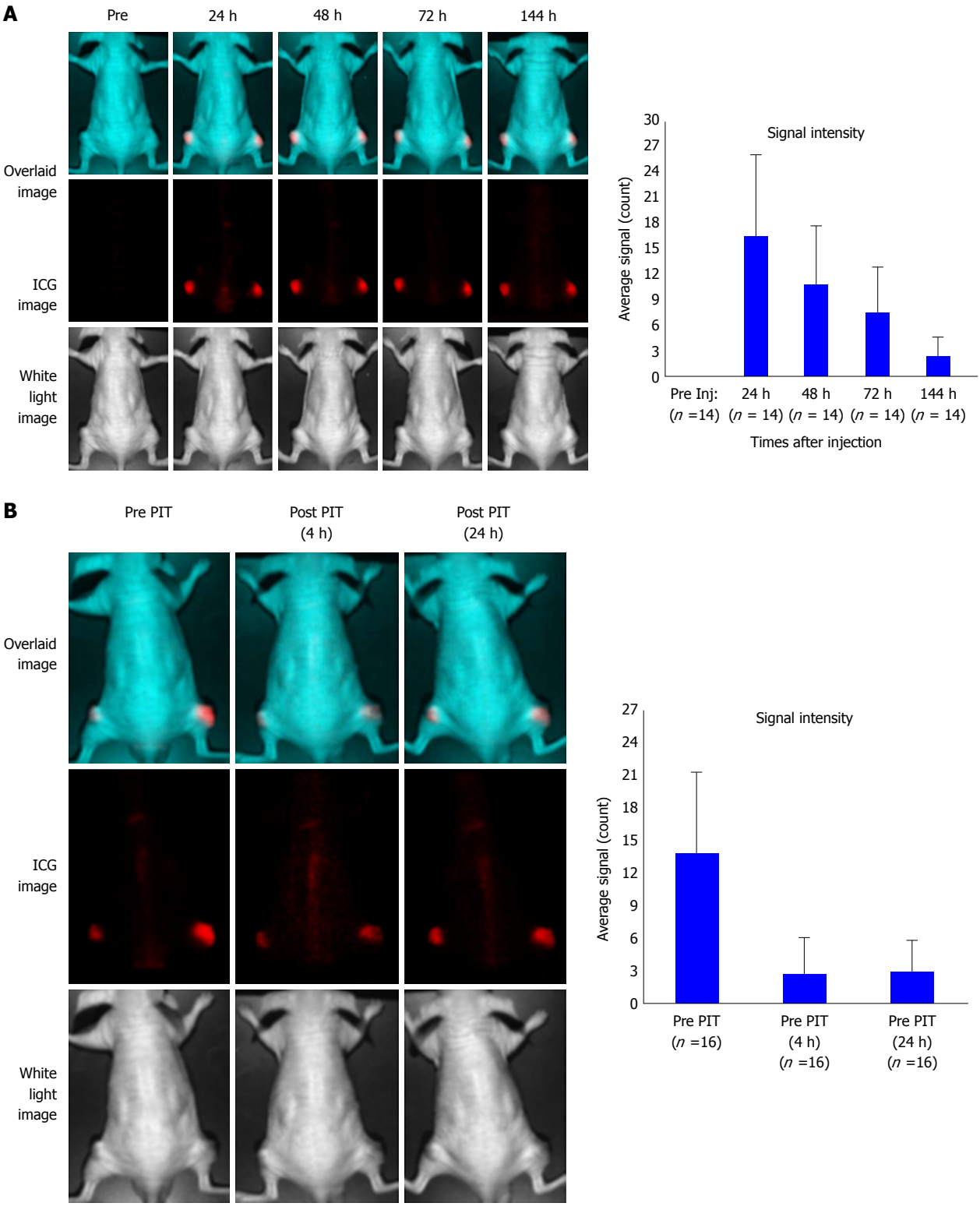

Figure 4 Serial near-infrared fluorescence imaging of a representative mouse bearing xenografted tumor. A: Imaging was performed pre- and post- injection of indocyanine green (ICG)-labeled anti-tissue factor antibody 1849 (1849-ICG) at indicated time points (24, 48, 72, and 144 h). The upper panel shows the overlaid image of the ICG spectrum image (middle panel) and the white light image (lower panel). Fluorescent signal intensity of BxPC-3 tumors is higher than that of the whole body. Adjoining bar graph shows the ICG specific signal intensity of the tumors over time with the peak intensity at 24 h after the injection. Data are presented as mean ± SD (n = 14); B: Images of tumor bearing mice before photoimmunotherapy (PIT) (left); 2 h (center) and 24 h (right) after PIT. ICG signal intensity in the tumor decreased initially after PIT and was restored in 24 h suggesting re-accumulation of 1849-ICG due to circulating 1849-ICG. Bar graph shows the ICG signal intensity of tumor before and after near-infrared-PIT. Data are presented as mean ± SD (n = 16). 1849-ICG: Indocyanine green-labeled anti-tissue factor antibody 1849; NIR: Near-infrared; PIT: Photoimmunotherapy.

CD44 mAb[33], anti-PD-L1 mAb[34], anti-PSMA mAb[30], anti-CD25 mAb[35], and anti-CEA mAb[31,32], with photosensitizer IR700DX, and used them as PIT agents. Although PIT is a promising therapeutic option, very few

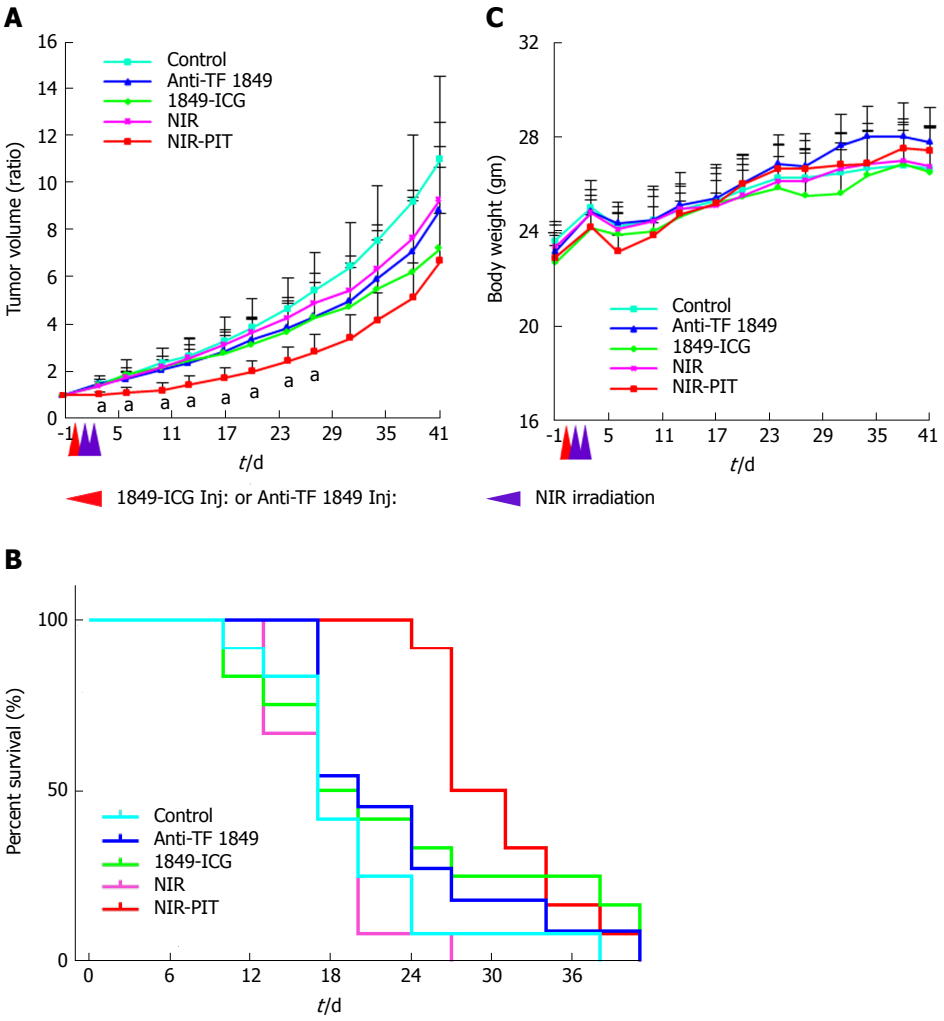

Figure 5 Photoimmunotherapeutic effects on BxPC-3 xenografts and body weight change in mice. A: Tumor volume change is expressed as the ratio of the volume on the indicated day and volume at 1 d before the start of near-infrared photoimmunotherapy (NIR-PIT). Tumors treated by NIR-PIT (red) showed significantly reduced growth rates compared to those, that received no treatment (light blue), NIR light exposure alone (pink), indocyanine green-labeled anti-tissue factor (TF) antibody 1849 (1849-ICG) alone (green) and anti-TF antibody 1849 (anti-TF 1849) alone (blue), for 27 d after the treatment start date. Values shown represent mean ± SD, $^{a}P < 0.05$, NIR-PIT vs other groups (n = 12 for each group except n = 11 in anti-TF 1849 group); B: Significantly prolonged survival was observed in NIT-PIT group vs other groups, $^{b}P < 0.05$, by Gehan-Breslow-Wilcoxon test (n = 12 for each group except n = 11 in anti-TF 1849 group); C: The average body weight did not differ significantly among all 5 groups of mice. Red arrowhead indicates the day of administration of 1849-ICG or Anti-TF 1849 and purple arrowheads indicate the day of NIR exposure. Anti-TF 1849: Anti-tissue factor antibody 1849; 1849-ICG: Indocyanine green-labeled anti-tissue factor antibody 1849; NIR: Near-infrared; PIT: Photoimmunotherapy.

PIT agents have been developed and examined. Therefore, there is a need to develop more PIT agents for treating various cancer patients.

High TF expression is commonly observed in a variety of solid tumors including pancreatic cancer and is associated with poor prognosis of pancreatic ductal adenocarcinoma[36]. Previously, we developed the anti-TF 1849, which has high affinity against TF, and succeeded to visualize TF-expressing tumors noninvasively, in an orthotopic glioma mouse model[13] and pancreatic xenograft tumor models (manuscript under preparation) by utilizing the ^{111}In-labeled anti-TF 1849. In the present study, we propose that TF is an attractive molecular target, and evaluate the photoimmunotherapeutic effect mediated by anti-TF 1849 labeled with a photosensitizing fluorophore ICG that is activated and cytotoxic upon irradiation with NIR light.

Our western blot analysis demonstrated the higher expression of TF in BxPC-3 pancreatic cancer cells compared to the SUIT-2 cells (Figure 2A). Other researchers have also reported the expression of TF in certain human pancreatic cancer cell lines[10]. These results encouraged us to use BxPC-3 as a representative TF-expressing pancreatic cancer model. Moreover, our results from *in vitro* and *in vivo* fluorescence imaging after overnight incubation of cells with 1849-ICG (Figure 2B) and tumor-bearing mice after 1849-ICG injection, respectively (Figure 4A), showed a strong ICG fluorescence signal in BxPC-3 cells and tumors; indicating the significantly increased accumulation of 1849-ICG in these cells and tumors. Therefore, we hypothesized that our pancreatic cancer xenograft expressed elevated levels of TF and would be bound specifically with 1849-ICG. Accumulation of 1849-ICG in tumors with fluorescence

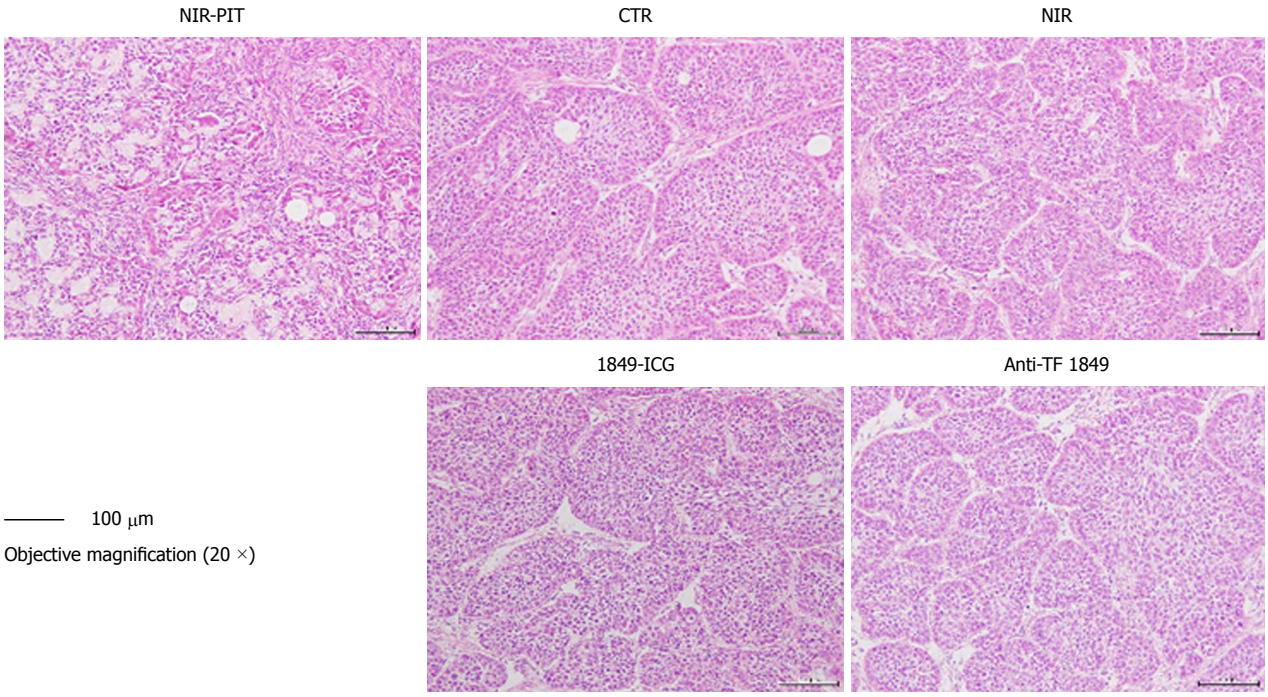

Figure 6 Histological examination of effects of near-infrared photoimmunotherapy 72 h after 2nd exposure to near-infrared light. Tumors were resected and stained with hematoxylin and eosin. After near-infrared photoimmunotherapy (NIR-PIT), tumors showed necrotic death-associated features including loss of tumor cells and cells nest pattern, scattering of damaged and hypertrophic tumor cells, and abundant fibrosis. No obvious damage was detected in the tumors of other control groups; receiving no treatment, NIR light alone, indocyanine green-labeled anti-tissue factor (TF) antibody 1849 (1849-ICG) alone and anti-TF antibody 1849 (anti-TF 1849) alone. Photos of tumor section were taken under 20 × objective magnification (scale bar = 100 μm). Anti-TF 1849: Anti-tissue factor antibody 1849; CTR: Control; 1849-ICG: Indocyanine green-labeled anti-tissue factor antibody 1849; NIR: Near-infrared; PIT: Photoimmunotherapy.

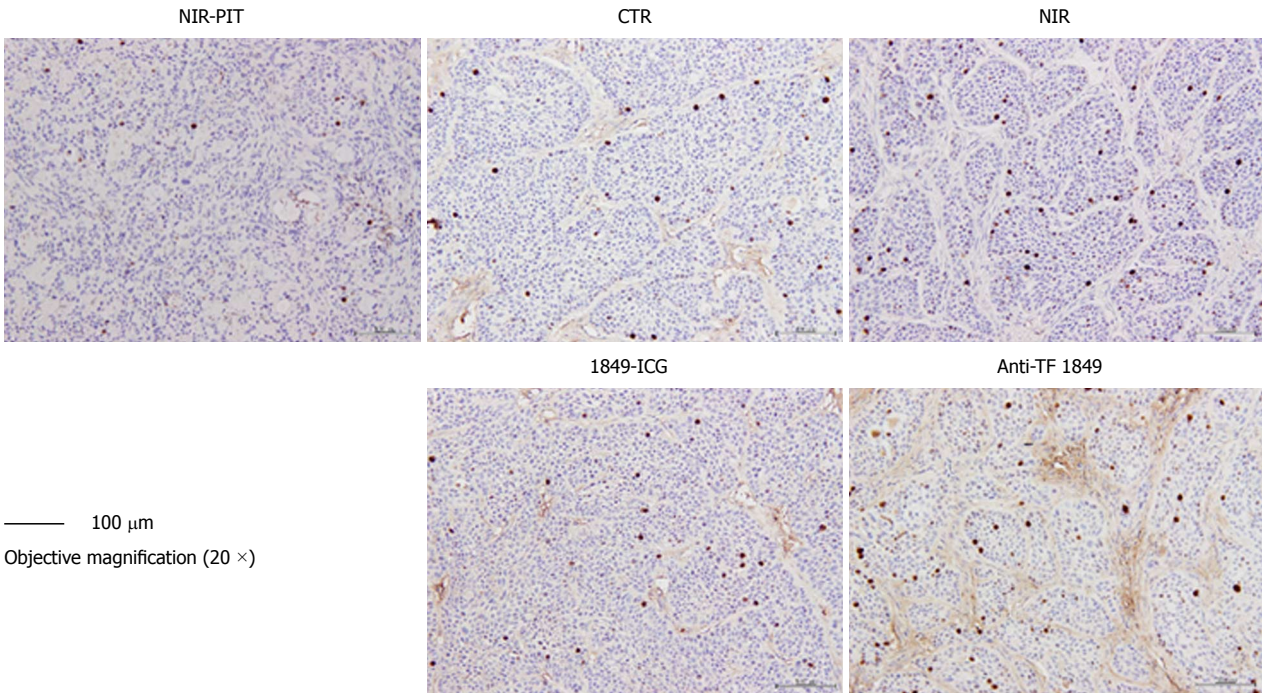

Figure 7 Ki-67 immunostaining of tumor sections 72 h after 2nd exposure to near-infrared light in near-infrared photoimmunotherapy. A marked reduction in Ki-67-positive cell numbers was observed in tumors treated with near-infrared photoimmunotherapy, compared with those of other control groups. Tumor section photos were taken under 20 × objective magnification (scale bar = 100 μm). Anti-TF 1849: Anti-tissue factor antibody 1849; CTR: Control; 1849-ICG: Indocyanine green-labeled anti-tissue factor antibody 1849; NIR: Near-infrared; PIT: Photoimmunotherapy.

image was serially quantified and was found to peak 24 h after injection. Following NIR-PIT, the ICG signal intensity in the tumor decreased initially, probably due to partial photobleaching of probe and cancer cell death.

Subsequently, the signal intensity tended to increase again, 24 h after PIT, indicating re-accumulation of circulating 1849-ICG in the surviving cells of the residual tumor. This phenomenon may ensure the effect of PIT by additional exposure of NIR 24 h later. Our present study is the first ever report of NIR-PIT targeting TF with 1849-ICG, although there have been studies regarding the targeting of TF for diagnostic imaging[14-16] or radioisotope therapy[17]. Since TF is expressed not only on tumor cell surface, but also, in tumor stroma[37] and on tumor-associated vascular endothelial cells[38], our NIR-PIT with 1849-ICG may possibly target all of them.

As the NIR-PIT regimen, we used a single 1849-ICG injection followed by NIR light exposure on two consecutive days. We intravenously injected the 100 μg 1849-ICG conjugate in 100 μL PBS to mice and irradiated the tumor with NIR light (50 J/cm^2) on two consecutive days. Even with this treatment regimen, tumor growth retardation was seen, and we could potentially obtain more optimal therapeutic efficacy with minimal adverse effects by increasing the injected dose of conjugate, the irradiation energy, fractionated doses and repeated treatment cycles. There have been reports that NIR-PIT, quickly and massively, kills target-expressing cancer cells within minutes after the NIR light exposure by provoking irreversible cellular membrane damage. As a result, extracellular water can enter the cells, resulting in swelling, blebbing, and rupture of the cells[24]. Moreover, antibody-photosensitizer conjugates selectively bind to target-positive cancer cells with insignificant non-target cellular uptake of the photosensitizer, inducing rapid necrotic damage, especially on cancer cells near blood vessels. Thus, it causes the dilatation of tumor blood vessels and dramatically increasing permeability so called the super EPR (SUPR) effect[39-41]. By means of this phenomenon after the initial NIR-PIT, antibody-photosensitizer conjugates can infiltrate more into the tumor microenvironment with enhanced permeability and penetration after the first dose of NIR-PIT, with a more homogenous access to the surviving cancer cells in tumors[42]. Therefore, an additional irradiation with NIR light can further augment the therapeutic efficacy of NIR-PIT[43].

To comprehensively evaluate the potential effects of 1849-ICG directed NIR-PIT, we performed *in vitro* cell viability imaging assay, longitudinal monitoring of tumor volume change and histological and IHC analyses of tumor sections. NIR-PIT-induced rapid cell death was seen by fluorescence microscopy (Figure 3). Relative tumor volume change showed significant inhibition of tumor growth in the NIT-PIT group compared to the control groups (Figure 4A). In the histological investigation, H&E-stained NIR-PIT-treated tumor sections exhibited necrotic death-associated features (were loss of tumor cells and cells nest pattern, scattering of damaged and hypertrophic tumor cells, and marked interstitial fibrosis), whereas no obvious damage was observed in tumors of the other groups (Figure 6). Furthermore, in the IHC examination, a decrease in number of proliferating cells was noticed in the tumors of mice treated with NIR-PIT (Figure 7). Although rapid and massive cell death was induced by NIR-PIT, to obtain the optimal and prolong antitumor effect, further studies with fractionated dosing of conjugate and repeated exposure of suitable irradiation doses and/or the strategic studies for combining it with other drugs or treatment modalities will be needed.

Kobayashi *et al*[39] and others utilized the IR700DX as the photosensitizer that has photostability, water solubility, and salt tolerance. In the present study, we employed a water-soluble anionic dye ICG as the photosensitizer, which is an already approved fluorescence imaging agent for clinical use by the United States Food and Drug Administration, since a couple of decades because of its safety[44]. Furthermore, the superior features of NIR properties of ICG over other visible fluorophores, such as less auto-fluorescence, better tissue penetration, and large stokes shifts that allow better rejection of excitation light and thus lower background fluorescence[45], encouraged us to use it for *in vivo* NIR imaging and NIT-PIT. NH_2-reactive ICG, that we employed here, can easily form a covalent bond with an amino group of anti-TF 1849 without any activation process. Previously, ICG has been reported to be an effective NIR light absorber for laser-mediated photodynamic/PTT[46-48]. Reindl *et al*[49] reported that ICG absorbs 800-nm NIR light, and nearly 90% of the absorbed light is converted to heat. Moreover, there were additional reports about that ICG induces photo-oxidative cell death mediated by a singlet oxygen[50] and heat generation[51]. Thus, photothermal effect and oxidative stress are involved in the mechanisms resulting in the anti-tumor effect of ICG-NIR therapy. The present study demonstrated that ICG is useful for PIT, suggesting that ICG-labeled antibodies are alternative option in addition to IR700DX-labeled.

In the last few years, with the advantage of tumor specificity of PIT over PDT, studies on PIT have increased, and evidences on NIR-PIT-induced immune responses were being reported[52]. The association of PIT and immune response is an interesting topic and needs to be investigated more extensively. Unfortunately, we could not include this issue in our present study.

The specific binding of the 1849-ICG conjugate with inherent fluorescent nature of ICG, which emits the fluorescence signals in the NIR range, enables using this conjugate in clinical practice for both anti-tumor PIT and *in situ* detection of pancreatic cancer. Thus, in the case of resectable pancreatic cancer, tumor margins may be identified by using the intraoperative or endoscopic/laparoscopic setting of ICG fluorescence imaging tools. Furthermore, PIT can be concurrently conducted as an additional therapy to residual tumor tissues. PIT may also be applied to disseminated peritoneal lesions of pancreatic cancer with minimal damage to surrounding healthy normal tissues. Although, the development of clinically usable devices for endoscopic/laparoscopic fluorescence imaging and NIR-PIT remain a hurdle, there

is a possibility to overcome it with advancing software and hardware technologies.

In conclusion, the current study reveals that 1849-ICG conjugate accumulated in a TF-overexpressing pancreatic cancer cell and xenografts model BxPC-3. A single dose of 1849-ICG conjugate administration accompanied by NIR light exposure (50 J/cm^2) for two consecutive days effectively inhibited tumor growth *in vivo* without producing any noticeable adverse effects. Taken together, our results suggest that NIR-PIT employing TF as a targeting antigen for the 1849-ICG is a promising new treatment modality for pancreatic cancer with a useful contemporaneous diagnostic utility, which could be ultimately applicable in clinical use.

ARTICLE HIGHLIGHTS

Research background

Pancreatic cancer is still one of major life-threatening diseases. Therefore, there is an urgent need to explore early diagnostic and new therapeutic options. Near infrared photoimmunotherapy (NIR-PIT) is a highly selective tumor treatment that utilizes antibody-photosensitizer conjugate systemic administration, accompanied by subsequent NIR light exposure. Tissue factor (TF) is a transmembrane protein and its overexpression is associated with increased tumor growth, tumor angiogenesis and metastatic potential in many malignancies, including pancreatic cancer.

Research motivation

Previously, we suggested that TF may be a promising target for cancer diagnostic imaging probe and have already reported the usefulness of anti-TF monoclonal antibody (anti-TF mAb) in cancer imaging and therapy. However, NIR-PIT using anti-TF mAb has not been attempted.

Research objectives

In this study, we aim to investigate the photoimmunotherapeutic effect induced by a rat IgG$_{2b}$ anti-TF monoclonal antibody 1849 (anti-TF 1849), conjugated to the NIR photosensitizer, indocyanine green (ICG), in a TF-expressing BxPC-3 pancreatic cancer model.

Research methods

An ICG-labeled antibody conjugate (1849-ICG) was generated by labeling an anti-TF 1849 with ICG. The expression levels of TF in two human pancreatic cancer cell lines were examined by western blotting. Specific binding of the 1849-ICG to BxPC-3 cells was examined by fluorescence microscopy. NIR-PIT-induced cell death was determined by cell viability imaging assay. *In vivo* longitudinal fluorescence imaging was used to explore the accumulation of 1849-ICG conjugate in xenograft tumors. To determine the effect of NIR-PIT, tumor-bearing mice were divided into 5 groups: (1) 100 μg of 1849-ICG i.v. administration followed by NIR light exposure (50 J/cm^2) on two consecutive days (Days 1 and 2); (2) NIR light exposure (50 J/cm^2) only on two consecutive days (Days 1 and 2); (3) 100 μg of 1849-ICG i.v. administration; (4) 100 μg of unlabeled anti-TF 1849 i.v. administration; and (5) the untreated control. Semiweekly tumor volume measurements, accompanied with histological and immunohistochemical (IHC) analyses of tumors, were performed 3 d after the 2nd irradiation with NIR light to monitor the effect of treatments.

Research results

High TF expression in BxPC-3 cells was observed *via* western blot analysis, concordant with the observed preferential binding with intracellular localization of 1849-ICG *via* fluorescence microscopy. NIR-PIT-induced cell death was observed by performing cell viability imaging assay. In contrast to the other test groups, tumor growth was significantly inhibited by NIR-PIT with a statistically significant difference in relative tumor volumes ($P < 0.05$). Tumors that received NIR-PIT showed evidence of necrotic cell death-associated features upon hematoxylin-eosin staining accompanied by a decrease in Ki-67-positive cells (a cell proliferation marker) by IHC examination.

Research conclusions

The TF-targeted NIR-PIT with the 1849-ICG conjugate can potentially open a new platform for treatment of TF-expressing pancreatic cancer.

Research perspectives

Because TF-targeted NIR-PIT is a promising new treatment modality with a useful contemporaneous diagnostic utility, we will approach to apply it in clinical use. In addition, the association of PIT and immune response is an interesting topic and we will explore it in the future study.

REFERENCES

1 **GBD 2015 Mortality and Causes of Death Collaborators**. Global, regional, and national life expectancy, all-cause mortality, and cause-specific mortality for 249 causes of death, 1980-2015: a systematic analysis for the Global Burden of Disease Study 2015. *Lancet* 2016; **388**: 1459-1544 [PMID: 27733281 DOI: 10.1016/S0140-6736(16)31012-1]

2 **Siegel RL**, Miller KD, Jemal A. Cancer statistics, 2018. *CA Cancer J Clin* 2018; **68**: 7-30 [PMID: 29313949 DOI: 10.3322/caac.21442]

3 **Kasthuri RS**, Taubman MB, Mackman N. Role of tissue factor in cancer. *J Clin Oncol* 2009; **27**: 4834-4838 [PMID: 19738116 DOI: 10.1200/JCO.2009.22.6324]

4 **van den Berg YW**, Osanto S, Reitsma PH, Versteeg HH. The relationship between tissue factor and cancer progression: insights from bench and bedside. *Blood* 2012; **119**: 924-932 [PMID: 22065595 DOI: 10.1182/blood-2011-06-317685]

5 **Leppert U**, Eisenreich A. The role of tissue factor isoforms in cancer biology. *Int J Cancer* 2015; **137**: 497-503 [PMID: 24806794 DOI: 10.1002/ijc.28959]

6 **Kakkar AK**, Lemoine NR, Scully MF, Tebbutt S, Williamson RC. Tissue factor expression correlates with histological grade in human pancreatic cancer. *Br J Surg*1995; **82**: 1101-1104 [PMID: 7648165 DOI: 10.1002/bjs.1800820831]

7 **Ueda C**, Hirohata Y, Kihara Y, Nakamura H, Abe S, Akahane K, Okamoto K, Itoh H, Otsuki M. Pancreatic cancer complicated by disseminated intravascular coagulation associated with production of tissue factor. *J Gastroenterol* 2001; **36**: 848-850 [PMID: 11777214]

8 **Khorana AA**, Ahrendt SA, Ryan CK, Francis CW, Hruban RH, Hu YC, Hostetter G, Harvey J, Taubman MB. Tissue factor expression, angiogenesis, and thrombosis in pancreatic cancer. *Clin Cancer Res* 2007; **13**: 2870-2875 [PMID: 17504985 DOI: 10.1158/1078-0432.CCR-06-2351]

9 **Hobbs JE**, Zakarija A, Cundiff DL, Doll JA, Hymen E, Cornwell M, Crawford SE, Liu N, Signaevsky M, Soff GA. Alternatively spliced human tissue factor promotes tumor growth and angiogenesis in a pancreatic cancer tumor model. *Thromb Res* 2007; **120** Suppl 2: S13-S21 [PMID: 18023707 DOI: 10.1016/S0049-3848(07)70126-3]

10 **Haas SL**, Jesnowski R, Steiner M, Hummel F, Ringel J, Burstein C, Nizze H, Liebe S, Löhr JM. Expression of tissue factor in pancreatic adenocarcinoma is associated with activation of coagulation. *World J Gastroenterol* 2006; **12**: 4843-4849 [PMID: 16937466]

11 **Tsumura R**, Sato R, Furuya F, Koga Y, Yamamoto Y, Fujiwara Y, Yasunaga M, Matsumura Y. Feasibility study of the Fab fragment of a monoclonal antibody against tissue factor as a diagnostic tool. *Int J Oncol* 2015; **47**: 2107-2114 [PMID: 26497165 DOI: 10.3892/ijo.2015.3210]

12 **Koga Y**, Manabe S, Aihara Y, Sato R, Tsumura R, Iwafuji H, Furuya F, Fuchigami H, Fujiwara Y, Hisada Y, Yamamoto Y, Yasunaga M, Matsumura Y. Antitumor effect of antitissue factor antibody-MMAE conjugate in human pancreatic tumor xenografts. *Int J Cancer* 2015; **137**: 1457-1466 [PMID: 25704403 DOI: 10.1002/ijc.29492]

13 **Takashima H**, Tsuji AB, Saga T, Yasunaga M, Koga Y, Kuroda JI, Yano S, Kuratsu JI, Matsumura Y. Molecular imaging using an anti-human tissue factor monoclonal antibody in an orthotopic glioma xenograft model. *Sci Rep* 2017; **7**: 12341 [PMID: 28951589 DOI: 10.1038/s41598-017-12563-5]

14 **Hernandez R**, England CG, Yang Y, Valdovinos HF, Liu B, Wong

HC, Barnhart TE, Cai W. ImmunoPET imaging of tissue factor expression in pancreatic cancer with ^{89}Zr-Df-ALT-836. *J Control Release* 2017; **264**: 160-168 [PMID: 28843831 DOI: 10.1016/j.jconrel.2017.08.029]
15 **Hong H**, Zhang Y, Nayak TR, Engle JW, Wong HC, Liu B, Barnhart TE, Cai W. Immuno-PET of tissue factor in pancreatic cancer. *J Nucl Med* 2012; **53**: 1748-1754 [PMID: 22988057 DOI: 10.2967/jnumed.112.105460]
16 **Shi S**, Hong H, Orbay H, Graves SA, Yang Y, Ohman JD, Liu B, Nickles RJ, Wong HC, Cai W. ImmunoPET of tissue factor expression in triple-negative breast cancer with a radiolabeled antibody Fab fragment. *Eur J Nucl Med Mol Imaging* 2015; **42**: 1295-1303 [PMID: 25801992 DOI: 10.1007/s00259-015-3038-1]
17 **Wang B**, Berger M, Masters G, Albone E, Yang Q, Sheedy J, Kirksey Y, Grimm L, Wang B, Singleton J, Soltis D. Radiotherapy of human xenograft NSCLC tumors in nude mice with a 90Y-labeled anti-tissue factor antibody. *Cancer Biother Radiopharm* 2005; **20**: 300-309 [PMID: 15989475 DOI: 10.1089/cbr.2005.20.300]
18 **Scholzen T**, Gerdes J. The Ki-67 protein: from the known and the unknown. *J Cell Physiol* 2000; **182**: 311-322 [PMID: 10653597 DOI: 10.1002/(SICI)1097-4652(200003)182:3<311::AID-JCP1>3.0.CO;2-9]
19 **Sudo H**, Tsuji AB, Sugyo A, Ogawa Y, Sagara M, Saga T. ZDHHC8 knockdown enhances radiosensitivity and suppresses tumor growth in a mesothelioma mouse model. *Cancer Sci* 2012; **103**: 203-209 [PMID: 22017350 DOI: 10.1111/j.1349-7006.2011.02126.x]
20 **Kano MR**, Bae Y, Iwata C, Morishita Y, Yashiro M, Oka M, Fujii T, Komuro A, Kiyono K, Kaminishi M, Hirakawa K, Ouchi Y, Nishiyama N, Kataoka K, Miyazono K. Improvement of cancer-targeting therapy, using nanocarriers for intractable solid tumors by inhibition of TGF-beta signaling. *Proc Natl Acad Sci USA* 2007; **104**: 3460-3465 [PMID: 17307870 DOI: 10.1073/pnas.0611660104]
21 **Agostinis P**, Berg K, Cengel KA, Foster TH, Girotti AW, Gollnick SO, Hahn SM, Hamblin MR, Juzeniene A, Kessel D, Korbelik M, Moan J, Mroz P, Nowis D, Piette J, Wilson BC, Golab J. Photodynamic therapy of cancer: an update. *CA Cancer J Clin* 2011; **61**: 250-281 [PMID: 21617154 DOI: 10.3322/caac.20114]
22 **Shirasu N**, Nam SO, Kuroki M. Tumor-targeted photodynamic therapy. *Anticancer Res* 2013; **33**: 2823-2831 [PMID: 23780966]
23 **Peer D**, Karp JM, Hong S, Farokhzad OC, Margalit R, Langer R. Nanocarriers as an emerging platform for cancer therapy. *Nat Nanotechnol* 2007; **2**: 751-760 [PMID: 18654426 DOI: 10.1038/nnano.2007.387]
24 **Mitsunaga M**, Ogawa M, Kosaka N, Rosenblum LT, Choyke PL, Kobayashi H. Cancer cell-selective in vivo near infrared photoimmunotherapy targeting specific membrane molecules. *Nat Med* 2011; **17**: 1685-1691 [PMID: 22057348 DOI: 10.1038/nm.2554]
25 **Burley TA**, Mączyńska J, Shah A, Szopa W, Harrington KJ, Boult JKR, Mrozek-Wilczkiewicz A, Vinci M, Bamber JC, Kaspera W, Kramer-Marek G. Near-infrared photoimmunotherapy targeting EGFR-Shedding new light on glioblastoma treatment. *Int J Cancer* 2018; **142**: 2363-2374 [PMID: 29313975 DOI: 10.1002/ijc.31246]
26 **Nakamura Y**, Ohler ZW, Householder D, Nagaya T, Sato K, Okuyama S, Ogata F, Daar D, Hoa T, Choyke PL, Kobayashi H. Near Infrared Photoimmunotherapy in a Transgenic Mouse Model of Spontaneous Epidermal Growth Factor Receptor (EGFR)-expressing Lung Cancer. *Mol Cancer Ther* 2017; **16**: 408-414 [PMID: 28151706 DOI: 10.1158/1535-7163.MCT-16-0663]
27 **Heryanto YD**, Hanaoka H, Nakajima T, Yamaguchi A, Tsushima Y. Applying near-infrared photoimmunotherapy to B-cell lymphoma: comparative evaluation with radioimmunotherapy in tumor xenografts. *Ann Nucl Med* 2017; **31**: 669-677 [PMID: 28741052 DOI: 10.1007/s12149-017-1197-9]
28 **Railkar R**, Krane LS, Li QQ, Sanford T, Siddiqui MR, Haines D, Vourganti S, Brancato SJ, Choyke PL, Kobayashi H, Agarwal PK. Epidermal Growth Factor Receptor (EGFR)-targeted Photoimmunotherapy (PIT) for the Treatment of EGFR-expressing Bladder Cancer. *Mol Cancer Ther* 2017; **16**: 2201-2214 [PMID: 28619755 DOI: 10.1158/1535-7163.MCT-16-0924]
29 **Jin J**, Krishnamachary B, Mironchik Y, Kobayashi H, Bhujwalla ZM. Phototheranostics of CD44-positive cell populations in triple negative breast cancer. *Sci Rep*2016; **6**: 27871 [PMID: 27302409 DOI: 10.1038/srep27871]
30 **Nagaya T**, Nakamura Y, Okuyama S, Ogata F, Maruoka Y, Choyke PL, Kobayashi H. Near-Infrared Photoimmunotherapy Targeting Prostate Cancer with Prostate-Specific Membrane Antigen (PSMA) Antibody. *Mol Cancer Res* 2017; **15**: 1153-1162 [PMID: 28588059 DOI: 10.1158/1541-7786.MCR-17-0164]
31 **Shirasu N**, Yamada H, Shibaguchi H, Kuroki M, Kuroki M. Potent and specific antitumor effect of CEA-targeted photoimmunotherapy. *Int J Cancer* 2014; **135**: 2697-2710 [PMID: 24740257 DOI: 10.1002/ijc.28907]
32 **Maawy AA**, Hiroshima Y, Zhang Y, Heim R, Makings L, Garcia-Guzman M, Luiken GA, Kobayashi H, Hoffman RM, Bouvet M. Near infra-red photoimmunotherapy with anti-CEA-IR700 results in extensive tumor lysis and a significant decrease in tumor burden in orthotopic mouse models of pancreatic cancer. *PLoS One* 2015; **10**: e0121989 [PMID: 25799218 DOI: 10.1371/journal.pone.0121989]
33 **Nagaya T**, Nakamura Y, Okuyama S, Ogata F, Maruoka Y, Choyke PL, Allen C, Kobayashi H. Syngeneic Mouse Models of Oral Cancer Are Effectively Targeted by Anti-CD44-Based NIR-PIT. *Mol Cancer Res* 2017; **15**: 1667-1677 [PMID: 28923838 DOI: 10.1158/1541-7786.MCR-17-0333]
34 **Nagaya T**, Nakamura Y, Sato K, Harada T, Choyke PL, Hodge JW, Schlom J, Kobayashi H. Near infrared photoimmunotherapy with avelumab, an anti-programmed death-ligand 1 (PD-L1) antibody. *Oncotarget* 2017; **8**: 8807-8817 [PMID: 27716622 DOI: 10.18632/oncotarget.12410]
35 **Nakajima T**, Sano K, Choyke PL, Kobayashi H. Improving the efficacy of Photoimmunotherapy (PIT) using a cocktail of antibody conjugates in a multiple antigen tumor model. *Theranostics* 2013; **3**: 357-365 [PMID: 23781283 DOI: 10.7150/thno.5908]
36 **Nitori N**, Ino Y, Nakanishi Y, Yamada T, Honda K, Yanagihara K, Kosuge T, Kanai Y, Kitajima M, Hirohashi S. Prognostic significance of tissue factor in pancreatic ductal adenocarcinoma. *Clin Cancer Res* 2005; **11**: 2531-2539 [PMID: 15814630 DOI: 10.1158/1078-0432.CCR-04-0866]
37 **Vrana JA**, Stang MT, Grande JP, Getz MJ. Expression of tissue factor in tumor stroma correlates with progression to invasive human breast cancer: paracrine regulation by carcinoma cell-derived members of the transforming growth factor beta family. *Cancer Res* 1996; **56**: 5063-5070 [PMID: 8895765]
38 **Contrino J**, Hair G, Kreutzer DL, Rickles FR. In situ detection of tissue factor in vascular endothelial cells: correlation with the malignant phenotype of human breast disease. *Nat Med* 1996; **2**: 209-215 [PMID: 8574967]
39 **Kobayashi H**, Choyke PL. Super enhanced permeability and retention (SUPR) effects in tumors following near infrared photoimmunotherapy. *Nanoscale* 2016; **8**: 12504-12509 [PMID: 26443992 DOI: 10.1039/c5nr05552k]
40 **Sano K**, Nakajima T, Choyke PL, Kobayashi H. The effect of photoimmunotherapy followed by liposomal daunorubicin in a mixed tumor model: a demonstration of the super-enhanced permeability and retention effect after photoimmunotherapy. *Mol Cancer Ther* 2014; **13**: 426-432 [PMID: 24356818 DOI: 10.1158/1535-7163.MCT-13-0633]
41 **Sano K**, Nakajima T, Choyke PL, Kobayashi H. Markedly enhanced permeability and retention effects induced by photo-immunotherapy of tumors. *ACS Nano* 2013; **7**: 717-724 [PMID: 23214407 DOI: 10.1021/nn305011p]
42 **Nagaya T**, Nakamura Y, Sato K, Harada T, Choyke PL, Kobayashi H. Improved micro-distribution of antibody-photon absorber conjugates after initial near infrared photoimmunotherapy (NIR-PIT). *J Control Release* 2016; **232**: 1-8 [PMID: 27059723 DOI: 10.1016/j.jconrel.2016.04.003]
43 **Mitsunaga M**, Nakajima T, Sano K, Choyke PL, Kobayashi H. Near-infrared theranostic photoimmunotherapy (PIT): repeated exposure of light enhances the effect of immunoconjugate. *Bioconjug Chem* 2012; **23**: 604-609 [PMID: 22369484 DOI: 10.1021/bc200648m]
44 **Dzurinko VL**, Gurwood AS, Price JR. Intravenous and indocyanine green angiography. *Optometry* 2004; **75**: 743-755 [PMID: 15624671]
45 **Sharma R**, Wendt JA, Rasmussen JC, Adams KE, Marshall MV,

Sevick-Muraca EM. New horizons for imaging lymphatic function. *Ann N Y Acad Sci* 2008; **1131**: 13-36 [PMID: 18519956 DOI: 10.1196/annals.1413.002]

46 **Shirata C**, Kaneko J, Inagaki Y, Kokudo T, Sato M, Kiritani S, Akamatsu N, Arita J, Sakamoto Y, Hasegawa K, Kokudo N. Near-infrared photothermal/photodynamic therapy with indocyanine green induces apoptosis of hepatocellular carcinoma cells through oxidative stress. *Sci Rep* 2017; **7**: 13958 [PMID: 29066756 DOI: 10.1038/s41598-017-14401-0]

47 **Tseng WW**, Saxton RE, Deganutti A, Liu CD. Infrared laser activation of indocyanine green inhibits growth in human pancreatic cancer. *Pancreas* 2003; **27**: e42-e45 [PMID: 14508139]

48 **Radzi R**, Osaki T, Tsuka T, Imagawa T, Minami S, Nakayama Y, Okamoto Y. Photodynamic hyperthermal therapy with indocyanine green (ICG) induces apoptosis and cell cycle arrest in B16F10 murine melanoma cells. *J Vet Med Sci* 2012; **74**: 545-551 [PMID: 22146339]

49 **Reindl S,** Penzkofer A, Gong SH, Landthaler M, Szeimies RM, Abels C, Baumler W. Quantum yield of triplet formation for indocyanine green. *J Photoch Photobio A* 1997; **105**: 65-68 [DOI: 10.1016/S1010-6030(96)04584-4]

50 **Bäumler W**, Abels C, Karrer S, Weiss T, Messmann H, Landthaler M, Szeimies RM. Photo-oxidative killing of human colonic cancer cells using indocyanine green and infrared light. *Br J Cancer* 1999; **80**: 360-363 [PMID: 10408838 DOI: 10.1038/sj.bjc.6690363]

51 **Urbanska K**, Romanowska-Dixon B, Matuszak Z, Oszajca J, Nowak-Sliwinska P, Stochel G. Indocyanine green as a prospective sensitizer for photodynamic therapy of melanomas. *Acta Biochim Pol* 2002; **49**: 387-391 [PMID: 12362980]

52 **Ogawa M**, Tomita Y, Nakamura Y, Lee MJ, Lee S, Tomita S, Nagaya T, Sato K, Yamauchi T, Iwai H, Kumar A, Haystead T, Shroff H, Choyke PL, Trepel JB, Kobayashi H. Immunogenic cancer cell death selectively induced by near infrared photoimmunotherapy initiates host tumor immunity. *Oncotarget* 2017; **8**: 10425-10436 [PMID: 28060726 DOI: 10.18632/oncotarget.14425]

P- Reviewer: Bramhall S **S- Editor**: Ma RY
L- Editor: A **E- Editor**: Yin SY

World Journal of Gastroenterology

Submit a Manuscript: https://www.f6publishing.com

World J Gastroenterol 2018 December 28; 24(48): 5505-5524

DOI: 10.3748/wjg.v24.i48.5505

ISSN 1007-9327 (print) ISSN 2219-2840 (online)

ORIGINAL ARTICLE

Basic Study

Integrated metabolomic profiling for analysis of antilipidemic effects of *Polygonatum kingianum* extract on dyslipidemia in rats

Xing-Xin Yang, Jia-Di Wei, Jian-Kang Mu, Xin Liu, Jin-Cai Dong, Lin-Xi Zeng, Wen Gu, Jing-Ping Li, Jie Yu

Xing-Xin Yang, Jia-Di Wei, Jian-Kang Mu, Jin-Cai Dong, Lin-Xi Zeng, Wen Gu, Jing-Ping Li, Jie Yu, College of Pharmaceutical Science, Yunnan University of Traditional Chinese Medicine, Kunming 650500, Yunnan Province, China

Xin Liu, Beijing Entry-Exit Inspection and Quarantine Bureau, Beijing 100026, China

ORCID number: Xing-Xin Yang (0000-0001-6594-772X); Jia-Di Wei (0000-0002-8108-0457); Jian-Kang Mu (0000-0001-9189-2515); Xin Liu (0000-0003-4788-5275); Jin-Cai Dong (0000-0001-6909-9676); Lin-Xi Zeng (0000-0002-3234-2377); Wen Gu (0000-0003-3766-5180); Jing-Ping Li (0000-0002-7452-6342); Jie Yu (0000-0001-8100-8896).

Author contributions: Yang XX and Yu J designed the research; Yang XX, Wei JD and Dong JC performed the research; Liu X contributed analytic tools; Zeng LX, Gu W and Li JP analyzed the data; Yang XX, Wei JD and Mu JK wrote the paper.

Supported by the National Natural Science Foundation of China, No. 81660596 and No. 81760733; the Application and Basis Research Project of Yunnan, China, No. 2016FD050 and No. 2017FF117-013; and the Fund for Young and Middle-aged Academic and Technological Leaders of Yunnan, No. 2015HB053.

Institutional animal care and use committee statement: Approval from the Institutional Ethical Committee on Animal Care and Experimentations of Yunnan University of Traditional Chinese Medicine was obtained for this study.

Conflict-of-interest statement: The authors declare that there is no duality of interest associated with this manuscript.

Data sharing statement: No additional data are available.

ARRIVE guidelines statement: The authors had read the ARRIVE guidelines, and the manuscript was prepared and revised according to the ARRIVE guidelines.

Manuscript source: Unsolicited manuscript

Corresponding author: Jie Yu, PhD, Professor, College of Pharmaceutical Science, Yunnan University of Traditional Chinese Medicine, 1076 Yuhua Road, Kunming 650500, Yunnan Province, China. cz.yujie@gmail.com
Telephone: +86-871-65933303
Fax: +86-871-65933303

Received: September 25, 2018
Peer-review started: September 25, 2018
First decision: October 24, 2018
Revised: October 31, 2018
Accepted: November 16, 2018
Article in press: November 16, 2018
Published online: December 28, 2018

Abstract

AIM

To identify the effects and mechanism of action of *Polygonatum kingianum* (*P. kingianum*) on dyslipidemia in rats using an integrated untargeted metabolomic method.

METHODS

A rat model of dyslipidemia was induced with a high-fat diet (HFD) and rats were given *P. kingianum* [4 g/(kg•d)] intragastrically for 14 wk. Changes in serum and hepatic lipid parameters were evaluated. Metabolites in serum, urine and liver samples were profiled using ultra-high

performance liquid chromatography/mass spectrometry followed by multivariate statistical analysis to identify potential biomarkers and metabolic pathways.

RESULTS

P. kingianum significantly inhibited the HFD-induced increase in total cholesterol and triglyceride in the liver and serum. *P. kingianum* also significantly regulated metabolites in the analyzed samples toward normal status. Nineteen, twenty-four and thirty-eight potential biomarkers were identified in serum, urine and liver samples, respectively. These biomarkers involved biosynthesis of phenylalanine, tyrosine, tryptophan, valine, leucine and isoleucine, along with metabolism of tryptophan, tyrosine, phenylalanine, starch, sucrose, glycerophospholipid, arachidonic acid, linoleic acid, nicotinate, nicotinamide and sphingolipid.

CONCLUSION

P. kingianum alleviates HFD-induced dyslipidemia by regulating many endogenous metabolites in serum, urine and liver samples. Collectively, our findings suggest that *P. kingianum* may be a promising lipid regulator to treat dyslipidemia and associated diseases.

Key words: Dyslipidemia; Lipid regulation; Metabolomics; Multivariate statistical analysis; *Polygonatum kingianum*; Ultra-high performance liquid chromatography/mass spectrometry

Core tip: We investigated the effects and the underlying mechanism of action of *Polygonatum kingianum* (*P. kingianum*) on high-fat diet (HFD)-induced dyslipidemia in rats using an integrated untargeted metabolomic method. The results indicated that *P. kingianum* alleviated HFD-induced dyslipidemia by regulating a large number of endogenous metabolites in serum, urine and liver. This involved phenylalanine, tyrosine, tryptophan, valine, leucine and isoleucine biosynthesis, and tryptophan, tyrosine, phenylalanine, starch, sucrose, glycerophospholipid, arachidonic acid, linoleic acid, nicotinate, nicotinamide and sphingolipid metabolism. *P. kingianum* may be a promising lipid regulator to remedy dyslipidemia and further alleviate its related diseases.

Yang XX, Wei JD, Mu JK, Liu X, Dong JC, Zeng LX, Gu W, Li JP, Yu J. Integrated metabolomic profiling for analysis of antilipidemic effects of *Polygonatum kingianum* extract on dyslipidemia in rats. *World J Gastroenterol* 2018; 24(48): 5505-5524
URL: https://www.wjgnet.com/1007-9327/full/v24/i48/5505.htm
DOI: https://dx.doi.org/10.3748/wjg.v24.i48.5505

INTRODUCTION

Dyslipidemia is a core characteristic of the metabolic syndrome, and is an important risk factor for atherosclerosis, coronary heart disease, stroke and other cardiovascular and cerebrovascular diseases. It is also closely related to many significant diseases such as diabetes and nephropathy[1]. Dyslipidemia is divided into two types, referred to as primary and secondary dyslipidemia. Primary dyslipidemia has a genetic history and may be caused by congenital enzyme defects. Secondary dyslipidemia is usually present in patients with diseases such as diabetes mellitus, hypothyroidism, nephrotic syndrome, biliary obstruction, pancreatitis, gout, alcoholism, and various liver disorders[2]. The improvement in living standards and associated lifestyle changes have led to dyslipidemia being considered one of the most important risk factors for metabolic diseases worldwide[3]. Therefore, management of dyslipidemia is of vital importance to prevent and cure a variety of acute and chronic human diseases.

The commonly used lipid regulators include statins, fibrates, nicotinic acid and variants, bile acid sequestrants and inhibitors of cholesterol absorption. These drugs can be effective for treating dyslipidemia, but have significant adverse effect profiles[4]. For example, statins may increase blood glucose concentrations, cause rhabdomyolysis or damage the liver and kidneys[5]. Traditional Chinese medicines (TCMs) are one of the world's oldest herbal medicines and have been applied extensively by TCM practitioners for thousands of years[6]. TCMs have an indispensable role in the prevention and treatment of human diseases, especially those that are complicated and chronic[7]. As a complementary therapy technique with fewer side effects than Western medicines, TCMs have been employed widely to regulate lipid metabolic disorders[8]. Thus, TCMs may serve as the basis for development of new lipid-regulating drugs or health products.

Rhizoma polygonati, first recorded in *Mingyi Bielu* in 220-450 AD (written by Hong-Jing Tao), has been used as a TCM and nutritional food for over 2000 years. *Polygonatum kingianum* Coll. et Hemsl., *Polygonatum sibiricum* Red. and *Polygonatum cyrtonema* Hua are described in the Chinese Pharmacopoeia (2015 edition) as legal sources of *Rhizoma polygonati*. *Polygonatum kingianum* (*P. kingianum*; Figure 1) is mainly distributed in the Chinese provinces of Yunnan, Sichuan, Guizhou and Guangxi. It is mainly comprised of saponins and polysaccharides, and has pharmacological activities that include immune system stimulation, anti-aging effects and blood glucose regulation[9,10]. Our previous research showed that the total saponins and total polysaccharides from *P. kingianum* had blood glucose and lipid regulating activities[11,12]. However, the lipid-regulating effects of *P. kingianum* and the mechanism for these remain unclear.

Metabolomics can comprehensively characterize small molecule metabolites in biological systems. It can also provide an overview of metabolic status and global biochemical events after external stimulation such as in disease models and after drug treatment[13]. Metabolomics is a novel method in pharmacological and phar-

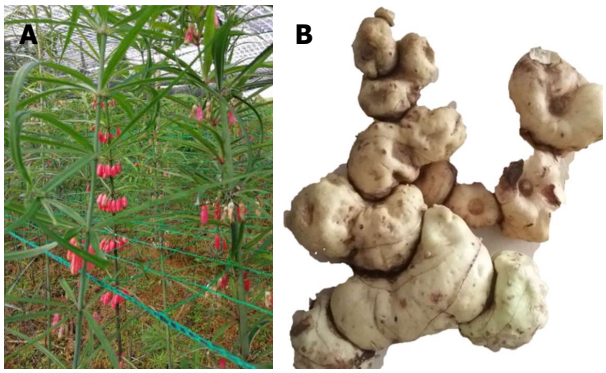

Figure 1 ***Polygonatum kingianum.*** A: Whole plant photograph of *Polygonatum kingianum (P. kingianum)*; B: Rhizome of *P. kingianum*, which represents the medicinal part of this plant used in this study.

macodynamic studies that is increasingly employed to assess the therapeutic and toxic effects of herbal TCMs and TCM prescriptions, and their mechanism of action[14].

In the present study, we investigated the lipid-regulating effects and the underlying mechanism of action of *P. kingianum* on high-fat diet (HFD)-induced dyslipidemia in rats. An integrated untargeted metabolomic method was used, which was based on ultra-high performance liquid chromatography/mass spectrometry (UHPLC/MS) analysis of serum, urine and liver samples (Figure 2). The results indicated that *P. kingianum* alleviated HFD-induced dyslipidemia by regulating many endogenous metabolites in serum, urine and liver samples. Taken together, these findings indicated that *P. kingianum* may be a promising lipid regulator to treat dyslipidemia and further alleviate associated diseases.

MATERIALS AND METHODS

Chemicals, reagents and materials

Kits for quantifying triglyceride (TG) and total cholesterol (TC) concentrations were purchased from ZhongshengBei Biotech Co., Ltd. (Beijng, China). Bicinchoninic Acid (BCA) Protein Determination Kit was obtained from Beyotime Institute of Biotechnology (Shanghai, China). Simvastatin was purchased from Hangzhou Merck East Pharmaceutical Co., Ltd. (Hangzhou, China). HPLC-grade formic acid and acetonitrile were acquired from Merck (Darmstadt, Germany). Basal rodent diet (calories provided from carbohydrates, proteins and fat were 62%, 26% and 12%, respectively) was obtained from Suzhou Shuangshi Experimental Animal Feed Technology Co., Ltd. (Suzhou, China). Cholesterol, refined lard, and eggs were supplied by Beijing Boao Extension Co., Ltd. (Beijing, China), Sichuan Green Island Co., Ltd. (Chengdu, China) and Wal-Mart Supermarket (Kunming, China), respectively. High-purity deionized water was purified using a Milli-Q system (Millipore, Bedford, MA, United States). All other reagents were of analytical grade or higher. The rhizome of *P. kingianum* was purchased from Wenshan Shengnong Trueborn Medicinal Materials Cultivation Cooperation Society (Wenshan, China) on 07 April 2017. Samples were authenticated by Professor Jie Yu and a voucher specimen (No. 8426) was deposited in the Key Laboratory of Preventing Metabolic Diseases of Traditional Chinese Medicine, Yunnan University of Traditional Chinese Medicine (Kunming, China).

Preparation of P. kingianum extract

P. kingianum rhizome was processed according to regulations in the Chinese Pharmacopoeia (2015 edition). Briefly, fresh *P. kingianum* rhizome was separated from fibrous roots, washed, cut into thick slices and dried at 50 ℃. The dried materials were then infiltrated in a 5-fold volume of Shaoxing rice wine (Beijing Ershang Wangzhihe Food Co., Ltd., Beijing, China), and then placed in a steam sterilizer (LDZX-50 KBS, Shanghai Shenan Medical Instrument Factory, Shanghai, China) at 120 ℃ for 2.5 h. After cooling for 3 h, the steamed materials were dried at 60 ℃.

The steamed and dried *P. kingianum* sample was pulverized, immersed in a 7-fold volume of water for 30 min and then decocted with water for 60 min. The filtrates were collected after leaching. The dregs were decocted successively with a 7-fold volume of water for a further 60 min, and the extracted liquids filtered. The two filtrates were then combined and condensed using an R-210 rotatory evaporator (Büchi Labortechnik AG, Flawil, Switzerland) under reduced pressure at 50 ℃. Finally, the concentrates were lyophilized to a powder using a FD5-3 freeze dryer (SIM International Group Co. Ltd., Newark, DE, United States). The obtained sample powder was stored in a desiccator at room temperature until use.

Animal experiments

Healthy male Sprague-Dawley rats (200 ± 50 g) were obtained from Dashuo Biotech. Co., Ltd. (Chengdu, China). They were adjusted to a controlled environment (22 ± 1 ℃ temperature; 60% ± 10% humidity; and a 12 h/12 h light/dark cycle) with free access to water and a commercial laboratory complete food. Experiments complied with the Guide for the Care and Use of Laboratory Animals as published by the United States of America National Institutes of Health and specifically approved by the Institutional Ethical Committee on Animal Care and Experimentations of Yunnan University of Traditional Chinese Medicine (R-062016003) (Kunming, China). All reasonable efforts were made to minimize animal suffering.

After one week of adaptive feeding, rats were randomized into four groups (n = 5 rats per group): normal control (normal saline), model (normal saline), simvastatin [1.8 mg/(kg•d)] and *P. kingianum* [4 g/(kg•d)] groups. The simvastatin group served as a positive control. The rats were given the treatments intragastrically once a day for 14 consecutive weeks. Simvastatin and *P. kingianum* were prepared separately in normal saline. Dyslipidemia was induced with an HFD (comprised of 1% cholesterol, 10% refined lard, 10%

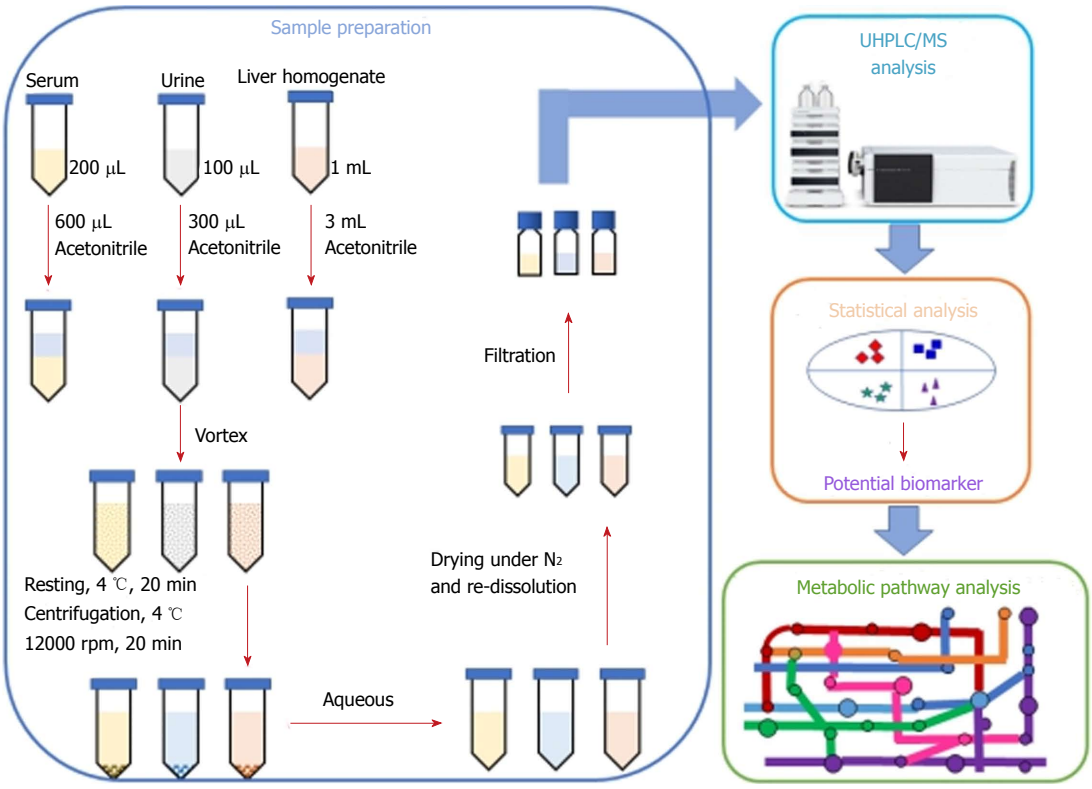

Figure 2 Workflow of the integrated untargeted metabolomic method based on ultra-high performance liquid chromatography/mass spectrometry analysis of serum, urine and liver samples. UHPLC/MS: Ultra-high performance liquid chromatography/mass spectrometry.

eggs and 79% basic feed) for 14 wk in all groups except for the normal control group.

Sample collection

To collect urine samples, rats in each experimental group were housed in metabolic cages for the last three weeks of the 14 wk of treatment. Samples were collected from the metabolic cages and transferred immediately into sterile tubes. After the last administration at week 14, rats were fasted for 12 h and then anesthetized with chloral hydrate. Fasting blood was collected from the hepatic portal vein, and the liver was harvested and stored at -80 ℃ until use. Blood samples were allowed to clot at 4 ℃ and centrifuged at 10000 *g* for 10 min, after which serum was collected and stored at -80 ℃ until assayed.

Measurement of lipid parameters in serum and liver

TG and TC concentrations were determined using 100 μL of serum and 100 μL of liver homogenate supernatant, in which the protein concentration was measured by BCA assay. All parameters were evaluated on a SpectraMax Plus 384 Microplate Reader (Molecular Devices, Sunnyvale, CA, United States) using commercially available diagnostic kits in accordance with the manufacturer's instructions.

Sample pre-treatment for UHPLC/MS analysis

Serum samples: Aliquots of serum (200 μL) were diluted with 600 μL of acetonitrile. After vortex-mixing and resting at 4 ℃ for 20 min, the samples were centrifuged at 12000 rpm and 4 ℃ for 15 min. The collected supernatants were dried under a gentle nitrogen stream. The obtained residues were re-dissolved in 100 μL of acetonitrile for metabolomics analysis.

Urine samples: Samples were lyophilized to a powder using a FD5-3 freeze dryer (SIM International Group Co. Ltd., Newark, DE, United States). The obtained sample powders were dissolved with 100 μL of water and then diluted with 300 μL of acetonitrile. After vortex-mixing and resting at 4 ℃ for 20 min, the samples were centrifuged at 12000 rpm and 4 ℃ for 15 min. The collected supernatants were dried with a gentle nitrogen stream. The residues were re-dissolved in 100 μL of acetonitrile for metabolomics analysis.

Liver samples: Samples were thawed at room temperature before pre-treatment. Liver tissue (0.2 g) from each rat was homogenized with 1.0 mL of normal saline and then diluted with 300 μL of acetonitrile. After vortex-mixing and resting at 4 ℃ for 20 min, the samples were centrifuged at 12000 rpm and 4 ℃ for 15 min. The collected supernatants were dried with a gentle nitrogen stream. The residues were re-dissolved in 100 μL of acetonitrile for metabolomics analysis.

Conditions of UHPLC/MS analysis

UHPLC/MS analyses were performed on an UHPLC Dionex Ultimate 3000 system coupled with a Thermo

Table 1 Body weight and food intake of rats

	Normal control	Model	Simvastatin	*P. kingianum*
Initial body weight (g)	200.87 ± 8.83	206.69 ± 8.51	205.03 ± 6.26	206.72 ± 7.82
Final body weight (g)	494.81 ± 37.43	518.08 ± 40.50	487.62 ± 30.26	480.14 ± 29.91
Body weight gain (g)	293.94 ± 28.61	311.39 ± 31.98	282.59 ± 24.01	273.42 ± 22.10
Food intake (g)	15670.81	15042.53	14969.08	14903.86

Values represent the mean ± SD from five animals. *P. kingianum*: *Polygonatum kingianum*.

Table 2 Effects of *Polygonatum kingianum* on total cholesterol and triglyceride concentrations in rat serum

Group	TC (mmol/L)	TG (mmol/L)
Normal group	1.42 ± 0.11^{c}	0.91 ± 0.21
Model group	1.56 ± 0.11^{a}	0.97 ± 0.22
P. kingianum group	1.43 ± 0.13^{c}	0.76 ± 0.13^{c}
Simvastatin group	1.15 ± 0.09^{b,d}	0.77 ± 0.09^{c}

Values represent the mean ± SD from five animals. $^{a}P < 0.05$, $^{b}P < 0.01$ *vs* the relative normal group. $^{c}P < 0.05$, $^{d}P < 0.01$ *vs* the relative model group. *P. kingianum*: *Polygonatum kingianum*; TC: Total cholesterol; TG: Triglyceride.

Scientific Q-Exactive TM hybrid quadrupole-orbitrap mass spectrometer with a heated-electrospray ionization probe (Thermo Fisher Scientific, San Jose, CA, United States). The UHPLC system consisted of a quaternary pump, an auto-sampler with a temperature control function, a column box, and a photodiode array (PDA) detector.

UHPLC conditions for all samples were: (1) chromatographic column: Thermo C18 column (100 mm × 2.1 mm I.D., 1.9 μm); (2) mobile phase: 0.1% formic acid (A) and acetonitrile (B) with a gradient program (0-3 min, 5% B; 3-5 min, 5% B → 23% B; 5-10 min, 23% B → 43% B; 10-13 min, 43% B → 64% B; 13-16 min, 64% B → 85% B; 16-18 min, 85% B → 100% B; 18-20 min, 100% B → 100% B); (3) flow rate: 0.2 mL/min; and (4) sample injection volume: 4 μL.

MS conditions for all samples were: (1) flow rate: 0.2 mL/min (split from UPLC effluent); (2) detection mode: positive and negative ion; (3) heat block and curved desolvation line temperature: 250 ℃; nebulizing nitrogen gas flow: 1.5 L/min; interface voltage: (+) 3.5 kV, (-) -2.8 kV; (4) mass range: MS, m/z 100-1000; MS^2 and MS^3, m/z 50-1000; (5) dynamic exclusion time: 10 s; and (6) workstation: Xcalibar 3.0.63 for liquid chromatography combined with data processing, molecular prediction, and precise molecular weight calculations.

Statistical analysis

Lipid concentrations in serum and liver are expressed as the mean ± standard deviation (SD). Statistical analyses were performed using SPSS software (13.0 for Windows; SPSS, Chicago, IL, United States). Differences between groups were analyzed by one-way analysis of variance (ANOVA, Dunnett's method). $P < 0.05$ (two-tailed) was considered statistically significant.

All UHPLC/MS raw files were exported in Xcalibur Raw File (.raw) format and converted to computable document format (.cdf) with Xcalibur 2.0 software (Thermo Fisher Scientific, Waltham, MA, United States). The converted file was then transferred into XCMS online (https://xcmsonline.scripps.edu) to output all data, including groups and comparisons. After that, multivariate statistical analysis, including principal components analysis (PCA) and orthogonal partial least squares discriminant analysis (OPLS-DA), was performed on SIMCA-P 14.1 software (Umetrics, Umeå, Sweden). Potential biomarkers were selected according to the parameters of variable importance in the projection (VIP > 1.0) from OPLS-DA. The metabolites were identified using METLIN database and compared with data reported previously. Finally, biochemical reactions involving the identified metabolites were found through the Kyoto Encyclopedia of Genes and Genomes (KEGG) in MetaboAnalyst4.0 online (http://www.metaboanalyst.ca).

RESULTS

Effects of HFD and P. kingianum on body weight and food intake

In the present study, a HFD rat model was used to investigate the potential effect of *P. kingianum* on HFD-mediated dyslipidemia that was induced by administration of an HFD over a 14-wk period. *P. kingianum* extract was administered by oral gavage at s dosage of 4 g/(kg•d) during HFD administration. During the experiment, none of the rats died, and they had healthy-looking fur, normal drinking habits, moved freely and rapidly responded to external stimuli. As shown in Table 1, the HFD slightly increased body weight, but *P. kingianum* and simvastatin showed a non-significant effect on body weight and food intake.

Effects of P. kingianum on lipids in serum and liver samples from HFD-fed rats

The effects of *P. kingianum* on lipids in serum and liver samples were first assessed in a rat model of HFD-induced dyslipidemia. As shown in Table 2, 14 wk of HFD feeding resulted in a significant increase in TC concentration, but had no significant effect on TG con-

Table 3 Effects of *Polygonatum kingianum* on total cholesterol and triglyceride concentration in rat liver

Group	TC (mmol/gprot)	TG (mmol/gprot)
Normal group	0.77 ± 0.19^{d}	1.46 ± 0.12^{d}
Model group	1.17 ± 0.22^{b}	2.83 ± 0.71^{b}
P. kingianum group	0.95 ± 0.15^{c}	1.20 ± 0.28^{d}
Simvastatin group	0.94 ± 0.15^{c}	1.37 ± 0.43^{d}

Values represent the mean ± SD from five animals. $^{a}P < 0.05$, $^{b}P < 0.01$ *vs* the relative normal group. $^{c}P < 0.05$, $^{d}P < 0.01$ *vs* the relative model group. *P. kingianum*: *Polygonatum kingianum*; TC: Total cholesterol; TG: Triglyceride.

centration in serum. These effects were significantly reduced by simvastatin, which is known to correct dyslipidemias[15]. Similar to simvastatin, *P. kingianum* remarkably prevented HFD-induced dyslipidemias. Furthermore, Table 3 shows that after 14 wk of HFD feeding, hepatic TC and TG concentrations were significantly increased compared with the normal control group. However, these effects were significantly reduced by *P. kingianum* and simvastatin treatment.

Metabolomic profiling of serum, urine and liver samples

Separation conditions of the three samples on the UHPLC column were optimized in terms of peak number, peak shape and reproducibility. Figures 3-5 shows representative total ion current profiles of the positive and negative ion modes of the four groups in serum, urine and liver, respectively. A large number of molecules were profiled by UHPLC/MS in the analyzed samples. Moreover, there were significant differences in peak number and intensity between the four groups within each of the three sample types. This indicated different metabolomic states in the different groups. Hence, after 14 wk of HFD feeding and administration of *P. kingianum* and simvastatin, the metabolites in serum, urine and liver samples were significantly different.

Multivariate statistical analysis of metabolomic data

PCA and OPLS-DA are frequently used for multivariate data analysis because of their ability to cope with highly multivariate, noisy, collinear and possibly incomplete data. PCA is an unsupervised pattern recognition method that is initially used to discern the presence of inherent similarities in profiles. OPLS-DA is a supervised pattern recognition approach based on a partial least squares algorithm that has higher sensitivity for biomarker detection than other methods.

Serum samples

Figure 6A shows the PCA score plots of serum samples in positive and negative ion modes. The normal control, model, simvastatin and *P. kingianum* groups were located in four different regions of the scatter score map. The four sample sets were basically separated. Additionally, the *P. kingianum* group was closer to the normal group than the simvastatin group and partially overlapped with the normal group. This indicated that the composition and concentration of metabolites in the *P. kingianum* group was more similar to the control group. Thus, *P. kingianum* treatment remarkably prevented HFD-induced pathological changes.

OPLS-DA was performed to further verify sample separation from the four groups, to maximize separation between groups and to identify biomarkers from them (Figure 6B). The OPLS-DA score plots were described by the cross-validation parameter, R^2Y, and Q^2, which represent the total explained variation for the X matrix and the predictability of the model, respectively. In positive and negative ion modes, the four groups were also significantly separated. The *P. kingianum* and simvastatin groups were both close to the control group, which further indicated that *P. kingianum* treatment strongly prevented HFD-induced pathological changes.

To further evaluate the component changes after treatment, an S-Plot loading diagram was established based on OPLS-DA. As shown in Figure 6C, each point represents a variable that shows the biomarker that caused the difference between the model and *P. kingianum* groups. The importance of each variable to the classification was evaluated by the VIP value, with molecules with a VIP > 1.0 selected as potential biomarkers.

Urine samples

Figure 7A shows the PCA score plots of urine samples in positive and negative ion modes. The control group was clearly distinguished from the other three groups, which overlapped partially. In the negative ion mode, there were abnormal sets in the control group, which might be due to individual sample differences that resulted in outlier sample points being outside the 95% confidence interval. The model group was significantly different from the control group. The *P. kingianum* and simvastatin groups had a tendency to deviate from the model group, while the *P. kingianum* group was closer to the cross than the simvastatin group. Compared with the model group, the *P. kingianum* group had a tendency to approach the part samples of the control group and deviate from the part samples of the control group. This was because the appearance of the outlier sample points seriously affected the clustering result. In the positive ion mode, outlier sample points appeared in the control group. The model group had a tendency to deviate to the left compared with the control group. The *P. kingianum* group partially overlapped with the simvastatin group, but did not approach the control group. This was considered to be

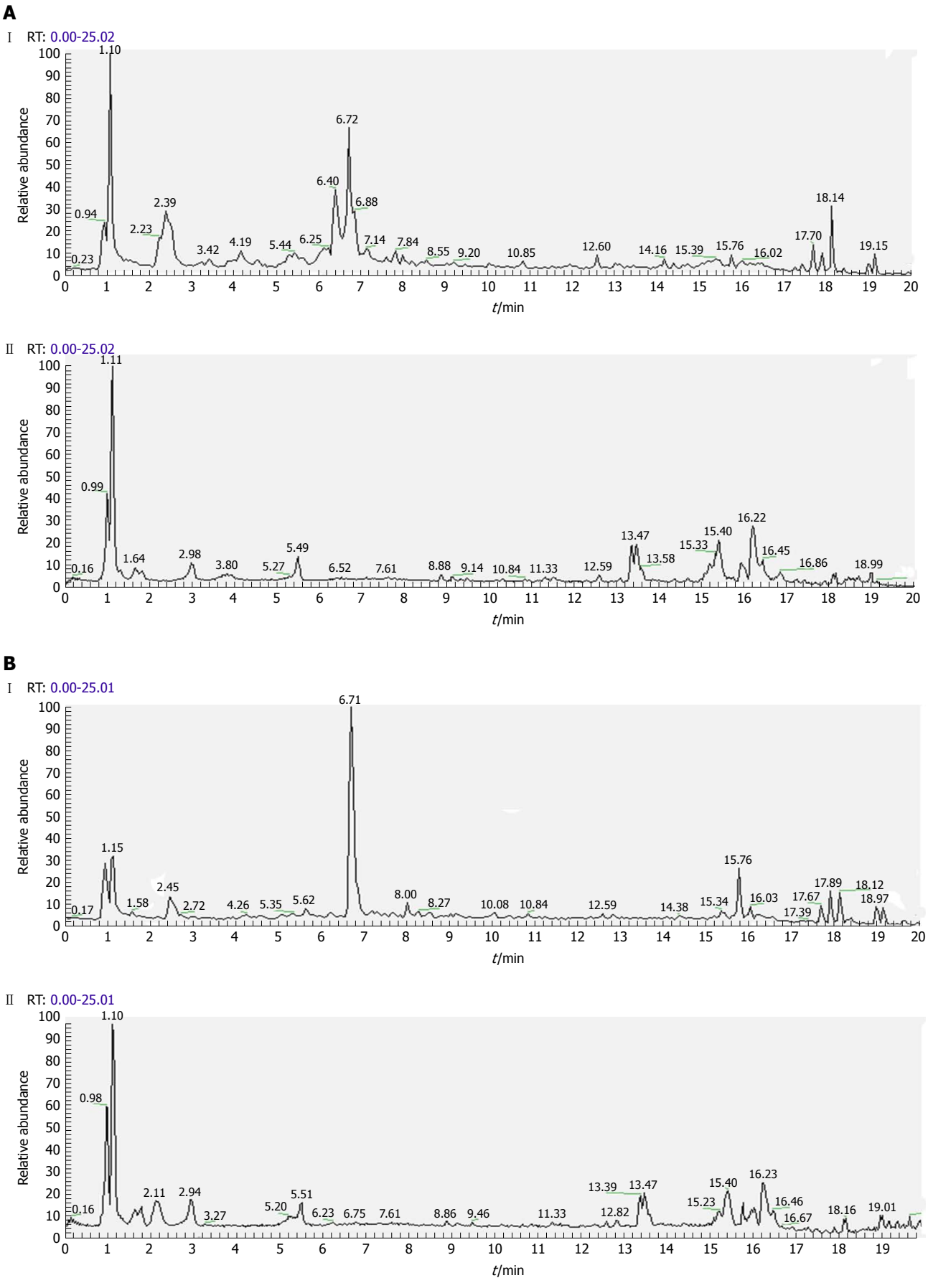
A
I RT: 0.00-25.02
Relative abundance
t/min
1.10
6.72
6.40
6.88
2.39
0.94
2.23
3.42
4.19
5.44
6.25
7.14
7.84
8.55
9.20
10.85
12.60
14.16
15.39
15.76
16.02
17.70
18.14
19.15
0.23
II RT: 0.00-25.02
Relative abundance
t/min
1.11
0.99
1.64
2.98
3.80
5.27
5.49
6.52
7.61
8.88
9.14
10.84
11.33
12.59
13.47
13.58
15.33
15.40
16.22
16.45
16.86
18.99
0.16
B
I RT: 0.00-25.01
Relative abundance
t/min
6.71
1.15
2.45
1.58
2.72
4.26
5.35
5.62
8.00
8.27
10.08
10.84
12.59
14.38
15.34
15.76
16.03
17.39
17.67
17.89
18.12
18.97
0.17
II RT: 0.00-25.01
Relative abundance
t/min
1.10
0.98
2.11
2.94
3.27
5.20
5.51
6.23
6.75
7.61
8.86
9.46
11.33
12.82
13.39
13.47
15.23
15.40
16.23
16.46
16.67
18.16
19.01
0.16

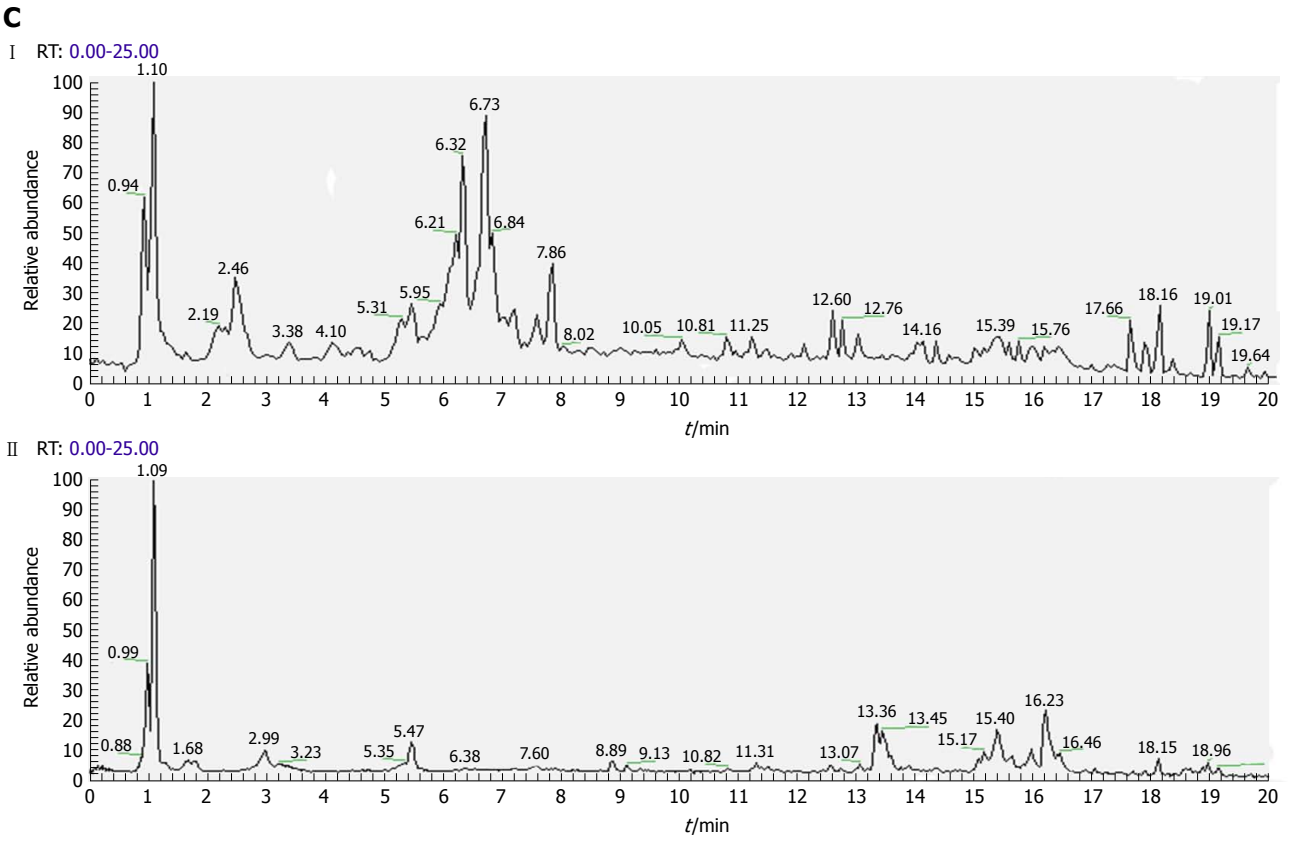

Figure 3 Representative total ion current profiles of serum samples in the negative (Ⅰ) and positive (Ⅱ) ion modes. A: Control group; B: Model group; and C: *Polygonatum kingianum* group.

related to the outlier sample points of the control group.

Figure 7B shows the OPLS-DA diagrams of urine samples in positive and negative ion modes. The results suggested that the samples from all groups were perfectly separated, and samples in each group were well clustered. The model group was significantly different from the control group, indicating that physiological metabolism in the urine of rats was seriously interfered with by the HFD. The sample points of the *P. kingianum* group showed a tendency to approach the control group, indicating that HFD-induced changes were relieved after *P. kingianum* administration. Figure 7C shows the S-Plot loading diagram of urine samples and the substances with a VIP > 1.0 that were selected as biomarkers.

Liver samples

Figure 8A displays the PCA score plots of liver samples in positive and negative ion modes. In the negative ion mode, all samples were distributed within the 95% confidence interval. The control group partially overlapped with the model group, which might be due to the unsupervised pattern recognition of PCA analysis. In the positive ion mode, there were outlier sample points in the control group. The *P. kingianum* group was significantly different from the control and model groups, indicating that *P. kingianum* administration interfered with metabolism in the rats.

Figure 8B showed the OPLS-DA diagrams of liver samples in positive and negative ion modes. The results suggested that the samples from all groups were perfectly separated, and the samples in each group were well clustered. The *P. kingianum* group was closer to the control group than the simvastatin group, which indicated that *P. kingianum* had significant effects on metabolomic changes in the liver. Figure 8C shows the S-Plot loading diagrams of urine samples and the substances with a VIP > 1.0 that were selected as biomarkers.

Potential biomarker identification

Nineteen compounds were identified from serum samples, including four in the negative ion mode and 15 in the positive ion mode. They were amino acids, carbohydrates and esters (Table 4). There were 24 compounds identified from urine samples, including seven in the negative ion mode and 17 in the positive ion mode. They were amino acids, organic acids and esters (Table 5). Finally, 38 compounds were identified from liver samples, including 18 in the negative ion mode and 22 in the positive ion mode. They were amino acids, organic acids and esters (Table 6).

Metabolic pathway analysis

Pathways with influence values greater than 0.1 were selected as the metabolic pathways[16]. Pathway impact plots were built to visualize the impact of altered metabolic pathways (Figure 9A). According to these, the

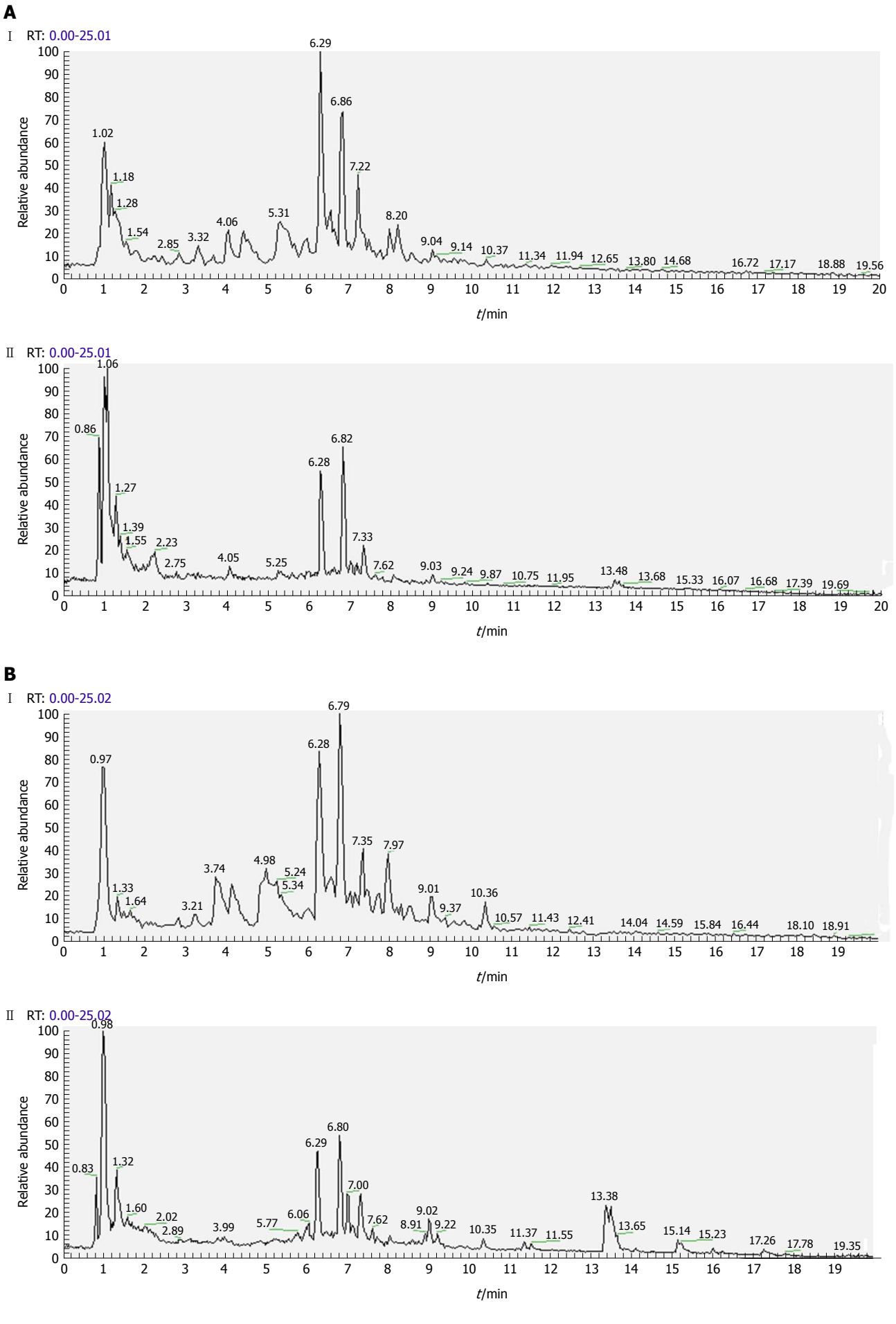
A
I RT: 0.00-25.01
Relative abundance
t/min
1.02
1.18
1.28
1.54
2.85
3.32
4.06
5.31
6.29
6.86
7.22
8.20
9.04
9.14
10.37
11.34
11.94
12.65
13.80
14.68
16.72
17.17
18.88
19.56
II RT: 0.00-25.01
Relative abundance
t/min
0.86
1.06
1.27
1.39
1.55
2.23
2.75
4.05
5.25
6.28
6.82
7.33
7.62
9.03
9.24
9.87
10.75
11.95
13.48
13.68
15.33
16.07
16.68
17.39
19.69
B
I RT: 0.00-25.02
Relative abundance
t/min
0.97
1.33
1.64
3.21
3.74
4.98
5.24
5.34
6.28
6.79
7.35
7.97
9.01
9.37
10.36
10.57
11.43
12.41
14.04
14.59
15.84
16.44
18.10
18.91
II RT: 0.00-25.02
Relative abundance
t/min
0.83
0.98
1.32
1.60
2.02
2.89
3.99
5.77
6.06
6.29
6.80
7.00
7.62
8.91
9.02
9.22
10.35
11.37
11.55
13.38
13.65
15.14
15.23
17.26
17.78
19.35

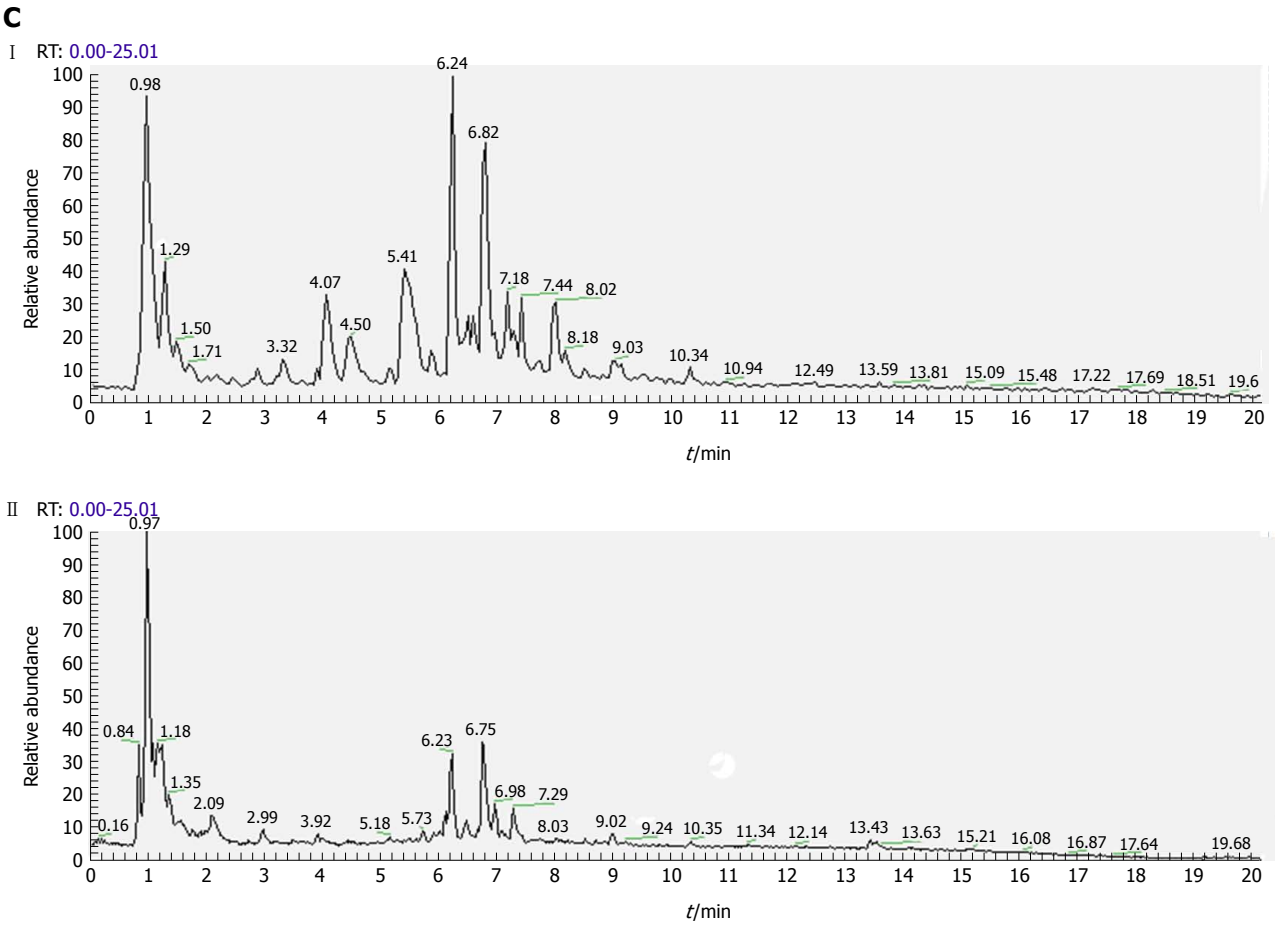

Figure 4 Representative total ion current profiles of urine samples in the negative (Ⅰ) and positive (Ⅱ) ion modes. A: Control group; B: Model group; and C: *Polygonatum kingianum* group.

major intervening pathways in serum samples involved phenylalanine, tyrosine, tryptophan, valine, leucine and isoleucine biosynthesis, and phenylalanine, starch, sucrose, glycerophospholipid, tryptophan and tyrosine metabolism (Figure 9A, Table 7). In urine samples, the major intervening pathway involved arachidonic acid metabolism (Figure 9B, Table 8). In liver samples, the major intervening pathways involved phenylalanine, tyrosine and tryptophan biosynthesis, and arachidonic acid, linoleic acid, nicotinate, nicotinamide, sphingolipid, tryptophan and tyrosine metabolism (Figure 9C, Table 9).

DISCUSSION

Dyslipidemia is mainly characterized by an increase in TC and TG concentrations in the serum and/or liver. We found that HFD feeding resulted in a significant increase in TC concentration in serum, and in TC and TG concentrations in the liver. This indicated that an HFD could induce hyperlipidemia. *P. kingianum* extract significantly inverted these HFD-induced changes, demonstrating that *P. kingianum* effectively ameliorated dyslipidemia in HFD-fed rats. Additionally, due to fundamental differences in plasma lipoprotein metabolism between rats and humans, it is valuable to use an optimal pathological model to evaluate the lipid-regulating effects of *P. kingianum*.

Metabolomics has been applied widely to the research of drug efficacy and the associated mechanism of action[17]. Currently, the most common samples analyzed in metabolomics are serum, urine, tissues/organs, feces, cells and sub-cells. We used serum, urine and liver samples for metabolomic analysis. The liver is the most important locus for substance metabolism, and also the main site for lipid and amino acid metabolism. External stimuli (*e.g.* a drug) may cause hepatic metabolites to change affecting the physiological function of the liver[18]. Serum reflects the overall status of an organism. When metabolic abnormalities occur in the liver, the metabolites in blood may change through the blood circulation. Urine is an important excretion pathway for metabolites and contains abundant metabolomic information about an organism. Eleven main metabolic pathways affected by *P. kingianum* administration were found in the three samples, including seven in serum and in the liver, and one in urine (Figure 10).

Phenylalanine, tyrosine and tryptophan biosynthesis and metabolism

Amino acids are the body's raw material for protein synthesis and are catabolic products. They participate in a

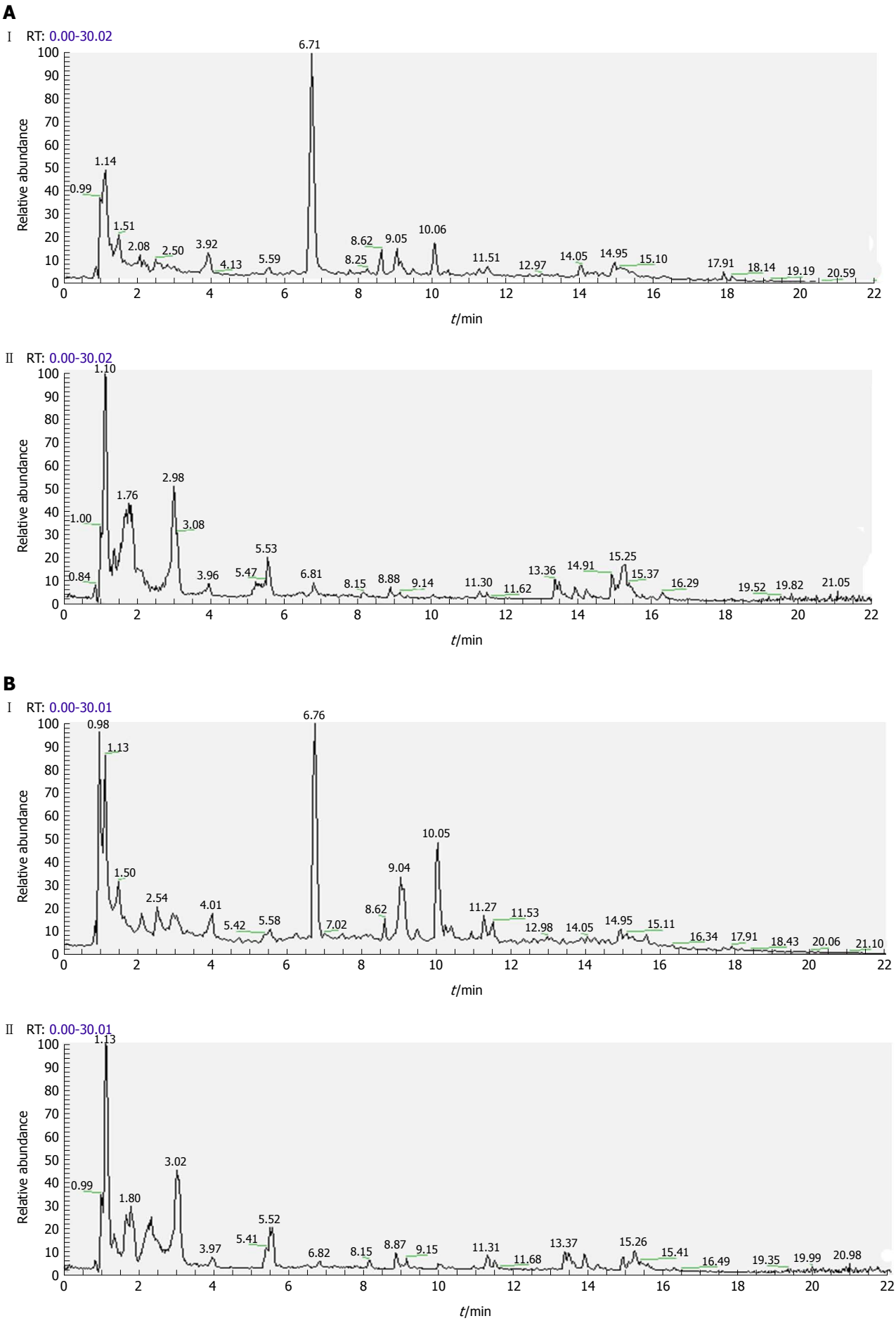
A
I RT: 0.00-30.02
Relative abundance
t/min
0.99
1.14
1.51
2.08
2.50
3.92
4.13
5.59
6.71
8.25
8.62
9.05
10.06
11.51
12.97
14.05
14.95
15.10
17.91
18.14
19.19
20.59
II RT: 0.00-30.02
Relative abundance
t/min
1.00
1.10
1.76
2.98
3.08
3.96
5.47
5.53
6.81
8.15
8.88
9.14
11.30
11.62
13.36
14.91
15.25
15.37
16.29
19.52
19.82
21.05
0.84
B
I RT: 0.00-30.01
Relative abundance
t/min
0.98
1.13
1.50
2.54
4.01
5.42
5.58
6.76
7.02
8.62
9.04
10.05
11.27
11.53
12.98
14.05
14.95
15.11
16.34
17.91
18.43
20.06
21.10
II RT: 0.00-30.01
Relative abundance
t/min
0.99
1.13
1.80
3.02
3.97
5.41
5.52
6.82
8.15
8.87
9.15
11.31
11.68
13.37
15.26
15.41
16.49
19.35
19.99
20.98

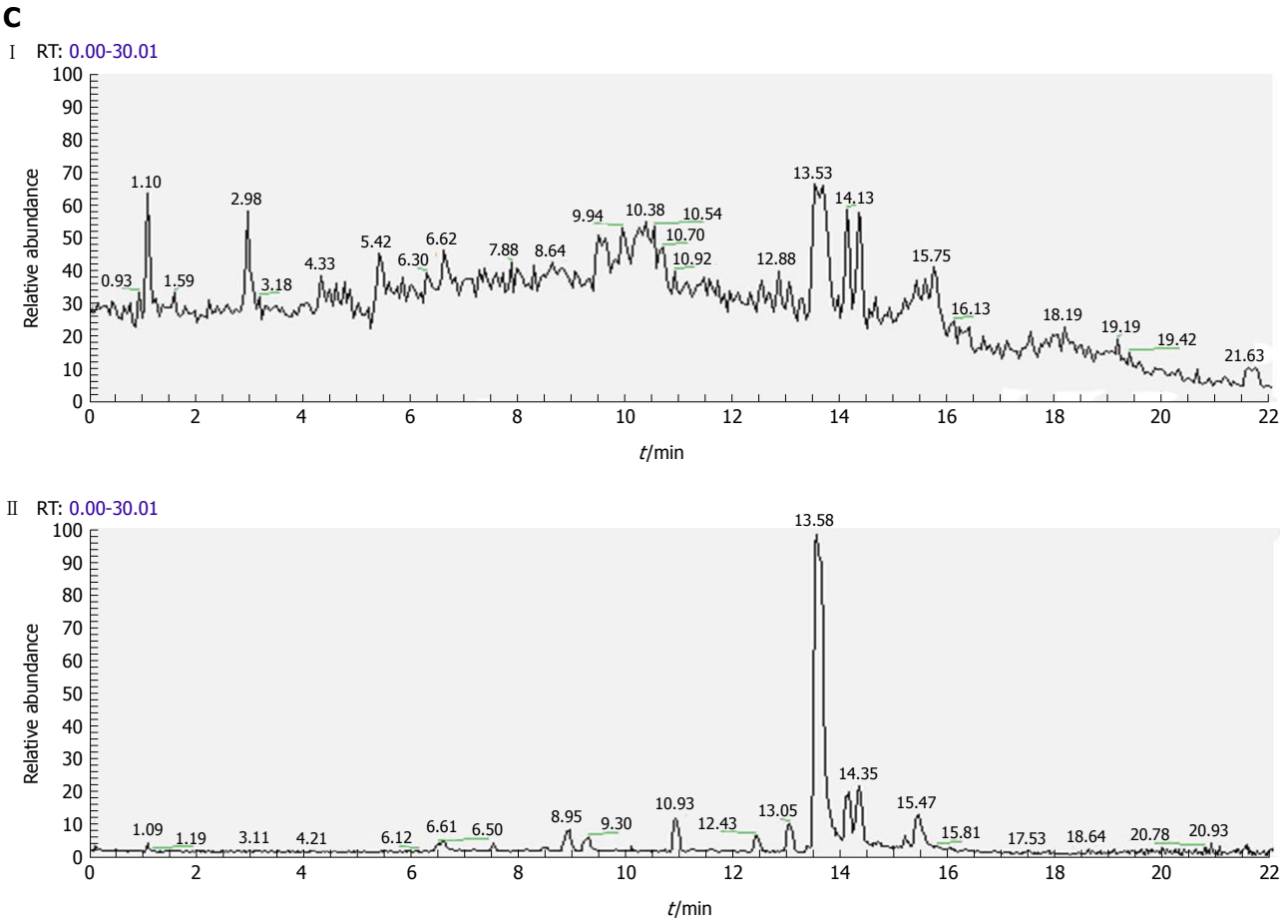

Figure 5 Representative total ion current profiles of liver samples in the negative (Ⅰ) and positive (Ⅱ) ion modes. A: Control group; B: Model group; and C: *Polygonatum kingianum* group.

variety of physiological and pathological processes, and their concentration often reflects the metabolic status of the body. In this study, a number of amino acid metabolic pathways were present in the serum and liver samples, with a decrease in these metabolites, indicating disordered amino acid metabolism. Dyslipidemia causes dysfunctional phenylalanine metabolism by inhibiting conversion of phenylalanine to tyrosine, which increases phenylalanine concentration in the blood. After *P. kingianum* administration, we showed decreased phenylalanine and increased tyrosine content in serum. Tyrosine is synthesized from phenylalanine and is necessary for synthesizing catecholamine hormones such as adrenaline (epinephrine). It also plays an important role in promoting energy metabolism, scavenging free radicals and relieving fatigue[19]. Tyrosine undergoes a series of metabolic reactions to form acetyl-CoA, which participates in the tricarboxylic acid (TCA) cycle. After *P. kingianum* administration, the tyrosine content was increased, which elevated the acetyl-CoA content and further accelerated lipid decomposition through the TCA cycle. Therefore, *P. kingianum* treatment reduced phenylalanine production and further increased tyrosine production by regulating phenylalanine, tyrosine and tryptophan biosynthesis, and phenylalanine and tyrosine metabolism.

Tryptophan, an essential amino acid for humans, has important functions for regulating lipid metabolism[20]. In addition, tryptophan can be converted to acetyl-CoA to participate in the TCA cycle. After *P. kingianum* administration, the tryptophan content was increased, which potentiated acetyl-CoA content and accelerated lipid decomposition. Thus, *P. kingianum* treatment increased tryptophan content and further relieved the disordered lipids by regulating tryptophan metabolism.

Valine, leucine and isoleucine biosynthesis

Biosynthesis of valine, leucine and isoleucine was involved in the serum samples. These amino acids can be broken down into glucose. We found that isoleucine was decreased by *P. kingianum* treatment, indicating a reduction in blood glucose. This affected the oxidation and decarboxylation of pyruvate, and further reduced lipid synthesis with glycerol to alleviate the lipid metabolic disorders.

Starch and sucrose metabolism

Starch and sucrose metabolism was involved in the serum samples. Glucose is the major energy source and metabolic intermediate of living cells. Starch is a

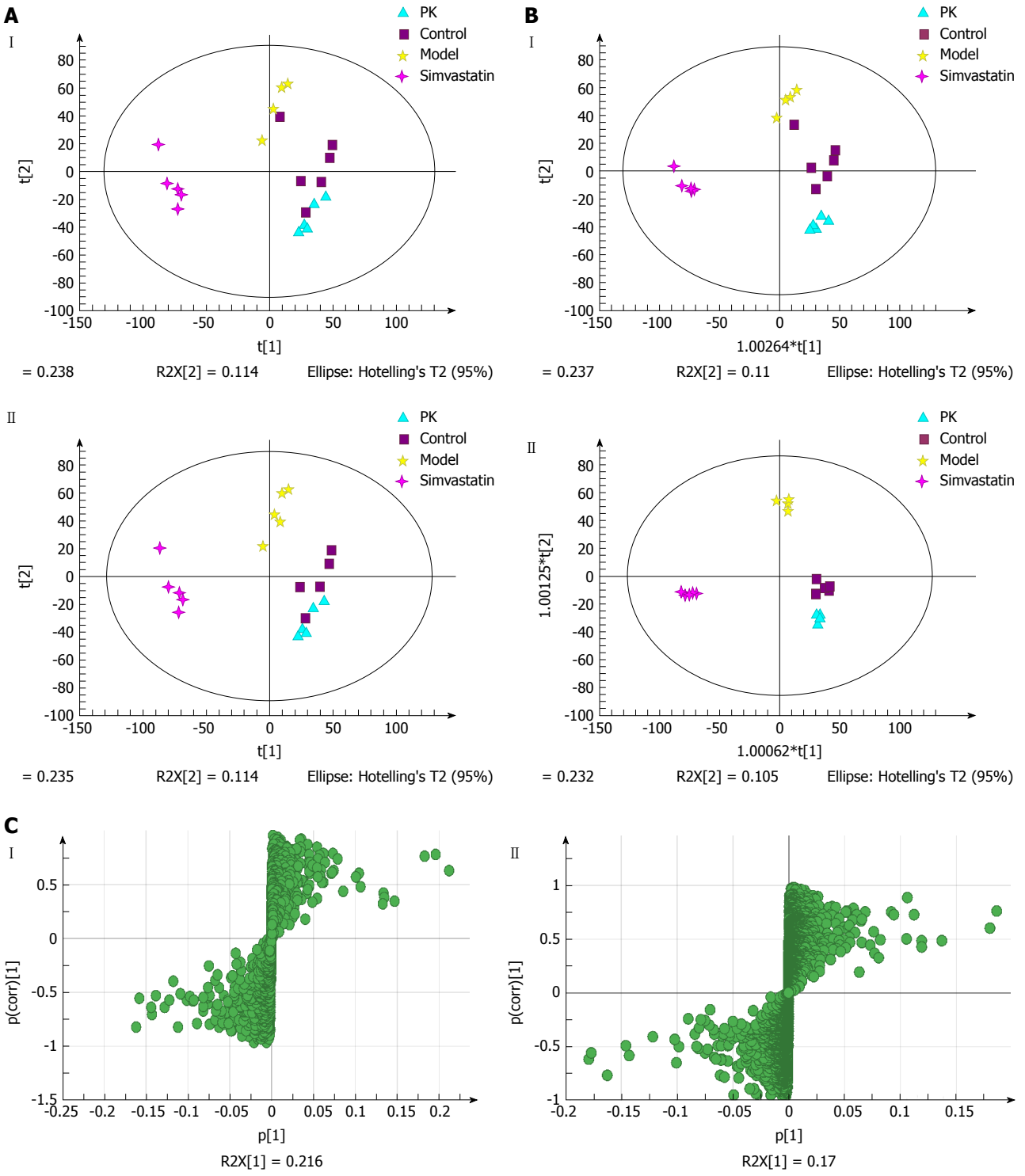

Figure 6 Multivariate statistical analysis of serum samples from model and *Polygonatum kingianum* groups in the negative (Ⅰ) and positive (Ⅱ) ion modes. A: Principal components analysis score plots; B: Orthogonal partial least squares discriminant analysis score plots; C: S-plot loading diagram. PK: *Polygonatum kingianum*.

polysaccharide that is composed of several glucose units. Sucrose is a disaccharide comprised of glucose and fructose molecules. Both sucrose and starch can be broken down into glucose by digestive juice. Glucose can be degraded to dihydroxyacetone phosphate by glycolysis. Dihydroxyacetone phosphate can be reduced to glycerol and can also be converted to pyruvate through glycolysis. Pyruvate is converted by oxidation and decarboxylation to acetyl-CoA, which can be used to synthesize fatty acids and further synthesize fat with glycerol[21]. We found that glucose content was reduced after *P. kingianum* administration, which signified that *P. kingianum* reduced lipid synthesis by regulating starch and sucrose metabolism.

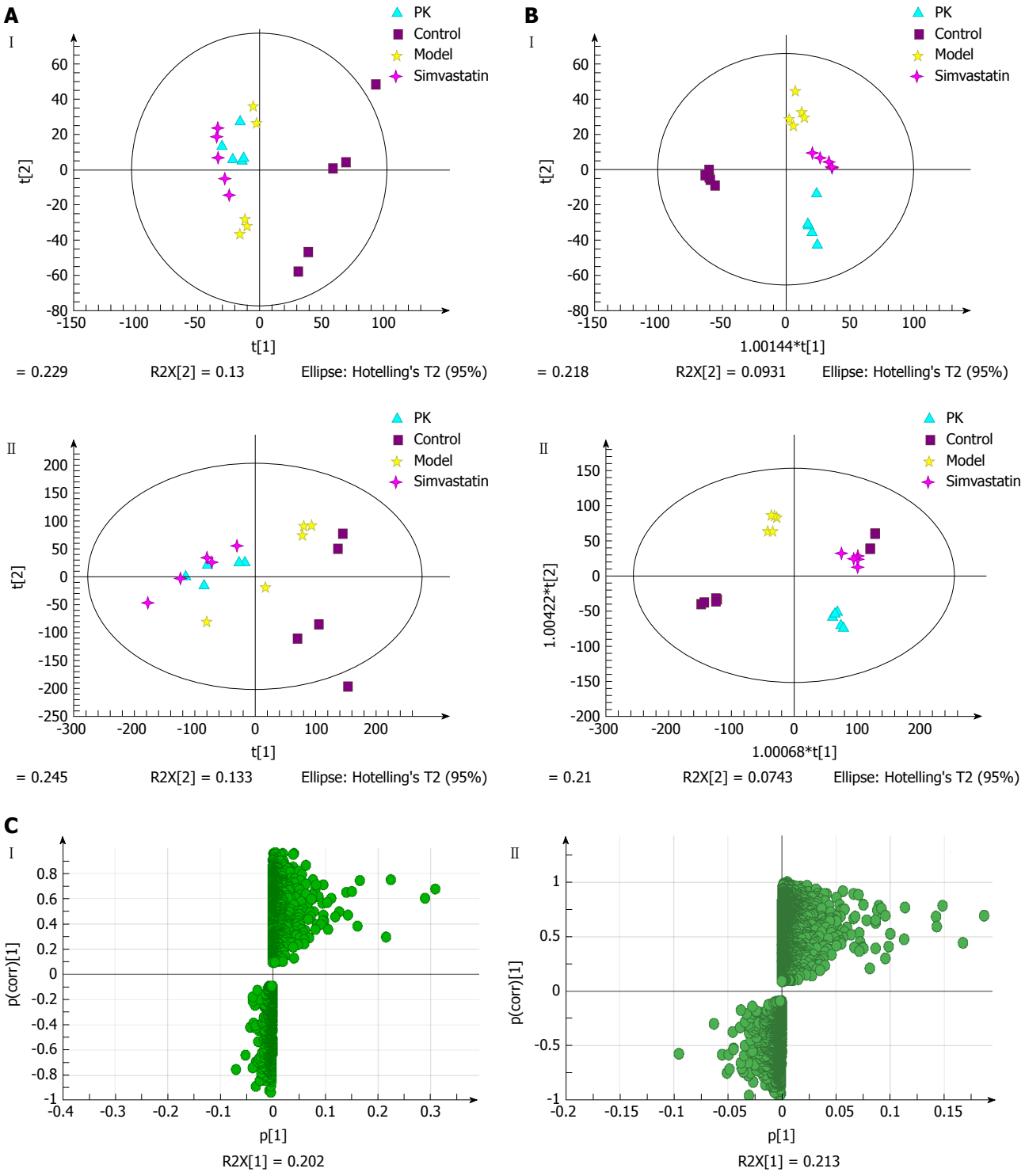

Figure 7 Multivariate statistical analysis of urine samples from model and *Polygonatum kingianum* groups in the negative (Ⅰ) and positive (Ⅱ) ion modes. A: Principal components analysis score plots; B: Orthogonal partial least squares discriminant analysis score plots; C: S-plot loading diagram. PK: *Polygonatum kingianum*.

Glycerophospholipid metabolism

Glycerophospholipid metabolism was involved in the serum samples. Phosphatidylcholine is the molecule from this pathway that was significantly changed after *P. kingianum* treatment. It is an important component of lipoproteins, a precursor of synthetic cholesterol and it facilitates cholesterol dissolution in bile[22]. Phosphatidylcholine can also disintegrate TGs and cholesterol in blood and in vascular walls, reducing lipid deposition in the vessel walls. It has been reported that people who eat a high-cholesterol diet with added phosphatidylcholine had lower blood cholesterol concentrations, supporting a hypolipidemic effect of phosphatidylcholine[23]. Fat is mainly transported by lipoprotein, while phospha-

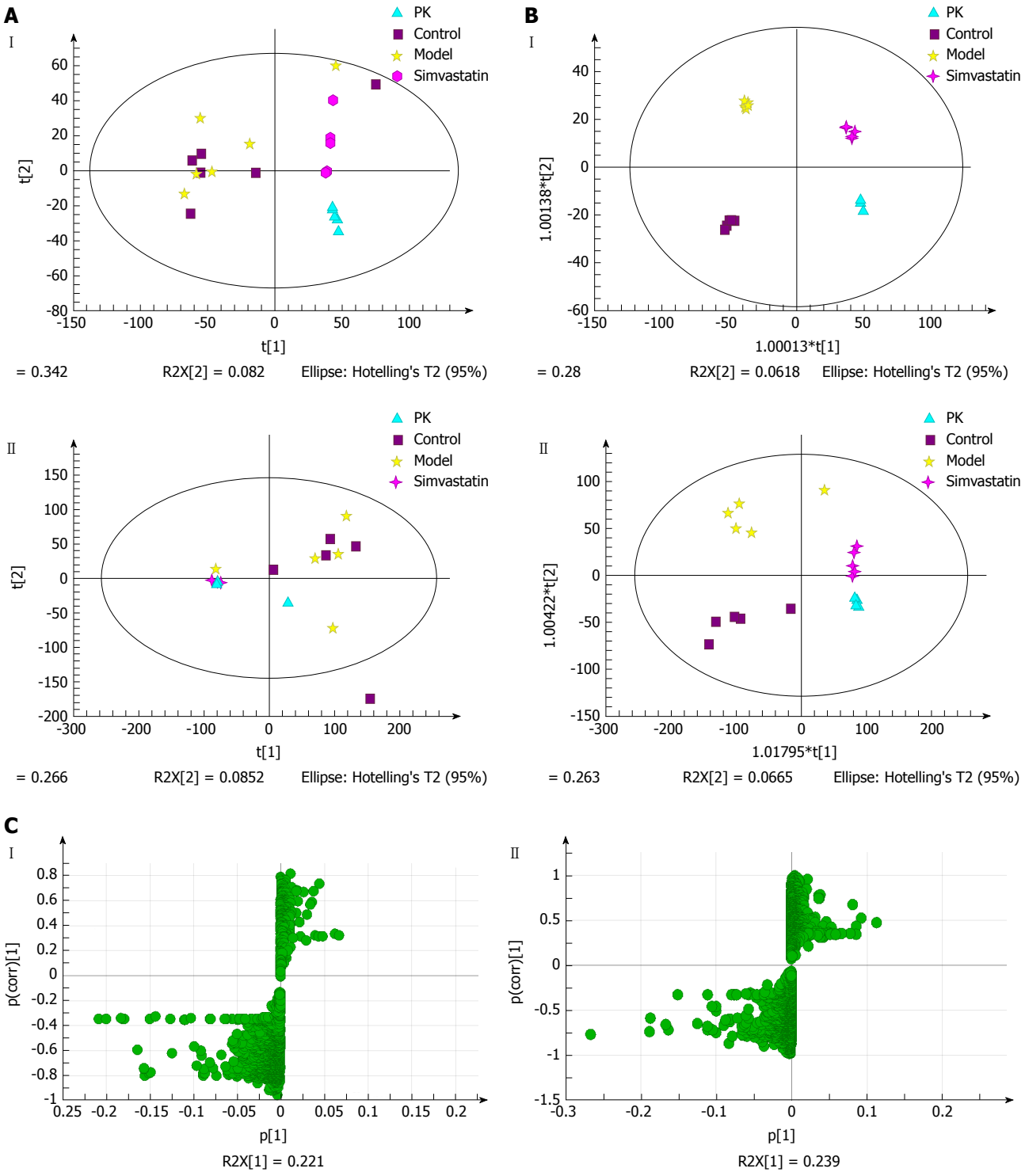

Figure 8 Multivariate statistical analysis of liver samples from model and *Polygonatum kingianum* groups in the negative (Ⅰ) and positive (Ⅱ) ion modes. A: Principal components analysis score plots; B: Orthogonal partial least squares discriminant analysis score plots; C: S-plot loading diagram. PK: *Polygonatum kingianum*.

tidylcholine is a vital substance for lipoprotein synthesis. Increased phosphatidylcholine content leads to accelerated hepatic lipoprotein synthesis, which potentiates TG conversion. Thus, insufficient hepatic phosphatidylcholine synthesis is an important contributor to fatty liver. We found that the phosphatidylcholine content was significantly increased after *P. kingianum* treatment, demonstrating that *P. kingianum* regulated glycerophospholipid metabolism to relieve dyslipidemia.

Arachidonic acid metabolism

Arachidonic acid metabolism was involved in the urine and liver samples, and was significantly changed by *P. kingianum* treatment. Cell stimulation results in decom-

Table 4 Potential biomarkers identified from serum samples

Retention time (min)	Molecular weight (Da)	VIP	Potential biomarker	Formula	Change trend Model-PKRP
ESI-					
0.928261	215.032	6.26699	2-C-Methyl-D-erythritol 4-phosphate	$C_5H_{13}O_7P$	down
8.30572	245.048	2.59774	Pimpinellin	$C_{13}H_{10}O_5$	down
17.7034	327.233	1.53493	3-Methyl-5-pentyl-2-furannonanoic acid	$C_{19}H_{32}O_3$	down
13.0574	437.291	1.03338	4,4'-Diaponeurosporene	$C_{30}H_{42}$	up
ESI+					
1.11629	132.102	21.806	Isoleucine	$C_6H_{13}NO_2$	down
0.997628	132.077	16.0576	3-Guanidinopropanoate	$C_4H_9N_3O_2$	up
1.0913	118.087	14.9589	Aminopentanoic acid	$C5H_{11}NO_2$	up
15.9773	496.338	14.2141	LysoPC(16:0)	$C_{24}H_{50}NO_7P$	up
2.1554	166.086	11.8849	L-Phenylalanine	$C_9H_{11}NO_2$	down
5.46147	205.097	10.6298	L-Tryptophan	$C_{11}H_{12}N_2O_2$	up
0.9767	203.053	10.4336	α-D-Glucose	$C_6H_{12}O_6$	down
18.5687	400.332	9.59788	Palmitoyl-L-carnitine	$C_{23}H_{45}NO_4$	down
1.09687	150.058	9.09347	L-Methionine	$C_5H_{11}NO_2S$	down
1.10844	182.081	8.07313	L-Tyrosine	$C_9H_{11}NO_3$	up
5.6576	202.086	6.72953	2'-Aminobiphenyl-2,3-diol	$C_{12}H_{11}NO_2$	down
6.83329	160.096	6.65796	4-Hydroxystachydrine	$C_7H_{13}NO_3$	up
0.960596	140.068	6.04106	Pentanoic acid	$C_5H_{11}NO_2$	down
15.0993	478.306	1.00334	1-Oleoyl lysophosphatidic acid	$C_{21}H_{41}O_7P$	down
10.4394	288.216	2.12052	L-Octanoylcarnitine	$C_{15}H_{29}NO_4$	down

VIP: Variable importance in the projection.

Table 5 Potential biomarkers identified from urine samples

Retention time (min)	Molecular weight (Da)	VIP	Potential biomarker	Formula	Change trend Model-PKRP
ESI-					
9.00895	213.113	1.42124	2,2'-(3-Methylcyclohexane-1,1-diyl) diacetic acid	$C_{11}H_{18}O_4$	up
3.93717	218.103	1.32234	Pantothenic acid	$C_9H_{17}NO_5$	up
14.0675	265.148	1.35019	Cumanin	$C_{15}H_{22}O_4$	up
1.11379	254.981	1.3057	Ascorbate-2-sulfate	$C_6H_8O_9S$	down
0.990052	308.099	1.2533	N-Acetylneuraminic acid	$C_{11}H_{19}NO_9$	down
3.03597	365.135	1.15211	Tetrahydropentoxyline	$C_{17}H_{22}N_2O_7$	down
17.8994	303.233	1.12374	Arachidonic acid	$C_{20}H_{32}O_2$	up
ESI+					
8.40988	173.117	1.51559	4-Hydroxynonenoic acid	$C_9H_{16}O_3$	up
6.14752	172.007	1.50165	L-Homocysteine sulfonic acid	$C_3H_9NO_3S_2$	up
10.4959	187.126	1.47714	1-Phenyl-5-propyl-1H-pyrazole	$C_{12}H_{14}N_2$	up
8.40656	155.106	1.46075	4-Oxo-2-nonenal	$C_9H_{14}O_2$	up
8.2458	190.115	1.44948	N6-Carbamoyl-DL-lysine	$C_7H_{15}N_3O_3$	up
1.89902	213.123	1.39163	Butethal	$C_{17}H_{22}N_2O_7$	up
13.7859	256.263	1.38483	Palmitic amide	$C_{16}H_{33}NO$	up
6.67969	172.097	1.34087	(3-Methylcrotonyl)glycine methyl ester	$C_8H_{13}NO_3$	up
17.9836	315.252	1.33499	9,10-DiHOME	$C_{18}H_{34}O_4$	up
3.91979	220.118	1.30061	Pantothenic acid	$C_9H_{17}NO_5$	up
7.08734	192.066	1.26102	5-Hydroxyindoleacetic acid	$C_{10}H_9NO_3$	up
0.839605	146.165	1.24838	Spermidine	$C_7H_{19}N_3$	up
0.924092	170.093	1.24502	1-Methylhistidine	$C_7H_{11}N_3O_2$	up
1.09509	189.123	1.23644	N-Alpha-acetyllysine	$C_8H_{16}N_2O_3$	up
9.40433	139.112	1.20585	2-Pentylfuran	$C_9H_{14}O$	up
7.33104	143.107	1.20454	2-Octenoic acid	$C_8H_{14}O_2$	up
3.91714	222.122	1.19506	Vinyl-L-NIO	$C_9H_{17}N_3O_2$	up

VIP: Variable importance in the projection.

position of arachidonic acid into a free form by phospholipase A2, with subsequent release into cytosol. The free form produces hundreds of bioactive metabolites by a series of metabolic enzymes. These metabolites have important regulatory effects on lipoprotein metabolism. Arachidonic acid closely relates to development of hyperlipidemia. In addition to effectively reducing blood lipids, it also decreases malondialdehyde. The latter reflects the degree of lipid peroxidation in tissue cells, indicating that arachidonic acid inhibits lipid peroxidation. Our

Table 6 Potential biomarkers identified from liver samples

Retention time (min)	Molecular weight (Da)	VIP	Potential biomarker	Formula	Change trend
					Model-PKRP
ESI-					
3.95787	218.103	9.02621	Pantothenic acid	$C_9H_{17}NO_5$	up
5.52016	203.082	5.17533	L-Tryptophan	$C_{11}H_{12}N_2O_2$	up
17.9144	303.232	2.67441	Arachidonic acid	$C_{20}H_{32}O_2$	up
8.18557	241.073	2.08795	Lumichrome	$C_{12}H_{10}N_4O_2$	down
17.6944	327.233	2.03102	Docosahexaenoic acid	$C_{22}H_{32}O_2$	down
9.27129	201.112	1.77891	Sebacic acid	$C10H18O_4$	down
18.1942	279.232	1.75755	Linoleic acid	$C_{18}H_{32}O2$	up
11.3188	464.302	1.75082	Glycocholic acid	$C_{26}H_{43}NO_6$	down
13.9455	313.24	1.66517	9,10-DiHOME	$C_{18}H_{34}O_4$	down
15.9588	319.227	1.58662	16R-HETE	$C_{20}H_{32}O_3$	up
7.08734	353.234	1.56066	PGE1	$C_{20}H_{34}O_5$	up
10.8984	227.128	1.45155	Traumatic acid	$C_{12}H_{20}O_4$	down
2.5168	251.079	1.41613	Deoxyinosine	$C_{10}H_{12}N_4O_4$	down
11.4285	221.081	1.39399	Apiole	$C_{12}H_{14}O_4$	down
16.2815	339.199	1.28069	Canrenone	$C_{22}H_{28}O_3$	down
11.4127	351.219	1.14883	PGE2	$C_{20}H_{32}O_5$	up
15.6357	343.228	1.0584	Medroxyprogesterone	$C_{22}H_{32}O_3$	down
19.0468	281.249	1.03242	Ethyl palmitoleate	$C_{18}H_{34}O_2$	down
ESI+					
5.58168	205.097	25.6421	L-Tryptophan	$C_{11}H_{12}N_2O_2$	up
1.12985	123.055	23.4569	Niacinamide	$C_6H_6N_2O$	up
3.94534	220.118	15.5283	Pantothenic acid	$C_9H_{17}NO_5$	down
1.07398	244.092	13.5445	Cytarabine	$C_9H_{13}N_3O_5$	down
1.65458	182.081	12.3842	L-Tyrosine	$C_9H_{11}NO_3$	up
0.901697	132.077	8.82297	3-Guanidinopropanoate	$C_4H_9N_3O_2$	down
0.990524	203.053	8.06945	L-(+)-Gulose	$C_6H_{12}O_6$	down
2.07851	269.088	7.66822	Inosine	$C_{10}H_{12}N_4O_5$	down
15.0942	302.305	7.59274	Sphinganine	$C_{18}H_{39}NO_2$	down
1.48196	153.04	7.19394	Xanthine	$C_5H_4N_4O_2$	down
6.38205	130.159	6.90221	Octylamine	$C_8H_{19}N$	down
1.21181	150.058	6.25979	L-Methionine	$C_5H_{11}NO_2S$	down
0.83538	146.165	6.24439	Spermidine	$C_7H_{19}N_3$	down
2.90983	285.083	5.64503	Xanthosine	$C_{10}H_{12}N_4O_6$	down
1.64612	165.055	5.16323	m-Coumaric acid	$C_9H_8O_3$	down
11.3366	181.122	4.58665	Dihydroactinidiolide	$C_{11}H_{16}O_2$	down
1.14382	204.123	4.29542	Succinylmonocholine	$C_9H_{17}NO_4$	down
2.20661	218.139	4.21655	Propionyl-L-carnitine	$C_{10}H_{19}NO_4$	down
5.73361	114.092	3.42289	ε-Caprolactam	$C_6H_{11}NO$	down
17.9613	305.248	1.8771	Arachidonic acid	$C_{20}H_{32}O_2$	up
13.2435	299.201	1.60893	Norethindrone	$C_{20}H_{26}O_2$	down
11.7171	181.122	1.58994	Dihydroactinidiolide	$C_{11}H_{16}O_2$	down

VIP: Variable importance in the projection.

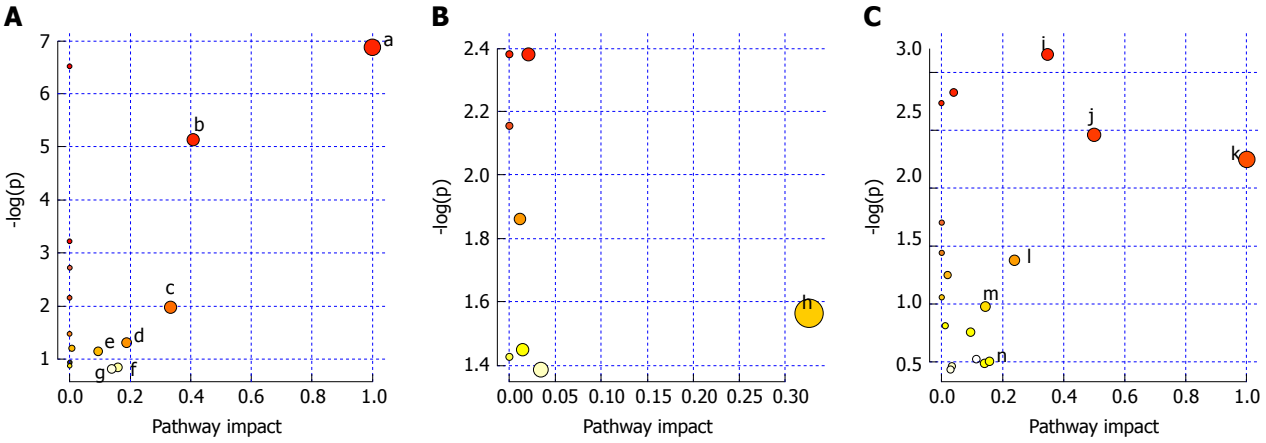

Figure 9 Analysis of metabolic pathways in serum (A), urine (B) and liver (C) samples. a: Phenylalanine, tyrosine and tryptophan biosynthesis; b: Phenylalanine metabolism; c: Valine, leucine and isoleucine biosynthesis; d: Starch and sucrose metabolism; e: Glycerophospholipid metabolism; f: Tryptophan metabolism; g: Tyrosine metabolism; h: Arachidonic acid metabolism; i: Arachidonic acid metabolism; j: Phenylalanine, tyrosine and tryptophan biosynthesis; k: Linoleic acid metabolism; l: Nicotinate and nicotinamide metabolism; m: Sphingolipid metabolism; n: Tryptophan metabolism; and o: Tyrosine metabolism.

Table 7 Results of metabolic pathway analysis of serum samples

No.	Pathway	Match status	*P* value	Impact	Details
1	Phenylalanine, tyrosine and tryptophan biosynthesis	2/4	8.19E-04	1.0	KEGG
2	Phenylalanine metabolism	2/9	0.0047415	0.40741	KEGG
3	Valine, leucine and isoleucine biosynthesis	1/11	0.126	0.33333	KEGG
4	Starch and sucrose metabolism	1/23	0.24635	0.18783	KEGG
5	Glycerophospholipid metabolism	1/30	0.30916	0.19753	KEGG
6	Tryptophan metabolism	1/41	0.39801	0.15684	KEGG
7	Tyrosine metabolism	1/42	0.40552	0.14045	KEGG

KEGG: Kyoto Encyclopedia of Genes and Genomes.

Table 8 Results of metabolic pathway analysis in urine samples

No.	Pathway	Match status	*P* value	Impact	Details
1	Arachidonic acid metabolism	1/36	0.20927	0.32601	KEGG

KEGG: Kyoto Encyclopedia of Genes and Genomes.

Table 9 Results of metabolic pathway analysis in liver samples

No.	Pathway	Match status	*P* value	Impact	Details
1	Arachidonic acid metabolism	3/36	0.042685	0.34677	KEGG
2	Phenylalanine, tyrosine and tryptophan biosynthesis	1/4	0.085643	0.5	KEGG
3	Linoleic acid metabolism	1/5	0.10592	1.0	KEGG
4	Nicotinate and nicotinamide metabolism	1/13	0.25318	0.2381	KEGG
5	Sphingolipid metabolism	1/21	0.37685	0.14286	KEGG
6	Tryptophan metabolism	1/41	0.60553	0.15684	KEGG
7	Tyrosine metabolism	1/42	0.61452	0.14045	KEGG

KEGG: Kyoto Encyclopedia of Genes and Genomes.

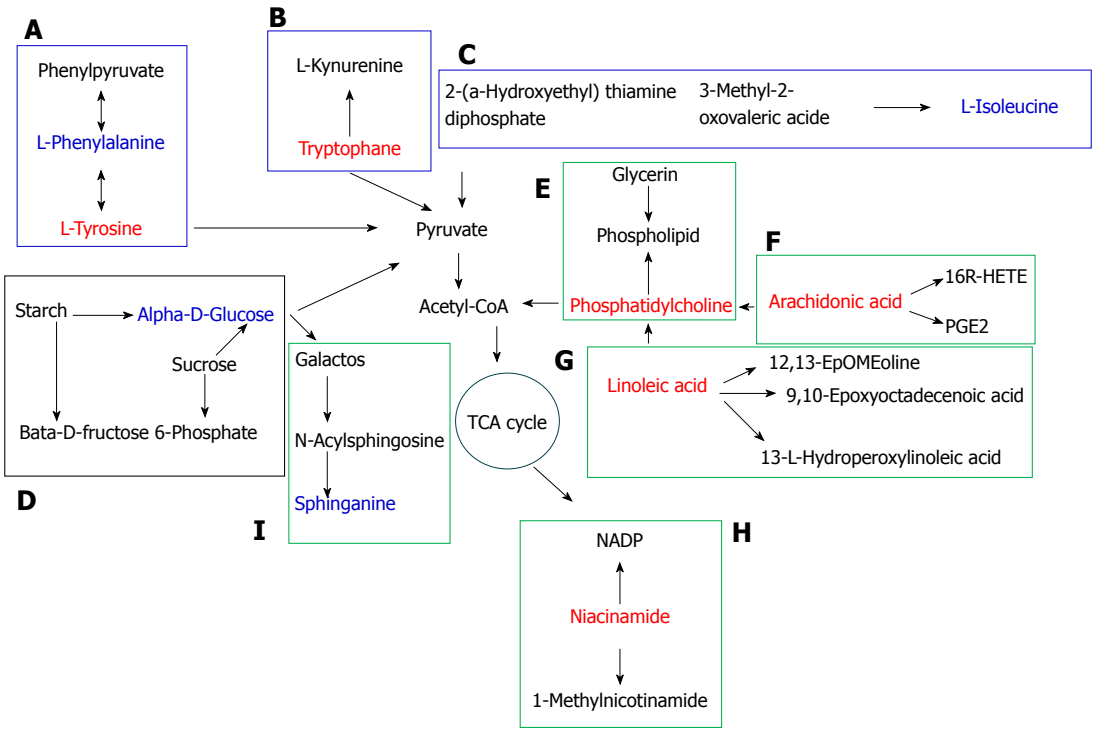

Figure 10 Metabolic pathway map of potential biomarkers. The red and blue font represents potential biomarkers that were up- and down-regulated by *Polygonatum kingianum* treatment, respectively. The blue, black and green box represents amino acid, sugar and lipid metabolism, respectively. A: Phenylalanine, tyrosine and tryptophan biosynthesis, and phenylalanine and tyrosine metabolism; B: Tryptophan metabolism; C: Valine, leucine and isoleucine biosynthesis; D: Starch and sucrose metabolism; E: Glycerophospholipid metabolism; F: Arachidonic acid metabolism; G: Linoleic acid metabolism; H: Nicotinate and nicotinamide metabolism; and I: Sphingolipid metabolism. TCA: Tricarboxylic acid.

results showed increased arachidonic acid in the urine and liver samples after *P. kingianum* treatment. Thus, *P. kingianum* regulated arachidonic acid metabolism to alleviate dyslipidemia.

Linoleic acid metabolism

Linoleic acid metabolism was involved in the liver samples, and linoleic acid was significantly altered with *P. kingianum* treatment. Previous studies found that linoleic acid accelerated fatty acid oxidation and glucose decomposition. Moreover, increased linoleic acid concentrations promoted proliferation and differentiation of fatty cells[24]. We found linoleic acid content to be significantly increased after *P. kingianum* administration, suggesting that *P. kingianum* regulated linoleic acid metabolism.

Niacin and nicotinamide metabolism

Niacin and nicotinamide metabolism was involved in the liver samples. Nicotinamide was the molecule from this pathway that was significantly altered by *P. kingianum* treatment. Nicotinamide is a metabolite produced by amidation of niacin. Niacin reduces synthesis of low density lipoprotein cholesterol, TC and TG, and increases synthesis of high density lipoprotein cholesterol. This indicates that niacin regulates lipid metabolism[25]. Our results showed that niacinamide content was increased by *P. kingianum* treatment. This suggests that *P. kingianum* increases niacin to alleviate dyslipidemia by regulating hepatic niacin and nicotinamide metabolism.

Sphingolipid metabolism

Sphingolipid metabolism was involved in the liver samples. Sphingolipids regulate important cellular functions, with metabolic abnormalities in these lipids closely related to various diseases. Previous studies found that obese individuals have disordered sphingolipid metabolism, which appears as accumulation of sphingolipids (*e.g.*, ceramide) in tissues and blood[26,27]. Sphingolipids can be metabolized to sphingosine. In our study, sphingosine content was decreased after *P. kingianum* treatment, suggesting that *P. kingianum* might decrease sphingolipid content to alleviate dyslipidemia by regulating hepatic sphingolipid metabolism.

Conclusion

Taken together, our data indicated that *P. kingianum* extract alleviated HFD-induced dyslipidemia by regulating a large number of endogenous metabolites in serum, urine and liver. This involved phenylalanine, tyrosine, tryptophan, valine, leucine and isoleucine biosynthesis, and tryptophan, tyrosine, phenylalanine, starch, sucrose, glycerophospholipid, arachidonic acid, linoleic acid, nicotinate, nicotinamide and sphingolipid metabolism. Thus, *P. kingianum* may be a promising lipid regulator to remedy dyslipidemia and further alleviate its related diseases.

ARTICLE HIGHLIGHTS

Research background

Dyslipidemia is an important risk factor for many vicious diseases such as diabetes and cardiovascular disease. Developing dyslipidemia regulators from traditional Chinese medicines (TCMs) to remedy lipid disorders represents attractive strategies for disease therapy. In China, *Polygonatum kingianum* (*P. kingianum*) has been used as an herb and nutritional food for centuries. Known pharmacological activities of *P. kingianum* include immune system stimulation, anti-aging effects and blood glucose regulation.

Research motivation

To date, studies on the effects of *P. kingianum* on dyslipidemia and the mechanism for these effects have not been investigated.

Research objectives

We aimed to identify the effects and mechanism of action of *P. kingianum* on dyslipidemia using an integrated untargeted metabolomic method.

Research methods

A rat model of dyslipidemia was induced with a high-fat diet (HFD) and rats were given *P. kingianum* [4 g/(kg•day)] intragastrically for 14 wk. Changes in serum and hepatic lipid parameters were evaluated. Metabolites in serum, urine and liver samples were profiled using ultra-high performance liquid chromatography/mass spectrometry followed by multivariate statistical analysis to identify potential biomarkers and metabolic pathways.

Research results

P. kingianum significantly inhibited the HFD-induced increase in total cholesterol and low density lipoprotein cholesterol in serum, and total cholesterol and triglyceride in the liver. *P. kingianum* also reduced hepatic high density lipoprotein cholesterol. *P. kingianum* significantly regulated metabolites in the analyzed samples toward normal status. Nineteen, twenty-four and thirty-eight potential biomarkers were identified in serum, urine and liver samples, respectively. These biomarkers involved 11 main metabolic pathways, including seven in serum and in the liver, and one in urine.

Research conclusions

P. kingianum alleviated HFD-induced dyslipidemia by regulating many endogenous metabolites in serum, urine and liver samples. This involved phenylalanine, tyrosine, tryptophan, valine, leucine and isoleucine biosynthesis, and tryptophan, tyrosine, phenylalanine, starch, sucrose, glycerophospholipid, arachidonic acid, linoleic acid, nicotinate, nicotinamide and sphingolipid metabolism.

Research perspectives

P. kingianum may be a promising lipid regulator to treat dyslipidemia and associated diseases.

REFERENCES

1 **Backstone RP.** Obesity-related diseases and syndromes: Insulin resistance, type 2 diabetes mellitus, non-alcoholic fatty liver disease, cardiovascular disease, and metabolic syndrome. In: Backstone RP. Obesity: The Medical Practitioner's Essential Guide. Cham: Springer, 2016; 83-108 [DOI: 10.1007/978-3-319-39409-1_5]

2 **Naheed DT,** Naheed T, Khan A. Dyslipidemias in type II diabetes mellitus patients in a teaching hospital of Lahore, Pakistan. *Pak J Med Sci* 2003; **19**: 283-286

3 **Athyros VG**, Doumas M, Imprialos KP, Stavropoulos K, Georgianou E, Katsimardou A, Karagiannis A. Diabetes and lipid metabolism. *Hormones* (Athens) 2018; **17**: 61-67 [PMID: 29858856 DOI: 10.1007/s42000-018-0014-8]

4 **Sirtori CR**. The pharmacology of statins. *Pharmacol Res* 2014; **88**: 3-11 [PMID: 24657242 DOI: 10.1016/j.phrs.2014.03.002]

5 **Caamaño BH**, Díaz JM, Bracho DG, Herrera H, Samur MC. Psychotic Acute Episode and Rhabdomyolysis after Lovastatin Ingestion. *Rev Colomb Psiquiatr* 2012; **41**: 672-679 [PMID: 26572120 DOI: 10.1016/S0034-7450(14)60037-8]

6 **Chan K**. Progress in traditional Chinese medicine. *Trends Pharmacol Sci* 1995; **16**: 182-187 [DOI: 10.1016/S0165-6147(00)89019-7]

7 **Yang XX,** Gu W, Liang L, Yan HL, Wang YF, Bi Q, Zhang T, Yu J, Rao GX. Screening for the bioactive constituents of traditional Chinese medicines-progress and challenges. *RSC Adv* 2017; **7**: 3089-3100 [DOI: 10.1039/c6ra25765h]

8 **Kwon HJ**, Hyun SH, Choung SY. Traditional Chinese Medicine improves dysfunction of peroxisome proliferator-activated receptor alpha and microsomal triglyceride transfer protein on abnormalities in lipid metabolism in ethanol-fed rats. *Biofactors* 2005; **23**: 163-176 [PMID: 16410638 DOI: 10.1002/biof.5520230305]

9 **Chen H,** Feng SS, Sun YJ, Yao ZY, Feng WS, Zheng XK. Advances in studies on chemical constituents of three medicinal plants from *Polygonatum* Mill. and their pharmacological activities. *Zhongcaoyao* 2015; **46**: 2329-2338

10 **Liu XQ,** Yi H, Yao L, Ma HW, Zhang JY, Wang ZM. Advances in plants of Polygonatum and discussion of its development prospects. *Zhongguo Yaoxue Zazhi* 2017; **52**: 530-534

11 **Lu JM**, Wang YF, Yan HL, Lin P, Gu W, Yu J. Antidiabetic effect of total saponins from *Polygonatum kingianum* in streptozotocin-induced daibetic rats. *J Ethnopharmacol* 2016; **179**: 291-300 [PMID: 26743227 DOI: 10.1016/j.jep.2015.12.057]

12 **Yan H**, Lu J, Wang Y, Gu W, Yang X, Yu J. Intake of total saponins and polysaccharides from *Polygonatum kingianum* affects the gut microbiota in diabetic rats. *Phytomedicine* 2017; **26**: 45-54 [PMID: 28257664 DOI: 10.1016/j.phymed.2017.01.007]

13 **Wang Z**, Zhang J, Ren T, Dong Z. Targeted metabolomic profiling of cardioprotective effect of *Ginkgo biloba* L. extract on myocardial ischemia in rats. *Phytomedicine* 2016; **23**: 621-631 [PMID: 27161403 DOI: 10.1016/j.phymed.2016.03.005]

14 **Tao Y**, Chen X, Li W, Cai B, Di L, Shi L, Hu L. Global and untargeted metabolomics evidence of the protective effect of different extracts of *Dipsacus asper* Wall. ex C.B. Clarke on estrogen deficiency after ovariectomia in rats. *J Ethnopharmacol* 2017; **199**: 20-29 [PMID: 28132861 DOI: 10.1016/j.jep.2017.01.050]

15 **Han W**, Li J, Tang H, Sun L. Treatment of obese asthma in a mouse model by simvastatin is associated with improving dyslipidemia and decreasing leptin level. *Biochem Biophys Res Commun* 2017; **484**: 396-402 [PMID: 28131832 DOI: 10.1016/j.bbrc.2017.01.135]

16 **Xie HH,** Xie T, Xu JY, Shen CS, Lai ZJ, Xu NS, Wang SC, Shan JJ. Metabolomics study of aconitine and benzoylaconine induced reproductive toxicity in BeWo cell. *Fenxi Huaxue* 2015; **43**: 1808-1813 [DOI: 10.1016/S1872-2040(15)60881-7]

17 **Chen H,** Yuan B, Miao H, Tan Y, Bai X, Zhao YY, Wang Y. Urine metabolomics reveals new insights into hyperlipidemia and therapeutic effect of rhubarb. *Anal Methods* 2015; **7**: 2113-3123 [DOI: 10.1039/c5ay00023h]

18 **Kaplowitz N**. Mechanisms of liver cell injury. *J Hepatol* 2000; **32**: 39-47 [PMID: 10728793 DOI: 10.1016/S0168-8278(00)80414-6]

19 **Holme E,** Mitchell GA. Tyrosine metabolism. In: Blau N, Duran M, Gibson K, Dionisi Vici C. ed. Physician's Guide to the Diagnosis, Treatment, and Follow-Up of Inherited Metabolic Diseases. Berlin, Heidelberg: Springer, 2014; 23-31 [DOI: 10.1007/978-3-642-40337-8_2]

20 **Owasoyo JO**, Neri DF, Lamberth JG. Tyrosine and its potential use as a countermeasure to performance decrement in military sustained operations. *Aviat Space Environ Med* 1992; **63**: 364-369 [PMID: 1599383]

21 **Catalano KJ**, Maddux BA, Szary J, Youngren JF, Goldfine ID, Schaufele F. Insulin resistance induced by hyperinsulinemia coincides with a persistent alteration at the insulin receptor tyrosine kinase domain. *PLoS One* 2014; **9**: e108693 [PMID: 25259572 DOI: 10.1371/journal.pone.0108693]

22 **Lagace TA**. Phosphatidylcholine: Greasing the Cholesterol Transport Machinery. *Lipid Insights* 2016; **8**: 65-73 [PMID: 27081313 DOI: 10.4137/LPI.S31746]

23 **Wang TJ**, Larson MG, Vasan RS, Cheng S, Rhee EP, McCabe E, Lewis GD, Fox CS, Jacques PF, Fernandez C, O'Donnell CJ, Carr SA, Mootha VK, Florez JC, Souza A, Melander O, Clish CB, Gerszten RE. Metabolite profiles and the risk of developing diabetes. *Nat Med* 2011; **17**: 448-453 [PMID: 21423183 DOI: 10.1038/nm.2307]

24 **West DB**, Delany JP, Camet PM, Blohm F, Truett AA, Scimeca J. Effects of conjugated linoleic acid on body fat and energy metabolism in the mouse. *Am J Physiol* 1998; **275**: R667-R672 [PMID: 9728060]

25 **Iwaki M**, Murakami E, Kakehi K. Chromatographic and capillary electrophoretic methods for the analysis of nicotinic acid and its metabolites. *J Chromatogr B Biomed Sci Appl* 2000; **747**: 229-240 [PMID: 11103908 DOI: 10.1016/S0378-4347(99)00486-7]

26 **Turinsky J**, O'Sullivan DM, Bayly BP. 1,2-Diacylglycerol and ceramide levels in insulin-resistant tissues of the rat in vivo. *J Biol Chem* 1990; **265**: 16880-16885 [PMID: 2211599]

27 **Samad F**, Hester KD, Yang G, Hannun YA, Bielawski J. Altered adipose and plasma sphingolipid metabolism in obesity: a potential mechanism for cardiovascular and metabolic risk. *Diabetes* 2006; **55**: 2579-2587 [PMID: 16936207 DOI: 10.2337/db06-0330]

P- Reviewer: Beltowski J **S- Editor**: Ma RY **L- Editor**: Wang TQ **E- Editor**: Yin SY

World Journal of Gastroenterology

Submit a Manuscript: https://www.f6publishing.com

World J Gastroenterol 2018 December 28; 24(48): 5525-5536

DOI: 10.3748/wjg.v24.i48.5525

ISSN 1007-9327 (print) ISSN 2219-2840 (online)

ORIGINAL ARTICLE

Retrospective Study

Safety of hepatitis B virus core antibody-positive grafts in liver transplantation: A single-center experience in China

Ming Lei, Lu-Nan Yan, Jia-Yin Yang, Tian-Fu Wen, Bo Li, Wen-Tao Wang, Hong Wu, Ming-Qing Xu, Zhe-Yu Chen, Yong-Gang Wei

Ming Lei, Lu-Nan Yan, Jia-Yin Yang, Tian-Fu Wen, Bo Li, Wen-Tao Wang, Hong Wu, Ming-Qing Xu, Zhe-Yu Chen, Yong-Gang Wei, Department of Liver Surgery, Liver Transplantation Center, West China Hospital of Sichuan University, Chengdu 610041, Sichuan Province, China

ORCID number: Ming Lei (0000-0001-7103-5700); Lu-Nan Yan (0000-0003-3603-3595); Jia-Yin Yang (0000-0003-2299-9188); Tian-Fu Wen (0000-0003-4668-4455); Bo Li (0000-0002-2124-7163); Wen-Tao Wang (0000-0002-9176-2718); Hong Wu (0000-0002-6329-2202); Ming-Qing Xu (0000- 0003-2442-5524); Zhe-Yu Chen (0000-0003-3506-0823); Yong-Gang Wei (0000-0003-0428-8366).

Author contributions: Lei M and Yan LN conceived and designed the study; Lei M and Yang JY analyzed the data; Lei M and Yan LN drafted the manuscript; Yan LN and Yang JY critically revised the manuscript; Yang JY, Wen TF, Li B, Wang WT, Wu H, Xu MQ, Chen ZY and Wei YG acquired the data and provided technical support; all authors have read and approved the final version to be published.

Institutional review board statement: This study was reviewed and approved by the Ethics Committee of the West China Hospital of Sichuan University.

Informed consent statement: Written informed consent was obtained from all participants.

Conflict-of-interest statement: All authors declare no conflicts of interest related to this article.

Data sharing statement: No additional data are available.

Manuscript source: Unsolicited manuscript

Corresponding author: Lu-Nan Yan, MD, Professor, Department of Liver Surgery, Liver Transplantation Center, West China Hospital of Sichuan University, 37 Guoxuexiang, Chengdu 610041, Sichuan Province, China. yanlunan688@126.com
Telephone: +86-28-85422867
Fax: +86-28-85422867

Received: November 9, 2018
Peer-review started: November 12, 2018
First decision: December 7, 2018
Revised: December 8, 2018
Accepted: December 13, 2018
Article in press: December 13, 2018
Published online: December 28, 2018

Abstract

BACKGROUND

Given the shortage of suitable liver grafts for liver transplantation, proper use of hepatitis B core antibody-positive livers might be a possible way to enlarge the donor pool and to save patients with end-stage liver diseases. However, the safety of hepatitis B virus core antibody positive ($HBcAb^+$) donors has been controversial. Initial studies were mainly conducted overseas with relatively small numbers of $HBcAb^+$ liver recipients, and there are few relevant reports in the population of mainland China. We hypothesized that the safety of $HBcAb^+$ liver grafts is not suboptimal.

AIM

To evaluate the safety of using hepatitis B virus (HBV) core antibody-positive donors for liver transplantation in Chinese patients.

METHODS

We conducted a retrospective study enrolling 1071 patients who underwent liver transplantation consecutively from 2005 to 2016 at West China Hospital Liver Transplantation Center. Given the imbalance in several baseline variables, propensity score matching was used, and the outcomes of all recipients were reviewed in this study.

RESULTS

In the whole population, 230 patients received HBcAb$^+$ and 841 patients received HBcAb negative (HBcAb$^-$) liver grafts. The 1-, 3- and 5-year survival rates in patients and grafts between the two groups were similar (patient survival: 85.8% *vs* 87.2%, 77.4% *vs* 81.1%, 72.4% *vs* 76.7%, log-rank test, P = 0.16; graft survival: 83.2% *vs* 83.6%, 73.8% *vs* 75.9%, 70.8% *vs* 74.4%, log-rank test, P = 0.19). After propensity score matching, 210 pairs of patients were generated. The corresponding 1-, 3- and 5-year patient and graft survival rates showed no significant differences. Further studies illustrated that the post-transplant major complication rates and liver function recovery after surgery were also similar. In addition, multivariate regression analysis in the original cohort and propensity score-matched Cox analysis demonstrated that receiving HBcAb$^+$ liver grafts was not a significant risk factor for long-term survival. These findings were consistent in both HBV surface antigen-positive (HBsAg$^+$) and HBsAg negative (HBsAg$^-$) patients.

Newly diagnosed HBV infection had a relatively higher incidence in HBsAg$^-$ patients with HBcAb$^+$ liver grafts (13.23%), in which HBV naive recipients suffered most (31.82%), although this difference did not affect patient and graft survival (P = 0.50 and P = 0.49, respectively). Recipients with a high HBV surface antibody (anti-HBs) titer (more than 100 IU/L) before transplantation and antiviral prophylaxis with nucleos(t)ide antiviral agents post-operation, such as nucleos(t)ide antiviral agents, had lower *de novo* HBV infection risks.

CONCLUSION

HBcAb$^+$ liver grafts do not affect the long-term outcome of the recipients. Combined with proper postoperative antiviral prophylaxis, utilization of HBcAb$^+$ grafts is rational and feasible.

Key words: Liver transplantation; Long-term outcome; Hepatitis B core antibody; Hepatitis B virus infection

Core tip: Considering the shortage of suitable liver grafts for liver transplantation, using hepatitis B virus core antibody positive (HBcAb$^+$) livers might be a possible way to enlarge the donor pool. However, the safety is controversial and not widely evaluated in Chinese patients. Our retrospective study enrolling 1071 patients found that HBcAb$^+$ grafts did not affect the long-term outcome. Although post-transplant hepatitis B virus (HBV) infection had a relatively higher incidence in HBV surface antigen-negative patients with such grafts, it did not affect patient and graft survival. We also found that sufficient anti-HBs titers in recipients might be a protective factor against *de novo* HBV infection. Combined with proper postoperative antiviral prophylaxis, utilization of HBcAb$^+$ grafts is feasible.

Lei M, Yan LN, Yang JY, Wen TF, Li B, Wang WT, Wu H, Xu MQ, Chen ZY, Wei YG. Safety of hepatitis B virus core antibody-positive grafts in liver transplantation: A single-center experience in China. *World J Gastroenterol* 2018; 24(48): 5525-5536
URL: https://www.wjgnet.com/1007-9327/full/v24/i48/5525.htm
DOI: https://dx.doi.org/10.3748/wjg.v24.i48.5525

INTRODUCTION

At present, liver transplantation is the only curative method for end-stage liver diseases. However, the limited organs available cannot meet the liver graft demand in Chinese patients. The shortage has promoted the enlargement of the donor pool, and accepting non-optimal livers offers a possibility to solve this troubling problem[1,2].

China is an area of high-intermediate hepatitis B virus (HBV) endemicity, with a prevalence of HBV infection close to 8%[3,4], and studies report that the number of HBV core antibody positive (HBcAb$^+$) liver grafts is up to 50% of the door pool[5-8]. However, liver grafts from HBcAb$^+$ donors carry the potential risk of HBV transmission, which limits the further use of such grafts, especially for patients naïve for HBV infection[9]. Indeed, several studies have found HBV covalently closed circular DNA (cccDNA) in some HBsAg$^-$ & HBcAb$^+$ liver grafts[5,7,10] and further verified the association between serum anti-HBc levels and intra-hepatic HBV cccDNA[11]. Thus, it is suggested that post-transplantation immunosuppression could trigger cccDNA and enhance its replication[12]. Additionally, early reports have confirmed the risk of post-transplantation HBV infection in HBcAb$^+$ liver graft recipients to be between 33% to 100%[7,10,13-17].

However, the lack of a larger study population[18-22], the wide variation in postoperative antiviral prophylaxis[7,20,21,23-25] and the clinical characteristics of the patients resulted in the availability of vague information concerning the risk of post-transplantation HBV infection in HBcAb$^+$ liver graft recipients. Moreover, the outcome of recipients receiving HBcAb$^+$ liver grafts has been discussed in previous studies with contradictory results. The survival rate of recipients with HBcAb$^+$ donors was lower than that of recipients with anti-HBc negative donors in two United States studies[19,26] in 1997 and was confirmed in another investigation 5 years later[18]. However, in a similar Spanish study, the difference in survival was not statistically significant (68% *vs* 76%, $P > 0.05$)[27]. And a UNOS-based study conducted in 2009[17] found that HBsAg$^-$ recipients receiving HBcAb$^+$ liver grafts had a significantly worse unadjusted graft survival, but the difference disappeared in multivariable

analysis. Furthermore, studies concerning the risk of post-transplantation HBV infection and the long-term graft and patient survival in HBcAb$^+$ liver graft recipients were mainly conducted overseas, and there are few relevant reports on the population of mainland China. Herein, we conducted a retrospective study enrolling 1071 patients who consecutively underwent liver transplantation from 2005 to 2016 in the Chinese population and aimed to evaluate the safety of utilization of HBcAb$^+$ liver grafts in a relatively large number of patients.

MATERIALS AND METHODS

Patients and data collection

This retrospective study concerns 1112 Chinese patients who consecutively underwent liver transplantation from 2005 to 2016 performed at the West China Hospital Liver Transplantation Center. Re-transplantation and multi-organ transplantation were excluded. We also did not include liver transplantations using HBV surface antigen-positive (HBsAg$^+$) and HCV-positive donors. All liver grafts were voluntarily donated after cardiac death or by living donors, and all donations were approved by the West China Hospital Ethics Committee in accordance with the ethical principles of the 1975 Declaration of Helsinki. Written informed consent was given by all participants, and those receiving HBcAb$^+$ liver grafts were fully informed of the possible risks before transplantation. Basic information of liver transplantations, the outcome and follow-up results were derived from The China Liver Transplant Registry.

Post-transplant therapy

Antiviral prophylaxis was given to all HBV-positive recipients, consisting of hepatitis B immunoglobulin (HBIG) and/or lamivudine or entecavir. A dosage of 2000 IU HBIG was intramuscularly injected during the anhepatic phase, followed by 800 IU intramuscularly daily for the first week, and then weekly for 3 wk, and monthly thereafter[28-30]. These patients maintained HBV prophylaxis indefinitely.

In HBV-negative recipients, considering that there were no practice guidelines on prophylaxis of *de novo* hepatitis B in China until 2016[31], the post-transplant antiviral prophylaxis varied from different periods. Generally, HBIG was administered to all patients the same way as in HBV-positive recipients, but the lasting time varied from 1-6 mo. Eighteen patients additionally received nucleos(t)ide analogue reverse transcriptase inhibitors (nRTI) including lamivudine (used in 15 patients), tenofovir (used in 1 patient) and entecavir (used in 2 patients).

The immunosuppressive therapy followed standard protocols, consisting of corticosteroids, tacrolimus and mycophenolate (1.0 g/d to 1.5 g/d) according to our previous report[32]. Methylprednisolone was started at a dose of 200 mg daily and was generally withdrawn within 3 mo. Tacrolimus was started at a dose of 0.05-0.10 mg/kg per day and was adjusted on the basis of liver function and trough concentration[32].

Post-transplant follow-up monitoring

All recipients were followed until June 2018 or until death or withdrawal. Patients were monitored regularly after liver transplantation, including clinical, biochemical and virological testing. Ultrasound examination was conducted every day for 2 wk after the operation and every month after discharge, with computed tomography performed every half a year[33].

Definitions of some clinical terms

HBV DNA > 100 copies/mL was detectable. Recurrence of HBV infection was defined as a detectable serum HBsAg and/or viral load (HBV DNA) in patients who were HBsAg positive at the time of transplantation, and *de novo* HBV infection was defined as a detectable serum HBsAg and/or viral load (HBV DNA) in patients without positive serum HBsAg or viral load before transplantation.

Primary non-function was defined according to criteria described by Ploeg *et al*[34] as a graft with poor initial function requiring re-transplantation or leading to death within 7 d after the primary procedure without any identifiable cause of graft failure[34]. Acute rejection was defined either by liver biopsy or recovery of liver function *via* high-dose methylprednisolone therapy[32]. If chronic rejection was suspected, liver biopsy was performed for confirmation[32].

Statistical analysis

Since some continuous covariates presented significant differences from the normal distribution, they are shown as medians and first and third quartiles. Categorical variables are described as absolute numbers and relative frequencies. For continuous variables, either the Mann-Whitney *U*-test or Student's-*t* test were performed, and the differences between rates were tested using the Chi square test or Fisher's exact test, if appropriate. The Kaplan-Meier method with log-rank test was used for cumulative survival analysis. Independent prognostic factors were identified using multivariate analysis based on the Cox proportional hazards model. The assumption for proportional hazard was evaluated using scaled Schoenfeld residuals.

Given the differences in the baseline characteristics between the two groups (Table 1), propensity score matching was used to balance out selection bias and potential confounding between the two groups[35]. Propensity scores were estimated using a non-parsimonious multivariable logistic regression model, which included all covariates that might have affected patient assignment to different groups. A nearest-neighbor 1:1 matching scheme with a caliper width of 0.1 was used for propensity score matching[36]. Statistical inference was performed in the matched cohort with the use of a Cox proportional-hazards regression model stratified on the matched pair to preserve the benefit of matching[36].

Table 1 Baseline clinical data between hepatitis B virus core antibody positive and hepatitis B virus core antibody negative liver graft recipients

Factor	Before propensity matching			After propensity matching		
	HBcAb$^+$ (n = 230)	HBcAb$^-$ (n = 841)	P value	HBcAb$^+$ (n = 210)	HBcAb$^-$ (n = 210)	P value
Baseline characteristic						
Gender (male)	77.4% (178)	80.10% (674)	0.36	80.5% (169)	79.5% (167)	0.90
Age (yr)	41.03 ± 15.58	42.04 ± 15.19	0.63	40.67 ± 16.57	40.55 ± 15.47	0.94
BMI	22.1 (19.7-24.2)	22.0 (19.8-24.4)	0.54	22.4 (19.7-24.4)	22.2 (19.7-24.2)	0.8
MELD	13.0 (9.0-21.0)	13.0 (9.0-20.0)	0.62	14.5 (10.0-20.8)	13.0 (9.0-20.0)	0.25
CTP	9.0 (7.0-11.0)	8.0 (7.0-10.0)	< 0.01	9.0 (7.0-11.0)	9.0 (7.0-11.0)	0.14
Creatinine (μmol/L)	67.0 (53.1-81.9)	71.9 (59.3-85.3)	< 0.01	68.4 (55.9-82.6)	67.5 (53.6-82.4)	0.36
Total bilirubin (μmol/L)	43.2 (18.8-198.3)	37.8 (18.9-139.9)	0.31	51.2 (22.8-201.9)	40.2 (18.6-195.0)	0.20
Albumin (g/L)	35.4 (30.9-40.5)	34.6 (30.1-40.1)	0.11	33.8 (30.1-40.1)	35.4 (31.1-41.3)	0.06
HBV-positive	64.78% (149)	77.28% (650)	< 0.01	62.9% (132)	69.0% (145)	0.18
HCV-positive	1.3% (3)	7.4% (62)	< 0.01	0.95% (2)	3.33% (7)	0.18
Etiology						
Liver cancer	48.26% (111)	46.13% (388)	0.57	43.3% (91)	49.5% (104)	0.20
Acute liver failure	11.30% (26)	4.99% (42)	< 0.01	8.57% (18)	11.4% (24)	0.32
Cirrhosis						
Biliary	9.13% (21)	7.84% (66)	0.53	8.57% (18)	9.05% (19)	0.86
HBV related	49.13% (113)	55.41% (466)	0.09	56.19% (118)	54.76% (15)	0.76
HCV related	0.86% (2)	1.90% (16)	0.28	0.95% (2)	2.38% (5)	0.45
Alcoholic	2.17% (5)	3.21% (27)	0.41	1.90% (4)	0.95% (2)	0.69
Autoimmune	1.74% (4)	1.07% (9)	0.41	0.95% (2)	0.95% (2)	1.00
Donor						
Gender (male)	74.35% (171)	79.30% (666)	0.12	61.4% (129)	61.9% (130)	0.92
Age	41.28 ± 13.01	33.66 ± 10.16	< 0.01	39.08 ± 10.59	40.82 ± 12.36	0.12
BMI	22.7 (20.8-24.6)	22.2 (20.8-23.9)	0.06	22.8 (21.4-24.8)	22.6 (20.8-24.5)	0.37
Serum Na$^+$ (mmol/L)	143.0 (140.1-153.6)	139.9 (136.2-142.7)	< 0.01	141.6 (138.5-143.9)	141.9 (140.0-153.5)	0.23
Creatinine (μmol/L)	73.1 (54.5-98.5)	74.6 (62.8-84.6)	< 0.01	75.3 (63.0-88.5)	74.4 (54.0-95.6)	0.39
Total bilirubin (μmol/L)	13.8 (9.4-18.9)	15.1 (10.2-23.3)	0.05	14.9 (10.1-21.7)	13.8 (9.4-18.7)	0.25
Albumin (g/L)	40.3 (32.6-45.3)	41.9 (36.2-46.6)	0.06	42.1 (36.2-46.7)	41.8 (34.9-46.0)	0.12
ALT (IU/L)	23.0 (16.0-45.0)	28.0 (16.0-47.0)	0.32	27.0 (17.8-46.2)	26.0 (16.0-43.0)	0.10
AST (IU/L)	27.0 (20.8-42.0)	26.0 (18.0-39.0)	0.15	27.0 (19.0-39.8)	27.5 (20.0-47.0)	0.12
Cold ischemic time (h)	5.0 (3.2-7.8)	6.0 (5.0-10.0)	0.05	5.5 (4.0-8.0)	5.5 (3.0-7.0)	0.11
Warm ischemic time (min)	6.0 (3.0-9.0)	4.5 (2.0-6.5)	0.05	6.0 (3.0-10.0)	5.0 (3.0-7.0)	0.08

Data are shown as the mean ± SD or medians with 25th-75th interquartile ranges when presenting significant differences from the normal distribution. For continuous variables, either the Mann-Whitney U-test or Student's-*t* test was performed, and the differences between rates were tested by Chi square test or Fisher exact test, if appropriate. CTP: Child-Pugh score; ALT: Glutamic-pyruvic transaminase; AST: Glutamic oxaloacetic transaminase; MELD: Model for end-stage liver disease.

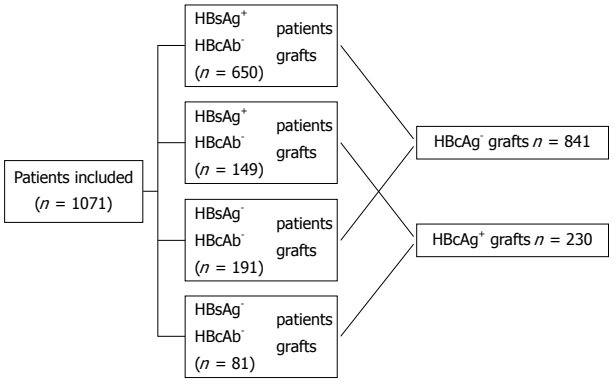

Figure 1 Flow diagram showing the allocation of hepatitis B virus core antibody positive liver grafts and hepatitis B virus surface antigen status in the whole cohort.

Analyses were further performed on the basis of HBsAg status of the recipients (HBsAg$^+$ and HBsAg$^-$ recipients). Propensity score matching was also conducted in HBsAg$^+$ and HBsAg$^-$ cohorts. The statistical methods of this study were reviewed by Jia-Wei Luo from West China School of Public Health, Sichuan University.

All reported *P*-values are two-sided, and *P*-values less than 0.05 were considered statistically significant. All data were analyzed using SPSS22.0 (IBM Corporation, Armonk, NY, United States) and R statistical software, version 2.3.15 (R Foundation, Inc.; http://cran.r-project.org/).

RESULTS

Study population and clinical characteristics

From 2005 to 2016, 1071 liver transplantation patients met our inclusion criteria, of which 230 patients received HBcAb$^+$ liver grafts and 841 patients received HBcAb$^-$ liver grafts. The median following time was 48.72 ± 33.37 mo (range from 0.1 to 128.1 mo). In these patients, 799 were HBsAg$^+$ (149 receiving HBcAb$^+$ liver grafts and 650 receiving HBcAb$^-$ liver grafts), and 272 were HBsAg$^-$ (81 receiving HBcAb$^+$ liver grafts and 191 receiving HBcAb$^-$ liver grafts) at the time of transplantation. A flow diagram of patient disposition is shown in Figure 1.

The clinical data of the recipients and donors between

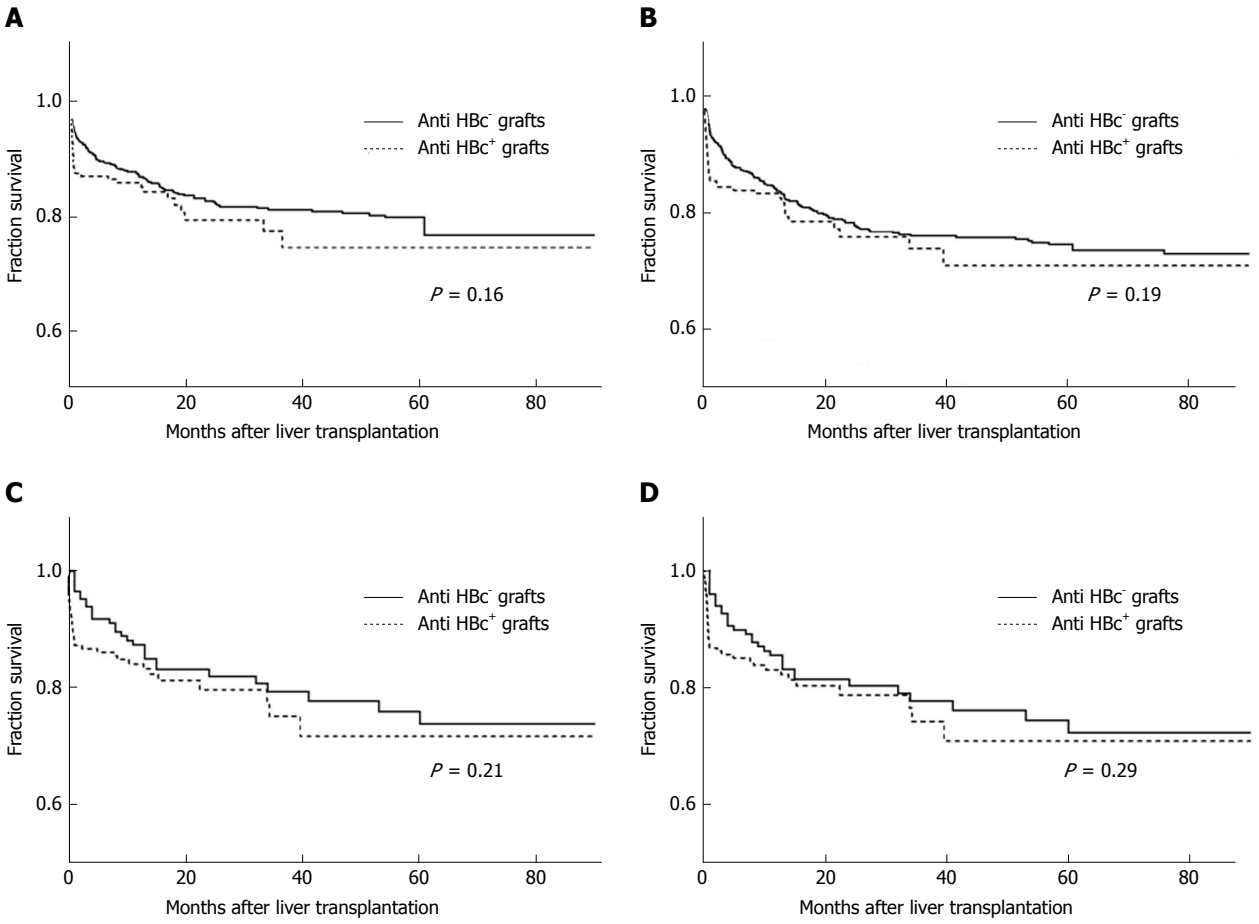

Figure 2 Patient survival and graft survival analysis of anti-hepatitis B core positive liver graft recipients and anti-hepatitis B core negative liver graft recipients. A: Patient survival in original cohort (n = 1071); B: Graft survival in original cohort (n = 1071); C: Patient survival in propensity score-matched cohort (n = 420); D: Graft survival in propensity score-matched cohort (n = 420).

the two groups are summarized in Table 1. There were differences between the two groups in several baseline variables. For example, recipients of HBcAb$^+$ grafts had a lower HBsAg$^+$ rate (64.78% *vs* 77.28%, $P < 0.01$) and a lower HCV-positive rate (1.3% *vs* 7.4%, $P < 0.01$). HBcAg+ donors were relatively older than HBcAg- donors (41.28 ± 13.01 *vs* 33.66 ± 10.16, $P < 0.01$). With the utilization of propensity score matching, 210 pairs of patients were generated, and the characteristics of the two groups were balanced (Table 1).

Postoperative mortality

In the original cohort, which included 1071 patients, the 1-, 3- and 5-year survival rates between the HBcAb$^+$ and HBcAb$^-$ liver graft recipients were similar (85.8%, 77.4% and 72.4% *vs* 87.2%, 81.1% and 76.7%, log-rank test, χ^2 = 1.97, P = 0.16, Figure 2A). Meanwhile, graft survival rates between the two groups were also comparable (83.2%, 73.8% and 70.8% *vs* 83.6%, 75.9% and 74.4%, log-rank test, χ^2 = 1.65, P = 0.19, Figure 2B). Propensity score matching was used for the differences in several baseline variables between the two groups as noted above, and the 1-, 3- and 5-year patient survival rates in the new HBcAb$^+$ and HBcAb$^-$ groups presented no significant differences (84.1%, 75.2% and 71.7% *vs* 87.4%,79.4% and 73.8%, log-rank test, χ^2 = 1.53, P = 0.21, Figure 2C). The corresponding 1-, 3- and 5-year graft survival rates in the HBcAb$^+$ group were 83.1%,74.3% and 70.7% compared with 85.6%, 77.8% and 72.3% in the controls (log-rank test, χ^2 = 1.10, P = 0.29, Figure 2D).

In HBsAg$^+$ patients, HBcAb$^+$ liver grafts did not have deleterious effects on survival when compared with HBcAb$^-$ grafts (log-rank test, χ^2 = 1.59, P = 0.20, Supplement Figure 1A), similar to the HBsAg$^-$ recipients (log-rank test, χ^2 = 0.81, P = 0.37, Supplement Figure 1B).

To identify the independent prognostic factors, Cox regression analysis was conducted in the whole cohort, and multivariate regression analysis showed that a higher BMI in the recipients was a strong indicator for worse patient (P = 0.001) and graft survival (P = 0.001) (Table 2). Blood transfusion amount and mechanical ventilation time were also shown as risk factors both for patient (P = 0.018 and 0.002, respectively) and graft survival (P = 0.021 and P = 0.004, respectively) (Table 2). However, parallel to the results of the survival curves, the multivariate regression analysis did not support HBcAb$^+$ liver grafts as an independent risk factor for death or graft loss after liver transplantation (P = 0.675 and P = 0.982, Table 2).

Table 2 Multivariable Cox analysis for patient and graft survival in the original cohort (n = 1071)

	Patient survival				Graft survival			
Equation variable	***P* value**	**HR**	**95%CI**		***P* value**	**HR**	**95%CI**	
Recipient								
BMI	0.001	1.006	1.002	1.010	0.001	1.007	1.002	1.011
MELD	0.942	1.002	0.948	1.059	0.912	1.003	0.949	1.059
CTP	0.429	1.049	0.835	1.263	0.398	1.046	0.834	1.258
HBsAb (negative *vs* positive)	0.208	1.058	0.768	1.347	0.258	1.027	0.739	1.374
Operation								
Anhepatic phase (min)	0.271	1.003	0.997	1.01	0.169	1.004	0.998	1.011
RBC transfusion (U)	0.018	1.055	1.009	1.104	0.021	1.052	1.006	1.103
After operation								
Mechanical ventilation (h)	0.002	1.003	1.001	1.006	0.004	1.004	1.001	1.006
Postoperative HBV infection (negative *vs* positive)	0.502	0.597	0.132	2.695	0.490	0.527	0.118	2.340
Donor								
Age	0.215	1.015	0.991	1.042	0.155	1.018	0.992	1.045
AST (IU/L)	0.65	1.002	0.993	1.011	0.563	1.002	0.994	1.011
Na (mmol/L)	0.243	1.016	0.988	1.045	0.408	1.011	0.983	1.041
Anti HBc-positive (negative *vs* positive)	0.675	1.175	0.551	2.505	0.982	1.008	0.480	2.118

HR: Hazard ratio; CTP score: Child-Pugh score; WIT: Warm ischemic time Na: Donor's serum Na^+ concentration.

Table 3 Multivariable Cox analysis and propensity score-matched analysis of patient survival

Group	**No. of patients**	**HR (95%CI)**	***P* value**
Entire cohort, multivariable-adjusted (n = 1071)			
HbcAb-positive grafts	230	1.18 (0.55,2.51)	0.68
HbcAb-negative grafts	841	Reference	
Entire cohort, propensity score-matched (n = 210 pairs)			
HbcAb-positive grafts	210	1.21 (0.73,2.03)	0.45
HbcAb-negative grafts	210	Reference	
HBsAg-positive cohort, multivariable-adjusted (n = 799)			
HbcAb-positive grafts	149	1.07 (0.98,1.17)	0.12
HbcAb-negative grafts	650	Reference	
HBsAg-positive cohort, propensity score-matched (n = 132 pairs)			
HbcAb-positive grafts	132	1.06 (0.93,1.20)	0.37
HbcAb-negative grafts	132	Reference	
HBsAg-negative cohort, multivariable-adjusted (n = 272)			
HbcAb-positive grafts	81	1.42 (0.71,2.81)	0.32
HbcAb-negative grafts	191	Reference	
HBsAg-negative cohort, propensity score-matched (n = 77 pairs)			
HbcAb-positive grafts	77	1.37 (0.60,3.14)	0.45
HbcAb-negative grafts	77	Reference	

Propensity score-matched analysis also revealed that receiving HBcAb$^+$ liver grafts was not associated with a significantly higher risk of death (Cox regression analysis, P = 0.45, 95%CI: 0.73-2.03, Table 3).

Consistent with the above results, both multivariate regression analysis in the original cohort and propensity score-matched Cox analysis did not support that receiving HBcAb positive liver grafts was associated with worse outcome for either HBsAg$^+$ or HBsAg$^-$ patients (Table 3).

During the observation period, 21 patients died in the entire cohort within 30 d. In patients receiving HBcAb$^+$ liver grafts, 5 patients died because of multi-organ failure with sepsis and 3 patients died of abdominal hemorrhage, while in the HBcAb$^-$ group, patients died within 30 d because of multi-organ failure with sepsis (n = 8), liver failure due to portal vein embolism (n = 2) and abdominal hemorrhage (n = 3). The death rates within 30 d of the two groups were not significantly different [Chi square test, 3.47% (8/230) *vs* 1.54% (13/841), P = 0.10]. None of the causes of death were HBV-related.

Postoperative complications

In the post-transplant observation, no differences between HBcAb$^+$ and HBcAb$^-$ graft recipients were observed in rates of major complications in either the early stage (within 30 d post LT) or the later period (beyond 30 d post LT; Tables 4 and 5)

In the entire cohort, 3 patients with HBcAb$^+$ liver graft underwent re-transplantations for primary non-function (n = 1), biliary complications (n = 1) and portal vein embolism (n = 1), while 7 recipients in the HBcAb$^-$ group underwent re-transplantations for primary non-function (n = 1), biliary complications (n = 2), portal vein embolism (n = 1) and hepatic artery embolism (n =

Table 4 Early stage major complications after operation between hepatitis B virus core antibody positive liver graft recipients and hepatitis B virus core antibody negative liver graft recipients (within 30 d post liver transplantation) %

Major complication	Before propensity matching			After propensity matching		
	Anti-HBc$^+$ (n = 230)	Anti-HBc$^-$ (n = 841)	P value	Anti-HBc$^+$ (n = 210)	Anti-HBc$^-$ (n = 210)	P value
Primary non-function	0.43 (1/230)	0.24 (2/841)	0.52	0	0	1.00
Biliary complications	0.87 (2/230)	1.30 (11/841)	0.75	0.47 (1/210)	0.47 (1/210)	1.00
Hepatic artery stenosis/embolism	2.61 (6/230)	1.54 (13/841)	0.26	2.38 (5/210)	1.43 (3/210)	0.72
Portal vein stenosis/embolism	3.91 (9/230)	2.49 (21/841)	0.25	3.33 (7/210)	0.95 (2/210)	0.17
Outflow tract stenosis/embolism	0.87 (2/230)	0.36 (3/841)	0.29	0.47 (1/210)	0.47 (1/210)	1.00
Bacterial infection	21.30 (49/230)	20.33 (171/841)	0.75	8.10 (17/210)	7.62 (16/210)	0.85
Intra-abdominal hemorrhage	7.39 (17/230)	5.35 (45/841)	0.24	5.24 (11/210)	2.38 (5/210)	0.20
Pleural effusion	10.86 (25/230)	15.21 (128/841)	0.09	5.71 (12/210)	3.33 (7/210)	0.24
Celiac effusion	11.74 (27/230)	14.86 (125/841)	0.23	7.62 (16/210)	8.10 (17/210)	0.85
Pneumonedema	0.43 (1/230)	0.36 (3/841)	> 0.9	0.47 (1/210)	0.47 (1/210)	1.00

Differences between rates were tested by Chi-square test or Fisher exact test, if appropriate.

Table 5 Later period major complications after operation between hepatitis B virus core antibody positive liver graft recipients and hepatitis B virus core antibody negative liver graft recipients (beyond 30 d post liver transplantation) %

Major complication	Before propensity matching			After propensity matching		
	Anti-HBc$^+$ (n = 230)	Anti-HBc$^-$ (n = 841)	P value	Anti-HBc$^+$ (n = 210)	Anti-HBc$^-$ (n = 210)	P value
Acute rejection	11.30 (26/230)	11.05 (93/841)	0.91	9.52 (20/210)	8.10 (17/210)	0.60
Chronic rejection	0.87 (2/230)	0.95 (8/841)	> 0.9	0.95 (2/210)	0.95 (2/210)	1.00
GVHD	0.43 (1/230)	0.59 (5/841)	> 0.9	0.47 (1/210)	0.47 (1/210)	1.00
Biliary complications	9.56 (22/230)	9.15 (77/841)	0.85	7.14 (15/210)	10.95 (23/210)	0.17
Hepatic artery stenosis/embolism	0.87 (2/230)	0.71 (6/841)	0.68	0.95 (2/210)	2.38 (5/210)	0.45
Portal vein stenosis/embolism	0.87 (2/230)	1.78 (15/841)	0.55	0.95 (2/210)	0.95 (2/210)	1.00
Outflow tract stenosis/embolism	0.43 (1/230)	0.71 (6/841)	> 0.9	0.47 (1/210)	0.47 (1/210)	1.00
Tumor recurrence	5.65 (13/230)	4.52 (38/841)	0.51	4.76 (10/210)	6.19 (13/210)	0.52
CMV infection	0.87 (2/230)	0.83 (7/841)	> 0.9	0.95 (2/210)	1.90 (4/210)	0.68
Opportunistic infection	2.17 (5/230)	1.43 (12/841)	0.38	1.43 (3/210)	2.38 (5/210)	0.72
Diabetes mellitus	7.82 (18/230)	7.97 (67/841)	0.94	7.14 (15/210)	4.76 (10/210)	0.3
Hypertension	4.78 (11/230)	3.57 (30/841)	0.39	3.33 (7/210)	2.38 (5/210)	0.77
Hyperlipemia	0.43 (1/230)	0.95 (8/841)	0.69	0.47 (1/210)	1.90 (4/210)	0.37

Differences between rates were tested by Chi square test or Fisher exact test, if appropriate. CMV: Cytomegalovirus; GVHD: Graft-*vs*-host disease.

3). The re-transplantation rates of the two groups were 1.30% (3/230) and 0.83% (7/841), without a significant difference (Fisher exact test, P = 0.45).

Furthermore, postoperative follow-up showed that there was no significant difference in liver function recovering after liver transplantation between the HBcAb$^+$ and HBcAb$^-$ groups (Figure 3).

HBV infection after liver transplantation

As was noted in the beginning, it is well acknowledged that HBcAb$^+$ liver grafts retain the capability to transmit HBV, especially to HBsAg$^-$ patients[7,9,23], which is one of the major concerns in utilization of such grafts.

First, we analyzed *de novo* HBV infection in the HBsAg negative cohort and its risk factors. We found that 9 patients receiving HBcAb$^+$ liver grafts developed hepatitis B after a mean time of 15.66 ± 5.52 mo, with an infection rate of 13.23% (9/68, 13 patients died within 1 mo after liver transplantation or without any post-transplant HBV serological data), whereas no patients receiving HBcAb$^-$ liver grafts were newly diagnosed with HBV after the operation (0/163, 28 patients died within 1 mo after liver transplantation or without any post-transplant HBV serological data). Thus, the data indicate a higher prevalence of *de novo* HBV infection in recipients of HBcAb$^+$ liver grafts (Fisher exact test, 13.23% *vs* 0, P < 0.0001).

Once the diagnosis of *de novo* hepatitis B was made, anti-viral therapy was switched to entecavir or tenofovir. Only one patient died 3 mo after a new diagnosis of HBV due to severe rejection-caused multi-organ failure without HBV flare-up. The other patients are still alive at present. The multivariate regression analysis revealed that the occurrence of newly diagnosed HBV infection is not an independent threat to patient and graft survival (P = 0.502 and 0.490, respectively, Table 2).

Considering the status of HBV surface antibody (anti-HBs) and HBV core antibody (anti-HBc), there were three different HBV serological statuses in recipients (Figure 4). There was a clear tendency that the HBV-naïve patients had the highest *de novo* HBV infection rate (31.82%, 7/22), while the anti-HBs+ recipients had the lowest *de*

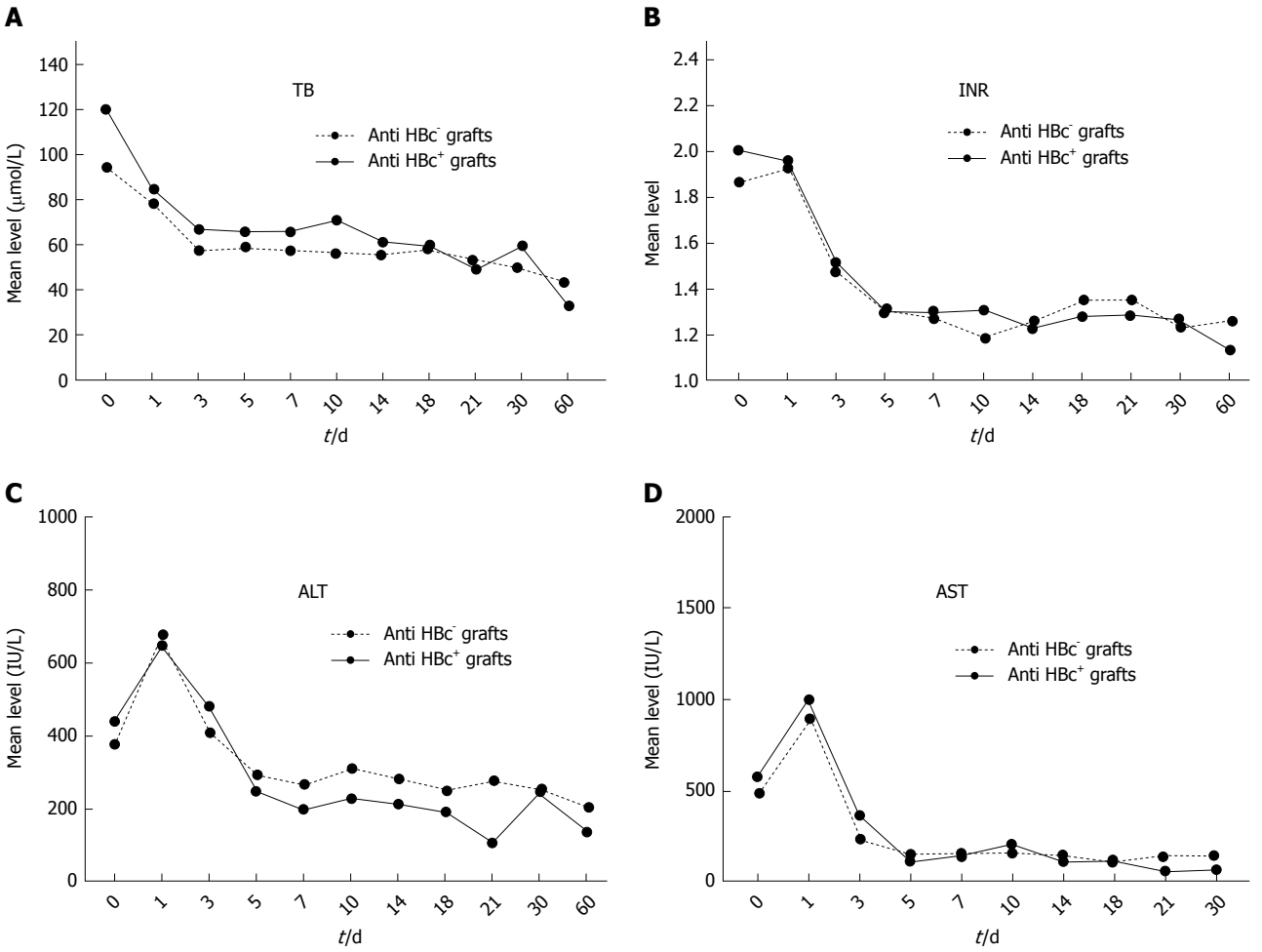

Figure 3 Comparison of graft function recovery after liver transplantation [0 d (right after operation) to 2 mo after operation] of patients who received hepatitis B virus core antibody positive grafts *vs* those who received hepatitis B virus core antibody negative grafts. Each plot represents the mean value of the illustrated parameter in either group. A: Total bilirubin level between the two groups; B: International normalized ratio level between the two groups; C: Alanine transaminase level between the two groups; D: Aspartate aminotransferase level between the two groups. ALT: Alanine transaminase; AST: Aspartate aminotransferase; TB: Total bilirubin; INR: International normalized ratio.

novo HBV infection rate (2.56%, 1/39). The comparison showed a significant difference (Fisher's exact test, P = 0.002). The results suggested that the presence of anti-HBs in recipients might be a protective factor against HBV infection.

Furthermore, the anti-HBs titer at the time of transplantation has a significant impact on the outcome of the HBV infection. We found that no patients with anti-HBs titer more than 100 IU/l before surgery (n = 21) developed *de novo* HBV infection, while those whose anti-HBs titers were less than 100 IU/l before surgery had a *de novo* infection rate of 19.15% (9/47) (Fisher exact test, P = 0.048, Figure 5).

Next, we divided the 68 patients into two groups with respect to antiviral prophylaxis: an HBIG monotherapy group (n = 50) and an nRTI combination group (n = 18). The corresponding *de novo* HBV infection rates of each group were 16.00% (8/50) and 5.55% (1/18). There was a higher risk tendency in the HBIG monotherapy group compared with the other, but without a significant difference (Fisher exact test, P = 0.43).

It is important to note that the only patient who developed HBV positivity in the nRTI combination group had an HBIG administration of 3 mo but did not use nRTI regularly until 8 mo after surgery and was diagnosed 4 mo later.

Finally, we also analyzed the recurrence of HBV infection in the HBsAg$^+$ cohort and found that 20 (2.5%) of the 799 HBsAg$^+$ patients developed recurrence of HBV infection, in which 7 patients received HBcAb$^+$ liver grafts and 13 received HBcAb$^-$ liver grafts. Thus, the recurrence rates between the two groups were 4.7% (7/149) and 2.0% (13/650); this difference was not statistically significant (Chi square test, P = 0.06).

DISCUSSION

Recent years have witnessed an increasing trend in the utilization of marginal organs, including HBV core antigen-positive liver grafts, to address the problem of organ shortage[8,37]. In early times, transplantation centers adhered to the principle that the occurrence of anti-HBc

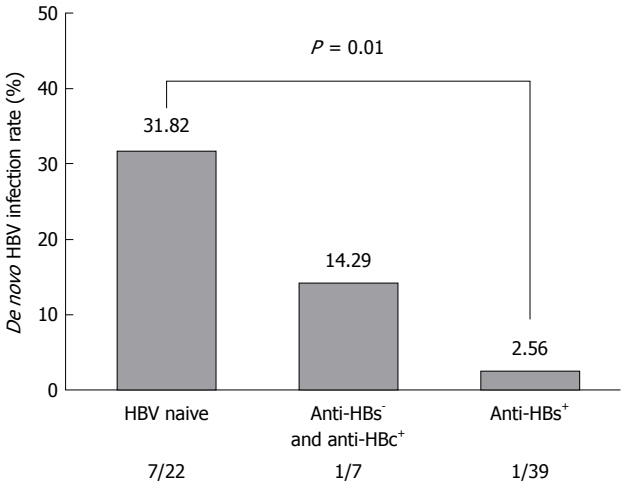

Figure 4 Overall *de novo* hepatitis B virus infection rate in hepatitis B virus surface antigen negative recipients who received liver grafts from anti-hepatitis B virus core positive donors in relation to their hepatitis B virus serological status before transplant.

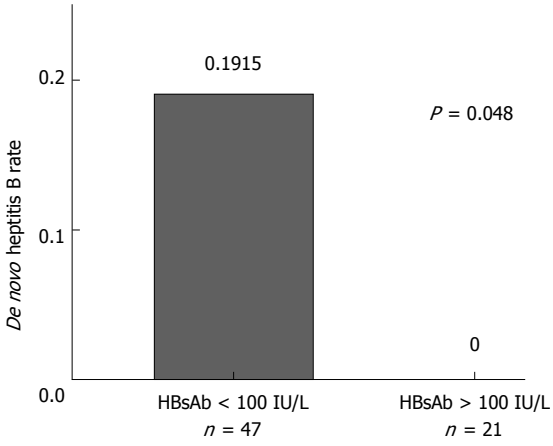

Figure 5 Hepatitis B virus infection rates post-transplant between recipients with hepatitis B virus surface antibody titer above and below 100 IU/L before transplantation.

in liver grafts was a contraindication to organ use in fear of deleterious effects[9,18,19]. However, as discussed above, the postoperative safety of receiving such grafts has become debatable over the following years.

Recent studies conducted in Austrian[20]and Italian[23] populations still associated HBcAb$^+$ livers with inferior outcomes, but without explained mechanisms. The Italian study[23] suggested that HBcAb positivity represents a surrogate marker of suboptimal graft quality. Nevertheless, none of the recorded causes of death or graft loss differed between HBcAb$^+$ or HBcAb$^-$ donors, and no graft loss was attributable to recurrence or *de novo* HBV infection, in line with other studies[20,38]. Notably, the authors in both articles[20,23] all acknowledged the high prevalence of HCV (20% to 50%) in the study population and the high rate of HCV recurrence[23] leading to cirrhosis in 20-30% of patients[39] when direct antiviral agents were not widely applied in the past. The Austrian study[20] also demonstrated that anti-HCV positivity was a strong indicator for worse patient survival (HR: 2.38, 95%CI: 1.18-4.78, P = 0.015), in agreement with an earlier report[40]. However, their findings in HCV infection rates were not the same as in our Chinese cohort (HCV infection rate: less than 8%), which might partially explain the difference in the impacts of HBcAb$^+$ liver grafts.

In our study, the number of HBcAb$^+$ liver grafts was greater than the numbers in most previous studies[7,18-20,22,26-27,41,42], which allows a more reliable conclusion. Our study was the largest single-center cohort of long-term follow-up in a Chinese population, which provides an important view in the utilization of such grafts.

Although the baseline data of HBcAb$^+$ donors and recipients shared similarity in most aspects with HBcAb$^-$ donors, as a real world study, differences existed between the two groups, consisting of a significantly higher Child-Pugh score and a higher prevalence of acute liver failure as transplantation reasons in HBcAb$^+$ graft recipients. These differences could be explained as the relatively "imperfect" liver grafts, for example, HBcAb$^+$ grafts were more likely to be allocated to patients with more severe and urgent conditions in short of proper grafts available in recent clinical practice. And it was notable that HBcAb$^+$ donors were older than HBcAb$^-$ donors, which was in line with previous studies[7,20,23,26] and reflected a higher prevalence of HBV infection and anti-HBc occurrence in older people, especially in epidemic areas.

Considering these confounding factors in a real world study, a new cohort of patients was generated in a propensity-score matching method, as we have introduced, to achieve appropriate analysis validity, which was neglected in most of the previous studies. Additionally, given the different HBsAg status in recipients, a subgroup analysis was conducted, and survival was compared as in the entire population.

Using multiple rigorous strategies, we were able to come to a firm conclusion that overall survival with HBcAb$^+$ liver grafts was not suboptimal, regardless of the HBsAg status of the recipients.

Monitoring after surgery in our study also showed that HBcAb$^+$ grafts did not increase the post-transplant complications in either the early stage or the later stage. Furthermore, liver function recovered in HBcAb$^+$ grafts at the same pace as in HBcAb$^-$ grafts.

Another barrier to HBcAb$^+$ graft utilization is the risk of HBV infection in recipients, especially for patients naïve to HBV infection[26]. In the era of prophylaxis with HBIG and nRTI, the dramatically high prevalence of HBV infection in HBcAb$^+$ liver recipients[7,10,13-17] has declined (in our cohort, *de novo* infection: 13.23%). Post-transplantation HBV infection did not affect patient and graft survival (P = 0.50 and 0.49, respectively, Table 2), the same as in previous articles[20,23]. Yet, there was no consensus on a prophylactic regimen for *de novo* HBV infection until 2015 in the United States[43] and 2016 in China[31]. Thus, a diverse array of protocols has been used worldwide in past time[7,20,21,23-25], from no

prophylaxis to the use of nucleos(t)ide antiviral agents, HBIG or their combination, resulting in varied HBV infection rates in different institutes[7]. In our cohort, there was a higher risk tendency of *de novo* HBV infection in the HBIG monotherapy group compared with patients with prophylaxis consisting of HBIG and nRTI (16.00% *vs* 5.55%), highlighting the importance of nucleos(t)ide antiviral agents in HBV prophylaxis. In addition, recent studies suggested that HBIG+ nRTI combination therapy did not provide superior protection over nRTI-only treatment[7,14,16,24,25,44]. The latest guidelines overseas[43,45] also recommend nRTI (lamivudine, entecavir or tenofovir) as prophylactic agents, excluding HBIG.

However, it is worth noting that the higher cost and lower compliance of HBIG injection prevented its long-term utilization in patients who were HBV-negative before transplantation, varying from weeks to months in our study and in other reports[7,14,25,44], which might increase the HBV infection rates in HBIG monotherapy prophylaxis, as we found above.

Additionally, recipient characteristics in HBV serology did have a significant impact on postoperative HBV infection when accepting HBcAb$^+$ grafts. In our results, HBV-naïve patients had the highest *de novo* HBV infection rate (31.82%), while the anti-HBs+ recipients had the lowest (2.56%), a tendency that was in accord with a previous systematic review[7]. Quantitative investigation on anti-HBs suggested that patients with an anti-HBs titer more than 100 IU/l before surgery had a lower risk of hepatitis B (P = 0.048, Figure 5). And in a recent study, patients were given HBV vaccinations as active immunizations with the aim of achieving anti-HBs > 1000 IU/L pre-transplant and > 100 IU/L post-transplant, which achieved satisfactory preventive results[46]. They also suggested that anti-viral prophylaxis could be safely discontinued in patients who obtain this immunity. Generally, these findings emphasize the prophylactic role of HBsAb and active immunization might be an economical alternative prophylaxis in patients who respond appropriately to vaccination.

Our study has limitations. It is based on retrospective data and patients at a single institution, which may be subject to bias and confounding, although we used multiple strategies (multivariable adjustment and propensity-score matching). In addition, because of the retrospective nature of our study, we were unable to obtain complete pre-LT HBV vaccination data. Further multicenter studies are needed to evaluate the ideal prophylaxis to prevent post-transplant *de novo* HBV infection.

In conclusion, our retrospective study revealed that HBcAb$^+$ liver grafts could be used with similar outcomes to HBcAb$^-$ grafts regardless of the HBsAg status of the recipients. Although HBcAb$^+$ liver recipients do have a higher *de novo* HBV infection rate in which HBV-naïve patients suffer more often, nucleos(t)ide antiviral agents have been regarded as effective antiviral prophylaxis that should be widely applied in clinical practice. Furthermore, maintaining sufficient anti-HBs titers in recipients might also be protective against *de novo* HBV infection.

ARTICLE HIGHLIGHTS

Research background

Given the shortage of suitable liver grafts for liver transplantation, proper use of hepatitis B core antibody-positive livers might be a possible way to enlarge the donor pool and to save patients with end-stage liver diseases. However, the safety of hepatitis B virus core antibody positive (HBcAb$^+$) donors has been controversial. Initial studies were mainly conducted overseas with relatively small numbers of HBcAb$^+$ liver recipients, and there are few relevant reports in the population of mainland China.

Research motivation

We performed this study to evaluate the safety of HBcAb$^+$ liver graft recipients in a Chinese population and to investigate the feasibility of wide utilization of such liver grafts.

Research objectives

The objectives of our study were: (1) to evaluate the long-term survival of HBcAb$^+$ liver graft recipients; and (2) to investigate the post-transplant hepatitis B virus infection rates of HBcAb$^+$ liver graft recipients and to elucidate possible risk factors.

Research methods

We conducted a retrospective study, enrolling 1071 patients who consecutively underwent liver transplantation from 2005 to 2016 at West China Hospital Liver Transplantation Center. Given the imbalance in several baseline variables, propensity score matching was used, and the outcomes of all recipients were reviewed in this study.

Research results

Our results revealed that the 1-, 3- and 5-year survival rates in patients and grafts between the HBcAb$^+$ and HBcAb$^-$ recipients showed no difference (P = 0.16 and 0.19, respectively), and receiving HBcAb$^+$ liver grafts was not a significant risk factor for long-term survival. Further studies illustrated that post-transplant major complication rates and liver function recovery after surgery were also similar. These findings were consistent in both HBsAg$^+$ and HBsAg$^-$ patients. Newly diagnosed HBV infection had a relatively higher incidence in HBsAg$^-$ patients with HBcAb$^+$ liver grafts (13.23%), in which HBV-naïve recipients suffered most (31.82%), whereas it did not affect patient and graft survival (P = 0.50 and 0.49, respectively). Recipients with high anti-HBs titers (more than 100 IU/L) before transplantation and antiviral prophylaxis with nucleos(t)ide antiviral agents post-operation had lower *de novo* HBV infection risks.

Research conclusions

HBcAb$^+$ grafts did not increase the post-transplant mortality, nor did they affect post-transplant major complication rates and liver function recovery. HBV-naïve recipients suffered post-transplantation *de novo* HBV infection more often, and sufficient anti-HBs titers in recipients might be a protective factor. Combined with proper postoperative antiviral prophylaxis, such as nucleos(t)ide antiviral agents, utilization of HBcAb$^+$ grafts is rational and feasible.

Research perspectives

Further multicenter studies are needed to investigate more interval time groups with a large sample size on the outcome of HBcAb$^+$ graft recipients. The findings of this study should spur more investigators to evaluate the ideal postoperative antiviral therapy, which may involve active immunization prophylaxis.

REFERENCES

1 **Alkofer B**, Samstein B, Guarrera JV, Kin C, Jan D, Bellemare S, Kinkhabwala M, Brown R Jr, Emond JC, Renz JF. Extended-donor criteria liver allografts. *Semin Liver Dis* 2006; **26**: 221-233 [PMID:

16850371 DOI: 10.1055/s-2006-947292]
2 **Merion RM**, Goodrich NP, Feng S. How can we define expanded criteria for liver donors? *J Hepatol* 2006; **45**: 484-488 [PMID: 16905221 DOI: 10.1016/j.jhep.2006.07.016]
3 **Liang X**, Bi S, Yang W, Wang L, Cui G, Cui F, Zhang Y, Liu J, Gong X, Chen Y, Wang F, Zheng H, Wang F, Guo J, Jia Z, Ma J, Wang H, Luo H, Li L, Jin S, Hadler SC, Wang Y. Epidemiological serosurvey of hepatitis B in China--declining HBV prevalence due to hepatitis B vaccination. *Vaccine* 2009; **27**: 6550-6557 [PMID: 19729084 DOI: 10.1016/j.vaccine.2009.08.048]
4 **Schweitzer A**, Horn J, Mikolajczyk RT, Krause G, Ott JJ. Estimations of worldwide prevalence of chronic hepatitis B virus infection: a systematic review of data published between 1965 and 2013. *Lancet* 2015; **386**: 1546-1555 [PMID: 26231459 DOI: 10.1016/S0140-6736(15)61412-X]
5 **Merrill RM**, Hunter BD. Seroprevalence of markers for hepatitis B viral infection. *Int J Infect Dis* 2011; **15**: e78-e121 [PMID: 21130675 DOI: 10.1016/j.ijid.2010.09.005]
6 **Bohorquez HE**, Cohen AJ, Girgrah N, Bruce DS, Carmody IC, Joshi S, Reichman TW, Therapondos G, Mason AL, Loss GE. Liver transplantation in hepatitis B core-negative recipients using livers from hepatitis B core-positive donors: a 13-year experience. *Liver Transpl* 2013; **19**: 611-618 [PMID: 23526668 DOI: 10.1002/lt.23644]
7 **Cholongitas E**, Papatheodoridis GV, Burroughs AK. Liver grafts from anti-hepatitis B core positive donors: a systematic review. *J Hepatol* 2010; **52**: 272-279 [PMID: 20034693 DOI: 10.1016/j.jhep.2009.11.009]
8 **Anwar N**, Sherman KE. Transplanting organs from hepatitis B positive donors: Is it safe? Is it ethical? *J Viral Hepat* 2018; **25**: 1110-1115 [PMID: 29968277 DOI: 10.1111/jvh.12962]
9 **Burton JR Jr**, Shaw-Stiffel TA. Use of hepatitis B core antibody-positive donors in recipients without evidence of hepatitis B infection: a survey of current practice in the United States. *Liver Transpl* 2003; **9**: 837-842 [PMID: 12884197 DOI: 10.1053/jlts.2003.50157]
10 **Kwan KW**, Lim TR, Kumar R, Krishnamoorthy TL. Understanding the hepatitis B core positive liver donor. *Singapore Med J* 2018 [PMID: 30182132 DOI: 10.11622/smedj.2018104]
11 **Caviglia GP**, Abate ML, Tandoi F, Ciancio A, Amoroso A, Salizzoni M, Saracco GM, Rizzetto M, Romagnoli R, Smedile A. Quantitation of HBV cccDNA in anti-HBc-positive liver donors by droplet digital PCR: A new tool to detect occult infection. *J Hepatol* 2018; **69**: 301-307 [PMID: 29621551 DOI: 10.1016/j.jhep.2018.03.021]
12 **Mason AL**, Xu L, Guo L, Kuhns M, Perrillo RP. Molecular basis for persistent hepatitis B virus infection in the liver after clearance of serum hepatitis B surface antigen. *Hepatology* 1998; **27**: 1736-1742 [PMID: 9620351 DOI: 10.1002/hep.510270638]
13 **Prakoso E**, Strasser SI, Koorey DJ, Verran D, McCaughan GW. Long-term lamivudine monotherapy prevents development of hepatitis B virus infection in hepatitis B surface-antigen negative liver transplant recipients from hepatitis B core-antibody-positive donors. *Clin Transplant* 2006; **20**: 369-373 [PMID: 16824156 DOI: 10.1111/j.1399-0012.2006.00495.x]
14 **Skagen CL**, Jou JH, Said A. Risk of *de novo* hepatitis in liver recipients from hepatitis-B core antibody-positive grafts - a systematic analysis. *Clin Transplant* 2011; **25**: E243-E249 [PMID: 21323735 DOI: 10.1111/j.1399-0012.2011.01409.x]
15 **Avelino-Silva VI**, D'Albuquerque LA, Bonazzi PR, Song AT, Miraglia JL, De Brito Neves A, Abdala E. Liver transplant from Anti-HBc-positive, HBsAg-negative donor into HBsAg-negative recipient: is it safe? A systematic review of the literature. *Clin Transplant* 2010; **24**: 735-746 [PMID: 20438579 DOI: 10.1111/j.1399-0012.2010.01254.x]
16 **Chang MS**, Olsen SK, Pichardo EM, Stiles JB, Rosenthal-Cogan L, Brubaker WD, Guarrera JV, Emond JC, Brown RS Jr. Prevention of *de novo* hepatitis B in recipients of core antibody-positive livers with lamivudine and other nucleos(t)ides: a 12-year experience. *Transplantation* 2013; **95**: 960-965 [PMID: 23545507 DOI: 10.1097/TP.0b013e3182845f97]
17 **Yu L**, Koepsell T, Manhart L, Ioannou G. Survival after orthotopic liver transplantation: the impact of antibody against hepatitis B core antigen in the donor. *Liver Transpl* 2009; **15**: 1343-1350 [PMID: 19790164 DOI: 10.1002/lt.21788]
18 **Muñoz SJ**. Use of hepatitis B core antibody-positive donors for liver transplantation. *Liver Transpl* 2002; **8**: S82-S87 [PMID: 12362304 DOI: 10.1053/jlts.2002.35783]
19 **Dodson SF**, Issa S, Araya V, Gayowski T, Pinna A, Eghtesad B, Iwatsuki S, Montalvo E, Rakela J, Fung JJ. Infectivity of hepatic allografts with antibodies to hepatitis B virus. *Transplantation* 1997; **64**: 1582-1584 [PMID: 9415560]
20 **Brandl A**, Stolzlechner P, Eschertzhuber S, Aigner F, Weiss S, Vogel W, Krannich A, Neururer S, Pratschke J, Graziadei I, Öllinger R. Inferior graft survival of hepatitis B core positive grafts is not influenced by post-transplant hepatitis B infection in liver recipients-5-year single-center experience. *Transpl Int* 2016; **29**: 471-482 [PMID: 26716608 DOI: 10.1111/tri.12741]
21 **Marciano S**, Gaite LA, Bisignano L, Descalzi VI, Yantorno S, Mendizabal M, Silva MO, Anders M, Orozco OF, Traverso R, Gil O, Galdame OA, Bandi JC, de Santibañes E, Gadano AC. Use of liver grafts from anti-hepatitis B core-positive donors: a multicenter study in Argentina. *Transplant Proc* 2013; **45**: 1331-1334 [PMID: 23726565 DOI: 10.1016/j.transproceed.2012.12.016]
22 **Lee S**, Kim JM, Choi GS, Park JB, Kwon CH, Choe YH, Joh JW, Lee SK. *De novo* hepatitis b prophylaxis with hepatitis B virus vaccine and hepatitis B immunoglobulin in pediatric recipients of core antibody-positive livers. *Liver Transpl* 2016; **22**: 247-251 [PMID: 26600319 DOI: 10.1002/lt.24372]
23 **Angelico M**, Nardi A, Marianelli T, Caccamo L, Romagnoli R, Tisone G, Pinna AD, Avolio AW, Fagiuoli S, Burra P, Strazzabosco M, Costa AN; Liver Match Investigators. Hepatitis B-core antibody positive donors in liver transplantation and their impact on graft survival: evidence from the Liver Match cohort study. *J Hepatol* 2013; **58**: 715-723 [PMID: 23201239 DOI: 10.1016/j.jhep.2012.11.025]
24 **Perrillo R**. Hepatitis B virus prevention strategies for antibody to hepatitis B core antigen-positive liver donation: a survey of North American, European, and Asian-Pacific transplant programs. *Liver Transpl* 2009; **15**: 223-232 [PMID: 19177436 DOI: 10.1002/lt.21675]
25 **Saab S**, Waterman B, Chi AC, Tong MJ. Comparison of different immunoprophylaxis regimens after liver transplantation with hepatitis B core antibody-positive donors: a systematic review. *Liver Transpl* 2010; **16**: 300-307 [PMID: 20209589 DOI: 10.1002/lt.21998]
26 **Dickson RC**, Everhart JE, Lake JR, Wei Y, Seaberg EC, Wiesner RH, Zetterman RK, Pruett TL, Ishitani MB, Hoofnagle JH. Transmission of hepatitis B by transplantation of livers from donors positive for antibody to hepatitis B core antigen. The National Institute of Diabetes and Digestive and Kidney Diseases Liver Transplantation Database. *Gastroenterology* 1997; **113**: 1668-1674 [PMID: 9352871]
27 **Prieto M**, Gómez MD, Berenguer M, Córdoba J, Rayón JM, Pastor M, García-Herola A, Nicolás D, Carrasco D, Orbis JF, Mir J, Berenguer J. *De novo* hepatitis B after liver transplantation from hepatitis B core antibody-positive donors in an area with high prevalence of anti-HBc positivity in the donor population. *Liver Transpl* 2001; **7**: 51-58 [PMID: 11150423 DOI: 10.1053/jlts.2001.20786]
28 **Shen S**, Jiang L, Xiao GQ, Yan LN, Yang JY, Wen TF, Li B, Wang WT, Xu MQ, Wei YG. Prophylaxis against hepatitis B virus recurrence after liver transplantation: a registry study. *World J Gastroenterol* 2015; **21**: 584-592 [PMID: 25593480 DOI: 10.3748/wjg.v21.i2.584]
29 **Jiang L**, Yan L, Li B, Wen T, Zhao J, Jiang L, Cheng N, Wei Y, Yang J, Xu M, Wang W. Prophylaxis against hepatitis B recurrence posttransplantation using lamivudine and individualized low-dose hepatitis B immunoglobulin. *Am J Transplant* 2010; **10**: 1861-1869 [PMID: 20659092 DOI: 10.1111/j.1600-6143.2010.03208.x]
30 **Jiang L**, Yan L, Wen T, Li B, Zhao J, Yang J, Xu M, Wang W. Hepatitis B prophylaxis using lamivudine and individualized low-dose hepatitis B immunoglobulin in living donor liver transplantation. *Transplant Proc* 2013; **45**: 2326-2330 [PMID: 23953544 DOI: 10.1016/j.transproceed.2013.03.028]
31 **Chinese Society of Organ Transplantation,** Chinese Medical Association, Chinese Society of Hepatology, Chinese Medical Association. The practice guideline on prophylaxis and treatment of hepatitis B for liver transplantation in China (2016 edition). *Zhonghua Gan Zang Bing Za Zhi* 2016; **24**: 885-891 [PMID: 28073407 DOI:

10.3760/cma.j.issn.1007-3418.2016.12.002]
32 **Shao ZY**, Yan LN, Wang WT, Li B, Wen TF, Yang JY, Xu MQ, Zhao JC, Wei YG. Prophylaxis of chronic kidney disease after liver transplantation--experience from west China. *World J Gastroenterol* 2012; **18**: 991-998 [PMID: 22408361 DOI: 10.3748/wjg.v18.i9.991]
33 **Yu S**, Yu J, Zhang W, Cheng L, Ye Y, Geng L, Yu Z, Yan S, Wu L, Wang W, Zheng S. Safe use of liver grafts from hepatitis B surface antigen positive donors in liver transplantation. *J Hepatol* 2014; **61**: 809-815 [PMID: 24824283 DOI: 10.1016/j.jhep.2014.05.003]
34 **Ploeg RJ**, D'Alessandro AM, Knechtle SJ, Stegall MD, Pirsch JD, Hoffmann RM, Sasaki T, Sollinger HW, Belzer FO, Kalayoglu M. Risk factors for primary dysfunction after liver transplantation-a multivariate analysis. *Transplantation* 1993; **55**: 807-813 [PMID: 8475556]
35 **Kurth T**, Walker AM, Glynn RJ, Chan KA, Gaziano JM, Berger K, Robins JM. Results of multivariable logistic regression, propensity matching, propensity adjustment, and propensity-based weighting under conditions of nonuniform effect. *Am J Epidemiol* 2006; **163**: 262-270 [PMID: 16371515 DOI: 10.1093/aje/kwj047]
36 **Austin PC**. The use of propensity score methods with survival or time-to-event outcomes: reporting measures of effect similar to those used in randomized experiments. *Stat Med* 2014; **33**: 1242-1258 [PMID: 24122911 DOI: 10.1002/sim.5984]
37 **Nadig SN**, Bratton CF, Karp SJ. Marginal donors in liver transplantation: expanding the donor pool. *J Surg Educ* 2007; **64**: 46-50 [PMID: 17320806 DOI: 10.1016/j.cursur.2006.08.001]
38 **Brock GN**, Mostajabi F, Ferguson N, Carrubba CJ, Eng M, Buell JF, Marvin MR. Prophylaxis against *de novo* hepatitis B for liver transplantation utilizing hep B core (+) donors: does hepatitis B immunoglobulin provide a survival advantage? *Transpl Int* 2011; **24**: 570-581 [PMID: 21401727 DOI: 10.1111/j.1432-2277.2011.01236.x]
39 **Gane EJ**. The natural history of recurrent hepatitis C and what influences this. *Liver Transpl* 2008; **14** Suppl 2: S36-S44 [PMID: 18825724 DOI: 10.1002/lt.21646]
40 **Berenguer M**, Prieto M, San Juan F, Rayón JM, Martinez F, Carrasco D, Moya A, Orbis F, Mir J, Berenguer J. Contribution of donor age to the recent decrease in patient survival among HCV-infected liver transplant recipients. *Hepatology* 2002; **36**: 202-210 [PMID: 12085366 DOI: 10.1053/jhep.2002.33993]
41 **MacConmara MP**, Vachharajani N, Wellen JR, Anderson CD, Lowell JA, Shenoy S, Chapman WC, Doyle MB. Utilization of hepatitis B core antibody-positive donor liver grafts. *HPB* (Oxford) 2012; **14**: 42-48 [PMID: 22151450 DOI: 10.1111/j.1477-2574.2011.00399.x]
42 **Douglas DD**, Rakela J, Wright TL, Krom RA, Wiesner RH. The clinical course of transplantation-associated *de novo* hepatitis B infection in the liver transplant recipient. *Liver Transpl Surg* 1997; **3**: 105-111 [PMID: 9346723]
43 **Huprikar S**, Danziger-Isakov L, Ahn J, Naugler S, Blumberg E, Avery RK, Koval C, Lease ED, Pillai A, Doucette KE, Levitsky J, Morris MI, Lu K, McDermott JK, Mone T, Orlowski JP, Dadhania DM, Abbott K, Horslen S, Laskin BL, Mougdil A, Venkat VL, Korenblat K, Kumar V, Grossi P, Bloom RD, Brown K, Kotton CN, Kumar D. Solid organ transplantation from hepatitis B virus-positive donors: consensus guidelines for recipient management. *Am J Transplant* 2015; **15**: 1162-1172 [PMID: 25707744 DOI: 10.1111/ajt.13187]
44 **Vizzini G**, Gruttadauria S, Volpes R, D'Antoni A, Pietrosi G, Filì D, Petridis I, Pagano D, Tuzzolino F, Santonocito MM, Gridelli B. Lamivudine monoprophylaxis for *de novo* HBV infection in HBsAg-negative recipients with HBcAb-positive liver grafts. *Clin Transplant* 2011; **25**: E77-E81 [PMID: 21039887 DOI: 10.1111/j.1399-0012.2010.01329.x]
45 **Terrault NA**, Lok ASF, McMahon BJ, Chang KM, Hwang JP, Jonas MM, Brown RS Jr, Bzowej NH, Wong JB. Update on prevention, diagnosis, and treatment of chronic hepatitis B: AASLD 2018 hepatitis B guidance. *Hepatology* 2018; **67**: 1560-1599 [PMID: 29405329 DOI: 10.1002/hep.29800]
46 **Wang SH**, Loh PY, Lin TL, Lin LM, Li WF, Lin YH, Lin CC, Chen CL. Active immunization for prevention of *De novo* hepatitis B virus infection after adult living donor liver transplantation with a hepatitis B core antigen-positive graft. *Liver Transpl* 2017; **23**: 1266-1272 [PMID: 28691231 DOI: 10.1002/lt.24814]

P- Reviewer: Gordon LG, Jin M, Roohvand F, Shimizu Y
S- Editor: Wang XJ **L- Editor**: Wang TQ **E- Editor**: Yin SY

Published by **Baishideng Publishing Group Inc**
7901 Stoneridge Drive, Suite 501, Pleasanton, CA 94588, USA
Telephone: +1-925-223-8242
Fax: +1-925-223-8243
E-mail: bpgoffice@wjgnet.com
Help Desk: https://www.f6publishing.com/helpdesk
https://www.wjgnet.com

ISSN 1007-9327